ATP MIMICS AS GLUTAMINE SYNTHETASE INHIBITORS –AN EXPLORATORY SYNTHETIC STUDY

THESIS

Submitted in fulfillment of the requirements

for the degree of

DOCTOR OF PHILOSOPHY

of Rhodes University

by

SHERIFF TOMILOLA SALISU

February 2008

TABLE OF CONTENTS

1. INTRODUCTION

1.1. Tuberculosis

1.1.1. History of tuberculosis in man 1
1.1.2. History of tuberculosis therapy 1
1.1.2.1. Bacillus Calmette-Guerin BCG 2
1.1.2.2. The antibiotic era in tuberculosis treatment 3
1.1.3. The problem of drug resistance in TB chemotherapy 4
1.1.4. Current TB treatment 5
1.1.5. The synergy between HIV/AIDS and tuberculosis 9
1.1.6. WHO TB control 9

1.2. Random drug discovery and rational drug design 10

1.2.1. Random drug discovery 10
1.2.2. Enzyme inhibition and rational drug design 12

1.3. Glutamine Synthetase 15

1.3.1. Structure and function of MTB-GS and GS II 15
1.3.2. Regulation of MTB-GS 17

1.4. The purine system 20

1.4.1. Adenine 21
1.4.1.1. Synthesis and reactions of adenine 21
1.4.2. Adenosine 23
1.4.3. Adenosine triphosphate 25
1.4.4. Other purine systems 29
1.4.4.1. Medicinal uses of purine systems 29
1.4.4.2. Synthesis of purine systems 30
1.4.4.3. Synthesis of Viagra 31
1.4.4.4. Reactions of purine systems 31

1.5. Aims of this research 34

2. DISCUSSION

2.1. Novel Adenosine analogues from adenosine 36
2.2. Novel ATP analogues from adenine 54

2.3. ATP mimics from allopurinol and Baylis-Hillman electrophiles 61

2.4. Truncated adenine mimics 78

2.4.1. ATP mimics from 3-aminobenzonitile 78
2.4.2. ATP mimics from resorcinol 89
2.4.3. ATP mimics from 3-aminophenol 92
2.4.4. ATP mimics from 3-aminobenzylalcohol 102
2.4.5. ATP mimics from 3-hydroxy- and 3-aminobenzoic acid 111

2.5. Application of NMR chemical shift prediction Programmes 115

2.5.1. NMR chemical shift prediction for adenosine analogues 115
2.5.2. NMR chemical shift prediction for adenine analogues 119
2.5.3. NMR chemical shift prediction for truncated analogues 120
2.5.4. NMR chemical shift prediction for allopurinol-derived Baylis-Hillman analogues 126

2.6. **Computer modelling of ATP mimics** 129

2.6.1. Docking of ATP and ATP mimics into the MTB-GS receptor site 129
2.6.1.1. Modelling of ATP in the GS active-site
2.6.1.2. Modelling of adenosine, adenine and allopurinol Derivatives in the GS active-site 132
2.6.1.3.Modelling of truncated adenine -derived mimics in the GS active-site 139

2.7. Conclusions 145

3. EXPERIMENTAL 147

4. REFERENCES 200

ACKNOWLEDGEMENTS

I thank ALLAH [SWT] for granting me this noble opportunity to get educated to PhD level.

A very big thank you goes to my supervisor Professor Perry Kaye, a source of inspiration and guide throughout my study. I cannot but mention the compassionate nature of my dear “Smiling Professor” who does not give up on any reaction. Other Department of Chemistry academic staffs are well acknowledged for their meaningful inputs at various times during the course of this research.

I thank my wife Mrs. Yetunde Wulaymah Salisu for her patience, support, prayers, love and care throughout the duration of this programme.

Mr. Andrew George Soper ‘ANDY’ is one I believe I cannot thank enough for his untiring assistance with NMR spectroscopy as well as any form of assistance I needed day or night; from tuning the probe to processing of spectra to even coming around to my place of residence to sort out problems with my PC. I can only say in my language ‘ E SE GAN NI O O O O!!!!’ meaning ‘a very big thank you’.

I am also grateful to Kevin Lobb for running protein NMR experiments as well as direction on modelling. Without his direction I would probably have run into a lot of problems with modelling.

Thanks to Tommie van de Walt and Martin Brits of the University of Witwatersrand mass spectrometric unit for running high- and low-resolution MS analysis. Many thanks to Dr. Irvy Gledhill of the Council for Science and Industrial Research (CSIR) for providing the glutamine synthetase enzyme PDB file that was used for docking studies.

Perhaps the most important people to thank for my completing my PhD successfully at Rhodes are the technical staff i.e. Andre Adriaan, Mr. Reuben Douglas, Mr. Fourie, Mr. Buys, Mr. Dokes Ntebe, Mr. Sonemann and Mr. Vuyisile Dondashe. The office

staff members Mrs Benita Tarr and Barbra too deserve a lot of thanks for the work they do behind the scenes to make the department as a whole run smoothly.

I thank my fellow colleagues who over the years have made my stay in the Department of Chemistry at Rhodes a pleasant one, for their support and encouragement. All fellow post grads in all research labs of the department are well acknowledged.

I am grateful to the CSIR and Rhodes University for financial support.

Dr. Moosa Motara and family are well recognized as good support. Professor Wole Familoni of the Chemistry Department, University of Lagos, Nigeria is also well acknowledged for his moral and academic support.

A lot of thanks go to family members and in-laws (in Nigeria) as well as well-wishers both within and outside the university community for their invaluable support throughout the duration of my study at Rhodes.

ABSTRACT

Using a mechanism-based approach to drug discovery, efforts have been directed towards developing novel ATP mimics that can act as GS inhibitors. The purine-based systems, adenosine, adenine and allopurinol, were identified as possible scaffolds for potential ATP mimics, while various *meta*-disubstituted benzenoid compounds, 3-aminobenzonitrile, 3-aminophenol, resorcinol, 3-aminobenzyl alcohol, 3-hydroxybenzoic acid and 3-aminobenzoic acid have been explored as adenine analogues.

These compounds were treated with different alkylating and acylating agents. Allylation of all the substrates was achieved using allyl bromide and N-9 alkylation of protected allopurinol was effected using a number of specially prepared Baylis-Hillman adducts. Acylation of the benzenoid precursors with chloroacetyl chloride, acetoxyacetyl chloride, acryloyl chloride and specially prepared 2,3,4,5,6-pentaacetylgluconoyl chloride afforded the corresponding mono- and /or diacylated products in varying yields (4-96%). Elaboration of the alkylated and acylated products has involved the reaction of hydroxy systems with diethyl chloro phosphate and chloro derivatives with triethyl phosphite in Arbuzov-type reactions to afford phosphorylated products.

In all cases, products were fully characterized using 1- and 2-D NMR analysis and, where appropriate, high-resolution mass spectrometry. The application of Modgraph and ChemWindow NMR prediction programmes has been explored and the resulting data have been compared with experimental chemical shift assignments to confirm chemical structures and, in some cases, to establish the position of allylation or acylation. Experimental assignments were found to be generally comparable with the Modgraph data, but not always with the ChemWindow values.

The docking of selected products in the ‘active-site’ of GS and their structural homology with ATP, both in their free and bound conformations have been studied using the ACCELERYS Cerius^2 platform. All the selected ATP mimics exhibit some form of interaction with the ‘active-site’ residues, and a number of them appear to be promising GS ligands.

ABBREVIATIONS

^{1}H	Proton NMR spectroscopy
CH_2Cl_2	Dichloromethane
$CHCl_3$	Chloroform
COSY	Correlation spectroscopy (^{1}H-^{1}H)
DABCO	1,4-Diazabicyclo[2.2.2.]octane
DEAD	Diethylazodicarboxylate
DMF	*N*,*N*'-Dimethylformamide
DHPA	Dihydroxypropyl Adenine
DMSO	Dimethyl sulfoxide
EtOAc	Ethyl acetate
EtOH	Ethanol
HMBC	Heteronuclear multiple bond coherence (^{1}H-^{13}C)
HPMPA	9-[2-Hydroxy-3-(phosphonomethoxy)propyl]adenine
HSQC	Heteronuclear single quantum coherence (^{1}H-^{13}C)
TBAF	Tetrabutylammonium fluoride
THF	Tetrahydrofuran

1. INTRODUCTION

1.1. Tuberculosis

Tuberculosis (TB) is a deadly disease that has killed millions of people for a very long time.[1,2] It primarily affects the lungs, though it does affect other parts of the body, being characterized by the formation of tiny lumps otherwise referred to as tubercles in the affected part of the body.[3] *Mycobacterium tuberculosis M.tb.*, a tubercle bacillus is the organism that causes TB.[4,5] Infected individuals with pulmonary TB transmit the disease when they cough, sneeze or talk by propelling many bacilli into the air. Hence, inhalation of the airborne bacilli by healthy people may lead to infection.[3,6,7] Approximately 1.6 m illion people fell casuality to this preventable disease in 2005 with the highest mortality rates in the poorest parts of the world. The World Health Organization (WHO) TB/HIV Working Group was established to formulate policies directed at combating the deadly combination of TB and HIV/AIDS.[7]

1.1.1. History of tuberculosis in man

Archaeological evidence, art and literature strongly suggest that TB has been plaguing mankind from time immemorial. As a result of its widespread nature, the disease has been known by many different names. Some of these include: *pulmonary TB*, described as lung sickness, white plague or consumption; *Lupus vulgaris*, otherwise referred to as skin TB; and *white swelling*, *i.e.* TB of the bones. Famous people that have fallen prey to TB include Voltaire (philosopher), Walter Scott (poet and novelist), Anton Chekov (playwright), Niccolo Paganini (violinist) and George Orwell (writer).[1,8]

1.1.2 History of Tuberculosis Therapy

It was not until the 16th century that tuberculosis was recognized as a contagious disease. The 19th century witnessed the establishment of sanatoria in different parts of the world to cater for TB patients. These were treatment institutions located in the

countryside where TB patients were believed to be cured by being exposed to fresh air, eating a healthy diet, exercising and resting under strict supervision. However, there is no scientific evidence that the sanatoria reduced the menace of TB. In the same century, organizations around the world, such as the National Association for the Prevention of Consumption and other forms of TB (NAPT) in the UK and the National Tuberculosis Association (NTA) in the USA, were also established to curb the menace of the then incurable and deadly disease.[1,9]

In 1890, an Italian physician Forlanini invented pneumothorax (otherwise referred to as lung collapse) therapy. This method involved compressing the part of the diseased lung(s) and then filling the pleural cavities with nitrogen through a needle. An extreme form of the method was thoracoplasty, which involved the removal of ribs from one side of the thorax to accomplish a permanent collapse of the diseased part of the lung; an obvious side effect was shortness of breath as a result of the decreased lung space.[1]

The ability to view the tubercle bacillus in 1882, which was made possible by the staining technique of Robert Koch[10] and the invention of X-rays by Wilhelm Roentgen in 1889,[1] gave a boost to the fight against TB. It was then realized that TB is not inherited as previously believed, but that transmission occurs from diseased to healthy individuals through the mycobacterium and that prevention is possible.[1,3]

1.1.2.1. Bacillus Calmette-Guerin BCG

BCG, a potent vaccine against TB, was developed[10] in 1924 by two French scientists, Calmette and Guérin, from an attenuated strain of *mycobacterium bovis*. Though not particularly effective in preventing infection, BCG has been administered in areas with high TB prevalence and incidence. It has been impossible to judge the efficacy of BCG because the original stocks were not kept. Scientists are working on making a better vaccine that can prevent TB following the successful mapping of the *M.tb.* genome in 1997.[11, 12,13,14]

1.1.2.2. The antibiotic era in tuberculosis treatment

In a method invented in 1885 by Cantani, an Italian bacteriologist, patients inhaled nonpathogenic bacteria so as to reduce the level of tuberculosis bacilli in the sputum. It was discovered in 1888 by Babes, a Romanian scientist, that products of certain *Gram positive* and *Gram negative* bacteria could inhibit the growth of *m.tb.*[15] Sanocrysin, a double thiosulphate of gold and sodium introduced by Holger Mollgaard in 1925 was used as an anti TB drug in 1925, but was discontinued because of its high toxicity.[15] Streptomycin **1**[16,17] was first used for a human patient in 1944,[1] but by 1947, *M. tb.* had begun to show resistance to streptomycin. The search continued to find drug(s) that could treat the disease or be used together with streptomycin. In 1949 *para*-aminosalicyclic acid (PAS)[18] **2** became available and, in combination with streptomycin, afforded better treatment for TB.[19]

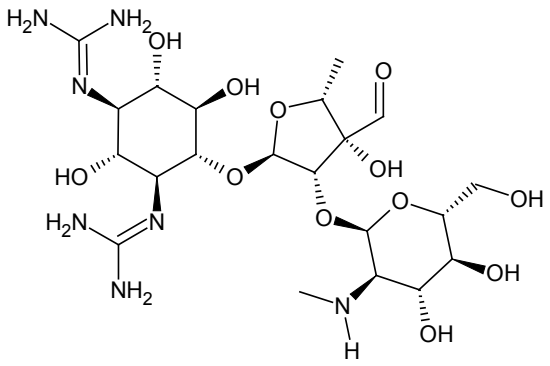

1

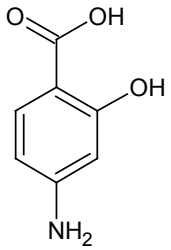

2

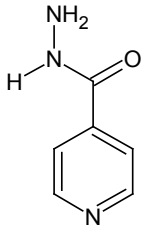

3

A new drug Isoniazid [INH][20] **3** was discovered in 1951 and, in combination with PAS, proved to be more effective than the combination of streptomycin and PAS.[14]

Other drugs made to treat TB include pyrazinamide **4** (1954),[21] cycloserine **5** (1955),[22] ethambuthol **6** (1962),[23] and rifampicin **7** (1963).[24]

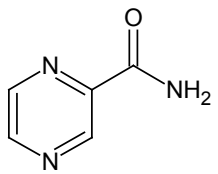

4

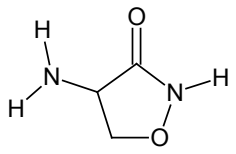

5

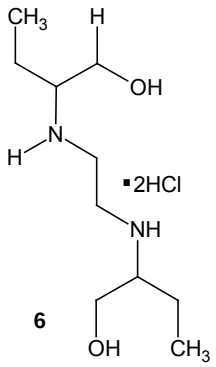

6

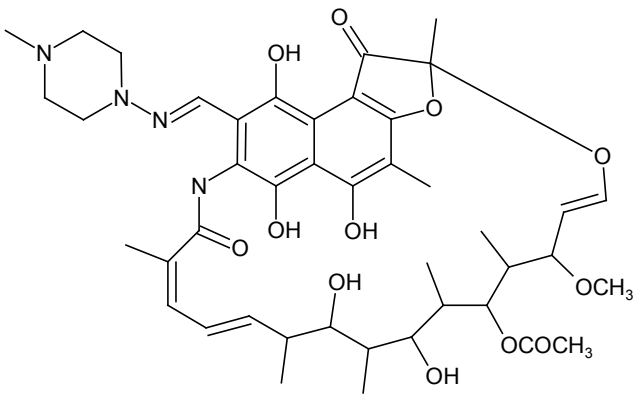

7

1.1.3 The problem of drug resistance in TB chemotherapy

Although the pathogen *M.tb.* does manage to evade the host-protective response in man's alveolar machrophages[3,25,26,27,28] to cause active TB disease in some infected individuals, chemotherapy has been effective in curing the disease.[29] However, TB continues to be a major threat to life as a result of drug resistance to chemotherapy.[7,30] Drug-resistant TB, otherwise referred to as multidrug resistant TB (MDR-TB), is defined as resistance to INH **3** and RIF **7,** whether there is resistance to other antitubercular drugs or not.[31] Extreme drug resistant TB (XDR) is caused by a new strain of *M.tb.* and is not curable even with the current available combination therapy that effectively treats MDR-TB.[32,33,34] Resistance to anti-TB agents is usually a consequence of poorly administered TB treatment.[32] Mycolic acids such as compound **8**[35] are essential components of the cell wall of the pathogen that causes TB. INH **3** is believed to act by inhibiting the synthesis of mycolic acids by mimicking nicotinamide **9** and being incorporated instead, thereby impairing the activity of the enzymes that require the latter.[29]

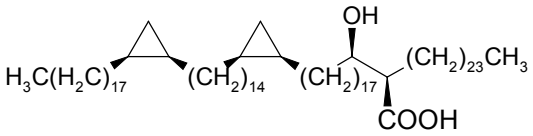

8

However, replacement of nicotinamide as the natural substrate, as a consequence of mutation in the *katG* and *inhA* genes of the bacteria, led to strains that are resistant to INH.[29] Similar mechanisms of resistance are encountered with other antitubercular drugs.

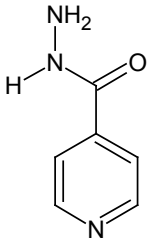

3

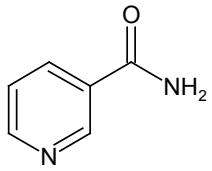

9

1.1.4. Current TB treatment

Both latent TB infection and active TB disease with the exception of XDR are curable with combination therapy.[36] Latent TB infection can be diagnosed with the aid of the tuberculin skin test,[29,36] while active TB, which may be drug-susceptible or drug-resistant,[29] can be diagnosed by chest X-ray, sputum smear, culture tests, polymerase chain reaction (PCR) and the recently developed *M.tb.* direct test (MTD).[36] The WHO and the International Union Against Tuberculosis and Lung disease (IUATLD) have formulated treatment regimens for all forms of TB plaguing society today, although there may be minor and major adverse reactions.

First-line TB drugs such as isoniazid, rifampicin, pyrazinamide, ethambutol and streptomycin suffice for the treatment of latent TB infection and drug-susceptible TB disease.[36,37] However, treatment of drug-susceptible TB with combination therapy may take up to 18 months, and resistance often develops as individuals find it difficult to maintain their medication for such a long time.[36] The mechanism of action of INH is not fully understood. However, INH has been observed to be bacteriostatic as it

stops replication of the mycobacterium. It is also bactericidal against semi-dormant populations as *M.tb.* loses its acid-fastness after being exposed to INH, which may be due to the drug interfering with the cell wall of the pathogen. New research has suggested that[38] INH is activated by the *katG* enzyme, which exhibits catalase-peroxidase activity. The isonicotinoyl radical **14** or perisonicotinic acid **16** (Figure 1) are very reactive intermediates that may result from action of the *katG* enzyme on INH leading to the formation of isonicotinaldehyde **10**, isonicotinic acid **11** and isonicotinamide **12**. It has been proposed that these activated species from the oxidation of INH with the *kat*G enzyme impair the activity of *inh*A, an enzyme that plays a vital role in the biosynthesis of the cell wall of *M.tb.*[38,39,40,41,42,43]

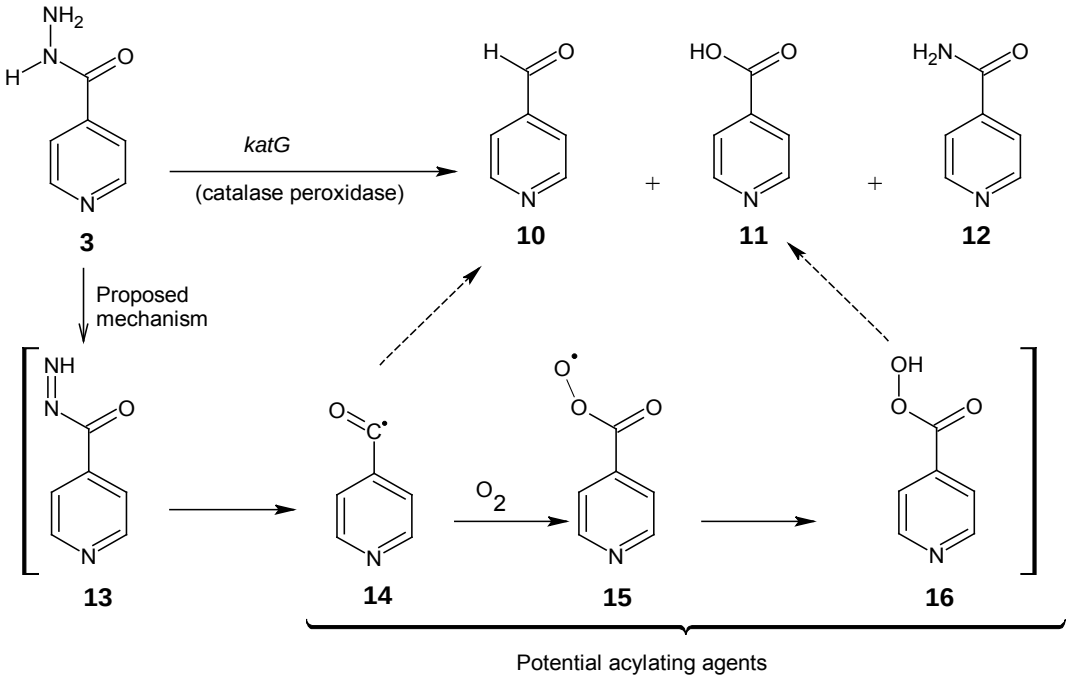

Figure 1. Catalase-peroxidase reaction of INH when administered.

Isonicotinic hydrazones **17** and isonicotinic hydrazides **18** are derivatives of INH that have been found to be less potent than INH.[44,45] When resistance or intolerance to first-line TB agents occurs, second-line TB drugs are administered. These drugs, which are expensive, toxic and usually accompanied by severe side effects,[46] include ethionamide **19**,[47] PAS **2**, cycloserine **5**, kanamycin **20**[48] and fluoroquinolones **21**.[49]

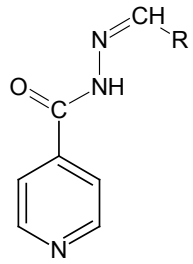

17

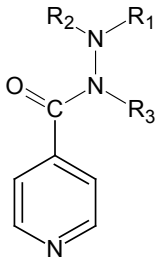

18

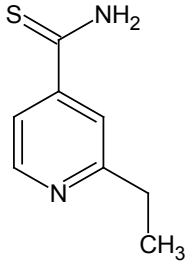

19

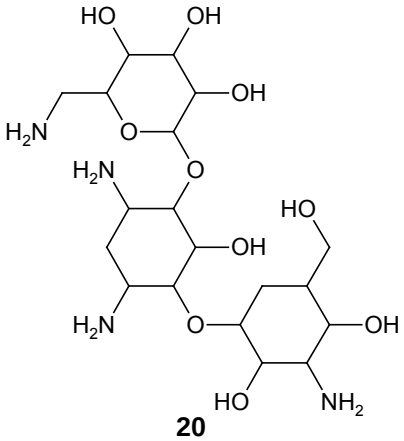

20

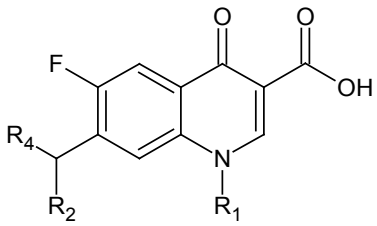

21

Ethionamide **19**,[47] a second line TB drug has been suggested to have a similar mechanism of action as INH. Ethionamide **19** is believed to be oxidized to ethionamide sulfoxide **22** by catalase-peroxidase, which impairs the activity of the *inhA* enoyl reductase enzyme by acylating the protein at the Cys 243 residue (Figure 2),[41,50] thus inhibiting the formation of compound **24**. In addition to demonstrating activity against *M.tb*., fluoroquionolones are active against other mycobacteria such as *M. xenopi* and *M. avium-intracellulare*.[49] Quinolones have the advantage of being active at low concentrations as well as having lower side effects when administered. It has been reported that non-fluorinated quinolones are not active against mycobacteria.[49] However, quinolone derivatives **25,** such as the piperazine analogues,

the pyrrolidine analogs and the 8-methoxy derivative, moxifloxacin **26,** show better activity than the earlier quinolones.[51,52]

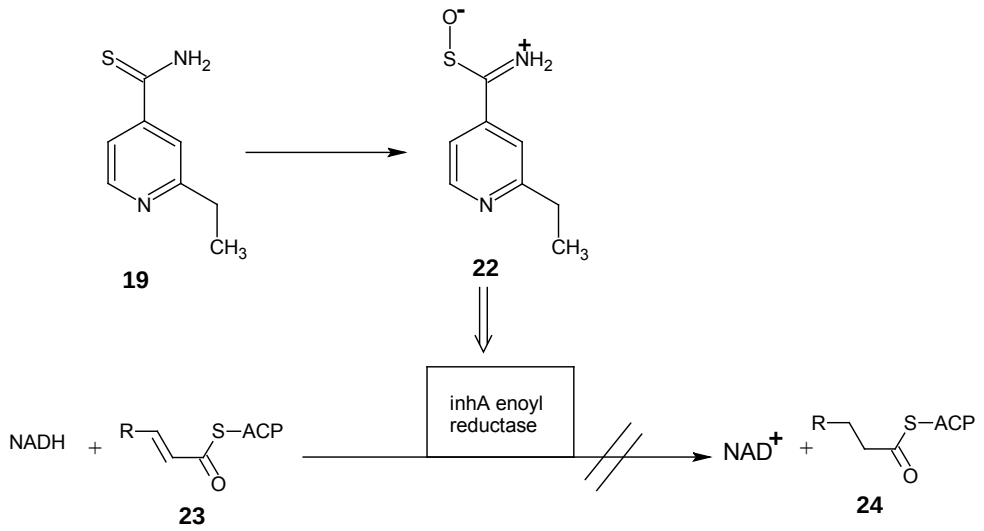

Figure 2. Mechanism of action of ethionamide.

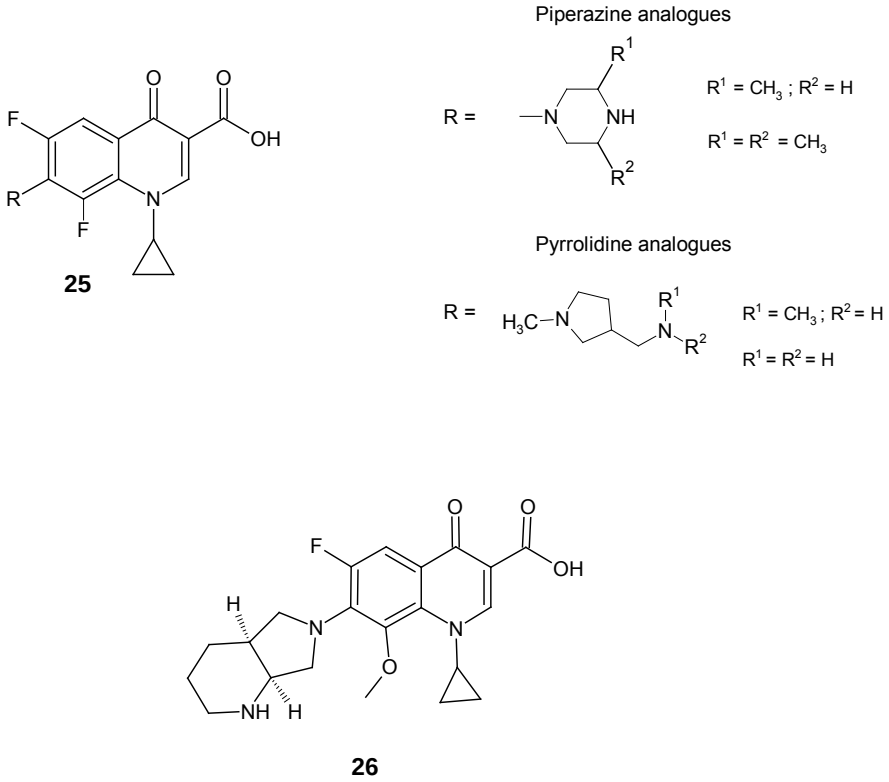

It is unfortunate that XDR-TB has defied cure even by second-line TB drugs. A recent 98% mortality was recorded within 25 da ys in patients, including those on a nti-

retrovirals in KwaZulu-Natal, afflicted with this new strain.[32] Hence, there is an urgent need to combat TB with a new approach, such as the target-based drug design.[53,54]

1.1.5. The synergism between HIV/AIDS and tuberculosis

The HIV/AIDS pandemic is a major factor in the resurgence of the global TB epidemic.[36,53] HIV weakens the immune system permitting the progression of latent TB infection to active TB disease in HIV positive individuals.[7,55] Hence TB is the leading cause of death of HIV infected people.[7,36] Research has also shown that extrapulmonary TB and MDR-TB are more common in people with compromised immune systems.[36] The lethal combination of HIV and TB is also complicated by the difficulty in diagnosing TB in HIV-positive individuals.[56] However, it is interesting to note that the treatment and prevention of TB using standard regimens prescribed by the WHO and IUATLD are effective in both HIV-positive and HIV-negative patients. The exception is that people taking protease inhibitors for HIV should substitute rifabutin for rifampin.[36]

1.1.6. WHO TB controls

The WHO has adopted a practical approach to combat the TB epidemic. The Direct Observed Therapy (DOT) strategy seeks to ensure compliance by the patient through observation by a family member or health worker. The DOTS (directly observed therapy, short course) strategy, [57,58,59,60,] which is the main strategy adopted by the WHO and the IUATLD for effective TB control, consists of five elements: " "Government commitment to a national tuberculosis programme as a specific health-system activity, integrated into comprehensive primary care, and supported technically at a national level; standardized, directly observed, short-course treatment prioritizing sputum smear-positive patients; case detection by means of a patient-friendly and clinically-efficient service based primarily on smear microscopy (passive case-finding); an ensured supply of all essential anti-tuberculosis drugs; and effective monitoring."[61]

1.2. Random drug discovery and rational drug design

1.2.1. Random drug discovery

Traditionally, different naturally occurring substances from plants, microbes, marine flora and fauna, arachnids and amphibians[62,63] are explored for their potency to act as cures for different ailments. This often random, broad-screening process involves looking for direct evidence of a physiological reaction in animal tests. As a consequence, biological, chemical and clinical practice has produced considerable data that has guided pharmaceutical drug research.[64,65,66,67] In many cases, of course, examination of the constituents of materials used as traditional medicines led to the isolation of active principles. For example, cocaine **27**[68] has local anesthetic properties and is extracted from the leaves of *Erythroxylon coca*, while quinine **28**[68] is an antimalarial obtained from the bark of *Cinchona* species.

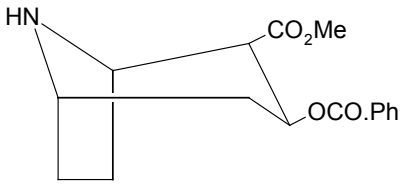

27

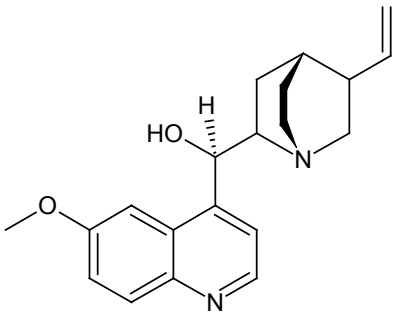

28

The need to reduce or eliminate side effects as well as improve the potency of natural drugs prompted the development of derivatives of these natural substances. Knowledge of synthetic chemistry, medicinal chemistry and pharmacology as well as imagination was needed to relate drug discovery to synthetic practice. Hence, medicinal chemists usually try to make active compounds (otherwise referred to as 'leads') by elaborating or mimicking known potent substances to develop better drugs.[69] Immediate examples are the hipolipidemics, Compactin **29**[65] and Pravastatin **30**.[65] Procaine **31**[68] and benzocaine **32**[68] are drugs that were synthesized to block the nerve activity like cocaine, but without the side-effects that lead to the abuse of

cocaine. Primaquine **33** and chloroquine **34** are two quinine analogues that became antimalarial standards for over five decades.[68]

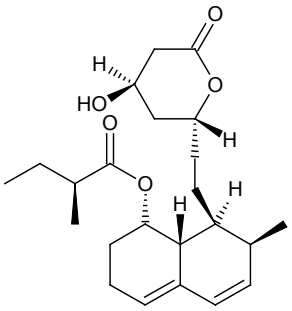

29

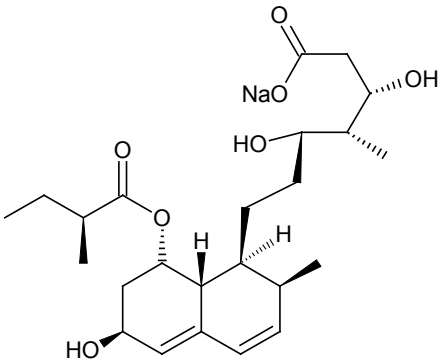

30

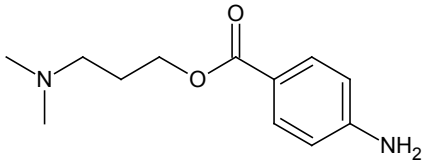

31

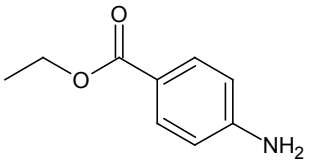

32

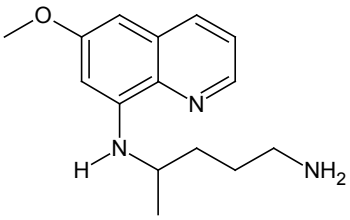

33

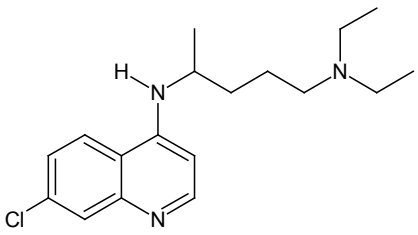

34

Today, random drug discovery has been made much easier with the availability of high through-put screening and combinatorial chemistry using computer-controlled robotic systems. Hence, hundreds to thousands of compounds can be synthesized simultaneously and their preliminary bioassays conducted much more rapidly than in the past. The success of random screening depends on a good bioassay system for the pharmacological action of interest.[69] One major criticism of random drug discovery is

that it is not guided by any specific biochemical theory of why some compounds work while others do not.[66]

1.2.2. Enzyme Inhibition and Rational drug design

Advances in molecular biology have afforded a better understanding of therapeutic targets at the molecular level.[53] Hence, it is now understood that the therapeutic targets of many medicinal agents extracted from natural products are specific enzyme systems. The bark of the willow tree, for example, has been known to have analgesic and antipyretic capabilities; the active ingredient, salicin, a glycoside, is metabolized *in vivo* to salicylic acid **35,** which inhibits the formation of the prostaglandins that mediate pain and fever by inhibiting the enzyme, cyclooxygenase.[70] Physostigmine **36**, a substance that is extracted from the West African Calabar bean, gives relief to glaucoma patients by inhibiting the enzyme, acetylcholinesterase, and, as a consequence, improving drainage and decreasing intra-ocular pressure.[70]

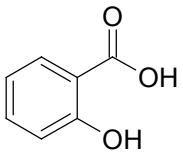

35

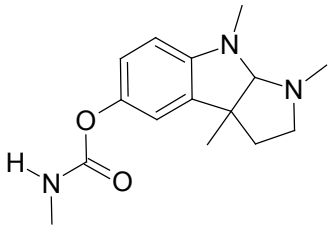

36

The antibacterial, prontosil **37,** inhibits the bacterial synthesis of folic acid **46** as a result of being metabolized into sulfanilamide **38** (Figure 3), a *para*-aminobenzoic acid mimic.[71] *Para*-aminobenzoic acid **42** is an essential metabolite in the synthesis of tetrahydrofolic acid which, in turn, is vital in the *in vivo* production of purines. The *para*-aminobenzoic acid mimic, sulfanilamide **38,** selectively inhibits the bacterial enzyme, dihydropteroate synthase (Figure 4) production of dihydrofolic acid **45**.[72] Dihydrofolic acid **45** is an important intermediate in the bacterial biosynthesis of folic acid (**46**). The rational approach to drug discovery has become more sophisticated with advances in molecular biology and information technology.[73] Hence, modern drug discovery is often based on knowledge of the enzyme receptor.[74,75] With a good understanding of the structure of a ligand and its receptor, it may be possible to propose molecules as lead compounds that will mimic the activity of a natural ligand.

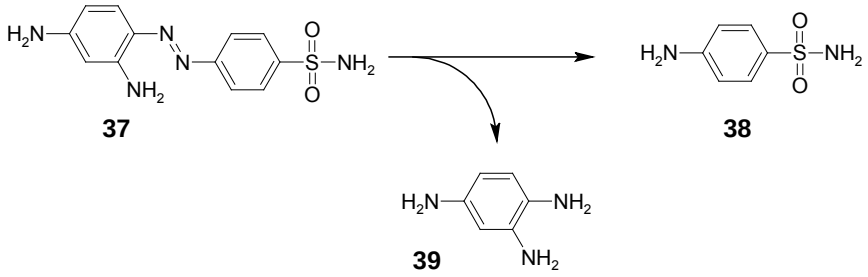

Figure 3. Metabolic reduction of prontosil to sulfanilamide.

The combinatorial synthesis of lead analogues,[76] high through-put screening, high-field NMR analysis, X-ray crystallography, molecular modelling,[77] quantum mechanical calculations[78] and quantitative structure activity relationship (QSAR) data may all contribute to the development of a rationally designed drug.[65] However, it is important to note that drug discovery is a long and difficult process in which the design of an inhibitor is only the first step. The pharmacokinetic profile of the inhibitor, its toxicities and side effects and animal and pre-clinical studies are all hurdles the inhibitor has to cross before it can be entered into clinical studies as a new drug candidate. Ritonavir **47**[80,81] and saquinavir[80,81] **48**, peptidomimetic inhibitors of both HIV-1 and HIV-2 proteases, as well as zanamivir **48**[67,82] (a therapeutic for influenza) are examples of products of the rational approach to drug discovery. Perhaps rational drug design will provide a solution to the resurgence of the TB pandemic, especially with the evolution of XDR-TB as a result of resistance to the currently available treatment regimen for MDR-TB.

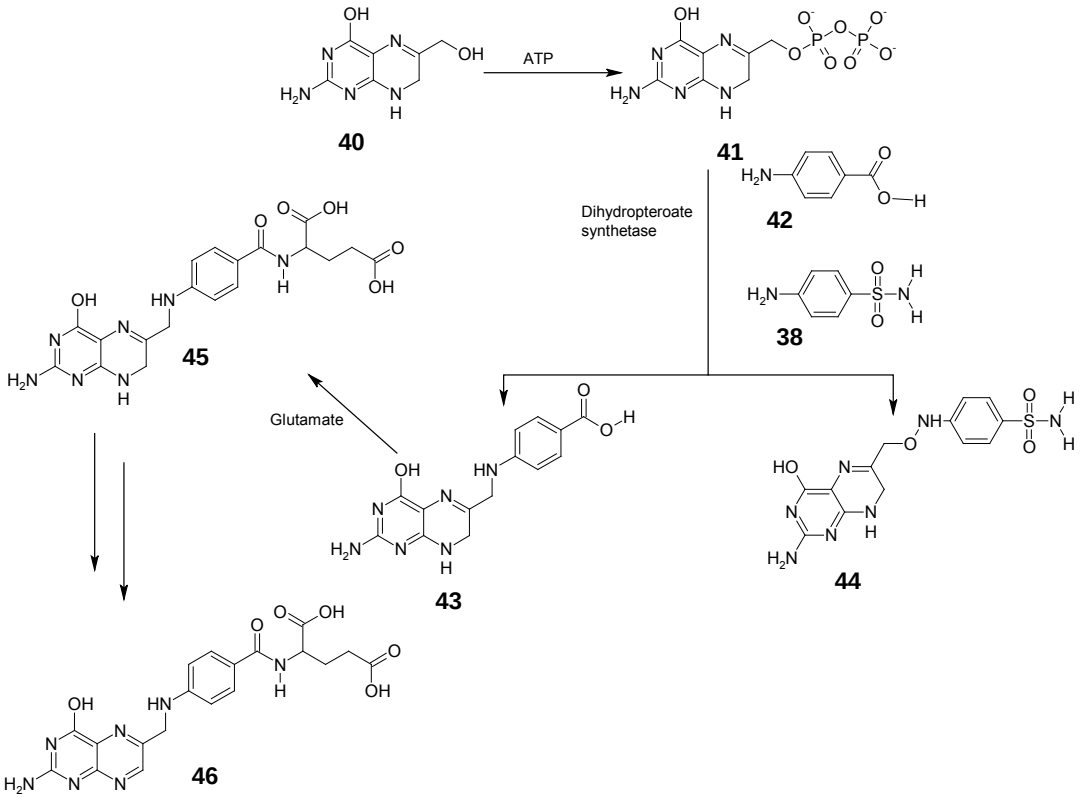

Figure 4. Inhibition of bacterial folic acid biosynthesis by sulfanilamide.

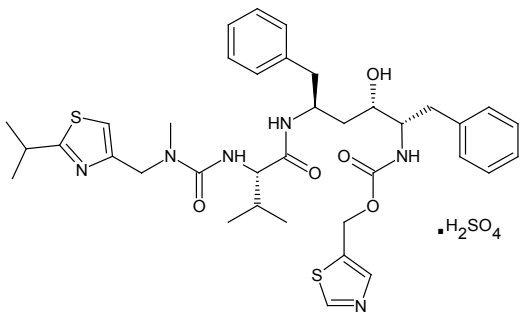

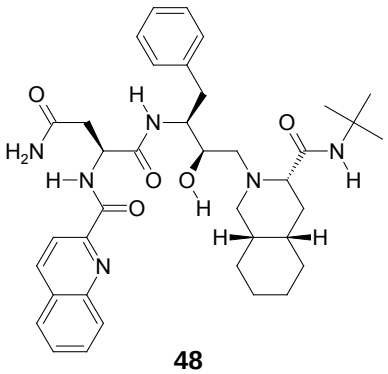

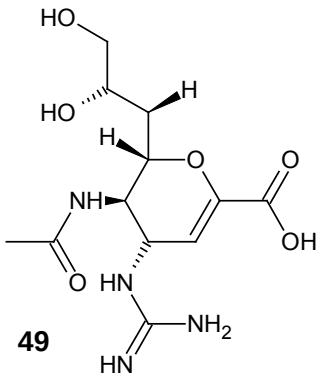

1.3. Glutamine synthetase GS

The survival of the *M.tb.* pathogen in the host to cause TB disease depends on its ability to protect itself in a kind of capsule that prevents its destruction in the phagocytic cells of human macrophages. Access to the cell is restricted and this capsule also determines what components are released into the host's tissues. Research has shown that this pathogenic mycobacterium releases extracellular proteins that are vital for its replication and virulence in the host's tissues.[83,84,85,86] The enzyme, glutamine synthetase (GS), is one of these released proteins and it has been shown to be essential for the formation of the cell wall of *M.tb.*[87] As well as catalyzing a number of other reactions, GS is an enzyme that is essential for nitrogen metabolism in living organisms.[88,89,90] Different types of GS are present in man and bacteria. Man, like other eukaryotes, expresses GS II while *M.tb*. like other prokaryotes express GS I [otherwise referred to as (MTB-GS)]. The modes of regulation of GS I and GS II are different.[88] Furthermore, pathogenic extracellular MTB-GS has been selectively inhibited by L-methionine-*S*-sulfoximine (MetSox) and by phosphinothricin. Hence, MTB-GS can be a therapeutic target.[85]

1.3.1. Structure and function of MTB-GS and GS II

MTB-GS is a very large enzyme consisting of 12 identical subunits of two face-to-face haxameric rings forming a dodecamer of mass 640 kDa.[91] Hydrogen bonding and hydrophobic interactions hold the dodecamer together. The junction between each pair of subunit forms an active site. There are thus 12 active sites and each of them is in the form of a bifunnel. The top of the bifunnel is the ATP binding site, while the bottom is the glutamate binding site. At the neck of the bifunnel are two divalent cation (Mn^{2+} or $Mg^{2+)}$ binding sites (referred to as n1 and n2, respectively) separated by 6Å. The n1 cation is essential in glutamate binding while the n2 cation is involved in phosphoryl transfer. The adenylylation loop is one of several loops with different functional importance resulting from the structure of the enzyme (Figure 5). [92] GS II exists as an 8-subunit oligomer[93] with a polypeptide chain of approximately 372 residues. Although there are similar residues in the active sites of GS I and GS II, performing similar functions, the adenylylation loop is absent in GS I.[88] Glutamine is

an essential source of nitrogen in the biosynthesis of many organic compounds, such as purines, pyrimidines and other amino acids in living systems. GS catalyzes the biosynthetic reaction (Scheme 1) that produces glutamine **52** as the product of the combination of glutamate **50** and ammonia in the presence of adenosine triphosphate (ATP). GS activity is dependent on the n2 cation. The coordination of the n2 cation with the γ-phosphate oxygens of ATP permits phosphoryl transfer to the γ-carboxylate group of glutamate leading to the formation of the γ-glutamyl phosphate intermediate **51**.[88] Glutamine **52** is formed when ammonia displaces the phosphoryl group as a free phosphate anion.[94]

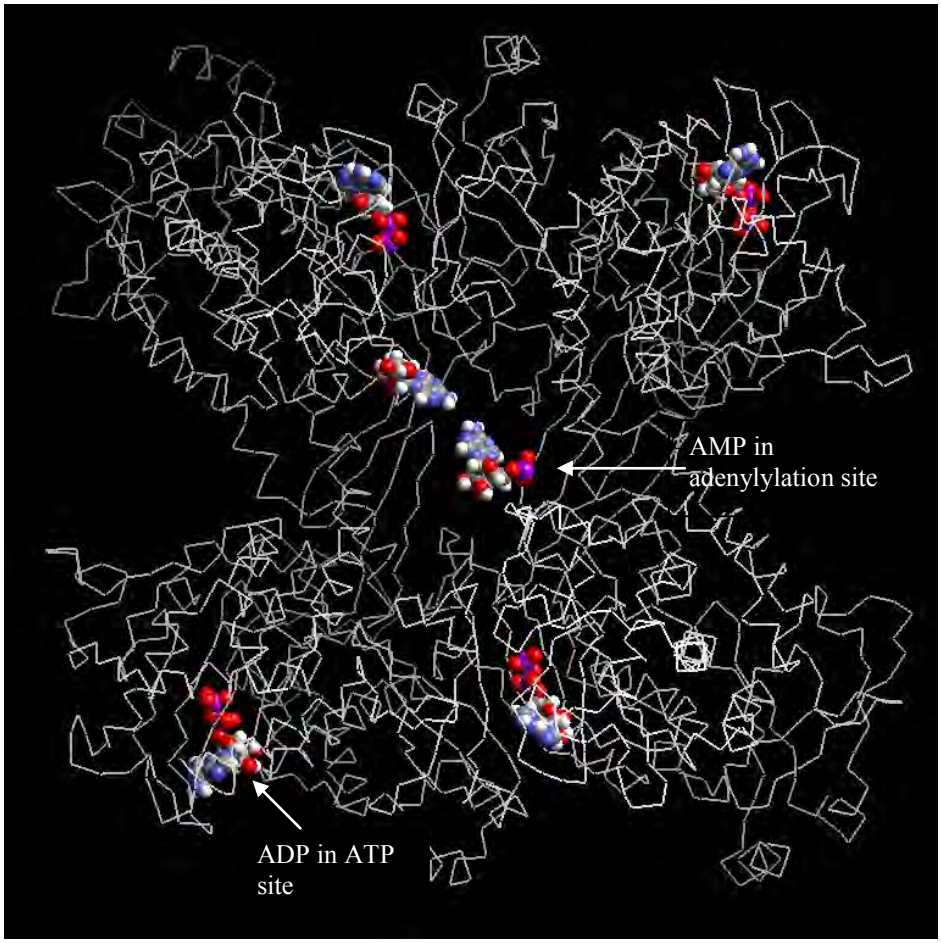

Figure 5. Trace display of reconstructed GS from *Salmonella typhimurium* downloaded from the PDB showing ADP in the ATP binding site and AMP in the adenylylation site. Downloaded at http://www.hort.purdue.edu/rhodcv/hort640c/ammonia/GSSt3D.htm

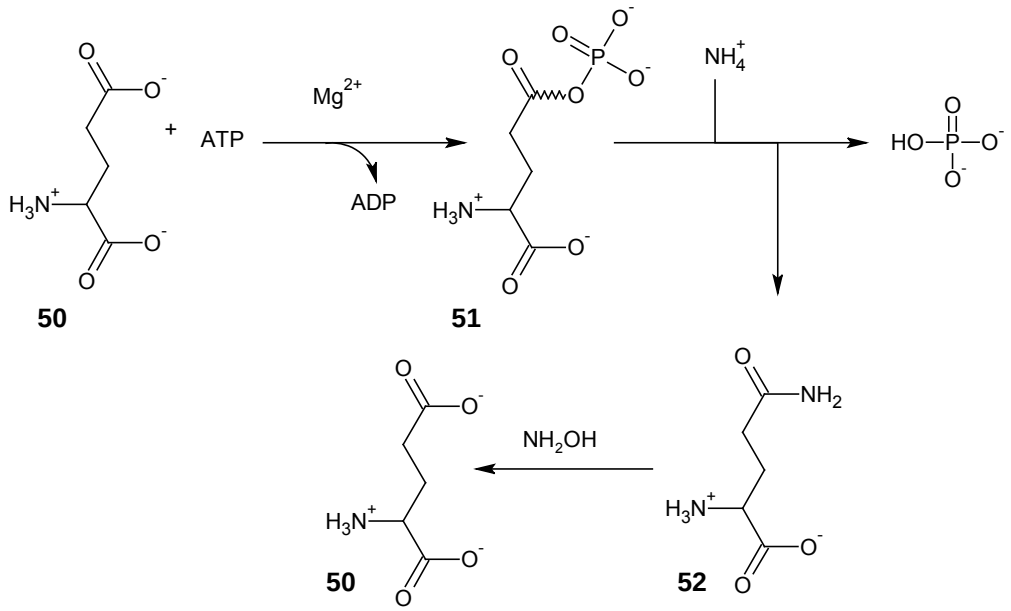

Scheme 1. Biosynthetic and transferase reactions

The transferase reaction is the reverse of the biosynthetic reaction, in which glutamine **52** is converted to γ-glutamylhydroxymate and ammonia in the presence of hydroxylamine.[88,95]

1.3.2. Regulation of MTB-GS: Feedback inhibition and covalent modification

Allosteric control or feedback inhibition[96,97] of MTB-GS occurs when there is sufficient glutamine in the system. A change in conformation at the relevant active site of the enzyme occurs so that other ligands, known as 'effectors', bind to the ATP and glutamate active sites.[96] Crystal structures of GS have revealed allosteric regulation by serine, glycine and alanine at the glutamate substrate site, while GDP, ADP and AMP bind allosterically to the ATP site.[88,98] MetSox **53** has been demonstrated to be a potent inhibitor of GS as it mimics glutamate and binds non-covalently but irreversibly with ATP at the glutamate binding site forming a tetrahedral intermediate.[88,99]

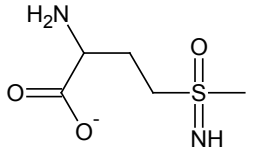

53

Covalent modification by adenylylation,[100,101,102,103] is another means of regulating the catalytic activity of GS I. An ATP dependent reaction, adenylylation, inactivates GS when ATP binds covalently to tyr[397] **54** on GS I as (AMP-*O*-Tyr[397]) **55** instead of the n1 metal ion in response to excess nitrogen in the cell (Figure 6). Each monomer on MTB-GS can be adenylylated and, as more sites are adenylylated, the catalytic activity of GS and the amount of glutamine produced both decrease. The reverse process, called deadenylylation, is the phosphorolytic removal of AMP as ADP. Both processes are catalyzed by adenylyl transferase **(AT)**.[104] Adenylylation does not occur in GS II due to the absence of the adenylylation loop.[88] Consequently, this mode of regulation of GS I represents a therapeutic target.[105] Efforts have been made to synthesize ATP mimics that will bind irreversibly to the relevant residues in the adenylylation site, preventing deadenylylation and the multiplication of mycobacterium in the host, which is man.

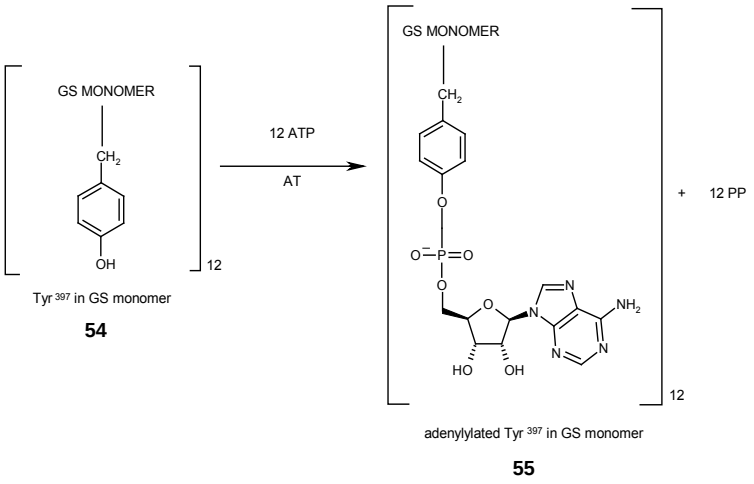

Figure 6. Covalent modification by adenylylation as a means or regulating MTB-GS.

Research has also shown the selective adenylylation of pathogenic MTB-GS in mixture of MTB-GS and nonpathogenic *mycobacterium bovis* (BCG) on addition of glutamine.[80] An enzymatic mechanism detailing the role of each residue in the bifunnel active site of GS during the biosynthetic reaction has been proposed and is summarized in Table 1.[88]

Table 1: A summary of the mechanism[88] of the biosynthetic reaction showing the role of each residue. Tyr^{397} is not in the bifunnel but lies in the adenylylation loop and is absent in GS II. Extracted from D. Eisenberg, H.S. Gill, G.M.U., Pfluegl, S.H. Rotstein, *Biochimica et Biophysica Acta*, 2000, **1477**, 122-145. Reproduced with permission from D. Eisenberg.

Residue	Role in enzymatic mechanism	Effector	Reference
Asp-50	Deprotonates ammonium substrate ion. Increases the affinity for ammonium binding	ADP	78, 106, 107
Ser-53	Increases intersubunit stability with Glu-327	ADP	78
Asp-64	Increases intersubunit stability with Arg-344	ADP	108
Glu-129	Coordinates the n2 ion and hydrogen bonds with His-271		78
Glu-131	Coordinates the amino group of glutamate and the n1 ion		78
Tyr-179	Coordinates the ammonium binding pocket		78, 106
Glu-212	Coordinates the ammonium binding pocket and the n1 ion		78
Glu 220	Coordinates the n1 ion		78
Asn-264	Coordinates the amino group of glutamate. Stabilizes the Glu-327 flap upon MetSox or PPT binding	Glu, Gln, Ser, Gly, Ala, Tl^+, PPT, MetSox	78, 109
Gly-265	Coordinates the amino group of glutamate.		78
His-269	Coordinates the n2 ion		110, 111
His-271	Coordinates the α-phosphate group of ADP/AMPPMP and Glu-129		108
Arg-321	Coordinates the carboxylate of glutamate		78
Glu-327	Stabilizes the tetrahedral adduct at the transition state. Accepts a proton from the adduct to form glutamine. Closes active site and shields intermediate from hydrolysis.	Ser, Tl^+, PPT, MetSox	112, 109, 78, 106, 107
Arg-339	Induces intersubunit stability by interacting with Asp-50	ADP	78
Arg-344	Coordinates the β-phosphate group of ADP/AMPPMP	ADP	78
Glu-357	Coordinates the n2 ion and Arg-344	ADP, AMPPMP	78
Arg-359	Coordinates the γ-phosphate group of glutamate		78
Tyr-397	**Adenylylation site (seen in bacterial GS only)**		113

1.4. The purine system

Many systems, of which ATP is one, containing the purine[114] backbone are biologically important. DNA and RNA, the "building blocks of life", are made of purine and pyrimidine bases.[115,116] Hormones and neurotransmitters are made up of nucleosides and nucleotides, while energy transfers occurring in many metabolic systems as well as intercellular signaling are a consequence of the interconversion of mono-, di- and triphosphate esters of nucleosides.[114] Pyrimidines **56** are six membered heterocycles with two nitrogen atoms while purines **57** are fused pyridine and imidazole heteroaromatic compounds with four nitrogen atoms.[114,117,118,119]

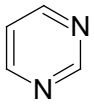

56

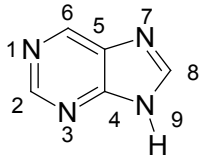

57

Purine **57** can alternate between the four tautomeric forms shown in Scheme 5. It exists in the 7-H tautomer in the crystalline state, while the 7-*H* and 9-*H* tautomers are predominant in solution.[120]

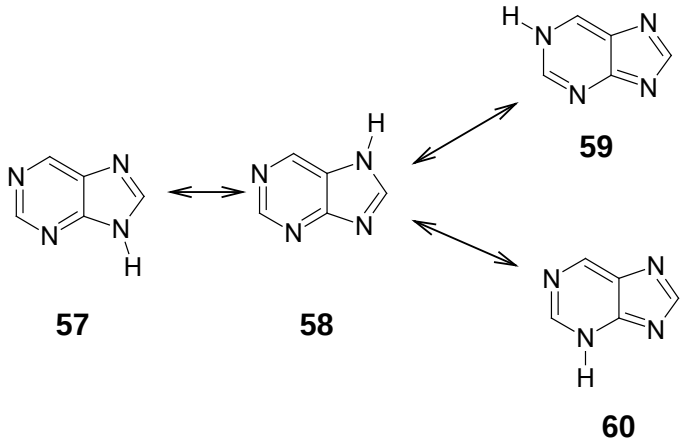

Scheme 2. Tautomerism in purine

Adenine **61**,[121] adenosine **62**[122] and adenosine triphosphate ATP **63**[123] are examples of aminopurines.

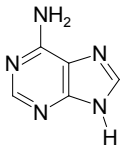

61

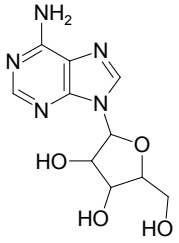

62

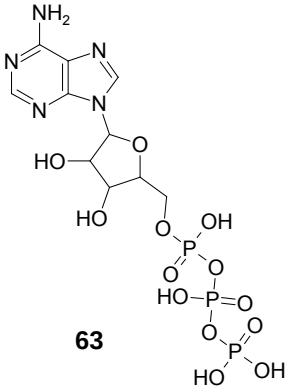

63

1.4.1. Adenine

Adenine **61** is a molecule of important biological significance as it is a constituent of RNA and DNA[114] as well as being an important component of ATP, a substance that is required to drive many biochemical reactions.[124]

1.4.1.1. Synthesis and reactions of adenine

Adenine **61** has been synthesized in 43% yield by treating formamide with $POCl_3$ at 120 °C in a closed vessel (Scheme3).[125]

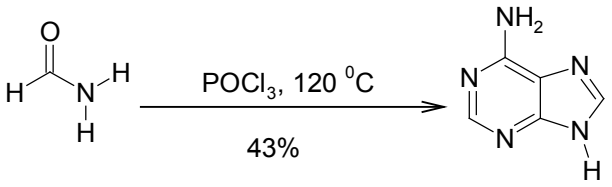

64 **61**

Scheme 3. Synthesis of adenine.

Alkylation and acylation can be carried out on the amino group on the pyrimidine ring as well as the nitrogen of the imidazole ring after deprotonation by a base. Synthesis of the diastereomeric acyclic nucleoside (**65a** and **65b)** and nucleotide (**74a** and **74b)** mimics have been reported according to schemes 4 and 5.[126] α,β-Methylfuranoside **67a** was obtained by methylating (+)-ribose with methanol in the presence of HCl. Tosylation of methylated ribose with tosyl chloride in pyridine at 4°C afforded the 5-tosylated derivative **68a** in 90% yield. In the presence of NaH, compound **68a** was

coupled to adenine under anhydrous conditions to afford compound **69a**. Oxidation of **69a** with sodium periodate at 4°C for one hour afforded the dialdehyde **70a** that was treated with aq. $NaBH_4$ to afford the target compound **65a** in 85% yield. Synthesis of the stereoisomeric analogue **65b** in 15-30% yield was achieved with (-)-ribose using the same approach.

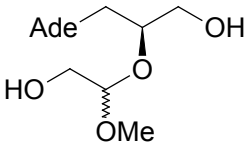

65a

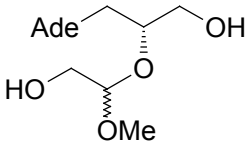

65b

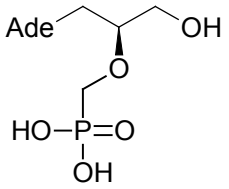

74a

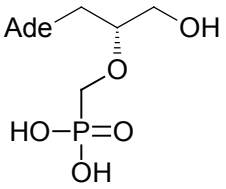

74b

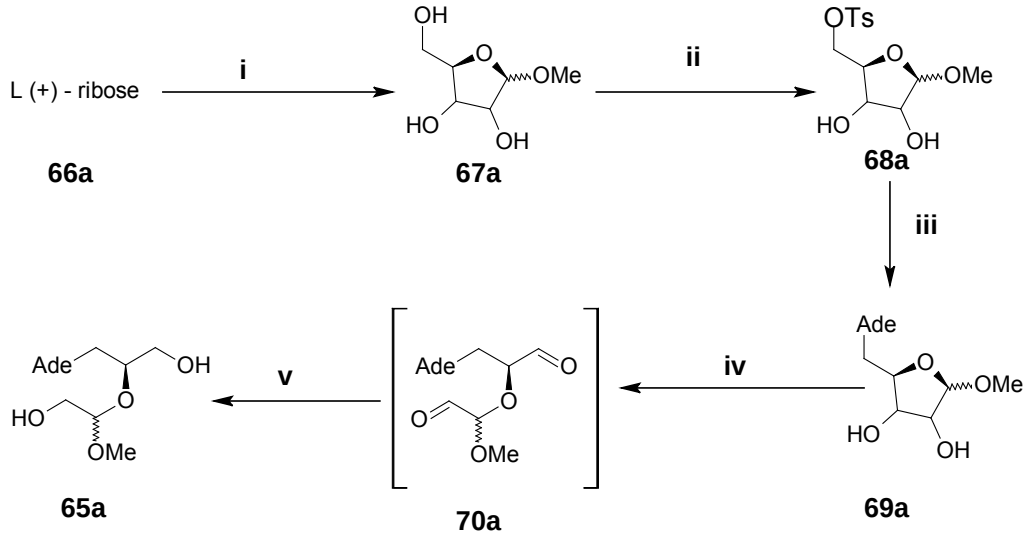

66a **67a** **68a** **69a** **70a** **65a**

Scheme 4. Synthesis of adenine nucleosides **65a**. Reagents and conditions: (i) AcCl/MeOH, rt, 16h; (ii) TsCl/Py, 4°C, 16h; (iii) Ade^-/DMF, 80°C, 5 days; (iv) $NaIO_4$, 4°C, 1h; (v) $NaBH_4$, 4°C, 3h.

The nucleotide **74b** was made from the nucleoside **65b**. Treatement of **65b** with 60% formic acid or Dowex 50 (H^+) afforded (*R*)-DHPA **71b**. The iodomethylphosphonate **72b** was obtained in 35% yield by reacting **71b** with 1.5 eq. of iodomethylphosphonic acid in the presence of DCC in pyridine. Intramolecular cyclisation of the iodomethylphosphonate to afford intermediate **73b** was achieved by treating **72b** with 5 eq. of NaH in DMF. Hydrolysis did afford pure **73b**; however, the nucleotide (*R*)-*cyclo*-HPMPA **74b** was isolated in 90% yield after treating crude **73b** with glacial acetic acid for 3 h. The corresponding (*S*)-DHPA **71a** was made from nucleoside **65a** affording access to (*S*)-*cyclo*-HPMPA **74a**.[126]

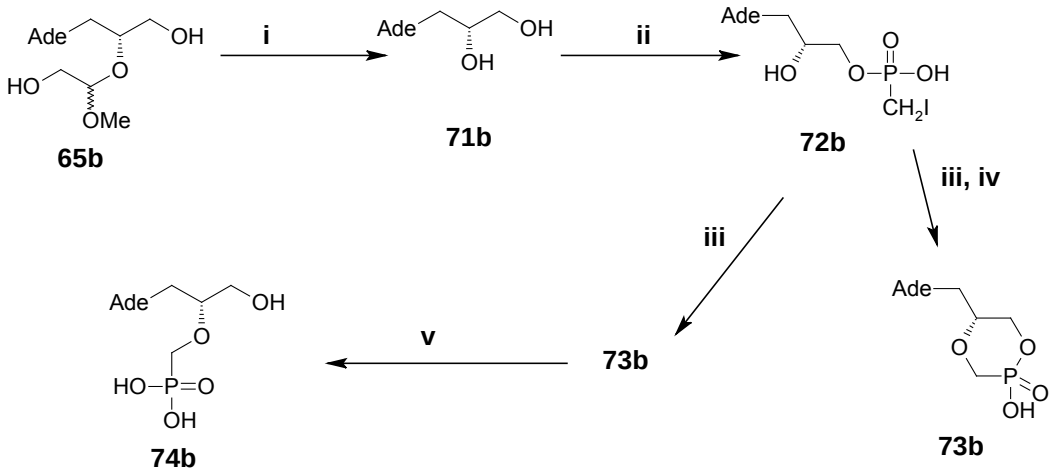

Scheme 5. Synthesis of adenine nucleosides **74a** and **74b**. Reagents and conditions: (i) H^+, 6h; (ii) $ICH_2P(O)(OH)_2$/DCC/Py, 16h; (iii) NaH/DMF,6h; (iv) H_2O, 3 h; (v) glacial AcOH, 3h.

1.4.2. Adenosine

Adenosine is a nucleoside with a ribose sugar attached to the imidazole ring *via* an *N*-glycosidic bond.[127]A molecule of great biological significance,[128] adenosine exerts different physiological effects on the nervous, immune and cardiovascular systems by activating A_1, A_{2A}, A_{2B}, and A_3 receptors. Hence, heart muscles, platelets as well as coronary arteries depend on adenosine for their proper function. Adenosine prevents aggregation of platelets and modulates the immunity of the cell, through interaction with A_{2A} receptors.[129,130] Research on blood cells has shown that adenosine and its

mimics may have a number of important roles, such as : (i) regulating nor mal immune responses; (ii) acting as anti-inflammatory and endogenous anti-aggregatory agents and (ii) as therapeutics.[129,130] Research has also shown that adenosine, as a neurotransmitter, stimulates A_1 receptors in the brain thereby inducing sleep. Interestingly, sleep time is decreased when coffee is consumed because blockage of the central adenosine receptors is effected by the methylxanthines in coffee.[131]

In the calf adenosine deamination reaction, adenosine is converted to inosine **76** (Scheme 6) *via the* hemi-aminal. Enzyme-catalysed reactions such as the deamination reaction proceed very rapidly in the active site of the enzyme.[132] However, transition-state mimics bind more strongly to the active site of the enzyme forming structurally and chemically similar structures to the transition state. Such stable intermediates provide information on the design of better inhibitors,[132,133] and are thus are very important in the mechanistic approach to drug discovery.

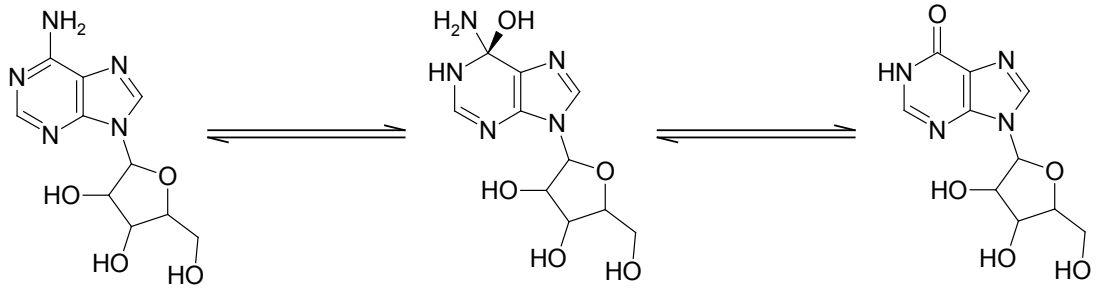

62 **75** **76**

Scheme 6. The calf adenosine deamination reaction.

Nucleosides such as adenosine have been synthesized by various routes.[134,135,136,137] Stemming from the therapeutic properties of natural hexopyranosyl nuclosides, the synthesis of ring- expanded mimics of adenosine has afforded many compounds with antiviral and anticancer activity. The asymmetric synthesis of the nucleoside **84** was recently reported[138] by researchers at West Virginia University, USA (Scheme 7). The synthesis commenced by protecting the two hydroxyl groups on commercially available furfuryl alcohol in a two-step reaction to afford the Boc-protected pyranone **77**.[139,140] The protected alcohol was then coupled to 6-chloropurine **78** in the presence of a palladium catalyst to afford the glycosylated 6-chloropurine pyranone 7**9** in 86%

yield. The alcohol **80** was obtained by exposing the pyranone **79** to $NaBH_4$ at -78 °C. Conversion of the alcohol to the olefin **81** was achieved with the reagent system (NBSH, PPh_3/DEAD, NMM). The diol **82** was obtained enantioselectively by dihydroxylating the olefin **81** with (OsO_4/NMO). Treatment of the diol **82** with ammonia at room temperature gave the amino derivative **83**. The desired hexopyranosyl nucleoside **84** was finally obtained in 94% yield by deprotection of the diol with TBAF at room temperature. This procedure can be extended to the synthesis of other compounds such as adenosine.

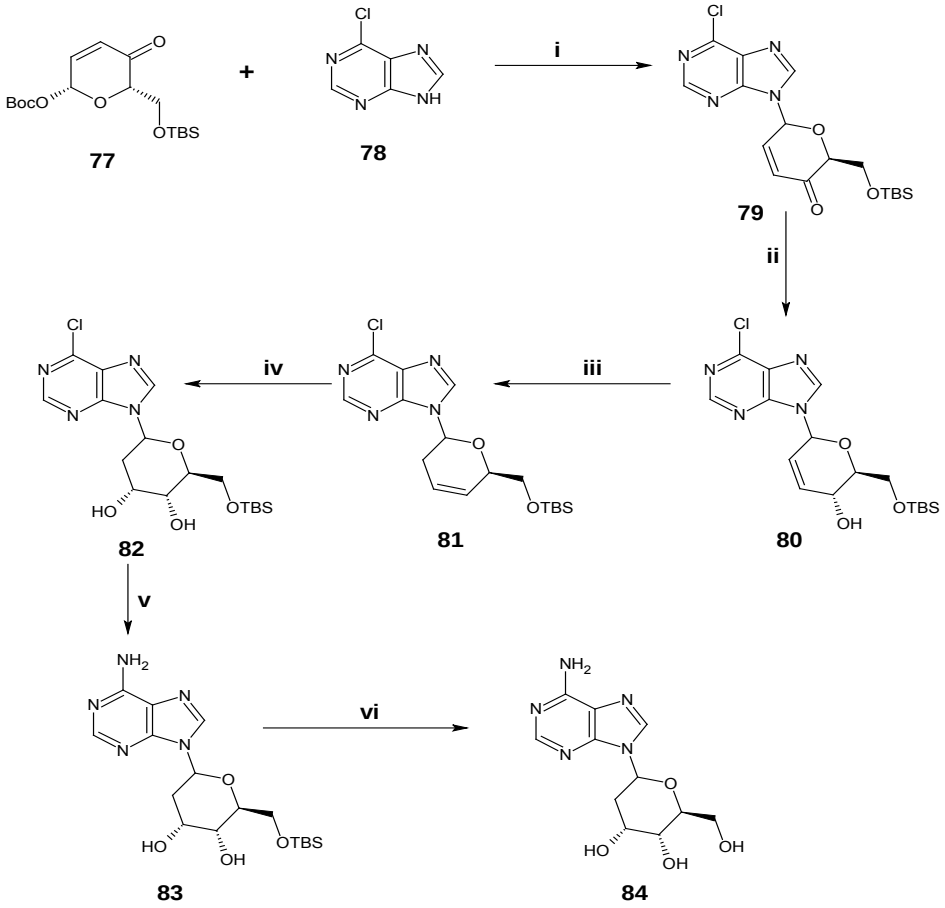

Scheme 7. Synthesis of the hexopyranosyl nucleoside **84** : (i) 0.5% $Pd_2(dba)_3.CHCl_3$, 2.5%PPh_3, THF, 0 °C, 86%; (ii) $NaBH_4$, MeOH/CH_2Cl_2, -78 C; (iii) NBSH, PPh_3, DEAD, NMM, -30 C; (iv) OsO_4, NMO, 95%; (v) NH_3, MeOH, 77%; (vi) TBAF, THF, rt, 94%.

1.4.3. Adenosine triphosphate ATP

Adenosine triphosphate **63**[81,82,83,84] consists of an adenine base, a ribose sugar and a phosphoryl ester group (Figure 7). The adenine base in ATP is linked to the ribose

sugar *via* a glycosidic bond which, in turn, is linked to phosphate groups through a phosphoester linkage. The phosphate groups are linked by phosphoanhydride linkages.[123]

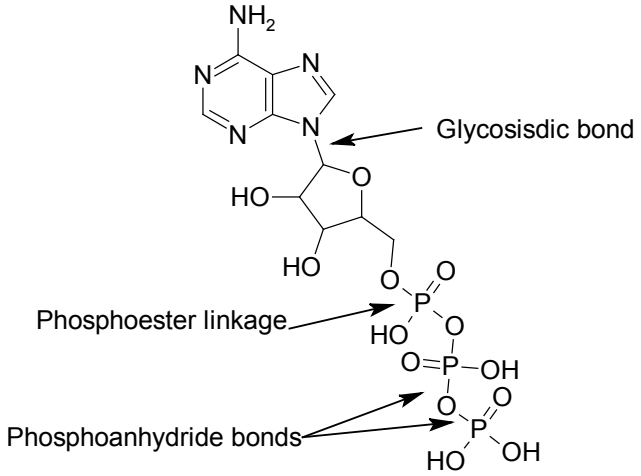

63

Figure 7. Adenosine triphosphate showing the glycosidic, phosphoester and phosphoanhydride linkages.

ATP **63** is a nucleotide formed (Scheme 8) as a result of the successive addition of phosphate groups to adenosine monophosphate (AMP) **85.** AMP is itself the produced by the esterification of adenosine **62** with phosphoric acid (Scheme 8).[141]

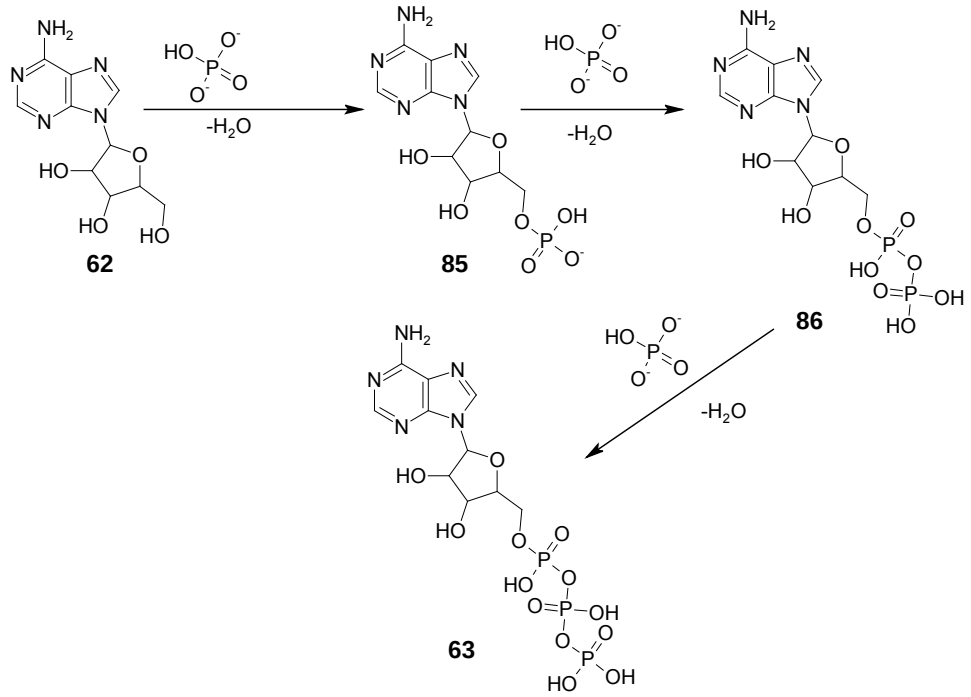

Scheme 8. Synthesis of ATP.

ATP is one of the most important molecules in living systems. Referred to as "energy currency", the energy released from hydrolysis of ATP is used to drive many biochemical reactions that are otherwise not thermodynamically feasible. ATP plays a very important role in mediating endergonic anabolic and exergonic catabolic processes as shown in Figure 8.[142]

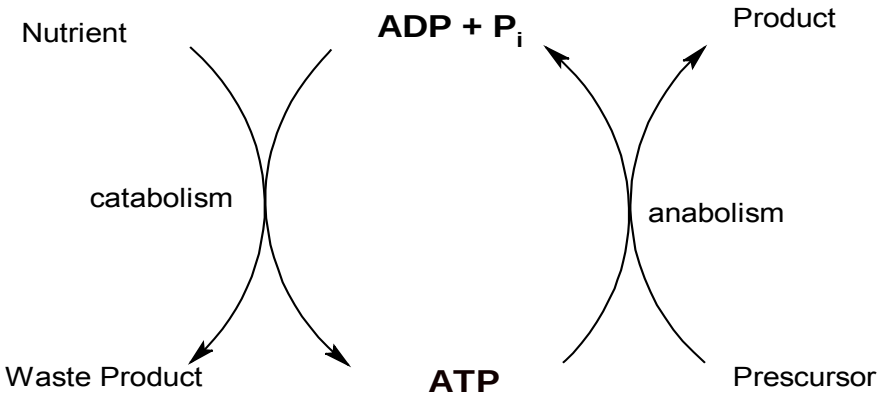

Figure 8. Coordination of anabolic and catabolic processes by ATP.

ATP is able to drive many of these biochemical reactions because of the high negative free energy that accompanies its hydrolysis. Hydrolysis of ATP is a spontaneous reaction since ATP is less stable than the hydrolysis products, adenosine diphosphate (ADP) and free phosphate which exert mutual electrostatic repulsion as a result of both being negatively charged; the terminal phosphoryl group in ATP is not resonance-stabilized as effectively as the inorganic free phosphate anion (Figure 9).[142]

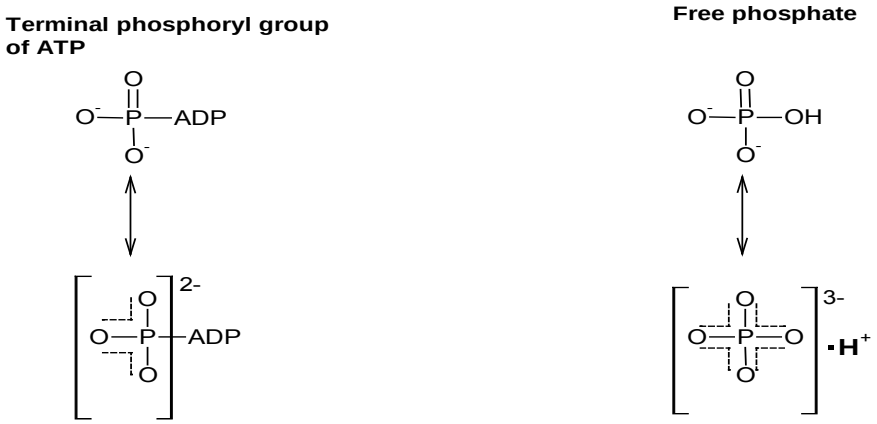

Figure 9. Resonance stabilisation of the terminal phosphoryl group in ATP and free inorganic phosphate.

1,3,7-Trimethylxanthine (caffeine) **87** and theobromine **88** are natural stimulants present in coffee and chocolate respectively. Synthetically, both natural products may be obtained by methylating xanthine with a reagent like methyl iodide.[143]

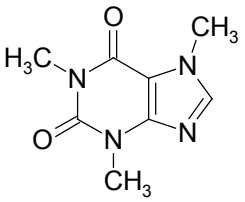

87

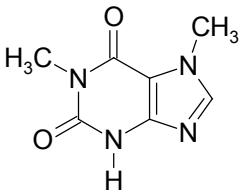

88

However, a more complicated methylation process is involved *in vivo*. Each of the phosphate groups and the methylene carbon of the sugar moiety in ATP can be attacked by hard and soft nucleophiles, respectively. A typical biochemical reaction in living systems is the nucleophilic attack by the amino acid methionine **89** to form *S*-adenosyl methionine (SAM) **90** (Scheme 9) in an S_N2 displacement[144] of the triphosphate moiety. SAM is a highly reactive methylating agent and, in plants, caffeine **88** is produced by SAM-mediated methylation of theobromine **88** (Scheme 10).[144]

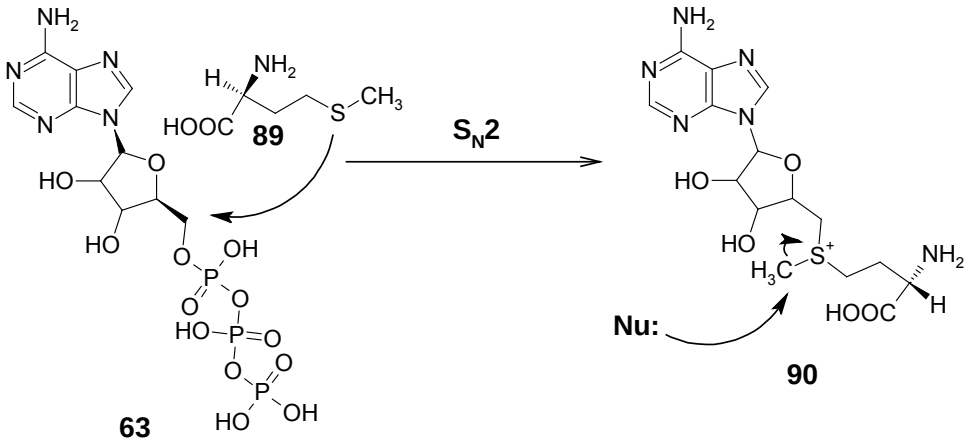

Scheme 9. Methylation of ATP by methionine

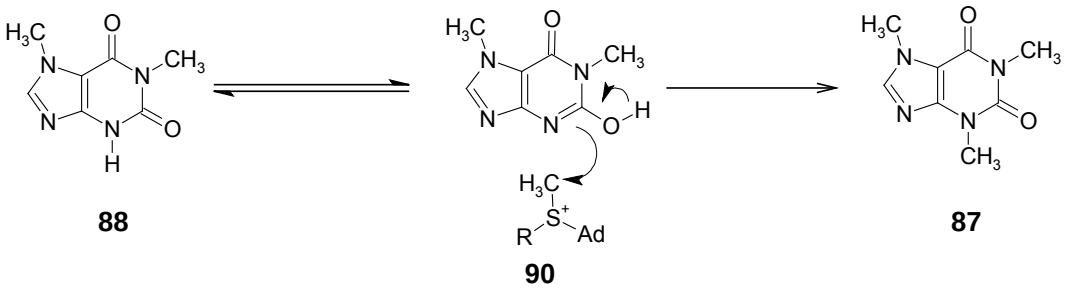

88 **90** **87**

Scheme 10. Formation of caffeine *via* methylation of theobromine by SAM

1.4.4. Other purine systems

1.4.4.1. Medicinal uses of purine systems

Purine systems with medicinal potential include: - (i) dideoxyinosine (DDI) **91**, a therapeutic agent for AIDS; (ii) acyclovir **92**, an antiviral agent for *Herpes*; and (iii) 6-mercaptopurine **93** that is administered to cancer and leukemia patients.[145]

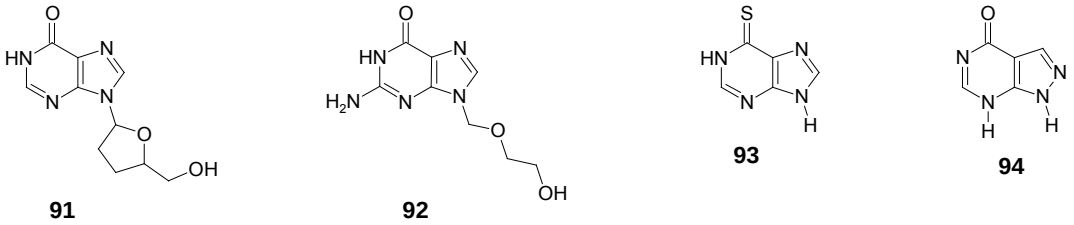

91 **92** **93** **94**

Allopurinol **94** is used for patients afflicted with gout,[146] while Sildenafil[146] (Viagra^{TM}) **95** is an effective therapeutic for impotence. Oxanosine **96** and tubercidin **97** are natural products, obtained from *Streptomyces*, and are used for treating cancerous and bacterial infections.[146]

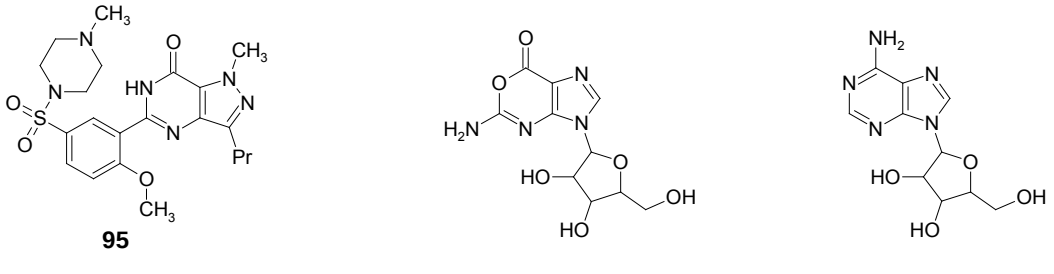

95 **96** **97**

1.4.4.2. Synthesis of purine systems

Various routes to purine derivatives have been developed. In the Traube synthesis, 8-substituted purines **100** can be obtained from di-aminopyrimidines **98** and an appropriate acylating agent as shown in Scheme 11.[147,148] The reaction proceeds *via* the amide **99** that is isolable.

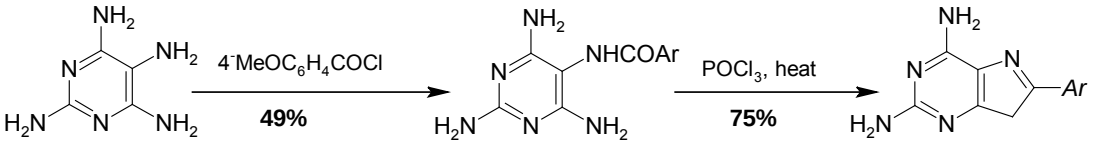

98 **99** **100**

Scheme 11. Synthesis of 8-substituted purines.

The 8,9-dimethylated xanthine derivative **104** has been synthesized successfully from the 5-aminoimidazole **102** that was generated *in situ* as outlined in Scheme 12.[149]

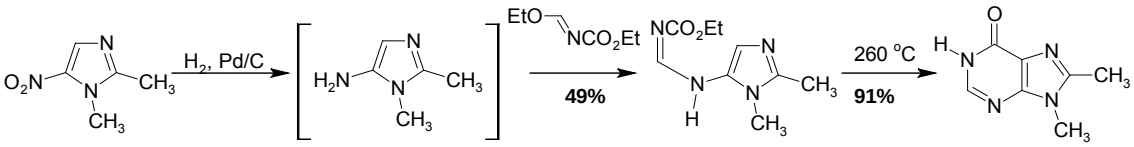

101 **102** **103** **104**

Scheme 12. Synthesis of dimethylated xanthine.

It is also possible to synthesize purines from the corresponding pyrimidine and imidazole derivatives in a cycloadditon reaction as outlined in Scheme 13.[150]

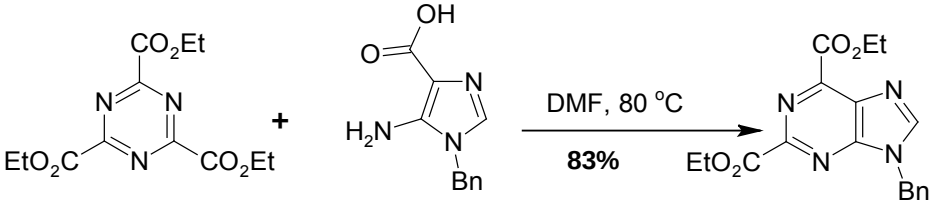

105 **106** **107**

Scheme 13. Synthesis of purines from pyrimidines and imidazoles.

1.4.4.3. Synthesis of Viagra

The pyrazole precursor **109** used in the synthesis of Viagra (Scheme 14) can be obtained by treating the ester **108** with aq. haydrazine. Methylation at the *N*-1 nitrogen followed by nitration then affords the intermediate **111** the pyrazole equivalent of 5-aminoimidazole-4-carboxylic acid (AICA) derivatives which are the starting materials for the synthesis of purines from imidazole. Reduction of the nitro group in the intermediate amide **112** and treatment of the resulting amine **113** with an aromatic acid chloride affords the amide **114**. Hydrolysis and cyclisation affords compound **115,** which on treatment with chlorosulphonic acid and *N*-methylpiperazine affords Viagra **95.**[151]

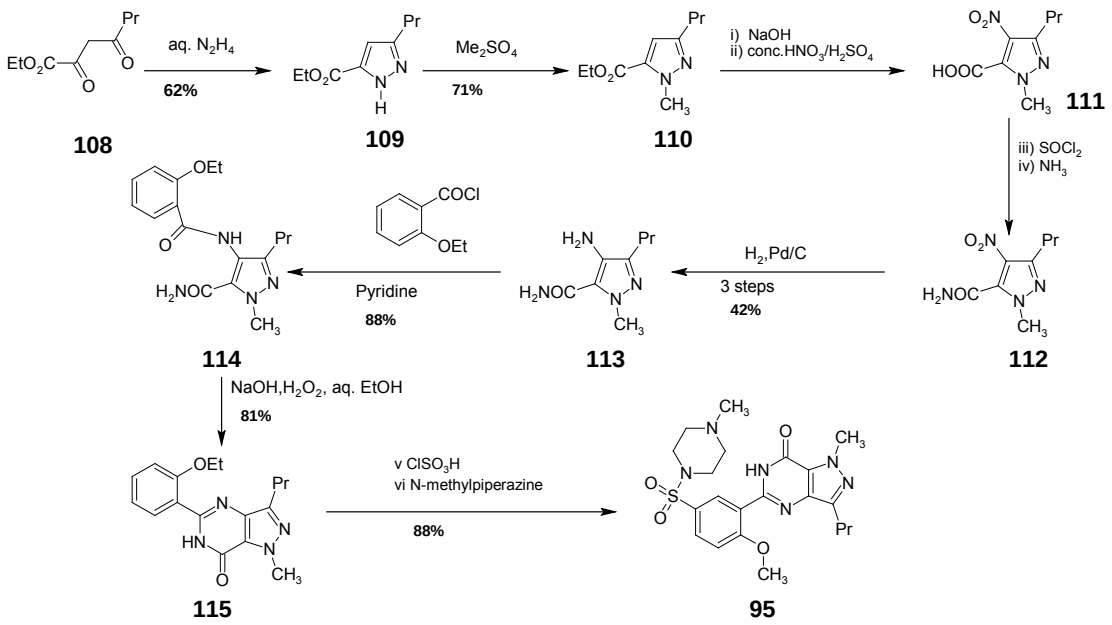

Scheme 14. Synthesis of Viagra.

1.4.4.4. Reactions of purine systems

Alkylation of the nitrogen atoms in both the pyrimidine and imidazole moieties is possible. Thus the 7,9-dimethylpurinium salt **116** is the product of the reaction between purine **56** and iodomethane (Scheme 15).[152]

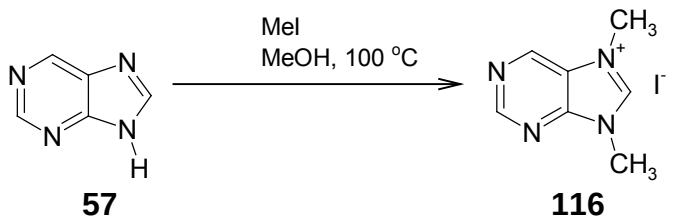

Scheme 15. Alkylation at nitrogen atoms in the imidazole ring of purine.

A mixture of 3,6-dimethylpurine and 6,9-dimethylpurine is obtained on methylating 6-methylpurine with dimethyl sulfate in alcoholic KOH (Scheme 16).[153]

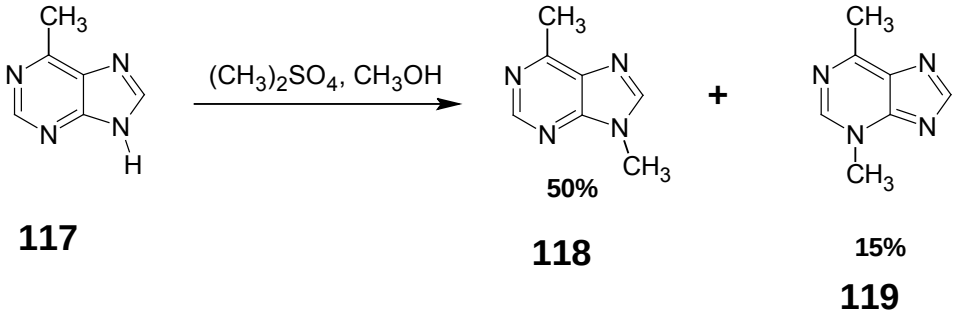

Scheme 16. Alkylation of nitrogen atoms in the pyrimidine and imidazole rings of purine.

Both the 7- and 9- substituted products (**121** and **122** respectively) are produced in basic solution when 6-chloropurine is alkylated with a benzyl halide.[154] However, substitution at *N*-9 (compound **123**) results from the reaction of 6-chloropurine with a dihydrofuran-derived carbocation (Scheme 17).[155]

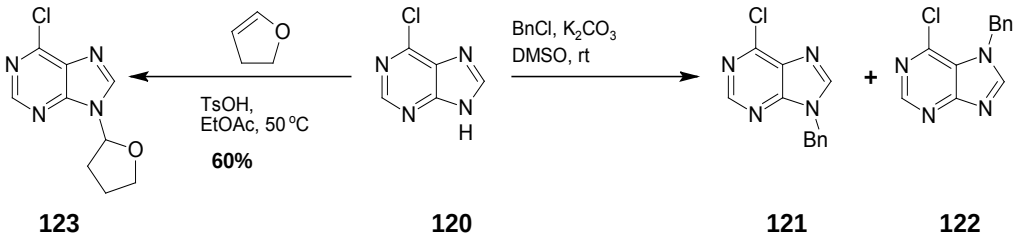

Scheme 17. Substitution at the 7- and 9- position in 6-chloropurine.

Reductive alkylation of adenine with formaldehyde (Scheme 18)[156] yields the monomethylated substitution product while treatment of adenine with the Mannich

product formed from the reaction of formaldehyde with morpholine (Scheme 19) affords the dimethylated derivative.[157]

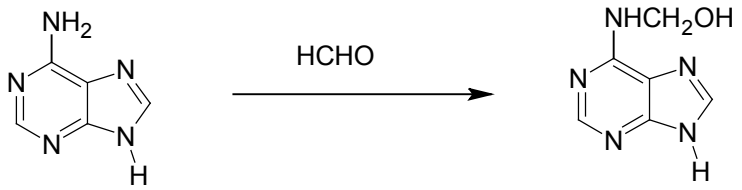

61 **124**

Scheme 18. Alkylation of adenine at the NH_2 position with HCHO

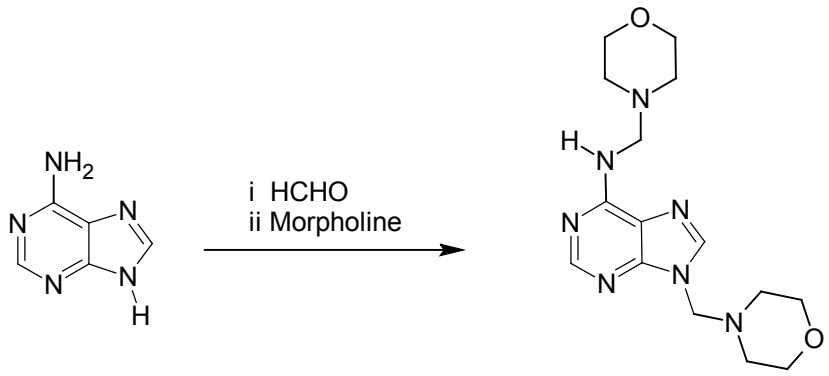

61 **125**

Scheme 19. Alkylation of adenine at the NH_2 position with Mannich product from morpholine and HCHO.

1.5. Aims of this research

With a detailed knowledge of the role of glutamine synthetase in pathogenic *Mycobacterium* tuberculosis,[75,76,77] our goal has been to prepare novel ATP mimics that will bind to the active site of MTB-GS, thereby inhibiting normal enzymatic function. In general we have focused on establishing access to a series of structural scaffolds and, in some cases, their elaboration to potential ATP mimics.

More specifically, the research has involved: -

(i) the synthesis and characterization of novel adenosine-, adenine- and allopurinol- based and truncated adenine derivatives;

(ii) the application of C-13 NMR shift prediction programmes to confirm experimental assignments; and

(iii) a study of the conformational preferences and receptor docking of potential ATP mimics into the MTB-GS active site using the ACCELERYS Cerius^2 platform.

2. DISCUSSION

The discussion will be focused on: - the syntheses of novel adenosine derivatives (**Section 2.1**), adenine derivatives (**Section 2.2**), allopurinol and Baylis-Hillman electrophiles (**Section 2.3**) and truncated systems (**Section 2.4**) as novel ATP analogues; the application of NMR prediction programme to confirm experimental data assignments (**Section 2.5**); computer modelling and docking of selected compounds into the GS active site (**Section 2.6**) and conclusions (**Section 2.7**)

ATP **63** comprises three parts: an adenine base, a ribose sugar and a phosphoryl ester group.[158,159] In our approach, each of these parts was altered in attempts to access a range of compounds as potential ATP mimics.

Adenosine triphosphate ATP

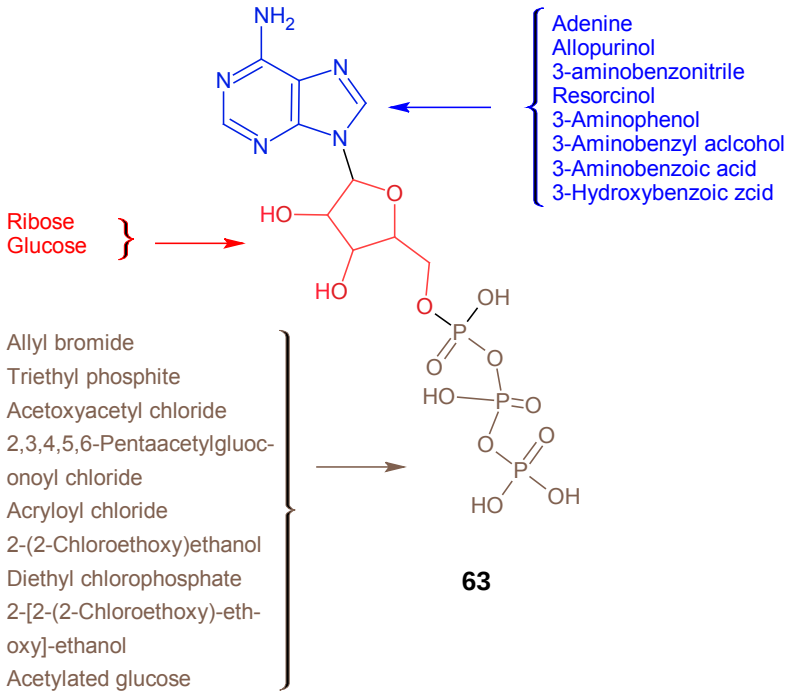

Figure 10. ATP with proposed moieties for derivatives.

2.1. Novel ATP analogues from adenosine

The method employed was to replace the primary hydroxyl hydrogen of adenosine with various groups through acylation and alkylation reactions (Figure 11).

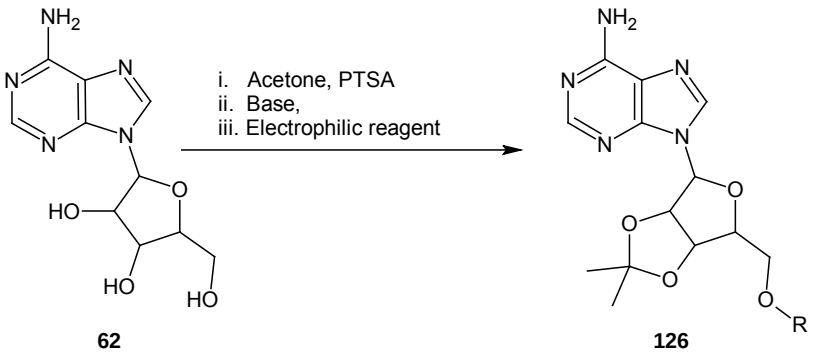

62 **126**

Figure 11. General approach for the synthesis of adenosine derivatives.

There are three hydroxyl groups on the ribose ring of adenosine and, although the primary hydroxyl group is more susceptible to acylation and alkylation, competition from the two secondary hydroxyl groups cannot be ruled out. However, the 1,2-dihydroxy groups can be selectively protected as a cyclic acetal. Acetals are not difficult to make, they are stable compounds and their removal does not generally pose any difficulty.[160] Protection of the vicinal 1,2-diol was successfully achieved by treating adenosine with acetone in the presence of an acid catalyst[161] following previous work in our research group by Hall.[162] The method involved stirring adenosine **62** in dry acetone in the presence of *para*-toluenesulfonic acid monohydrate as catalyst[163] at room temperature overnight to produce adenosine 3',4'-acetonide **127** in 93% yield (Scheme 20). The structure of the acetal obtained was confirmed by NMR and low- resolution mass spectroscopy. The two acetonide methyl singlets were observed at 1.22 and 1.38 ppm respectively in the ^{1}H NMR spectrum (Figure 12); while the quaternary carbon of the acetal was found to resonate at 114.0 ppm in the ^{13}C NMR spectrum (Figure 13).

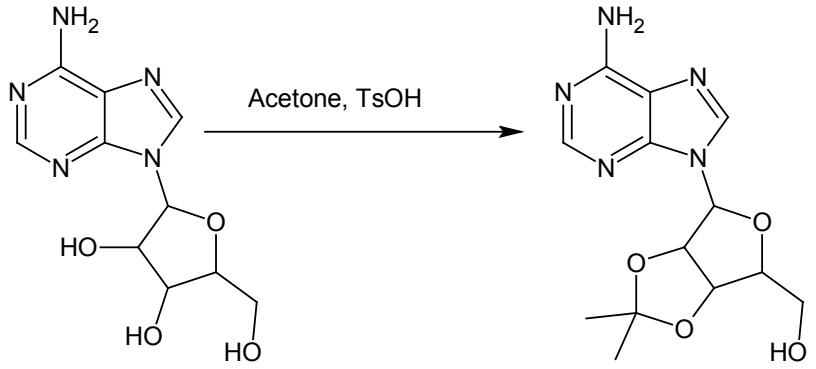

62 **127**

Scheme 20. Protection of adenosine with acetone.

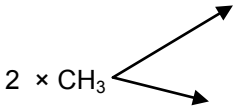

Figure 12. 400 MHz ^{1}H NMR spectrum of adenosine 3',4'-acetonide **127** in $CDCl_3$.

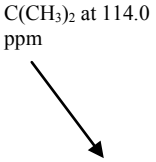

Figure 13. 100 MHz ^{13}C NMR spectrum of adenosine 3',4'-acetonide **127** in $CDCl_3$.

With the acetonide **127** in hand, a number of novel adenosine derivatives were synthesized in low to moderate yields by treating adenosine 3',4'-acetonide **127** with different alkylating and acylating agents[164] following deprotonation of the primary hydroxyl group using either NaH or BuLi. These reactions afforded a set of primary substitution products which could then be elaborated further (Figure 14). In a number of cases the acylating agent had to be specially prepared.

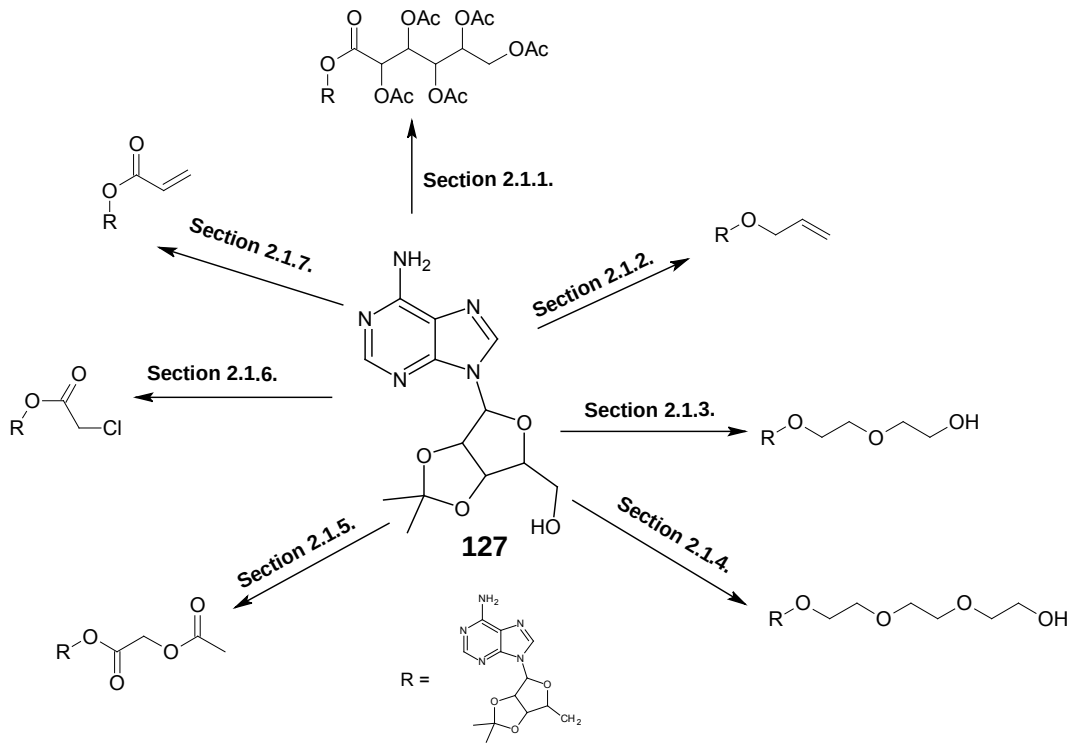

Figure 14. Routes to adenosine derivatives.

2.1.1. Preparation of 2-(6-aminopurin-9-yl)-3,4-dihydroxy-5-[(2,3,4,5,6–penta-acetoxyhexanoyloxy)methyl]tetrahydrofuran 3,4-acetonide 132

The route to the pentaacetoxy derivative **132** is shown in Scheme 21. The required acylating agent, 2,3,4,5,6-pentaacetylgluconoyl chloride **131**, was synthesized by stepwise acetylation[165] of the primary and secondary hydroxyl groups in D-gluconolactone **128**. In the first step, the lactone **128** was treated with acetic anhydride in the presence of $ZnCl_2$ catalyst followed by hydrolysis with ice-water to open the lactone ring. In the second step, 2,3,4,6-tetraacetylgluconic acid **129**[165] was treated with the same reagent and catalyst to afford 2,3,4,5,6-pentaacetylgluconic acid **130**. Pentacetylation was confirmed by the series of signals integrating for the 15 acetyl protons in the ^{1}H NMR spectrum and 5 methyl signals and 6 carbonyl carbon signals in the ^{13}C NMR spectrum. An initial attempt to make the acid chloride[165] **131** by stirring 2,3,4,5,6-pentaacetylgluconic acid **130** with PCl_5 in diethyl ether at room temperature was unsuccessful. However, 2,3,4,5,6-pentaacetylgluconoyl chloride **131** precipitated out as a white solid in 50% yield on stirring 2,3,4,5,6-pentaacetylgluconic acid **130** with oxalyl chloride[166] under nitrogen at room temperature for *ca.* 0.5 h. 2,3,4,5,6-D-pentaacetylgluconic acid **130** melted at 142-144°C while the acid chloride

131 melted at 41-42°C. The adenosine acetonide **127** was treated immediately with the acid chloride **131,** using pyridine as both solvent and base[167,168] to obtain 2-(6-aminopurin-1-yl)-3,4-dihydroxy-5-[(2,3,4,5,6-pentaacetoxyhexanoyloxy)methyl]tetra-hydrofuran 3,4-acetonide **132** as a yellow oil in 10% yield. Evidence for the formation of compound **132** was largely provided by NMR, mid-IR and mass spectrometric data.

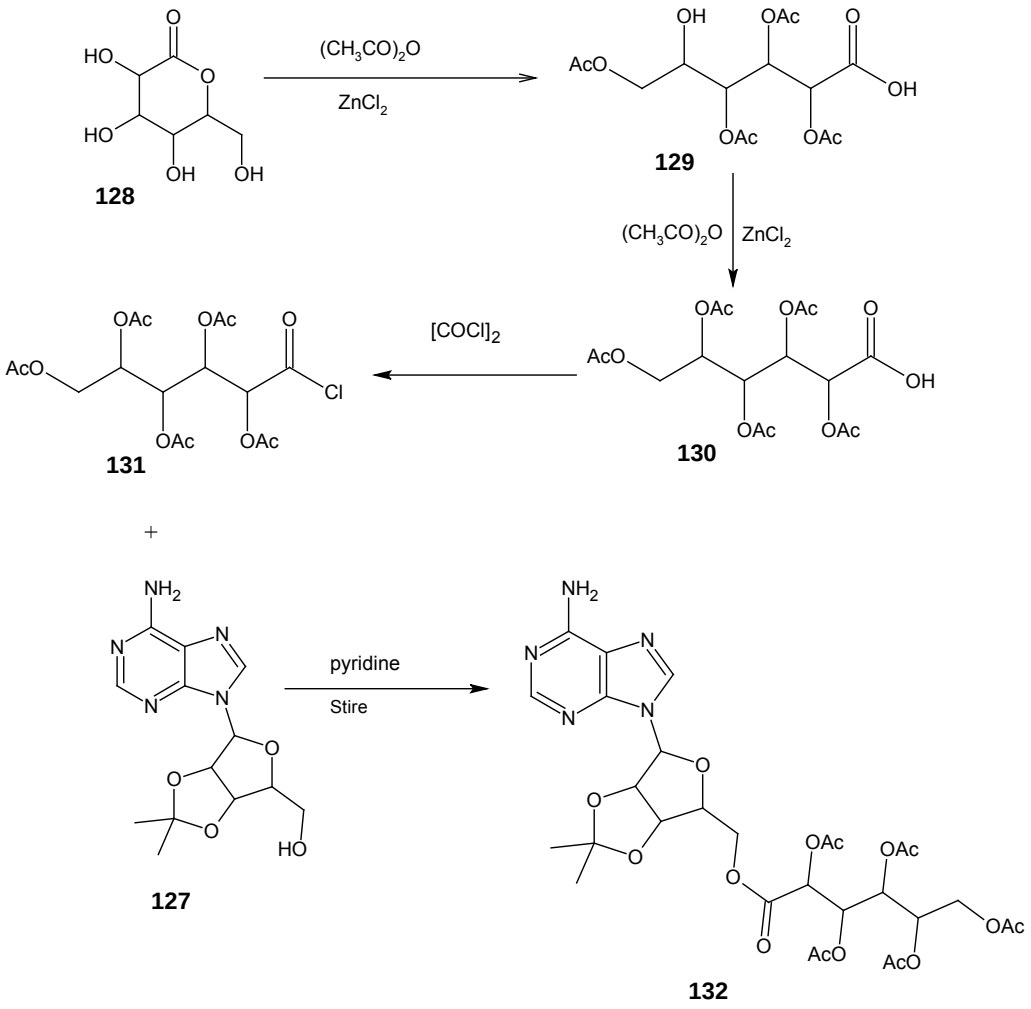

Scheme 21. Synthesis of the acetylated derivative **132**.

The amino nitrogen on the adenine ring was clearly not acylated in the isolated product as the NH_2 proton signal integrates for 2 protons at 5.88 ppm in the ^1H NMR spectrum (Figure 15). There is also no correlation between NH and gluconoyl C=O (C-1") in the HMBC spectrum (Figure 16).

Figure 15. 400 MHz ^{1}H NMR spectrum of the acetylated derivative **132** in $CDCl_3$.

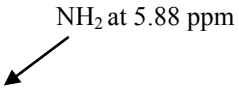

Figure 16. HMBC NMR spectrum of the acetylated derivative **132** in $CDCl_3$ showing the absence of any correlation between NH_2 and C-1".

2.1.2. Preparation of 2-(6-aminopurin-1-yl)-3,4-dihydroxy-5-[(allyloxy)methyl]-tetrahydrofuran 3,4-acetonide 133

The *O*-allylated derivative **133** was expected to provide access to the diol **134** and the bis-phosphorylated derivative **136** as outlined in Scheme 22. On treating the acetonide **127** with NaH and allyl bromide[169] in refluxing THF, the allylated derivative **133** was obtained in 9% yield. In the ^{1}H NMR spectrum (Figure 17), the 1"-methylene protons resonate as a pa ir of doublets at *ca.* 4 ppm; while the vinylic methylene protons resonate as overlapping multiplets at *ca.* 5.78 ppm, each of the allylic protons resonates as a dd (CH_a at 4.98 ppm and CH_b at 5.29 ppm respectively).

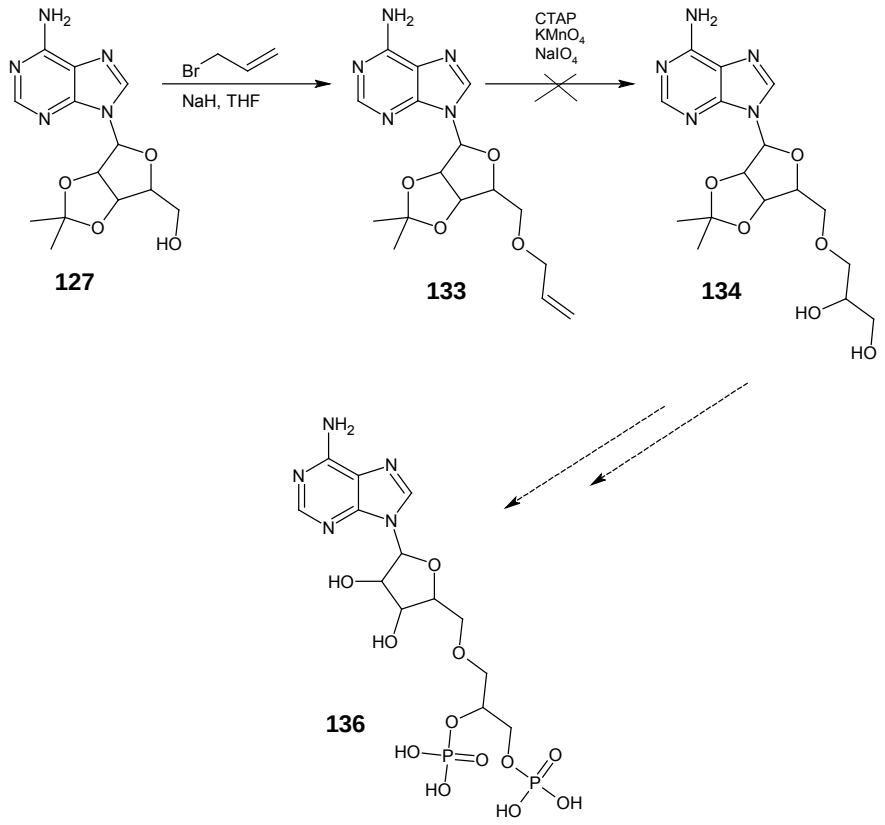

Scheme 22. Proposed route to the nucleotide **136**.

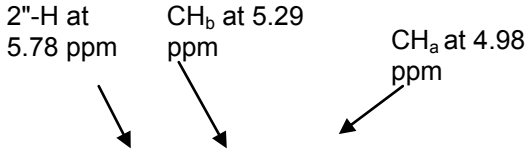

Figure 17. 400 MHz ^{1}H NMR spectrum of the allylated derivative **133** in $CDCl_3$.

Attempts to improve the efficiency of this reaction were made using different reaction conditions; the highest yield was 24% (Table 2). Unfortunately, attempts at dihydroxylating the allylated derivative **133** with various reagents including $NaIO_4$ in the presence of $RuCl_3$[170] catalyst, $KMnO_4$[171,172,173] and CTAP[173,174] were unsuccessful.

Table 2. Yields of the allylated derivative **134** under various reaction conditions.

Conc. of **134**/[M]	Solvent	Base	% Yield
0.5	THF	NaH	9.0
0.1	THF	NaH	21
0.01	THF	NaH	24
0.5	Pyridine	NaH	9.2
0.5	THF	Na	7.2
0.5	DMF	NaH	3.5
0.03	Acetone	K_2CO_3[175]	0.0

2.1.3. Preparation of 2-(6-aminopurin-9-yl)-3,4-dihydroxy-5-(7-hydroxy-2,5-dioxaheptyl)tetrahydrofuran 3,4-acetonide 137 and 2-(6-aminopurin-9-yl)-5[7-diethylphosphoryoxy)-2,5-dioxaheptyl]-3,4-dihydroxytetrahydrofuran 3,4-acetonide 138

The deprotonated acetonide **127** was alkylated[169] with 2-(2-chloroethoxy)ethanol in refluxing THF to afford 2-(6-aminopurin-9-yl)-3,4-dihydroxy-5-(7-hydroxy-2,5-dioxaheptyl)tetrahydrofuran 3,4-acetonide **137** in 72% yield (Scheme 23). In the ^{1}H NMR spectrum (Figure 18), the methylene protons (7", 6", 4", 3" and 1"-H_a) resonate as a series of multiplets at *ca.* 3.6-3.8 ppm. FAB mass spectrometric analysis showed the presence of the M+1 peak at *m/z* 396 with an intensity of 3% relative to the base peak at *m/z* 136.

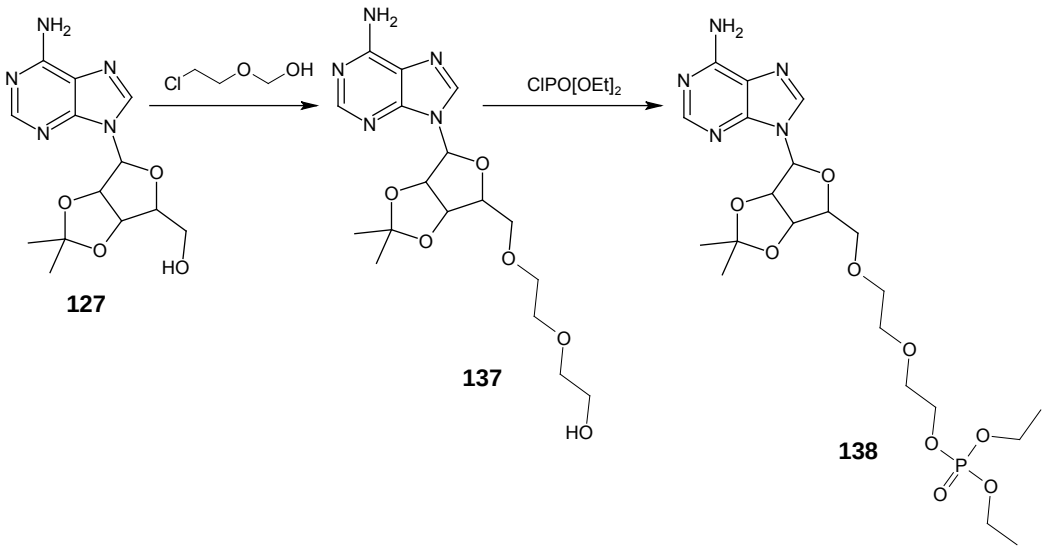

Scheme 23. Synthesis of the phosphorylated derivative **138**.

An initial attempt to phosphorylate compound **137** with tetrabutylammonium dihydrogen phosphate[176] under reflux in an inert atmosphere of argon was not successful. However, 2-(6-aminopurin-9-yl)-5[7-diethylphosphoryloxy)-2,5-dioxaheptyl]-3,4-dihydroxy - tetrahydrofuran 3,4-acetonide **138** was successfully isolated pure on t reating compound **137** with BuLi and diethyl chlorophosphate.[177] The methylene protons (7", 6", 4", 3" and 1") now resonate at slightly higher chemical shifts *ca.* 4.0-4.3 ppm (Figure 18). The ^{31}P signal is at 0.8 ppm (Figure 19) compared with 6.3 ppm in the diethyl chlorophosphate.

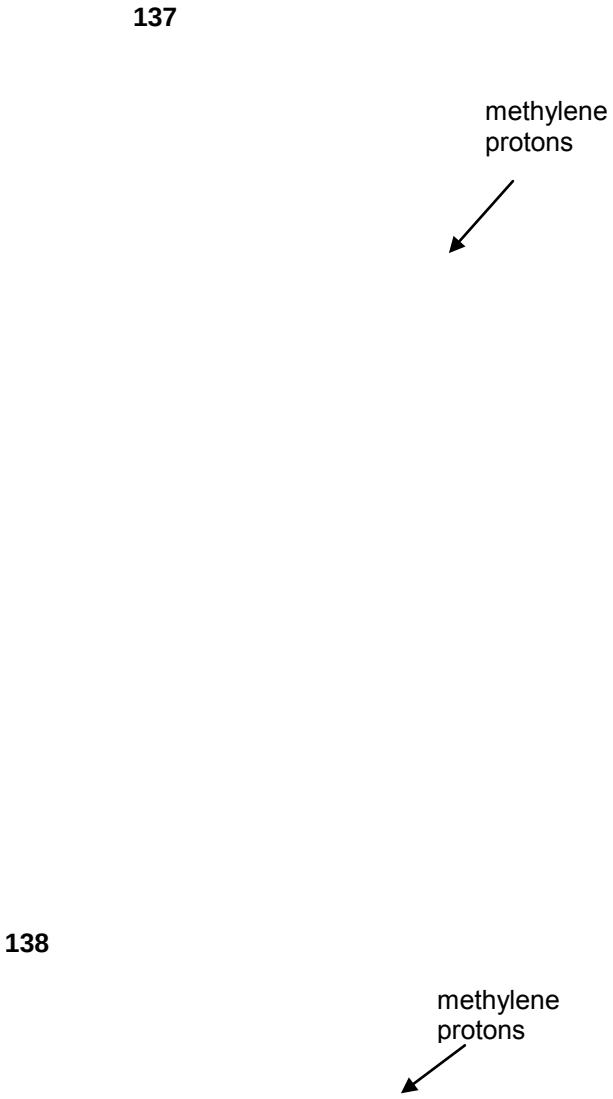

Figure 18. 400 MHz ^{1}H NMR spectra of the alkylated derivative **137** and phosphonate **138** in $CDCl_3$.

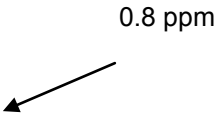

Figure 19. 162 MHz ^{31}P NMR spectrum of **138** in $CDCl_3$.

The mid-IR absorption spectrum of 2-(6-aminopurin-9-yl)-5[7-diethylphosphoryl-oxy)-2,5-dioxaheptyl]-3,4-dihydroxytetrahydrofuran 3,4-acetonide **138** shows a phosphate ester absorption band at 1028 cm^{-1} (Figure 20).

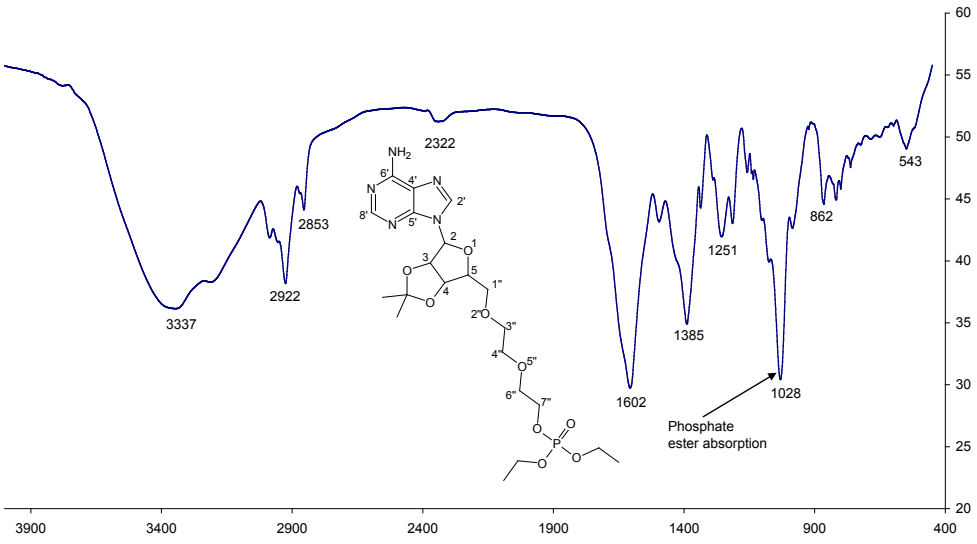

Figure 20. Mid-IR absorption spectrum of the phosphorylated derivative **138** as a thin film.

2.1.4. Preparation of 2-(6-aminopurin-9-yl) -3,4-dihydroxy- 5-(10-hydroxy-2,5,8-trioxadecyl)tetrahydrofuran 3,4-acetonide 139 and 2-[6-(8-hydroxy-3,6,-dioxa octylamino)purin-9-yl]-3,4-dihydroxy-5-(10-hydroxy-2,5,8- trioxadecyl)tetrahydrofuran 3,4-acetonide 139A

On treating the acetonide **127** with NaH[169] and 2-[2-(2-chloroethoxy)ethoxy]ethanol, in refluxing THF, the desired monoalkylated derivative 2-(6-aminopurin-9-yl)-3,4-dihydroxy-5-(10-hydroxy-2,5,8-trioxadecyl)tetrahydrofuran 3,4-acetonide **139** was isolated in 2% yield as well as the competing di-alkylated product, 2-[6-(8-hydroxy-3,6,-dioxaoctylamino)purin-9-yl]-3,4-dihydroxy-5-(10-hydroxy-2,5,8-trioxadecyl)tetrahydrofuran 3,4-acetonide **139A**, in 3% yield (Scheme 24). In the ^{1}H NMR spectra of compound **139** and **139A** (Figure 22), the methylene signals of compound **139** can be observed at *ca.* 3.58-3.96 ppm while those of the competing product **139A** can be observed in a similar region *ca.* 3.51-3.81 ppm. The 2'-H methine proton of **139**, however, resonates at 7.83 ppm while that of **139A** resonates downfield at 8.50 ppm as a consequence of the presence of the 8-hydroxy-3,6-dioxaoctylamino substituent on the purine ring.

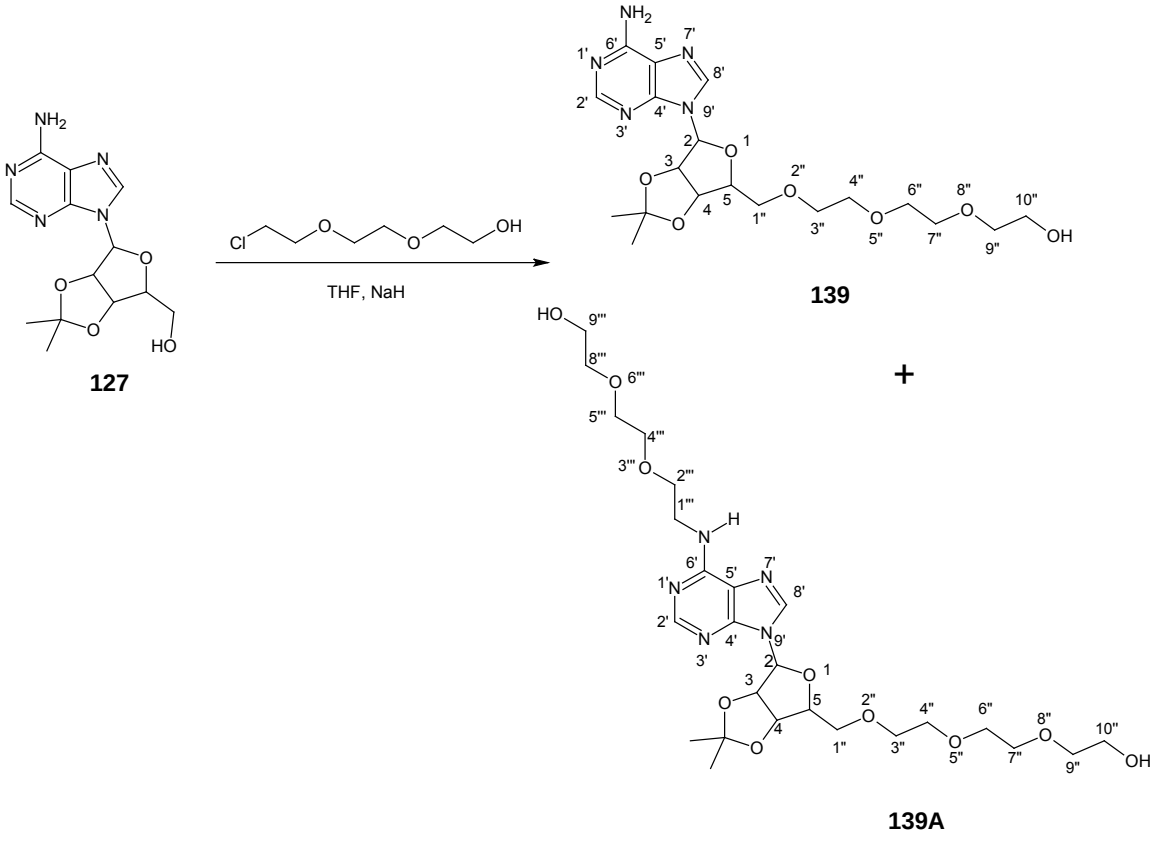

Scheme 24. Synthesis of compounds **139** and **139A**

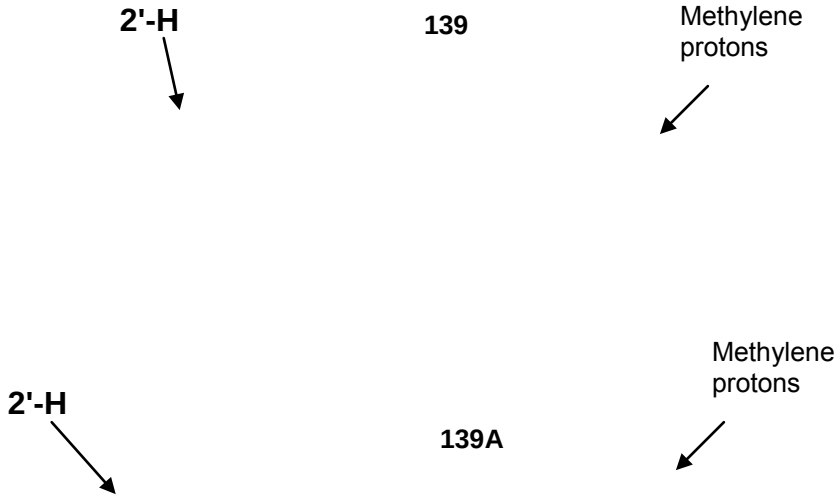

Figure 21. Comparism of ^{1}H NMR spectra of compound **139** and compound **139A** in $CDCl_3$.

2.1.5. Preparation of 2-(6-aminopurin-9-yl)-5-acetoxyacetyl-3,4-dihydroxytetrahydrofuran 3,4-acetonide 140 and 2-[6-(acetoxyacetylamino)purin-9-yl)-5-acetoxyacetyl 3,4-dihydroxytetrahydrofuran 3,4-acetonide 140A

On treating the acetonide **127** with NaH and acetoxyacetyl chloride[169,178] in refluxing THF, the ester 2-(6-aminopurin-9-yl)-5-acetoxyacetyl-3,4-dihydroxytetrahydrofuran 3,4-acetonide **140** was isolated in 34% yield as well as the di-acylated product, 2-[6-(acetoxyacetylamino)purin-9-yl)-5-acetoxyacetyl-3,4-dihydroxytetrahydrofuran 3,4-acetonide **140A** in 40% yield (Scheme 25). There is one C*H*$_3$CO signal at 2.13 ppm in ^{1}H NMR spectrum of compound **140** while there are (2 × C*H*$_3$CO) signals at 2.11 and 2.22 ppm respectively in the ^{1}H NMR spectrum of compound **140A** (Figure 22). The signal of the NH_2 on C-6' of the purine ring of compound **140** can be seen at 5.71 ppm while NH signal of compound **140A** can be seen at 9.4 ppm. The methylene protons of the acetoxyacetyl moiety attached to the ribose sugar of both products resonate as singlets at *ca.* 4.5 ppm while the methylene protons of the amide group of the di-acylated product resonate as a singlet at 5.30 ppm. FAB mass spectrometric

analysis of the ester **140** showed the presence of the M+1 peak at *m/z* 408 with an intensity of 96% relative to the base peak at *m/z* 136, while FAB mass spectrometric analysis of the di-acylated product showed the presence of the M+1 peak at *m/z* 508 with an intensity of 100% as the base peak.

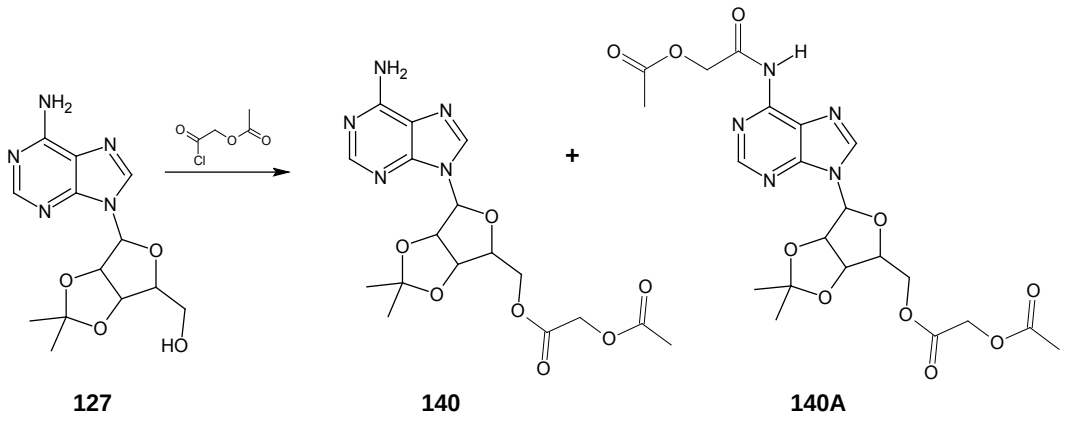

127 **140** **140A**

Scheme 25. Synthesis of the esters mono-ester **140** and di-ester **140A**.

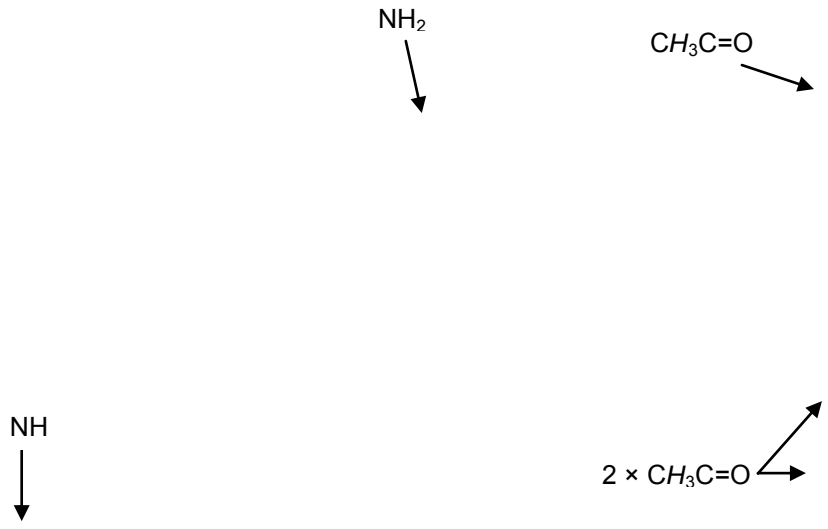

Figure 22. Comparison of ^{1}H NMR spectra of compounds (a) **140** and (b) **140A** in $CDCl_3$.

2.1.6. Preparation of 2-(6-aminopurin-9-yl)-5-[(2-chloroacetoxy)methyl]-3,4-di hydroxyltetrahydrofuran 3,4-acetonide 141 and 2-[6-(2-chloroacetamido)purin-9-yl]- 5-[(2-chloroacetoxy)methyl]-3,4-dihydroxytetrahydrofuran 3,4-acetonide 141A

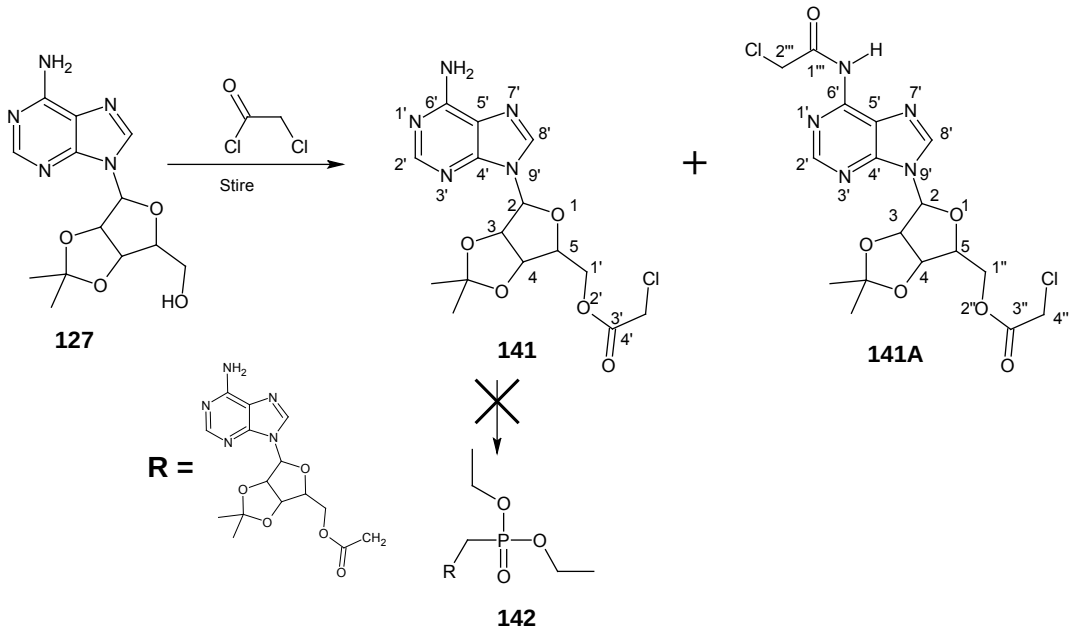

Scheme 26. Synthesis of compounds **141** and **141A**

The ester 2-(6-aminopurin-9-yl)-5-[(2-chloroacetoxy)methyl]-3,4-dihydroxytetrahydrofuran 3,4-acetonide **141** was synthesized in 94% yield by stirring the acetonide **127** with chloroacetyl chloride[179] under argon at room temperature for *ca.* 0.5 h (Scheme 26). In a separate reaction, on treating **127** with the same acid chloride under the same reaction conditions, compound **141A** was obtained as well as the desired product **141**. While each of the CH_2Cl methylene signals were observed at 4.00 ppm as shown in Figure 23, the methylene protons next to the amide group on the purine ring of **141A** resonate as a singlet at 4.70 ppm. The 8'-H methine proton of compound **141** resonates at 7.88 ppm, while the corresponding proton in compound **141A** resonates at 8.72 ppm. Attempts to synthesize compound **142** by refluxing compound **141** with triethyl phosphite (Arbuzov reaction)[180] were unsuccessful.

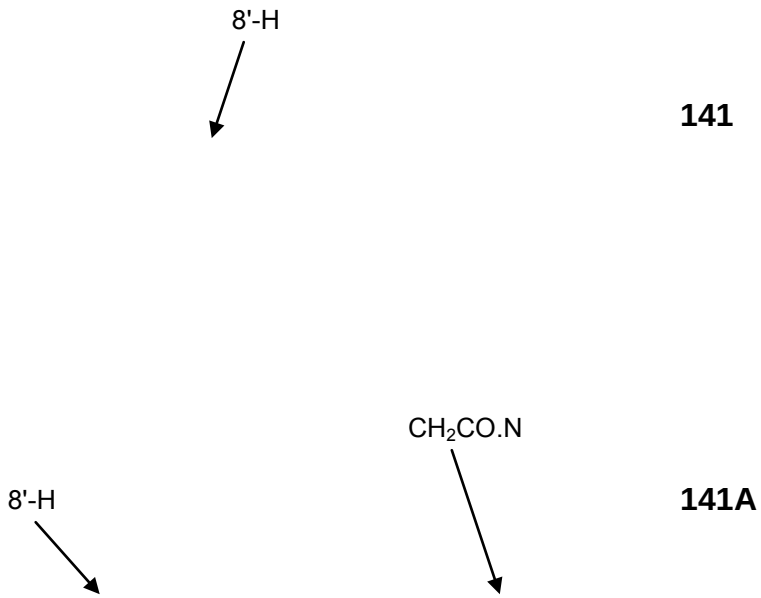

Figure 23. Comparison of 400MHz ^{1}H NMR spectra of compounds **141** and **141A** in $CDCl_3$.

2.1.7. Preparation of 5-[(acryloyloxy)methyl]-2-(6-aminopurin-9-yl)-3,4-dihydroxytetrahydrofuran 3,4-acetonide 143

The acrylic ester **143** was obtained as light yellow oil in 4% yield on t reating deprotonated **127** with acryloyl chloride under reflux (Scheme 27).

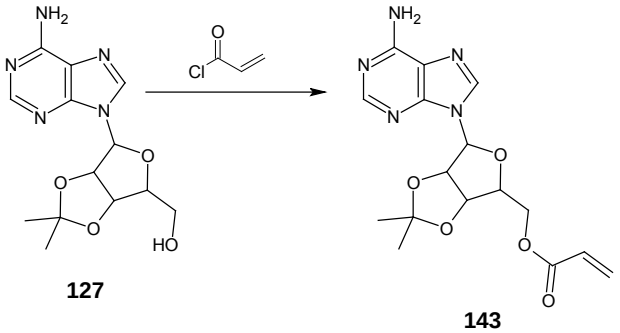

Scheme 27. Synthesis of the acrylic ester **143**.

Formation of the acrylic ester **143** was confirmed by the downfield shift of the 1"-methylene proton signals in compound **143** relative to the precursor **127** (Figure 24). Both methine protons on the heteroaromatic ring of the acrylic ester **143** resonate at about the same chemical shifts (7.84 and 8.34 ppm) as in the precursor **127** confirming that there was no acylation of the amino group on the purine ring. The NH_2 protons also integrate to approximately 2 at 5.87 ppm in the ^1H NMR spectrum of the acrylic ester product. The formation of the acrylic ester was further confirmed by the presence of the molecular ion at *m/z* 361.137825 with 30% abundance relative to the base peak at *m/z* 55.018601 in the high-resolution mass spectrometric analysis.

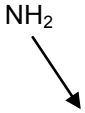

Figure 24. 400 MHz ^1H NMR spectrum of acrylic ester **143** in $CDCl_3$.

The mid-IR spectrum of compound **143** showed an ester carbonyl absorption band at 1714 cm^{-1}.

2.1.8. Preparation of 4-bromomethyl-2,2-dimethyl[1,3]dioxolane 145

The vicinal 1,2-diol moiety of 3-bromo-1,2-dihydroxypropane **144** was protected by stirring it with acetone in the presence of *p*ara-toluenesulfonic acid monohydrate

catalyst[163] to obtain 4-bromomethyl-2,2-dimethyl[1,3]dioxolane **145** in 65% yield (Scheme 28). The protection was confirmed by the observation of two clearly defined methyl singlets at 1.35 and 1.43 ppm respectively in the ^{1}H NMR spectrum (Figure 25) as well as six carbon signals in the ^{13}C NMR spectrum (Figure 26). However, attempts at alkylating[169] the deprotonated acetonide **127** with the dioxolane **145** was unsuccessful.

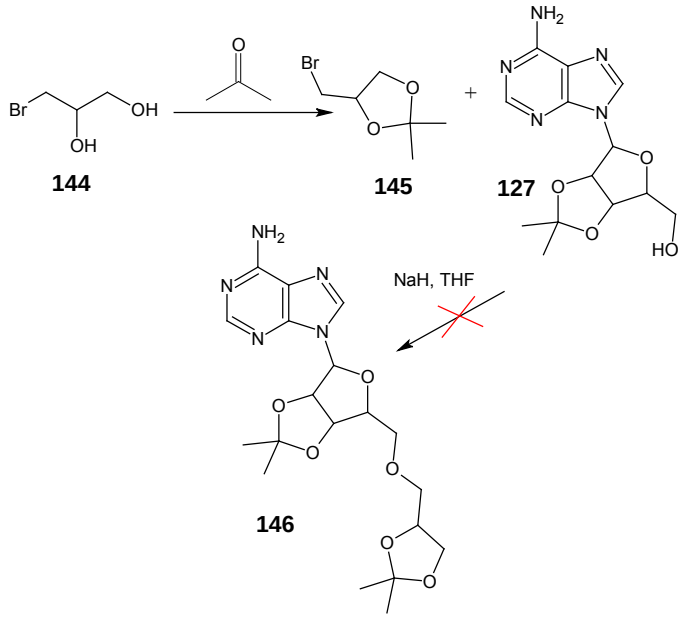

Scheme 28. Proposed synthesis of the derivative **146**.

Figure 25. 400 MHz ^{1}H NMR spectrum of the dioxolane **145** in $CDCl_3$.

Figure 26. 100 MHz ^{13}C NMR spectrum of the dioxolane **145** in $CDCl_3$.

2.2. Novel ATP analogues from adenine

The approach employed was to replace the proton on the N-9 nitrogen of adenine with various electrophiles after deprotonation of adenine to afford primary products (Figure 27) that could be elaborated further. In one case the electrophile had to be specially prepared.

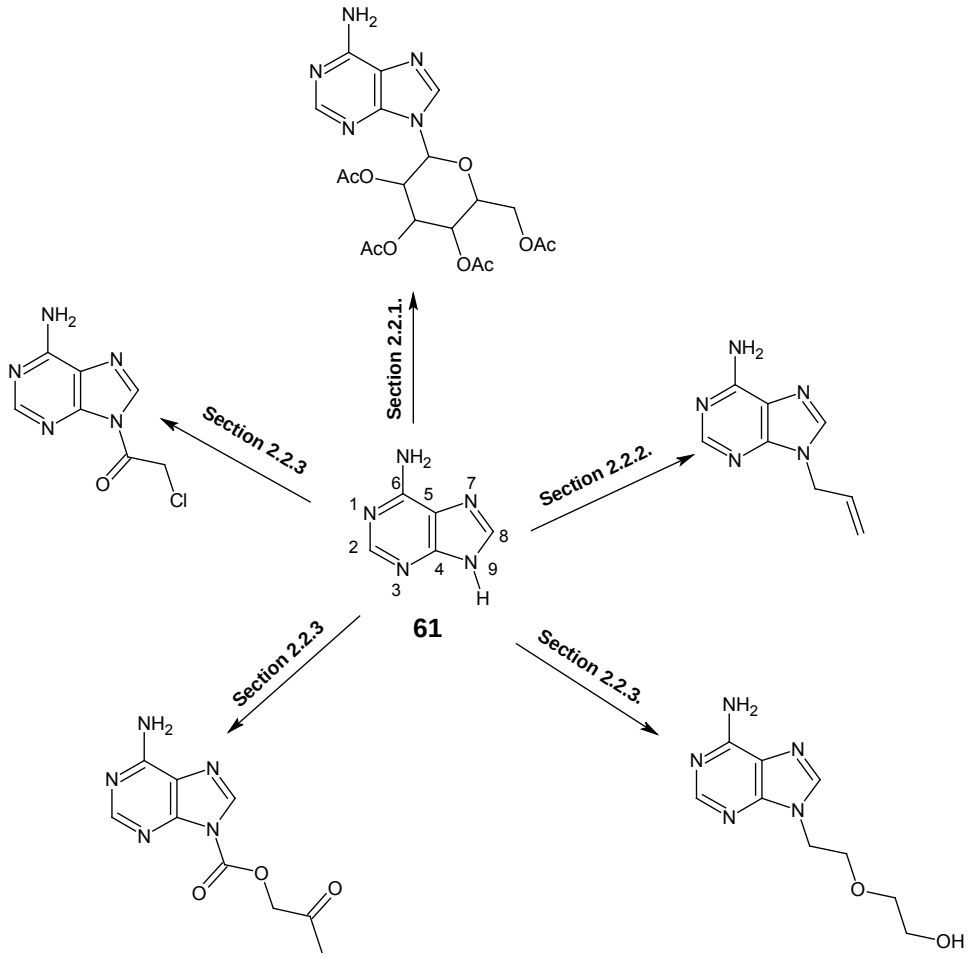

Figure 27. General approach for the synthesis of adenine derivatives.

2.2.1. Preparation of 3,4,5-triacetoxy-6-acetoxymethyl-2-(6-aminopurin-9-yl)-pyran 149

Acetylated glucose (3,4,5,6-tetraacetoxy-2-acetoxymethylpyran) **148** was synthesized in 87% yield by heating glucose **147** with acetic anhydride in the presence of $ZnCl_2$ catalyst[181] (Scheme 29). ^1H NMR analysis (Figure 28) indicated the presence of the desired product. Thus the anomeric proton (2-H) resonates as a doublet at 6.3 ppm with a coupling constant of 3.7 Hz, a down-field shift of 0.1 ppm from its value in glucose, while the five acetoxy methyl groups resonate between 1.94 and 2.23 ppm. Five methyl carbons and five C=O carbons can be observed in the ^{13}C NMR spectrum (Figure 29). Low-resolution mass spectrometric analysis reveals the presence of the molecular ion at m/z 390 with 3% abundance relative to the base peak at m/z 98, while mid-IR absorption at 1750 cm^{-1} was observed for the ester carbonyl group.

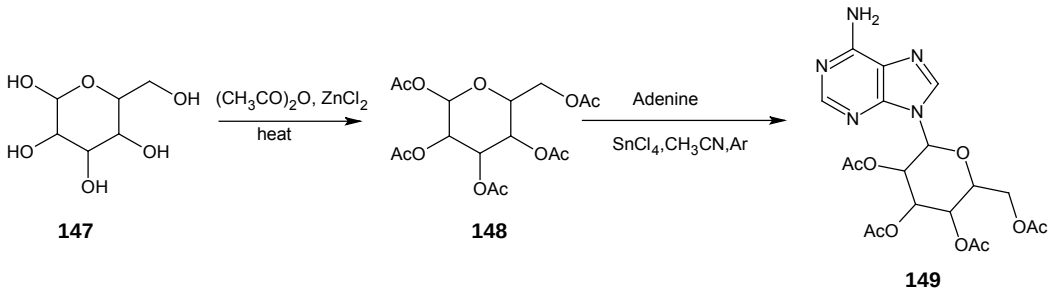

Scheme 29. Synthesis of the adenine derivative **149**.

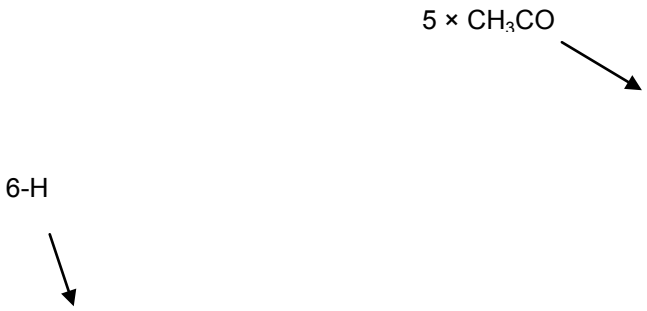

Figure 28. 400MHz ^{1}H NMR spectrum of compound **148** in $CDCl_3$.

Figure 29. 100MHz ^{13}C NMR spectrum of the acetylated product **148** in $CDCl_3$.

The acetylated glucose **148** was then coupled with adenine in a tin tetrachloride catalyzed[182] glycosidation reaction using acetonitrile[183] as solvent to afford of 3,4,5-triacetoxy-6-acetoxymethyl-2-(6-aminopurin-9-yl)pyran **149** in 30% yield. In the ^{1}H NMR spectrum (Figure 30), the anomeric proton (2-H) now resonates at 5.88 ppm with a coupling constant of 5.9 H z *ca.* 0.4 ppm upfield of the pentaacetylated precursor, while the anomeric carbon has a chemical shift of 80.3 ppm in the ^{13}C NMR spectrum (Figure 30) - an upfield shift of 8.8 ppm . Low-resolution mass spectrometric analysis of compound **149** showed the presence of the M-1 peak at *m/z* 464 as the base peak. Mid-IR absorption at 1744 c m^{-1} was observed for the ester carbonyl groups.

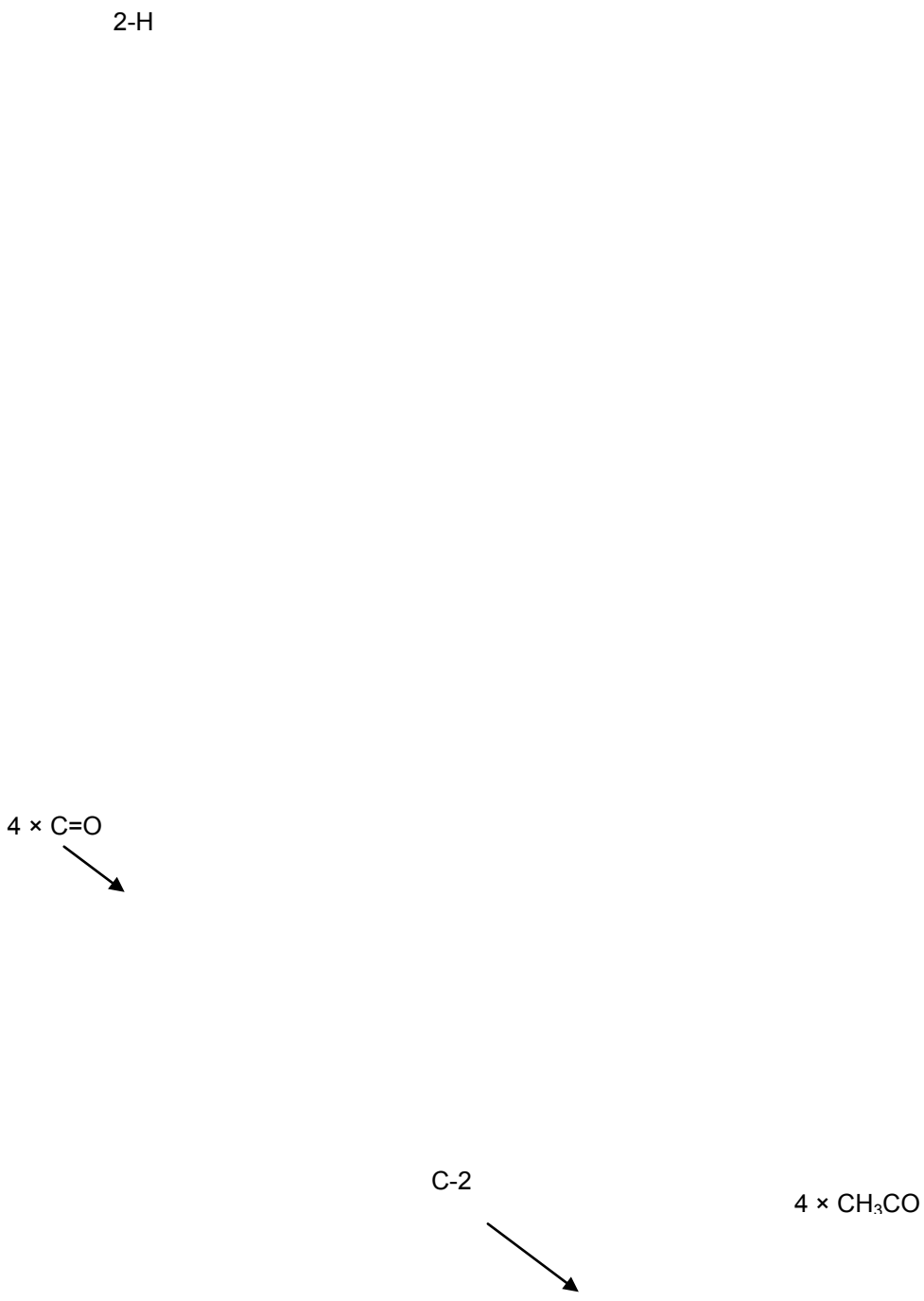

Figure 30 (i) 400MHz ^{1}H NMR spectrum of acetylated derivative **149** and (ii) 100MHz ^{13}C NMR spectrum of acetylated derivative **149** in $CDCl_3$.

2.2.2. Preparation of 6-(*N*-allylamino)purine 150 and 9-allyl-6-(*N*-allylamino)-purine 150A

Deprotonation of adenine in DMF followed by treatment with allyl bromide[169] under reflux yielded the mono- and di-allylated products **150** and **150A** (Scheme 30). NMR as well as high-resolution mass spectroscopy confirmed the formation of both allylated products. All protons are accounted for in the ^{1}H NMR spectra of both compounds (Figures 31 and 32). The NH proton of the mono-allylated product resonates as a singlet at 11.12 ppm while its 2'-H methine proton resonates at 6.06 ppm as a tdd. The molecular ion peak of the mono-allylated product **150** was clearly visible at *m/z* 175 as the base peak while the spectrum of the di-allylated product **150A** exhibited a molecular ion at *m/z* 215 with 95% abundance relative to the base peak at *m/z* 200.

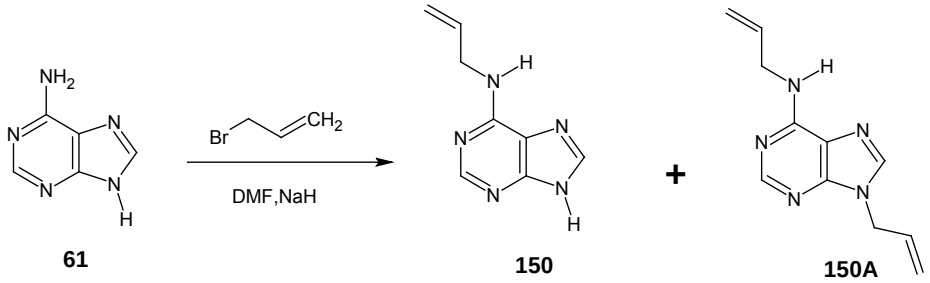

Scheme 30. Synthesis of the adenine derivatives **150** and **150A**

Figure 31. 400MHz ^{1}H NMR spectrum of the adenine derivative **150** in $CDCl_3$.

Figure 32. 400MHz ^{1}H NMR spectrum of the adenine derivative **150A** in $CDCl_3$.

2.2.2. Attempted Preparations

Attempts were made to couple deprotonated adenine with each of 2-(chloroethoxy)ethanol, acetoxyacetyl chloride and chloroacetyl chloride (Scheme 31). Unfortunately all these acylation reactions were unsuccessful. The reason for these failed reactions may be the steric bulk of the purine nucleophile in the case of chloroacetyl chloride and acetoxyacetyl chloride. 2-(chloroethoxy)ethanol, on t he other hand, might have undergone intramolecular cyclisation in the presence of NaH (Figure 33) hence preventing its reaction with the nucleophilic deprotonated adenine.

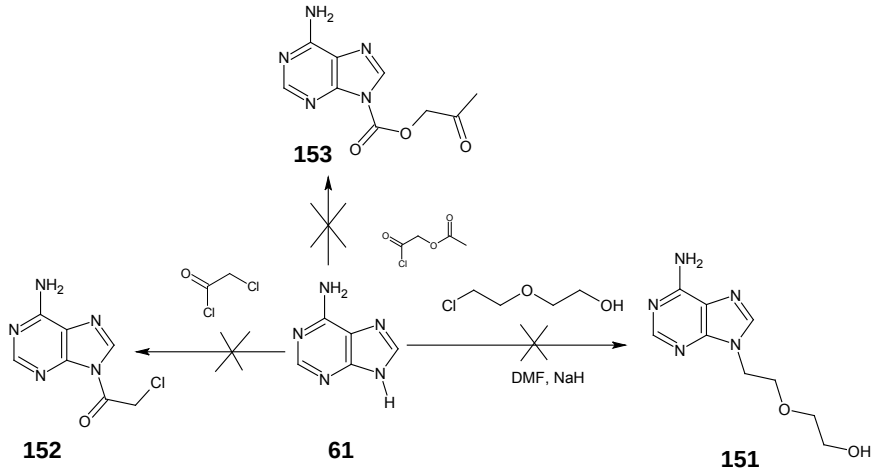

Scheme 31. Attempted preparations of adenine derivatives.

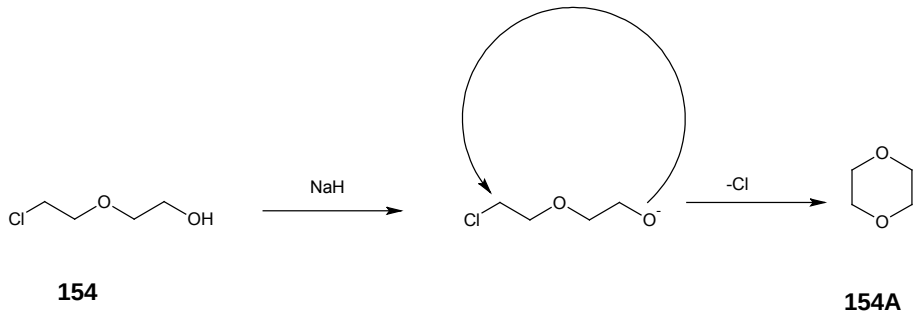

Figure 34. Possible intramolecular cyclisation of 2-(chloroethoxy)ethanol in the presence of NaH.

2.3. ATP mimics from allopurinol and Baylis-Hillman electrophiles

The approach was to replace the hydrogen of the imidazole ring in allopurinol with different electrophiles, after deprotonation by a base, to afford novel ATP mimics. Hence, the hydroxyl group on a llopurinol was protected with dihydropyran[184] (Scheme 32) to avoid competition between the NH and OH moieties in the molecule. ^{1}H NMR analysis (Figure 34) showed the formation of compound **157** with all the protons accounted for in their expected positions, and the 2'-methine proton having moved upfield by 0.4 ppm relative to its position in dihydropyran. In the ^{13}C NMR spectrum (Figure 35) the C-3' carbon has been shifted upfield by 71.2 ppm as a

consequence of being converted from an sp^2 centre in dihydropyran to an sp^3 carbon in the protected allopurinol.

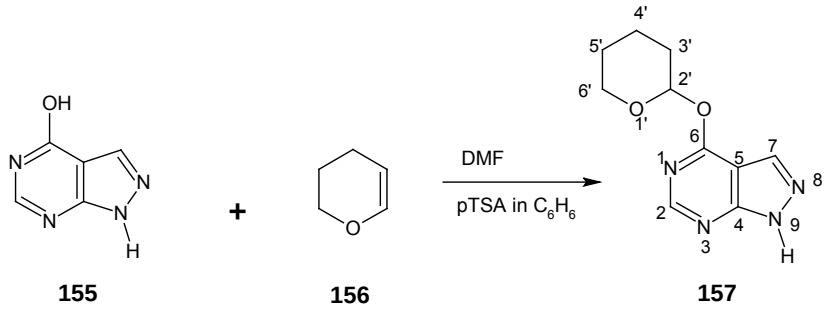

155 **156** **157**

Scheme 32. Protection of allopurinol.

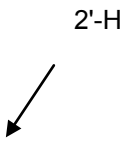

Figure 34. 400MHz ^{1}H NMR spectrum of the protected allopurinol **157** in $CDCl_3$.

C-3'

Figure 35. 100MHz ^{13}C NMR spectrum of the protected allopurinol **157** in $CDCl_3$.

With the protected allopurinol in hand, an attempt was made to synthesize the range of primary substitution products illustrated in Figure 38.

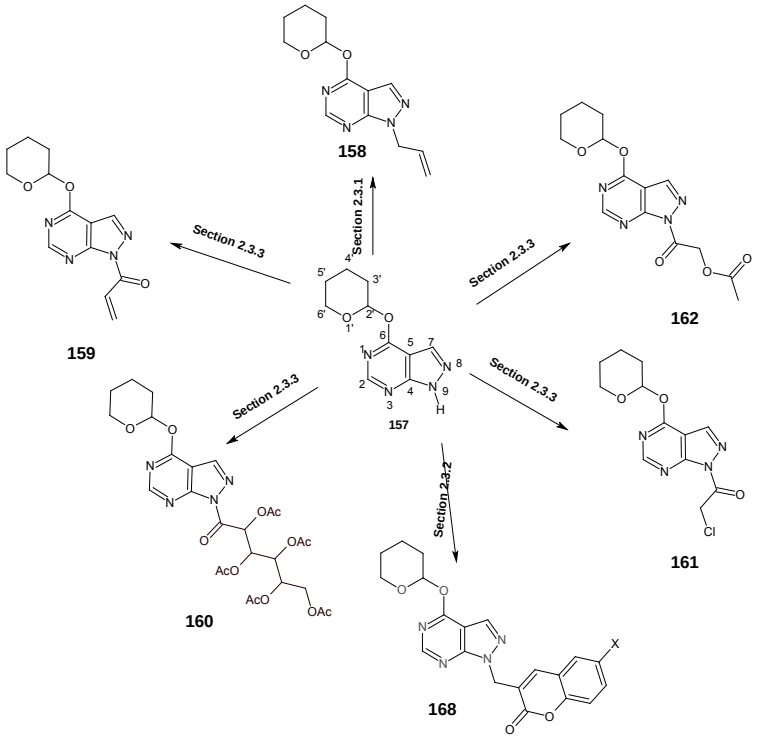

Figure 36. General approach to allopurinol derivatives.

2.3.1. Preparation of 9-allyl-4-(tetrahydropyran-2-yloxy)-1*H*-pyrazolo[3,4-*d*]pyrimidine 161

The protected allopurinol **157** was deprotonated using sodium hydride and then treated with allyl bromide[169] (Scheme 33) under reflux and the allylated derivative **158** was obtained in 87% yield. The ^{1}H NMR and ^{13}C NMR (Figure 37) spectra both confirm the formation of the product. The 2"-methine proton resonates at 5.94 ppm as a multiplet due to coupling with adjacent vinylic and methylene protons, while all 13 carbon atoms are accounted for (Figure 38). Mass spectrometric analysis shows the presence of the molecular ion at *m/z* 260 relative to the base peak at *m/z* 177.

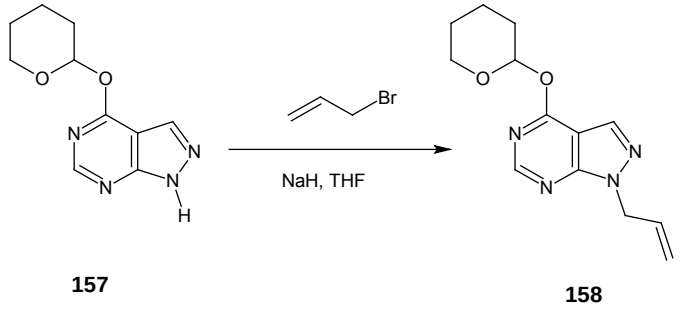

157 **158**

Scheme 33. Preparation of the allopurinol derivative **158**.

Figure 37. 600MHz ^{1}H NMR spectrum of the allopurinol derivative **158** in $CDCl_3$.

Figure 38. 100MHz ^{13}C NMR spectrum of the allopurinol derivative **158** in $CDCl_3$.

Attempts to acylate the pyrazole nitrogen[178] of protected allopurinol with various acylating agents (Scheme 34) were, also unsuccessful - paralleling the difficulties encountered in acylating adenine at the N-9 nitrogen.

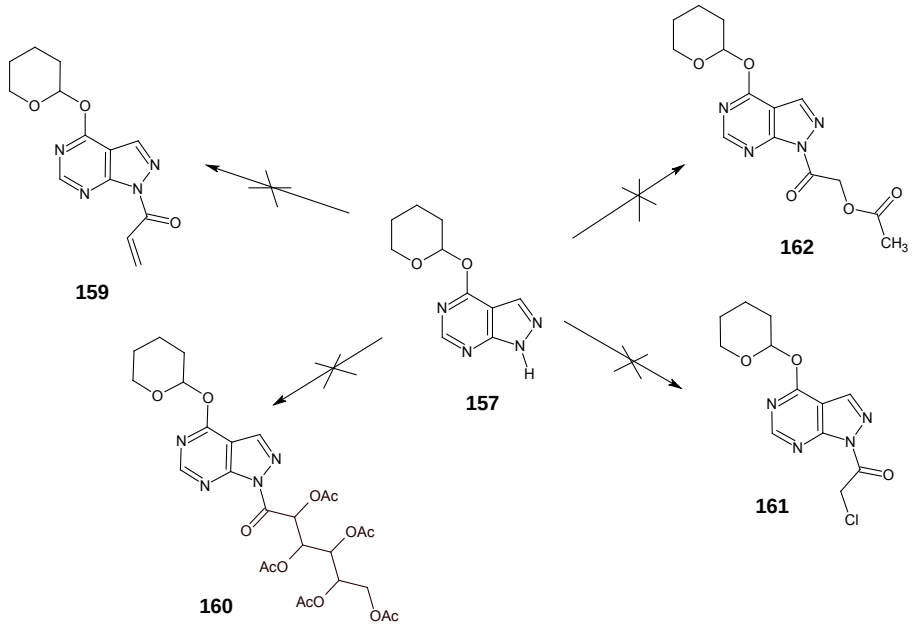

Scheme 34. Attempted acylations of compound **157**.

2.3.2. Preparation of *tert*-butyl 3-(5-bromo-2-hydroxyphenyl)-3-hydroxy-2-methylene propanoate 165a and *tert*-butyl 3-hydroxy-3-(2-hydroxyphenyl)-2-methylenepropanoate 165b

In separate reactions, 5-bromo-2-hydroxybenzaldehyde **163a** and salicylaldehyde **163b** were stirred with *tert*-butyl acrylate in the presence of DABCO as catalyst to obtain **165a** and **165b**, respectively (Scheme 35), following previous work done in the research group by Musa.[179] Each of these Baylis-Hillman adducts was then reacted with deprotonated allopurinol. ^{1}H NMR and other spectroscopic analysis confirmed the formation of the Baylis-Hilman products. The intramolecular cyclisation product **166b** was also obtained as side product in the reaction between salicylaldehyde and *tert*-butyl acrylate. This product arises from a conjugate addition-elimination (or S_N1 displacement) reaction affording a chromene instead of the coumarin analogue. The vinylic protons of compound **165b**, 3"-H_a and 3"-H_b, resonate at 5.49 ppm and 6.23 ppm, respectively (Figure 39). The 3-H methine proton singlet at 5.69 ppm and the 3-OH and 2'-OH signals at 4.36 ppm and 8.14 ppm disappear in the spectrum of the compound **166b** to give way for the 2-methylene singlet (Figure 40) at 4.94 ppm as a consequence of the intramolecular cyclisation of **165b**. The 3-H methine proton at 5.69 ppm on a sp^3 carbon in compound **165b** moves downfield to 7.32 ppm (4-H in **166b**) since it now resides on a sp^2 carbon.

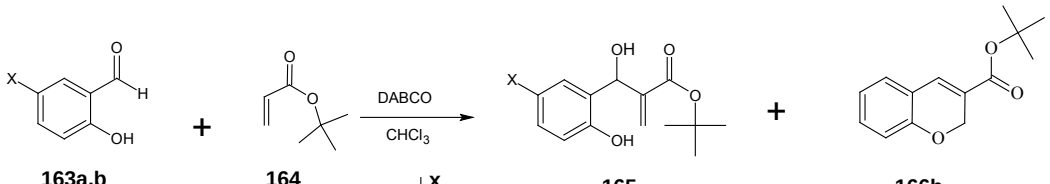

X
a: Br
b: H

Product	% Yield
165a	88
165b	4.1
166b	0.37

Scheme 35. General preparation of Baylis-Hilman products.

There is also a considerable shift upfield in the position of the carbonyl carbon in the ^{13}C NMR spectra from 166.7 ppm in **165b** (Figure 41) to 163.8 ppm in **166b** (Figure 42). High-resolution mass spectrometric analysis of compound **166b** shows the presence of the M-1 ion at *m/z* 231.101945 with 30% abundance relative to the base

peak at *m/z* 57.070785, while the mid-IR spectrum shows carbonyl absorption at 1700 cm^{-1}.

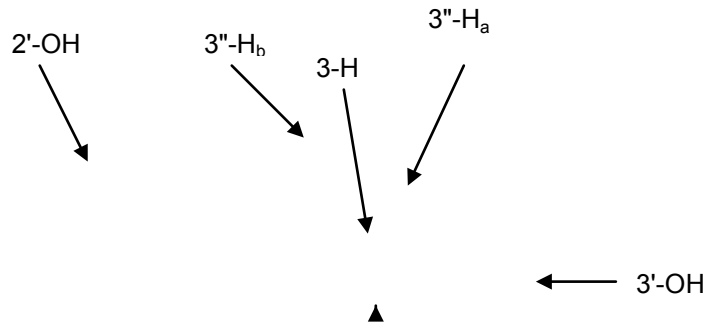

Figure 39. 400MHz ^{1}H NMR spectrum of the B-H product **166b** in $CDCl_3$

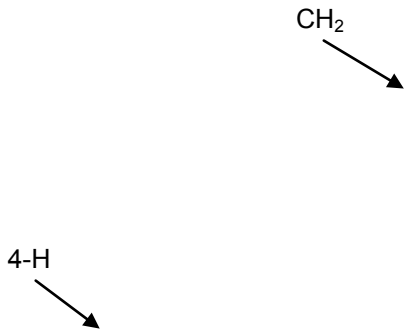

Figure 40. 400MHz ^{1}H NMR spectrum of the chromene **165b** in $CDCl_3$.

Figure 41.100MHz ^{12}C NMR spectrum of the Baylis-Hillman product **165b** in $CDCl_3$.

Figure 42. 100MHz ^{13}C NMR spectrum of the Baylis-Hillman product **166b** in $CDCl_3$.

2.3.2. Preparation of 6-bromo-3-(chloromethyl)coumarin 167, 6-bromo-3-(acetoxymethyl)coumarin 168 and 6-bromo-3-(hydroxymethyl)coumarin 169

Cyclisation of the Baylis-Hillman adduct **165a** in a refluxing mixture of HCl/CH_3COOH[185] yielded the desired 6-bromo-3-(chloromethyl)coumarin product **167** in 31% yield together with two side-products, 6-bromo-3-(acetoxymethyl)-coumarin **168** (1.8%) and 6-bromo-3-(hydroxymethyl)coumarin **169** (7.3%) as shown in Scheme 36. The chemical structures of the side-products were confirmed by spectroscopic methods. The formation of the ester **168** resulted from direct interception by acetic acid **(165a → 168)** and/or the reaction of the excess acetate ion with the desired alkyl halide product **167**, while the formation of the alcohol **169** is attributed to the hydrolysis of the ester **168**. All the protons and carbons of the ester **168** are accounted for as shown in Figures 43 and 44. The methyl protons resonate at 2.16 ppm and the 1'-methylene protons resonate as a singlet at 5.06 ppm, while the 4-H proton resonates as a singlet at 7.94 ppm. In the ^{13}C NMR spectrum the lactone carbonyl and the acetyl carbonyl carbons resonate at 159.5 and 170.4 ppm, respectively. Mass spectrometric analysis of the ester **168** shows the presence of the molecular ion at *m/z* 297 with 18% abundance relative to the base peak at *m/z* 43. Mid-IR spectroscopic analysis of the compound **168** shows the lactone carbonyl absorption band overlapping the coumarin carbonyl band at 1720 cm^{-1}.

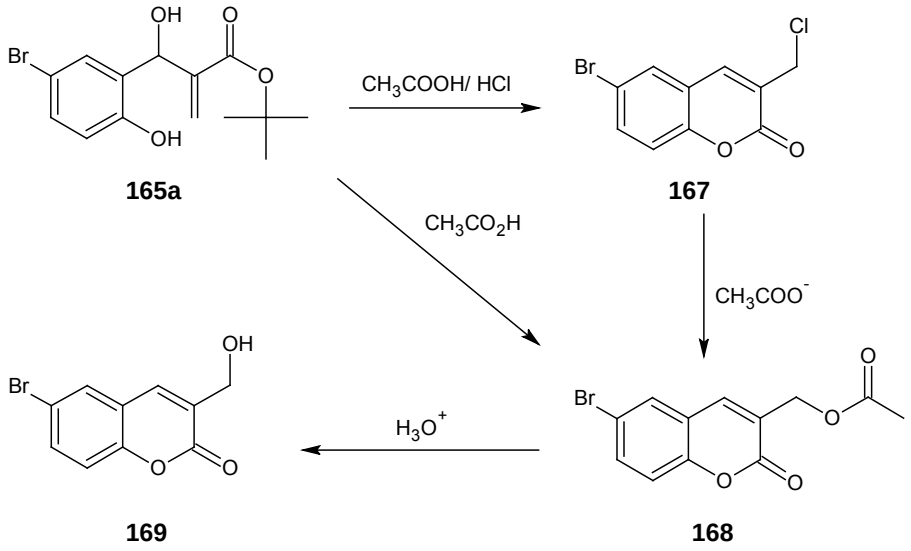

Scheme 36. Synthesis of the coumarin derivatives **167**, **168** and **169**.

Figure 43 400MHz ^{1}H NMR spectrum of compound **168** in $CDCl_3$.

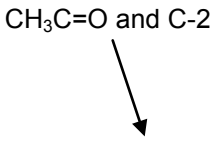

Figure 44 100MHz ^{13}C NMR spectrum of compound **168** in $CDCl_3$.

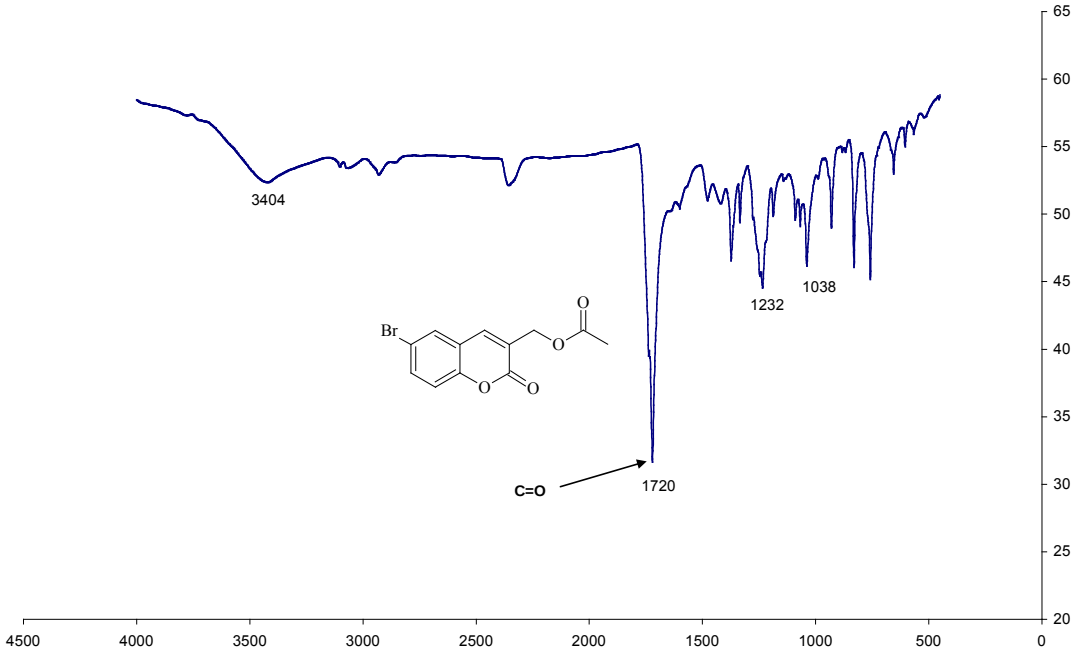

Figure 45. Mid-IR absorption of compound **168**.

All the protons and carbons of the alcohol **169** are accounted for as shown in Figures 46 and 47. The hydroxymethylene protons (CH_2OH) signal is a multiplet at 4.36 ppm while the hydroxyl proton resonates as a triplet at 5.52 ppm. All the carbon signals are accounted for in the ^{13}C NMR spectrum with the sp^2 C-4 carbon resonating at 135.6 ppm while the lactone carbonyl signal appears at 159.1 ppm. Mass spectrometric analysis of the alcohol **169** shows the presence of the molecular ion peak at *m/z* 255 with 83% abundance relative to the base peak at *m/z* 225. Mid-IR spectroscopic analyses of the compound **169** show a hydroxyl absorption band at 3409 cm^{-1} and a coumarin carbonyl absorption band at 1630 cm^{-1}.

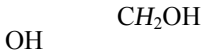

Figure 46. 400MHz ^{1}H NMR spectrum of the alcohol **169** in DMSO-d_6.

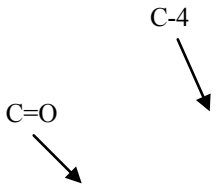

Figure 47. 100MHz ^{13}C NMR spectrum of the alcohol **169** in DMSO-d_6.

The Baylis-Hillman adducts **165a** and **165b** each have two electrophilic sites (Figure 48) at which they may be susceptible to attack by a nucleophile. The 2-

(chloromethyl)coumarin **167,** on the other hand has three different electrophilic sites, as shown in Figure 48, at which it may be susceptible to nucleophilic attack.

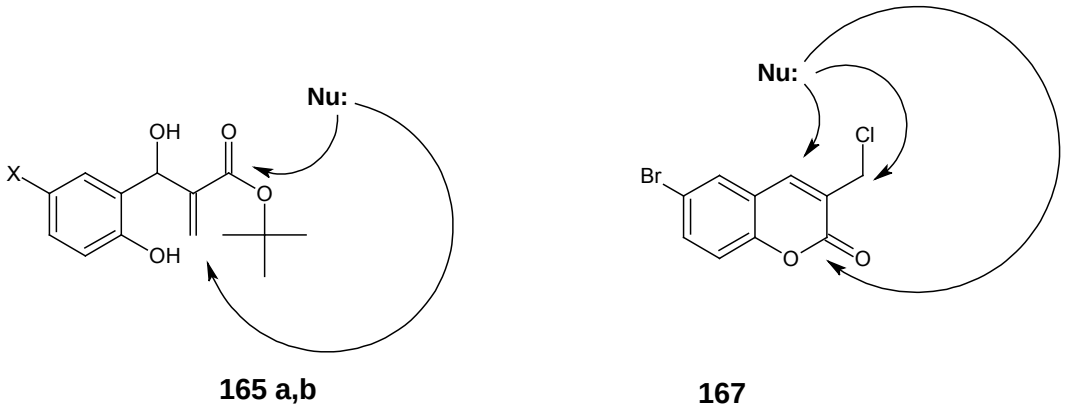

165 a,b **167**

Figure 48. Nucleophilic sites in compounds **165a,b** and compound **167**

2.3.2.3. Reaction of protected allopurinol 157 with 2-(chloromethyl)coumarin 167

The 2-(chloromethyl)coumarin **167** was refluxed[169,178] with deprotonated protected allopurinol **157** to afford the coumarin derivative **170a** in 31% yield (Scheme 37). The structure of the coumarin derivative **170a** was confirmed by spectroscopic methods. The significant downfield shift of the 1'-methylene protons from 4.53 ppm in the precursor **167** to 5.02 ppm in the product **170a** (Figure 49) and the downfield shift of the 1'-methylene carbon signal from 40.8 ppm in the precursor to 45.7 ppm in the product are clear evidence that the nucleophilic attack occurred at the 1'- centre of the coumarin. Furthermore there was no significant change in the chemical shift of the carbonyl carbon [159.4 ppm in the alkyl halide compared with 160.7 ppm in the product derivative (Figure 50)]. All other protons and carbon signals are accounted for in the respective spectra (Figures 49 and 50). High-resolution mass spectrometric analysis of **170a** shows the presence of the M-1 ion at *m/z* 456.043762 with 19% abundance relative to the base peak at *m/z* 84.048546.

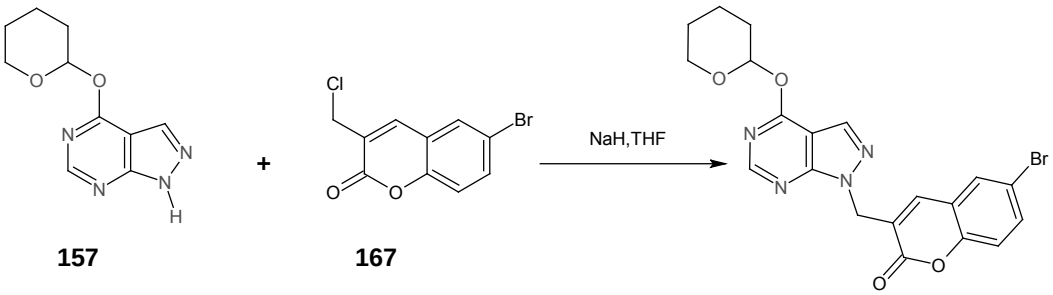

157 **167** **170a**

Scheme 37. Synthesis of the coumarin derivative **170a**.

Figure 49. 400MHz ^{1}H NMR spectra in $CDCl_3$ of compound 167 and compound **170a** in $CDCl_3$.

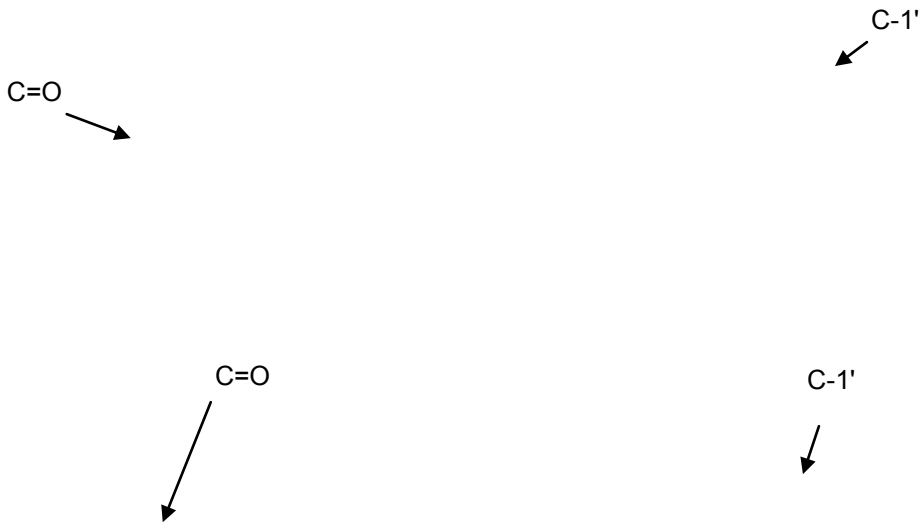

Figure 50. 100MHz ^{13}C NMR spectra of **167** in $CDCl_3$ and **170a** in $CDCl_3$ showing no significant change in chemical shift of the C=O signal.

2.3.2.4. Reaction of protected allopurinol with Baylis-Hillman adducts 165a and 165b

The Baylis-Hillman adducts **165a** and **165b** were refluxed[169,178] separately with deprotonated protected allopurinol to afford products **170a** and **170b** respectively (Scheme 38). In the presence of NaH, intramolecular cyclisation (Figure 51) seems to have occurred in both **165a** and **165b** before the nucleophilic S_N1 attack by the deprotected allopurinol to yield **170a** and **170b**. The chemical structure of each of these allopurinol derivatives was elucidated by spectroscopic methods. The only difference between **170a** and **170b** is the presence of the Br atom on C-6 of the coumarin moiety. Hence, a comparison of the proton NMR spectra of both compounds indicate the presence of 6 protons in the aromatic region of compound **170a** while compound **170b** has 7 protons in the same region (Figure 52). MS analysis of **170a** shows the presence of the molecular ion at *m/z* at 378.132008 with 35%

abundance relative to the base peak at *m/z* 84.057287, while mid-IR spectroscopic analysis of the compound shows carbonyl absorption at 1698 cm^{-1}.

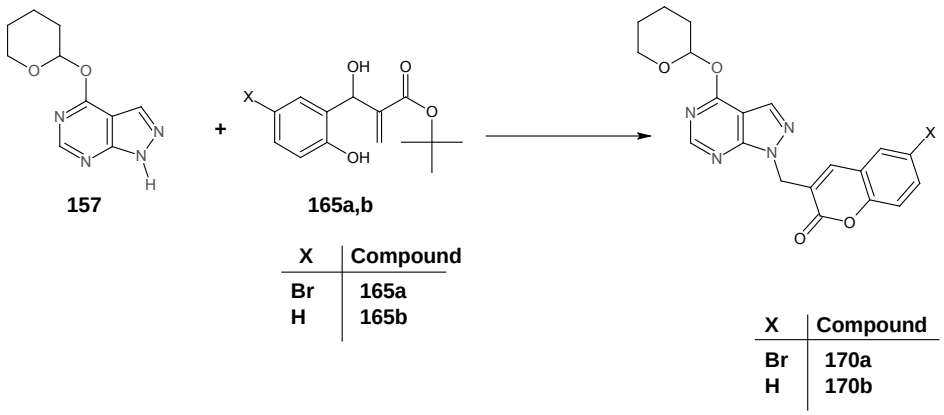

Scheme 38. Synthesis of allopurinol derivatives **170a** and **170b**.

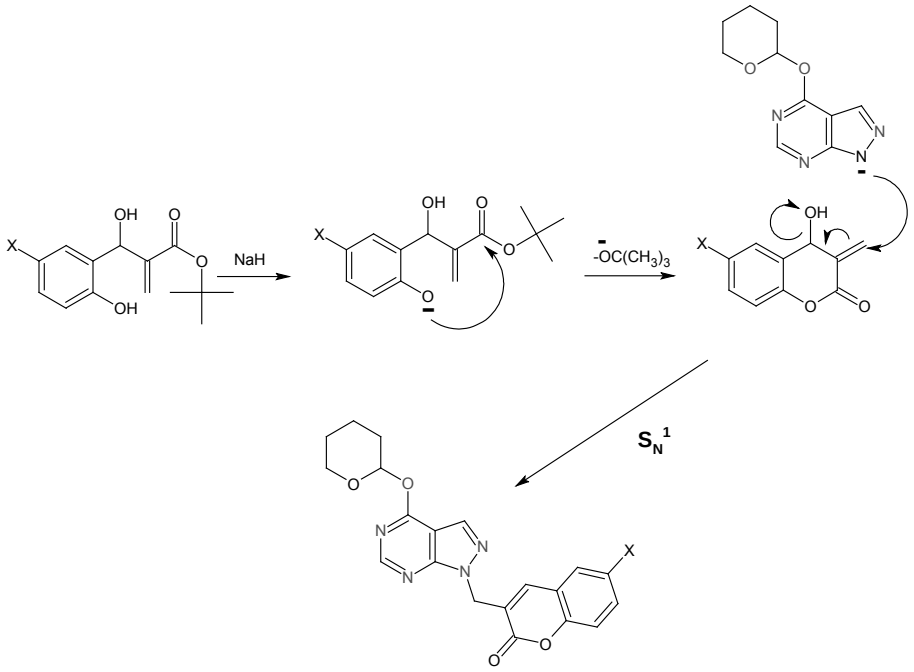

Figure 51. Proposed mechanism for the formation of **170a** and **170b**

170a

170b

Figure 52. Comparison of 400MHz ^{1}H NMR spectra of compounds **170a** and **170b** in $CDCl_3$.

2.4. Truncated adenine mimics

It was envisaged that benzenoid compounds with suitable *meta* substituents could serve as truncated analogues of the 6-aminopurine (adenine) nucleus. Drugs in chemical use often have relatively simple structures and when treated with base, followed by reaction with various electrophiles (as outlined in the Figure 53), it was hoped that such systems would provide convenient access to novel and effective ATP analogues.

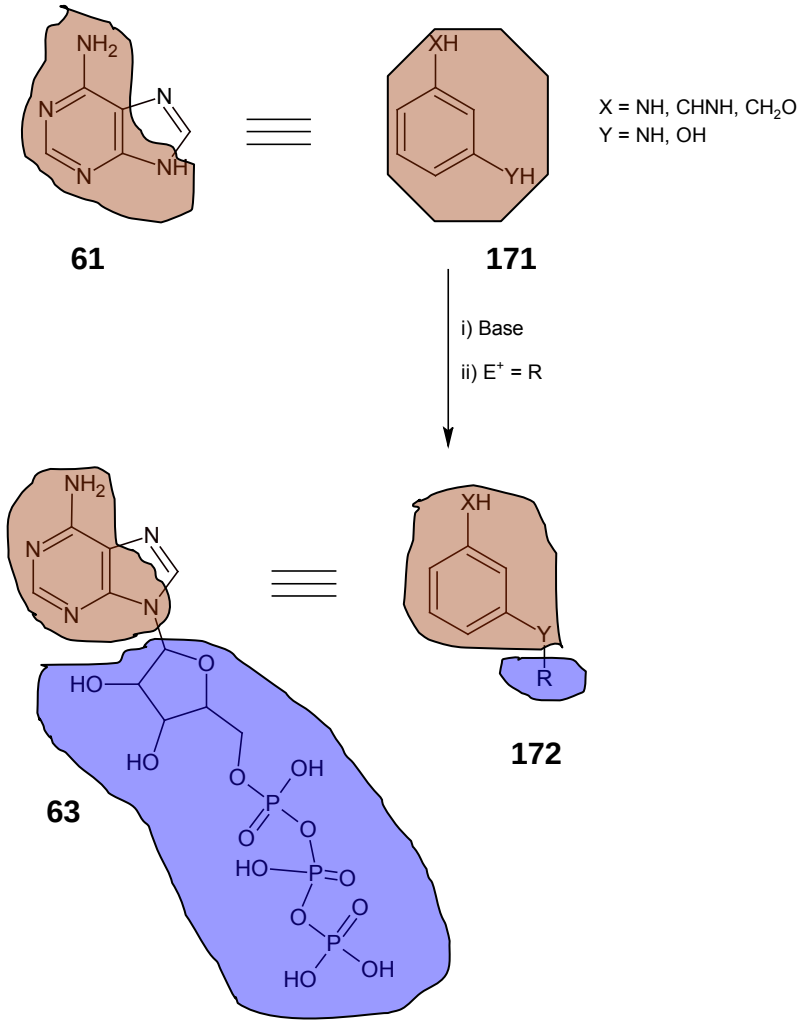

Figure 53. General approach to novel truncated ATP analogoues.

2.4.1. ATP mimics from 3-aminobenzonitrile 173

3-Aminobenzonitrile was identified as a synthon for the construction of truncated ATP analogues (Figure 54). Deprotonation and treatment with a range of electrophiles

was expected to afford a number of intermediates that could be elaborated further (Figure 54).

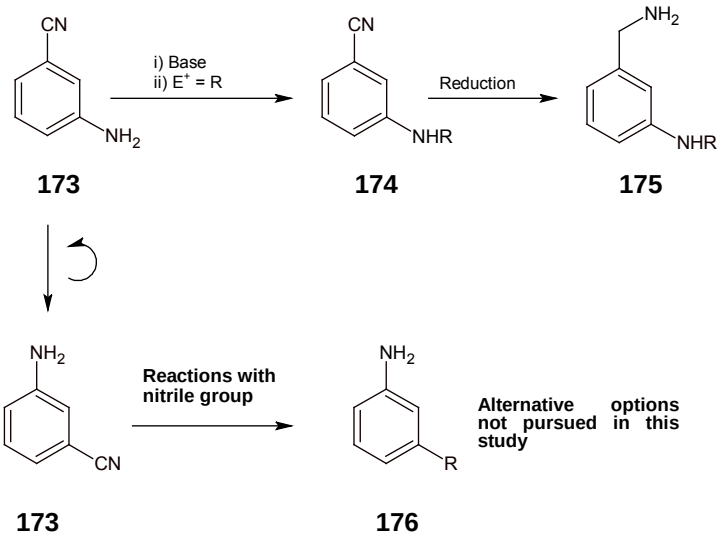

Figure 54. Construction of truncated ATP mimics from 3-aminobenzonitrile.

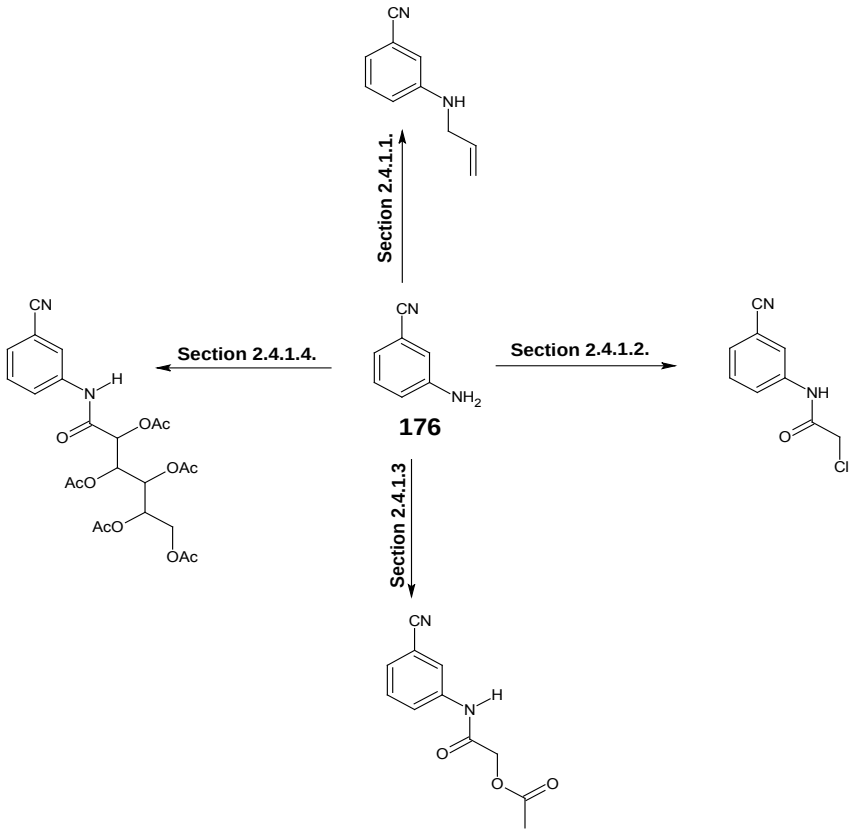

Figure 55. Proposed preparation of derivatives of 3-aminobenzonitrile **173**.

2.4.1.1. N-*Allyl-3-cyanoaniline 177 and* N,N-*diallyl-3-cyanoaniline 177a*

The alkene **177** was expected to provide access[177] to the phosphorylated derivative **180** *via* the dihydroxylated derivative **179** as shown in Scheme 39. Treatment of **173** with 1 equivalent of NaH at 0°C followed by allyl bromide[169] under reflux yielded the mono-allylated product **177** in 45% yield (Scheme 39). Using 2 equivalent of NaH and the same reaction conditions, both the mono-allylated derivative **177** (31%) and the di-allylated derivative **177a** (8%) were obtained. NMR, mass spectrometric and mid-IR spectroscopy were employed to confirm the formation of these products. Figures 56 a nd 57 s how the ^{1}H NMR spectra of compounds **177** and **177a** respectively. The vinylic methine proton in compound **177** resonates as a multiplet at 5.89 ppm while the two vinylic methine protons in the di-allylated product resonate as a multiplet at 5.81 ppm. The NH signal for the mono-allylated product **177** is evident as a singlet at 4.13 ppm. MS analysis of compound **177** indicates the presence of the molecular ion at *m/z* 158 as the base peak, while high-resolution MS analysis of **177a** indicates the presence of the M+1 peak at *m/z* 199.119390 with 9% abundance relative to the base peak at *m/z* 41.040152. Mid-IR analysis of compound **177** (Figure 58) showed an NH absorption band at 3391 cm^{-1} and the cyanide absorption band at 2228 cm^{-1}, while the di-allylated analogue **177a** (Figure 59) show only the cyanide absorption band at 2228 cm^{-1}. In attempts directed at improving the yield, the reaction was also carried out under various reaction conditions. The maximum yield obtained was 45% using 1 equivalent of NaH in THF (Scheme 39). Unfortunately, repeated attempts to either dihydroxylate compound **177** with CTAP,[174] $KMnO_4$[174] or $NaIO_4$[170] or to make the epoxide[186] **178** were unsuccessful, precluding access to the targeted diphosphate **180**.

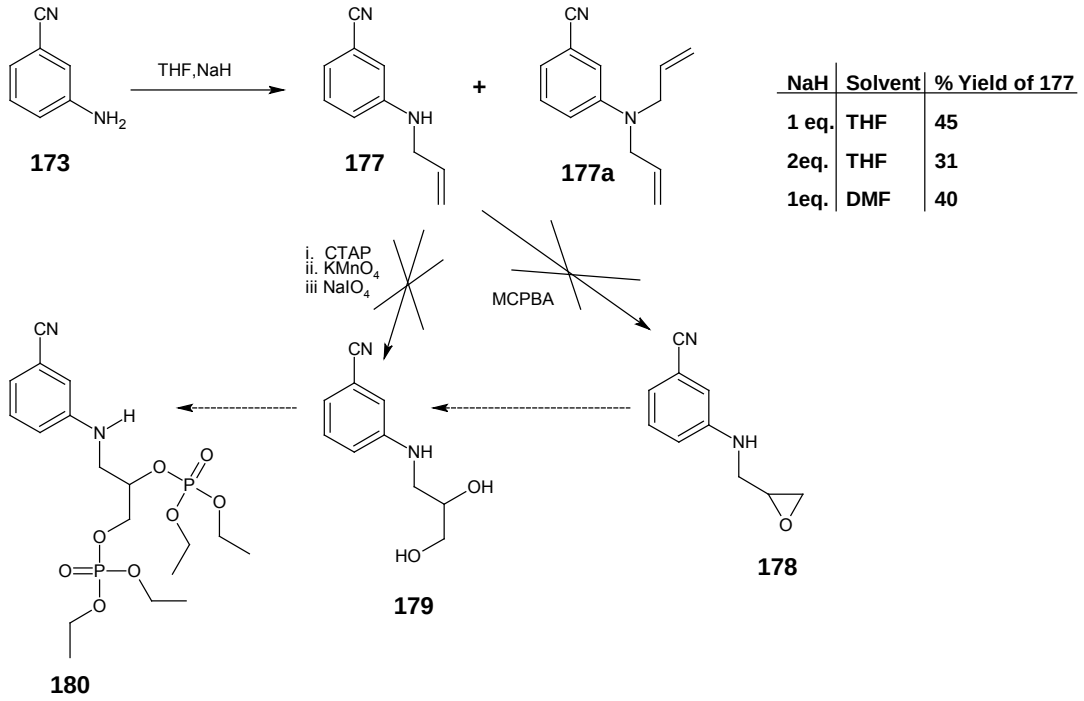

Scheme 39. Synthesis of compounds **177** and **177a**.

2'-H

Figure 56. 400MHz ^{1}H NMR spectrum of compound **177** in $CDCl_3$.

2'-H and 2"-H

Figure 57. 400MHz ^{1}H NMR spectrum of compound **177a** in $CDCl_3$.

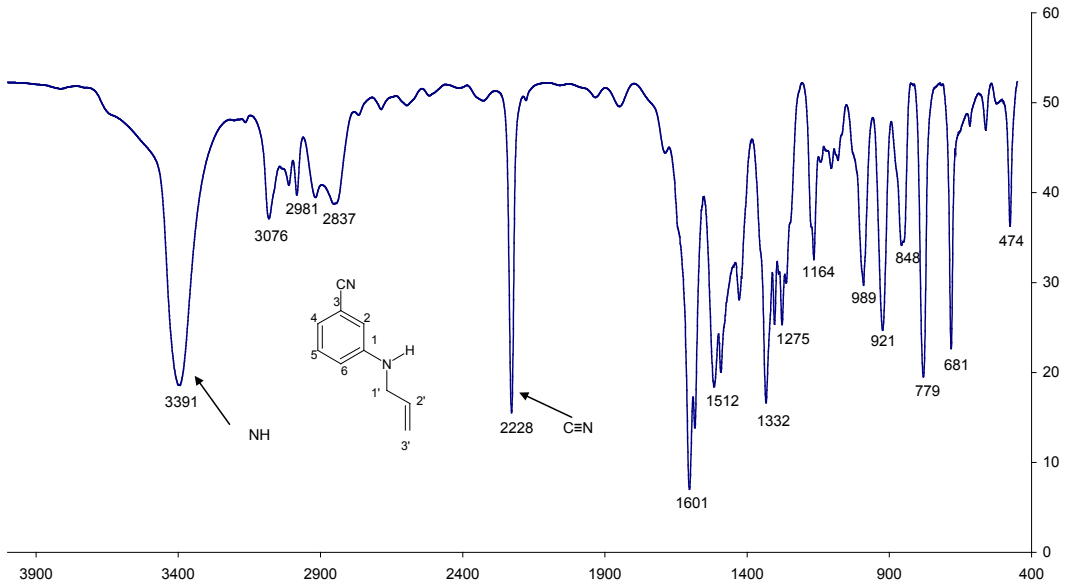

Figure 58. Mid-IR absorption of spectrum of compound **177**.

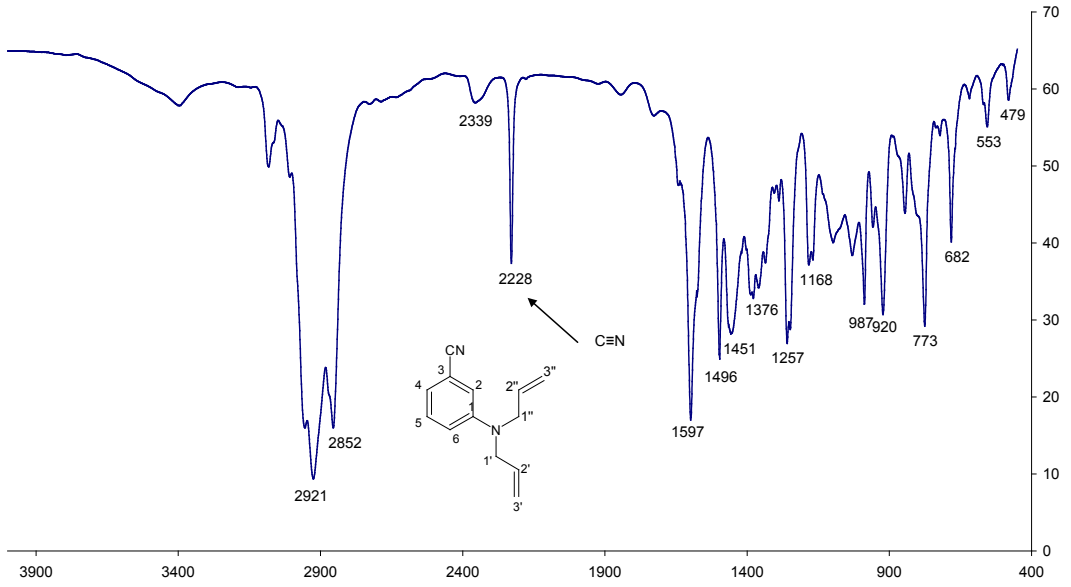

Figure 59. Mid-IR absorption of spectrum of **177a**.

*2.4.1.2. Preparation of 2-chloro-*N*-(3-cyanophenyl)acetamide 181 and diethyl [(3-cyanophenyl)carbamoyl]methyl phosphonate 182*

The chloroacetamide **181** was obtained in high yield of 95% by stirring 3-cyanoaniline **173** with chloroacetyl chloride[179] (Scheme 40). ^{1}H NMR analysis of the product **181** (Figure 60) reveals the CH_2Cl signal at 4.20 ppm as a singlet, while high-resolution mass spectrometric analysis revealed the molecular ion peak at *m/z* 194.02431 with 45% abundance relative to the base peak at *m/z* 118.05162. Phosphorylation of the chloroacetamide **181** with triethyl phosphite in an Arbuzov reaction[180] afforded the phosphonate **182** in 84% yield. The protons and carbon signals corresponding to the CH_2P methylene group are both observed to be split by the coupling to the ^{31}P nucleus in the ^{1}H and ^{13}C NMR spectra respectively (Figures 61 and 62). The carbonyl carbon is also observed to be split by the ^{31}P nucleus with a coupling constant of 4.5 Hz. The ^{31}P NMR spectrum (Figure 63) shows a signal at 18.30 ppm corresponding to the phosphorous atom. The high-resolution mass spectrum of the phosphonate **182** shows the molecular ion at *m/z* 296.01963 with 65% abundance relative to the base peak at *m/z* 179.08244. Attempts to effect catalytic hydrogenation of the nitrile moiety in compound **182**, in the presence of platinum on carbon catalyst, however, were unsuccessful.

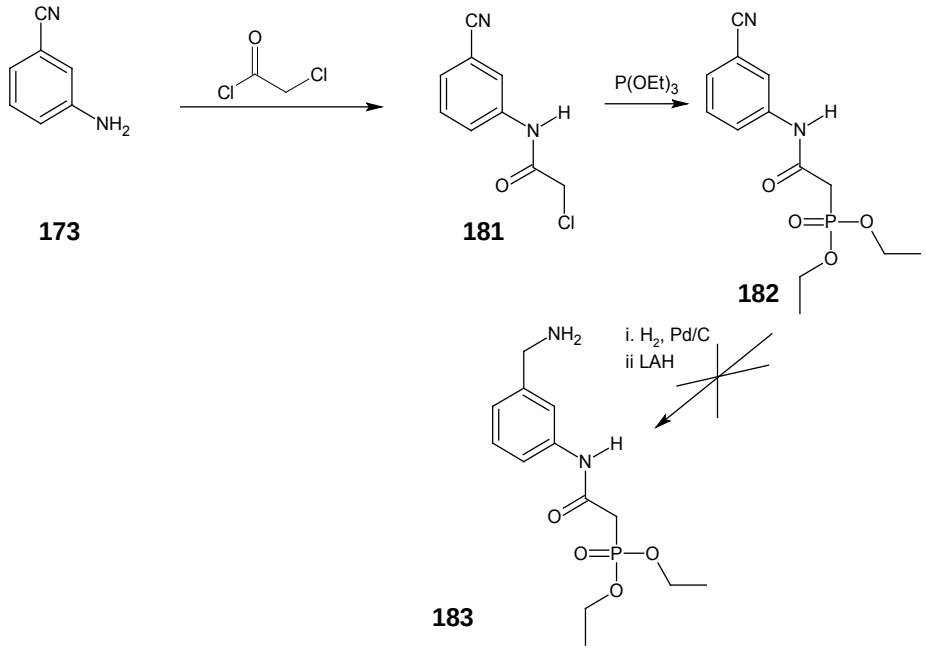

Scheme 40. Synthesis of compounds **181** and **183**.

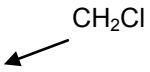

Figure 60. 400 MHz ^{1}H NMR spectrum of the chloroacetamide **181** in $CDCl_3$.

Figure 61. 400 MHz ^{1}H NMR spectrum of compound **182** in $CDCl_3$.

Figure 62. 100 MHz ^{13}C NMR spectrum of compound **182** in $CDCl_3$, showing splitting of the CH_2P and C=O signals by ^{31}P.

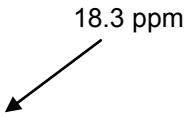

Figure 63. 162 MHz ^{31}P NMR of the phosphonate **182**.

*2.4.1.3. Preparation of 2-acetoxy-***N***-(3-cyanophenyl)acetamide 184***

Treatment of deprotonated 3-aminobenzonitrile **173** with acetoxyacetyl chloride[178] afforded 2-acetoxy-*N*-(3-cyanophenyl)acetamide **184** in 85% yield (Scheme 41). Formation of the product **184** was confirmed by spectroscopic methods. The HMBC NMR spectrum (Figure 64) shows the correlation between the NH proton and the carbonyl carbon of the carbamoyl group while the mid-IR spectrum showed an amide C=O absorption band at 1675 cm^{-1} and an ester C=O absorption band at 1735 cm^{-1}. Mass spectrometric analysis revealed the M+1 peak at *m/z* 219 with 60% abundance relative to the base peak at *m/z* 177. Attempted reduction of the nitrile group, in this case with lithium aluminium hydride[187] was also unsuccessful, and the difficulties associated with this seemingly straightforward transformation will have to be addressed in future studies.

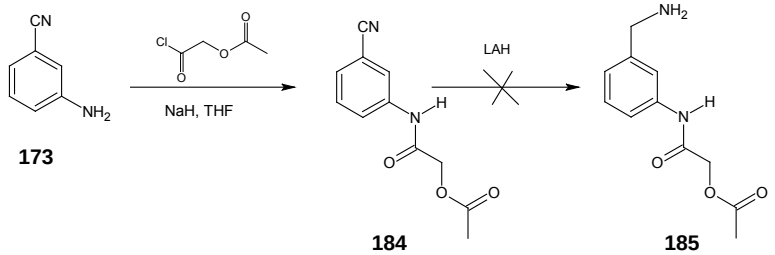

Scheme 41. Synthesis of 2-acetoxy-*N*-(3-cyanophenyl)acetamide **185**.

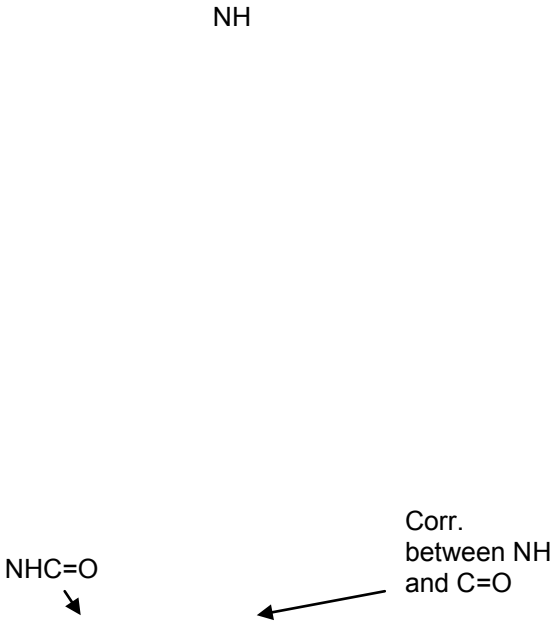

Figure 64. HMBC NMR spectrum of compound **184** in $CDCl_3$.

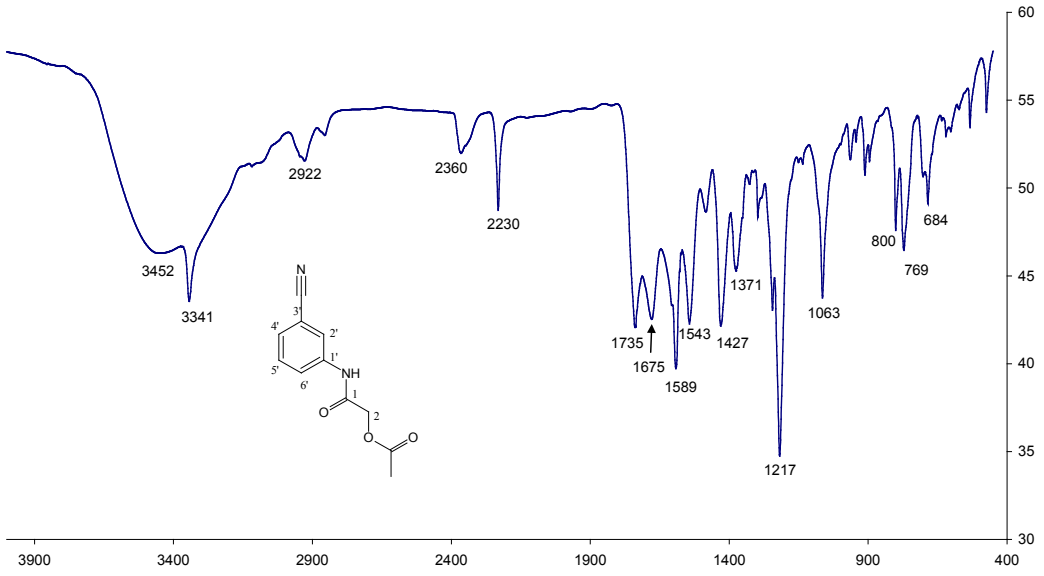

Figure 65. Mid-IR spectrum of compound **185** as solid deposit.

*2.4.1.4. Preparation of 2,3,4,5,6-pentaacetyl-*N*-(3-cyanophenyl)-gluconamide 186*

3-Aminobenzonitrile **173** was stirred with 2,3,4,5,6-pentaacetylgluconoyl chloride[167,168] **131** in pyridine to afford the gluconamide derivative **186** in 41% yield (Scheme 42), formation of which was confirmed by spectroscopic methods. The HMBC NMR spectrum (Figure 66) again shows the correlation between the NH proton and the carbonyl of the carbamoyl group. Mass spectrometric analysis of the gluconamide **186** shows the presence of the molecular ion at *m/z* 506 with 24% abundance relative to the base peak at *m/z* 505.

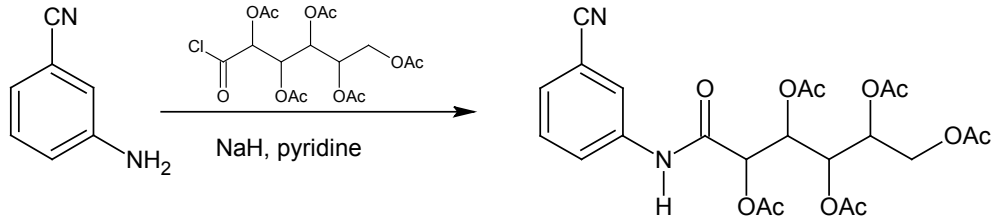

173 **186**

Scheme 42. Synthesis of the acetylated derivative **187**.

Figure 66. HMBC NMR spectrum of the gluconamide **186** in $CDCl_3$.

2.4.2. ATP mimics from resorcinol 187

Deprotonation of one of the hydroxyl groups of resorcinol with 1 equivalent of NaH,[169] followed by treatment with different alkylating and acylating agents,[169,178] afforded a set of primary substitution products as outlined in Scheme 43.

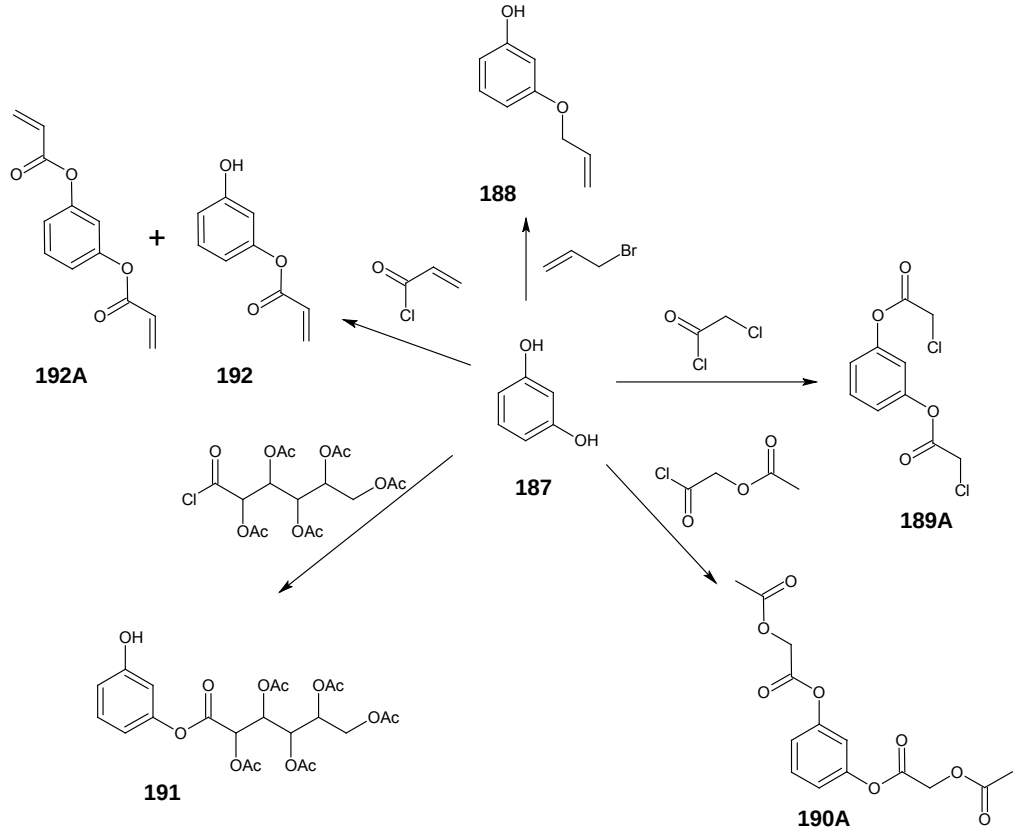

Scheme 43. ATP mimics derived from resorcinol.

Resorcinol **187** in dry THF was deprotonated with 1 equivalent of NaH and then treated with 1 equivalent of allyl bromide[169] under reflux to afford the allylated derivative **188** in 28% yield (Scheme 43). However, all attempts at dihydroxylating **188** with oxidizing agents, such as CTAP, $KMnO_4$ and $NaIO_4$ in the presence of $RuCl_3$ catalyst were unsuccessful.

Resorcinol **187** was similarly deprotonated and boiled under reflux with 1 equivalent of chloroacetyl chloride.[179] The reaction was repeated several times but each time the di-acylated product **189A** was obtained instead of the desired mono-acylated product.

When 1 equivalent acetoxyacetyl chloride was used instead of chloroacetyl chloride, the di-acylated product **190A** was obtained repeatedly instead of the desired mono-acylated product.

However, when resorcinol **187** was stirred with 2,3,4,5,6-pentaacetylgluconoyl chloride **131** in pyridine,[167,168] the desired mono-ester **191** was obtained in 24% yield (Scheme 43). The ^{1}H NMR spectrum of compound **191** (Figure 68) shows the expected acetyl and methine protons, while MS analysis revealed the molecular ion peak at *m/z* 498.

Resorcinol was again deprotonated with 1 equivalent of NaH and then treated with 1 equivalent of acryloyl chloride[169] (Scheme 43). In this case however, both the mono-acrylic and di-acrylic esters were obtained in very low yields. Attempts to improve the yield of the monoester by using 1 equivalent of KOH in ethanol as base appeared to result in the di-acrylic ester alone. Spectroscopic analysis confirmed the formation of both products. ^{1}H NMR spectra of both esters are shown in Figures 69 and 70 and it is clearly evident from integration data that both products have been isolated. Mass spectrometric analysis of the mono-ester **192** shows the presence of the molecular ion at *m/z* 164 in 97% abundance relative to the base peak at *m/z* 27, while the mass spectrum of the di-ester **192A** shows the presence of the molecular ion at *m/z* 218 with 80% abundance relative to a base peak at *m/z* 27.

Generally the desired mono-acylation proved difficult to achieve, except in the case of gluconoylation. Acylation of one of the resorcinol hydroxyl groups would increase the acidity of the remaining hydroxyl group relative to resorcinol itself thus favouring further deprotonation and formation of the di-acylated product (Figure 67). Formation of the mono-gluconoyl derivative can be argued to be due to steric hindrance by the first gluconoyl moiety on the molecule making the now more acidic second hydroxyl group less accessible to acylation.

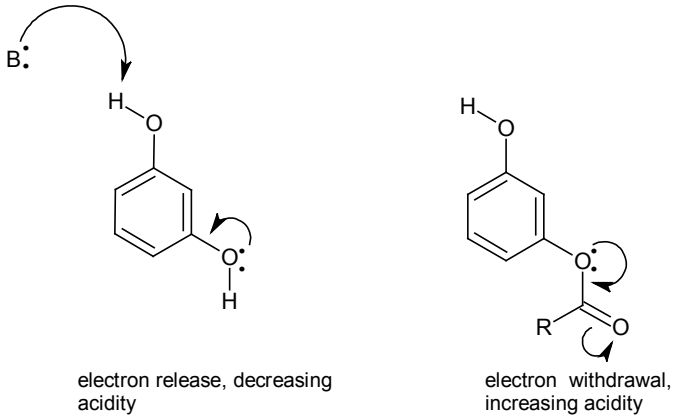

Figure 67. Explanation for di-acylation in resorcinol derivatives.

Figure 68. 400 MHz ^{1}H NMR spectrum of compound **191** in $CDCl_3$.

Figure 69. 400 MHz ^{1}H NMR spectrum of the mono-acrylic ester **192** in $CDCl_3$.

Figure 70. 400 MHz ^{1}H NMR spectrum the of di-acrylic ester **192A** in $CDCl_3$.

2.4.3. ATP mimics from 3-aminophenol

Deprotonation of the amino substituent on 3 -aminophenol **193** with NaH and treatment with different alkylating and acylating agents was expected to afford a set of primary substitution products (Figure 71). While regioselectivity might have been expected to be a major problem, the use of one equivalent of NaH[169] for deprotonation

of the substrate worked very well in achieving mono-alkylation and mono-acylations at the amino nitrogen.

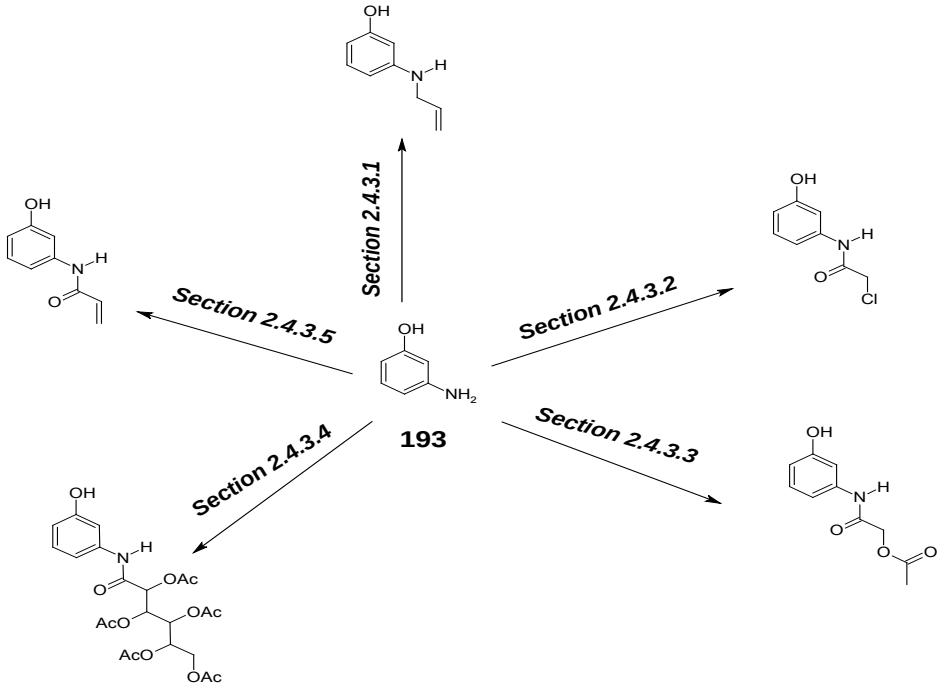

Figure 71. General approach to 3-aminophenol derivatives.

2.4.3.1. Preparation of N*-allyl-3-hydroxyaniline 194,* N*-allyl-3-allyloxyaniline 194A and* N,N*-diallyl-3-hydroxyaniline 194B*

Treatment of 3-aminophenol **193** with NaH and allyl bromide[169] afforded **194,** the desired allylated intermediate with two other allylated products **194A** and **194B**.

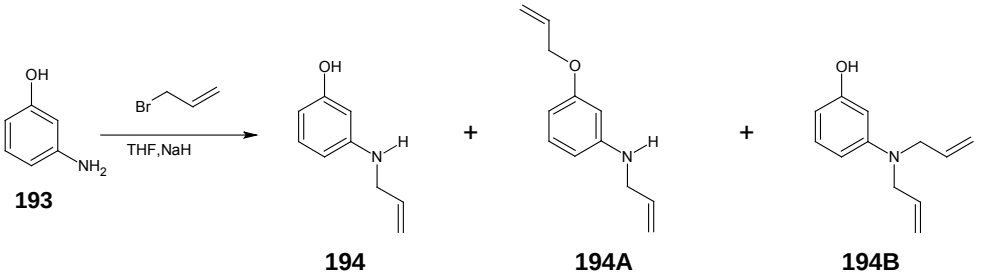

Scheme 44. Synthesis of compounds **194**, **194A** and **194B**.

In the comparative ^{1}H NMR spectra (Figure 72) of *N*-allyl-3-hydroxyaniline **194**, *N*-allyl-3-allyloxyaniline **194A** and *N*,*N*-diallyl-3-hydroxyaniline **194B**, the 1'-methylene

protons have similar chemical shift values (*ca.* 3.8 ppm), while the methyleneoxy protons in the *O*-allylated moiety **194A** resonate downfield at 4.51 ppm because of the greater de-shielding effect of the oxygen atom. It is also observed that the 2'-H (5.97 ppm) and 2"-H (6.07 ppm) vinylic methine protons in the *N*,*O*-di-allylated product **194A** resonate as multiplets at slightly different chemical shifts, while the corresponding methine protons in the *N*,*N*-di-allylated product **194B** resonate as a multiplet at 5.58 ppm being in the same chemical environment. The C-3' vinylic carbons in the *N*-allylated systems **194** and **194A** (Figure 73) resonate at similar chemical shift values (*ca.* 116 ppm), while the corresponding nuclei in the *N*,*O*-di-allylated system resonate at different chemical shift values. MS analysis of the products gave the following results: compound **194** showed the presence of the molecular ion at *m/z* 149 as the base peak, compound **194A** showed the presence of the molecular ion at *m/z* 189 with 95% abundance relative to the base peak at *m/z* 121, while **194B** showed the presence of the molecular ion at *m/z* 189 as the base peak.

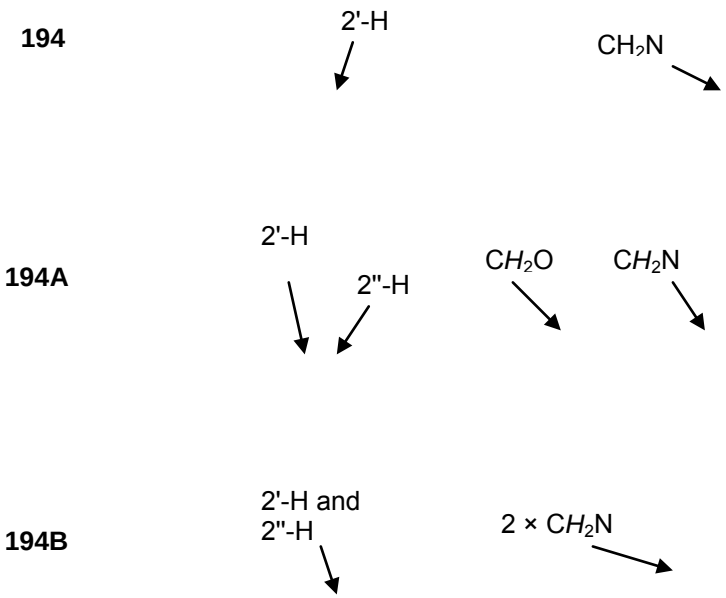

Figure 72. Comparative 400 ^{1}H NMR spectra of **194**, **194A** and **194B**, in CDCl3.

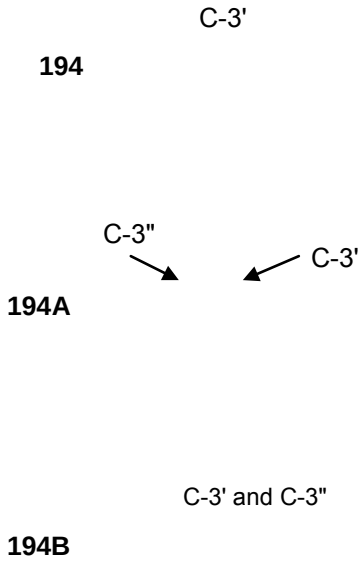

Figure73. Comparative partial 100 MHz ^{13}C NMR spectra of compounds **194**, **194A** and **194B** in $CDCl_3$.

Attempts to di-hydroxylate the mono-allylated product **194** with different agents such as CTAP, KMnO4 and $NaIO_4$ were unsuccessful - a pattern observed with earlier systems.

*2.4.3.2. Preparation of 2-chloro-***N***-(3-hydroxyphenyl)acetamide 195 and diethyl {[(3-hydroxy-phenyl)carbamoyl)methyl}phosphonate 196*

2-Chloro-*N*-(3-hydroxyphenyl)acetamide **195** was obtained in 76% yield by treating 3-aminophenol in dry THF under nitrogen with NaH followed by chloroacetyl chloride[179] under reflux (Scheme 45). The correlation between the NH proton and the carbonyl carbon can be observed in the HMBC spectrum of compound **195,** confirming that the substitution had occurred at the amino group and not the hydroxyl group (Figure 74).

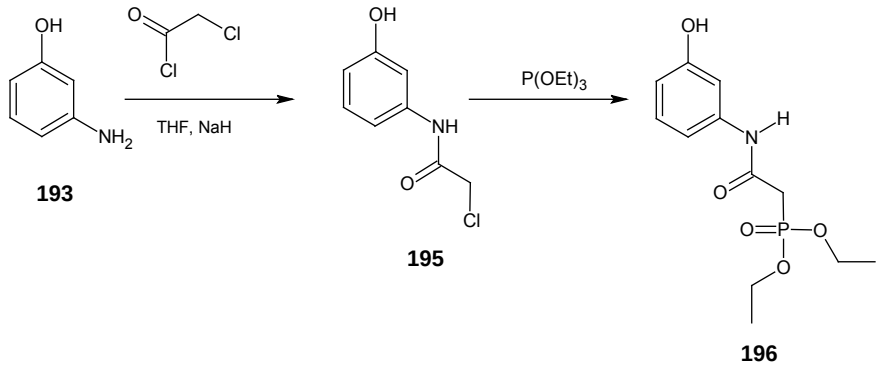

Scheme 45. Route to the phosphonate ester **197**.

Figure 74. HMBC NMR spectrum of **195** in DMSO-d_6.

Phosphorylation of **195** with triethyl phosphite (Arbuzov reaction)[180] afforded the diethyl phosphonate ester **196** in 48% yield. The protons and carbon of the CH_2P group both resonate as doublets due to coupling to the ^{31}P nucleus in the ^{1}H and ^{13}C NMR spectra, respectively (Figure 75). The C=O is also observed to be split by the ^{31}P with a coupling constant of 4.1Hz ^{31}P. The phosphorous ^{31}P signal is at 24.2 ppm.

Figure 75. Coupling of ^{31}P to (**a**) C*H*$_2$ and (**b**) *C*H$_2$ and C=O in compound **196**.

Interestingly, the phosphonate ester **196** was found to inhibit the DOX-P reductoisomerase enzyme of the malaria parasite *Plasmodium faciparum* (*Pf*DXR)

both *in vitro* (in Biochemistry Department at Rhodes) and from Saturation Transfer Difference (STD)[188,189] NMR spectroscopy experiments (in Chemistry). The protein-ligand interaction was confirmed by the presence of ligand proton signals in the *Pf*DXR protein spectrum (Figure 76). The implication of this observation is that although, the phosphonate ester **196** was made to inhibit the *Mycobacterium tuberculosis* enzyme glutamine synthetase, it is to be explored in our group as a potential therapeutic for malaria, and analogues are currently being made!

Figure 76. 600 MHz ^{1}H STD NMR spectrum of **196** and *Pf*DXR showing interaction between protein and ligand.

*2.4.3.3. Preparation of 2-acetoxy-***N***-(3-hydroxyphenyl)acetamide 197*

2-Acetoxy-*N*-(3-hydroxyphenyl)acetamide **197** was isolated pure on treating deprotonated 3-aminophenol **193** with acetoxyactyl chloride[178] (Scheme 46). All the proton and carbons are accounted for in the ^{1}H NMR and ^{13}C NMR spectra, respectively. The methyl signal is visible at 2.11 ppm while the methylene carbon resonates at 62.5 ppm The OH and NH protons resonate at 9.39 ppm and 9.92 ppm, respectively, while the amide and ester carbonyls resonate at 165.2 ppm and 169.9 ppm, respectively, as determined from the correlations between corresponding proton

and carbon signals in the HMBC spectrum (Figure 77). High-resolution mass spectroscopic analysis shows the presence of the molecular ion at *m/z* 209.068446 with 40% abundance relative to the base peak at *m/z* 109.053492.

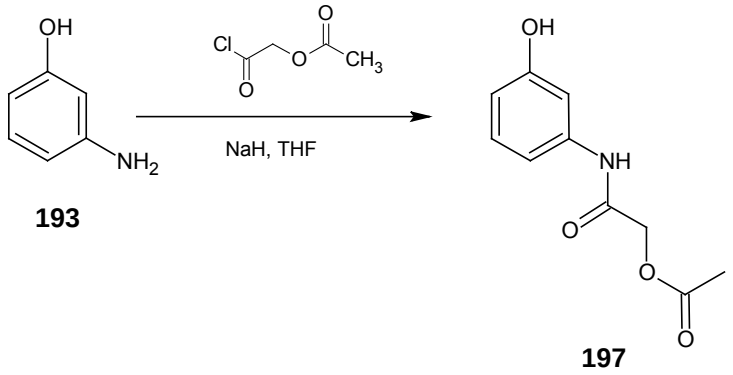

Scheme 46. Route to the ester **197**.

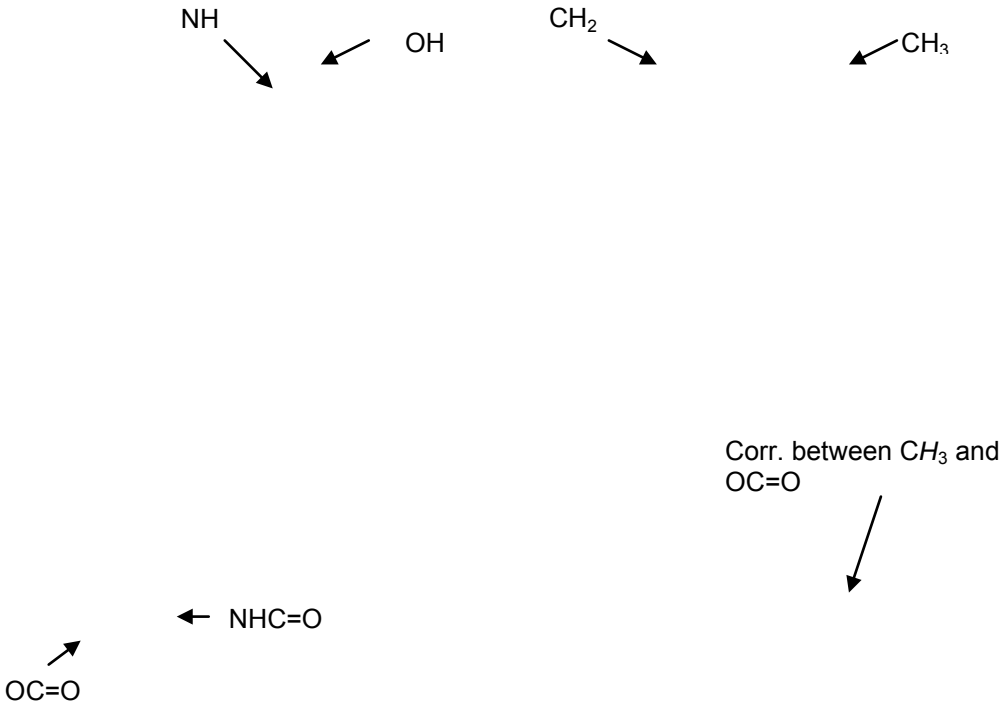

Figure 77. HMBC NMR spectrum of compound **197** in DMSO-d_6.

*2.4.3.4. Preparation of 2,3,4,5,6-pentaacetyl-*N*-(3-hydroxyphenyl)gluconamide 198*

2,3,4,5,6-Pentaacetyl-*N*-(3-hydroxyphenyl)gluconamide **198** was isolated successfully from the reaction between 3-aminophenol **193** and acid chloride[178] **131** (Scheme 47). The five acetoxymethyl groups are accounted for by the fifteen protons corresponding to the series of singlets that resonate between 2.24 and 2.01 ppm in the ^{1}H NMR spectrum (Figure 78). In the ^{13}C NMR spectrum, the presence of only four carbon signals corresponding to five methyl carbons is attributed to the coincidence of two of the signals. Mass spectrometric analysis confirmed the formation of **198** as the molecular ion is prominent at *m/z* 497.450192 as the base peak.

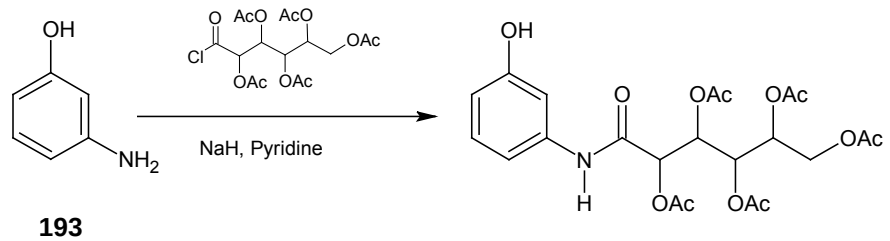

193 **198**

Scheme 47. Route to the acetylated derivative **198**.

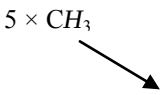

Figure 78. 400 MHz ^{1}H NMR spectrum of compound **198** in $CDCl_3$.

Figure 79. 100 MHz ^{13}C NMR spectrum of compound **198** in $CDCl_3$.

2.4.3.5. Reaction of 3-aminophenol with acryloyl chloride

Treatment of 3-aminophenol **193** in dry THF with 1 equivalent of NaH at 0°C, followed by 1 equivalent of acryloyl chloride,[169] afforded both the mono-acylated and di-acylated products **199** and **199A**. The products were separated and fully characterized but the yield of the acrylamide **199** was too small for the reaction to be carried further.

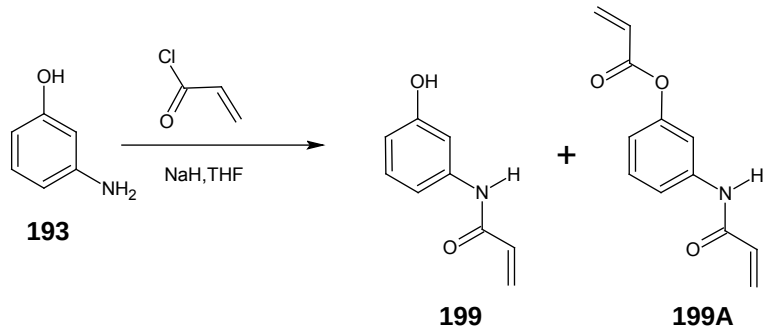

Scheme 48. Route to acrylic amide **199** and acrylic ester **199A**

2.4.4. ATP mimics from 3-aminobenzyl alcohol

Deprotonation of the amino substituent of 3-aminobenzyl alcohol **199** with NaH and treatment with different alkylating and acylating agents was expected to afford a further set of primary substitution products as scaffolds for elaboration to ATP mimics (Figure 80).

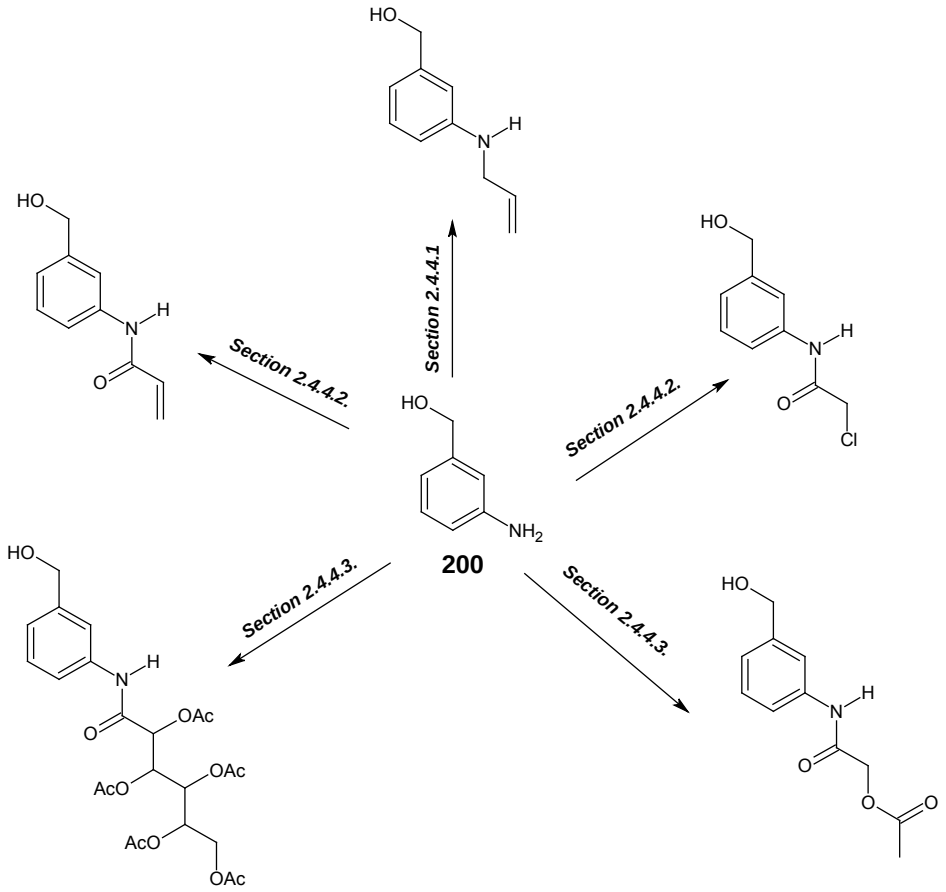

Figure 80. General approach to 3-aminobenzyl alcohol derivatives.

2.4.4.1. Reaction of 3-aminobenzylalcohol with allyl bromide

Treatment of 3-aminobenzyl alcohol **200** with NaH and allyl bromide[169] afforded the desired product *N*-allyl-3-(hydroxymethyl)aniline **201** in 10% yield together with *N*-allyl-3-(allyloxymethyl)aniline **201A,** *N*,*N*-diallyl-3-(hydroxymethyl)aniline **201B** and 3-(allyloxymethyl)aniline **201C** (Scheme 49). The structures of all four products were confirmed by spectroscopic methods, the assignments being based largely on a comparison of the allyl group signals in each compound. Thus, from the inspection of the spectra of all four products (Figure 81), it is apparent that the *N*-allyl methylene protons resonate at *ca.* 3.8 ppm, the *O*-allyl methylenes at *ca.* 4.0 ppm and the hydroxymethylene protons at *ca.* 4.6 ppm. The structural assignments are consistent with the ^{13}C, DEPT135, HSQC and HMBC data and are supported by the ^{13}C NMR predicted values (Section 2.5).

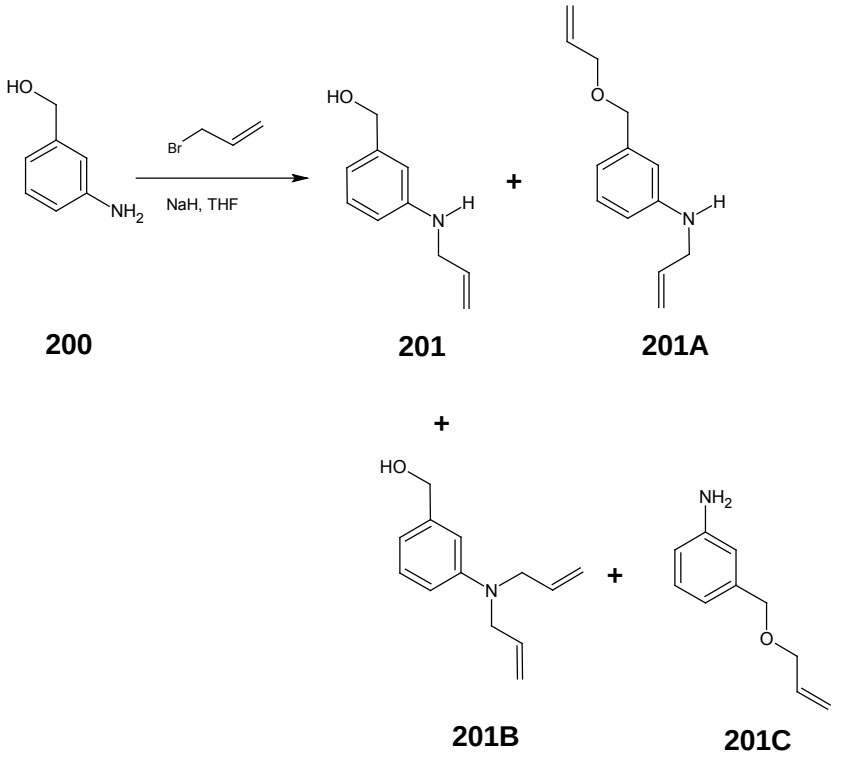

Scheme 49. Allylation of 3-aminobenzylalcohol **200**.

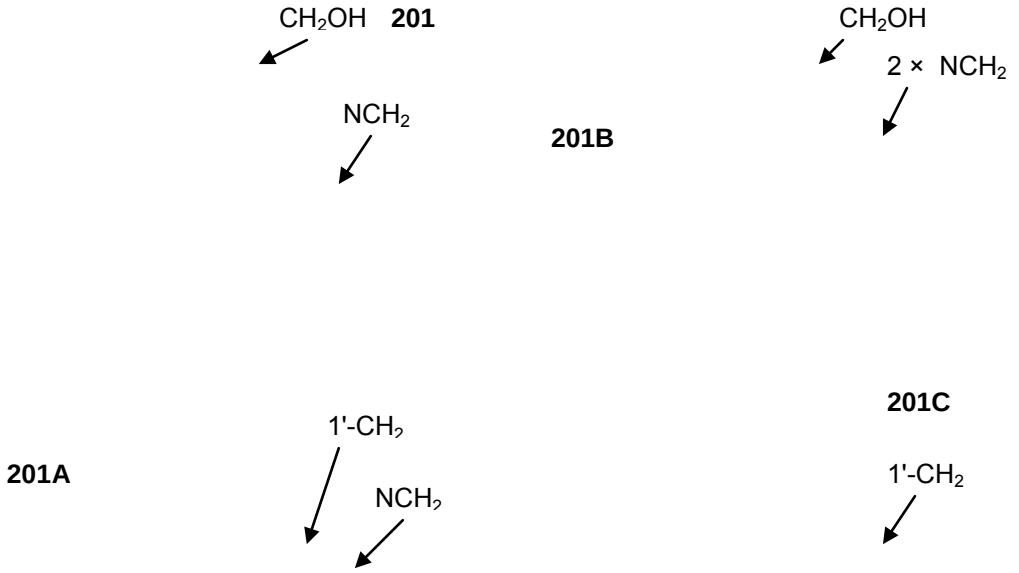

Figure 81. Comparison of 400 MHz ^{1}H NMR spectra of compounds **201**, **201A, 201B** and **201C** in $CDCl_3$.

2.4.4.2. Reaction of 3-aminobenzyl alcohol with chloroacetyl chloride and acryloyl chloride

The *N,O*-bis-chloroacetylated product **202A** was obtained in 95% yield on stirring 3-aminobenzyl alcohol **200** with chloroacetyl chloride[179] under nitrogen. In another reaction a mixture of both the amide **202** and the bis-chloroacetylated product **202A** were obtained on refluxing deprotected (using NaH) 3-aminobenzyl alcohol **200** with 1 equivalent of chloroacetyl chloride (Scheme 50). In the HMBC spectrum of the amide **202** (Figure 82), the chloromethylene protons were observed to correlate with the carbonyl carbon only, while hydroxymethylene protons correlate with aromatic carbons. The hydroxymethylene protons resonate as a singlet at 4.50 ppm while the chloromethylene proton singlet is at 4.42 ppm. The two pairs of chloromethylene protons in the bis-acylated product **202A** may be differentiated by examining the HMBC spectrum (Figure 83). The carbonyl carbon signal at 167.1 ppm correlates with the 1'-methyleneoxy signal at δ 5.19 ppm as well as with the 4'-chloromethylene signal at 4.01 ppm, making it possible to distinguish between the amide and ester methylene signals as well as the corresponding carbonyl carbon signals. The Mid-IR spectrum of compound **202A** shows both an ester C=O absorption band at 1747 cm^{-1}

and an amide C=O absorption band at 1664 cm^{-1} (Figure 84). MS analysis showed the presence of the molecular at *m/z* 199 in 10% abundance relative to the base peak at m/z 198 for compound **202**, while the molecular ion for compound **202A** was observed at *m/z* 276 as the base peak.

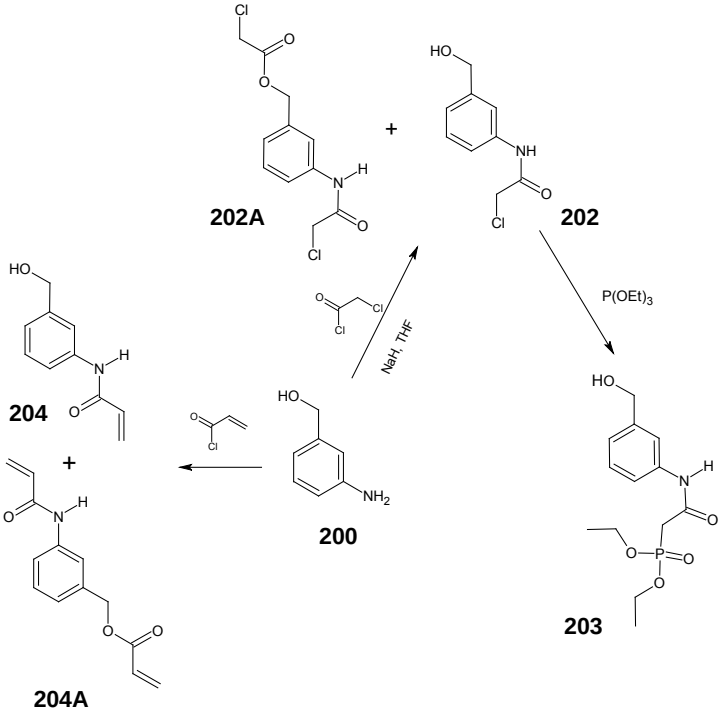

Scheme 50. Routes to the Arbuzov product **203**, and acryloyl chloride derivatives **204** and **204A**.

Phosphorylation of the mono-acylated product **202** (Scheme 50) with triethyl phosphite (Arbuzov reaction)[180] afforded the expected phosphonate ester **203** in 37% yield. The protons and carbon signals for the CH_2P moiety are both split due to coupling with the ^{31}P nucleus (Figures 85 and 86), while the C=O signal exhibits a doublet with a coupling constant of 129.9 H z due to coupling with ^{31}P. The phosphorous ^{31}P signal is observed at 23.5 ppm. High-resolution MS analysis of **203** showed the presence of the molecular at *m/z* 301.275911 as the base peak.

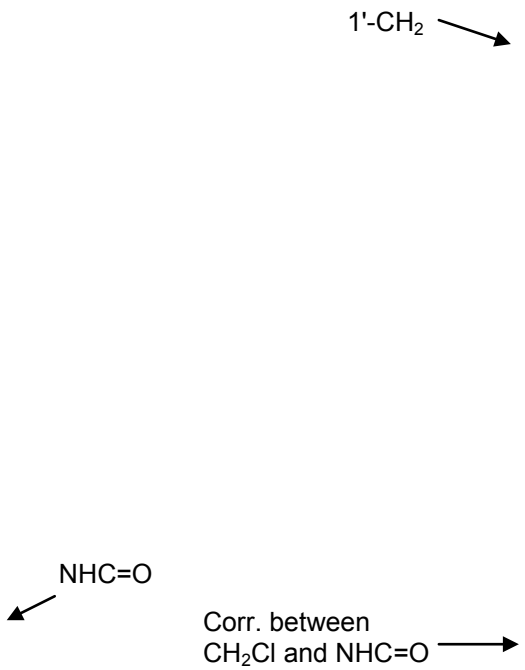

Figure 82. HMBC spectrum of the mono-acylated product **202** in $CDCl_3$.

Reaction of 3-aminobenzyl alcohol **200** in dry THF with 1 equivalent NaH at 0°C, followed by 1 equivalent acryloyl chloride, afforded a mixture of both the acrylamide **204** and the acrylate ester **204A** (Scheme 50). The products were separated and characterized spectroscopically, but the yields were too low for the reactions to be carried further in the available time.

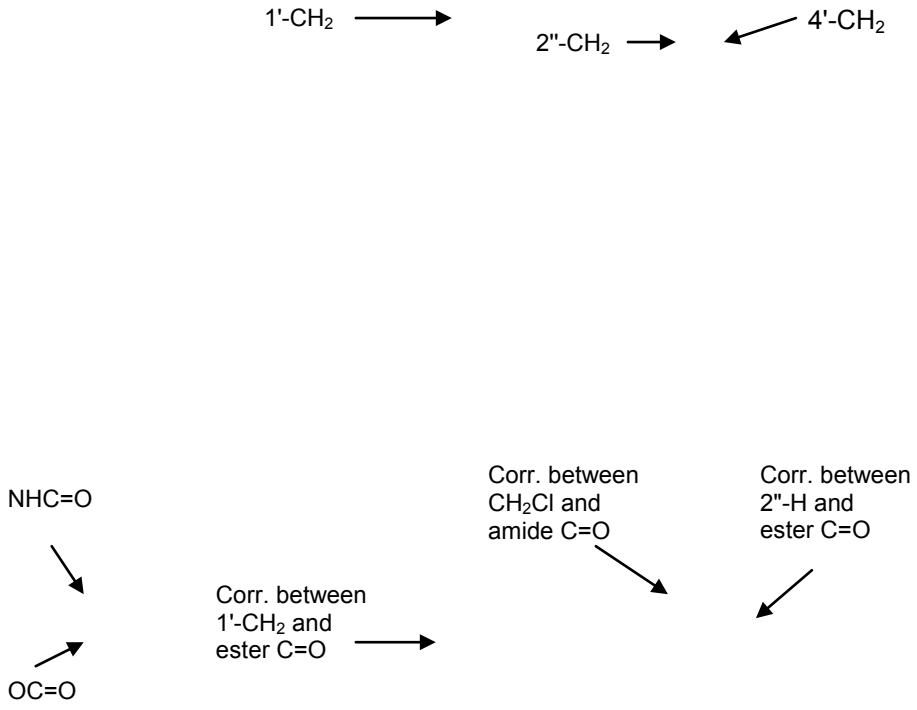

Figure 83. Partial HMBC spectrum of the di-acylated product **202A** in $CDCl_3$.

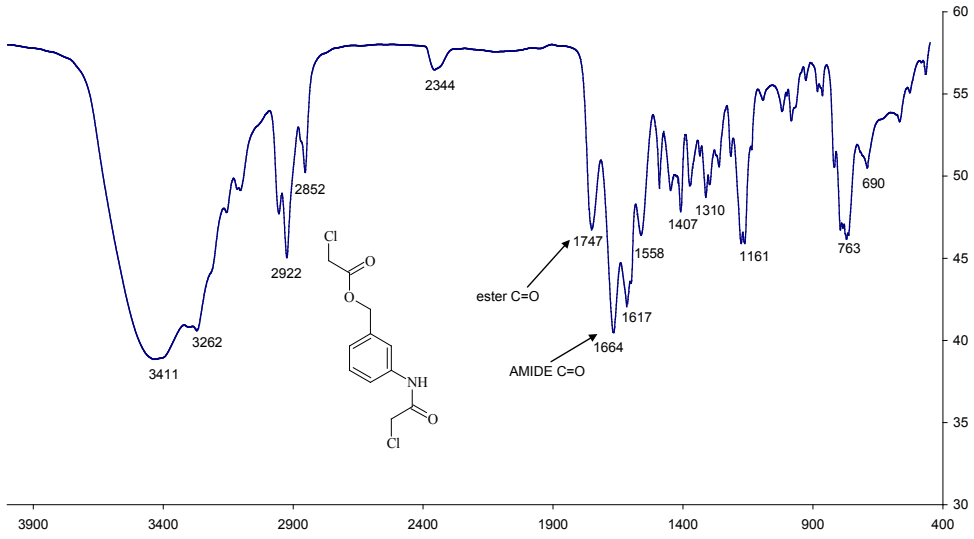

Figure 84. Mid-IR spectrum of **202A** as solid deposit.

Figure 85. 400MHz ^{1}H NMR of compound **203** in $CDCl_3$.

Figure 86. 100 MHz ^{13}C NMR spectrum of compound **203** in $CDCl_3$.

2.4.4.3. Reaction of 3-aminobenzyl alcohol with acetoxyacetyl chloride and 2,3,4,5,6-pentaacetylgluconoyl chloride

2-Acetoxy-*N*-[(3-hydroxymethyl)phenyl]acetamide **205** was isolated pure on treating deprotonated 3-aminobenzyl alcohol **200** with acetoxyacetyl chloride[179] (Scheme 51). In the HMBC spectrum (Figure 87), correlation is obtained between the methyl signal at 2.19 ppm and the ester carbonyl signal at 169.6 ppm, while the amide C=O carbon resonating at 165.3 ppm correlates with the 2-methylene signal at 4.63 ppm. High-resolution mass spectrometric analysis shows the presence of the molecular ion at *m/z* 223.08369 as the base peak.

The 2,3,4,5,6-pentaacetyl-*N*-(3-hydroxyphenyl)gluconamide derivative **206** was also isolated successfully from the reaction between 3-aminobenzyl alcohol **200** and the gluconoyl chloride[167,168] **131** (Scheme 51). The five acetoxymethyl groups are accounted for by the fifteen protons resonating as a series of singlets between 2.02 and 2.24 ppm in the ^{1}H NMR spectrum (Figure 88); the overlapping carbon-13 signals at *ca.* 20 ppm correspond to the five methyl groups in the ^{13}C NMR spectrum of **206**, but six discrete signals are evident in the carbonyl carbon region at *ca.* 163-171 ppm (Figure 89). MS analysis confirmed the formation of compound **206** with the molecular ion appearing at *m/z* 511.16685 as the base peak.

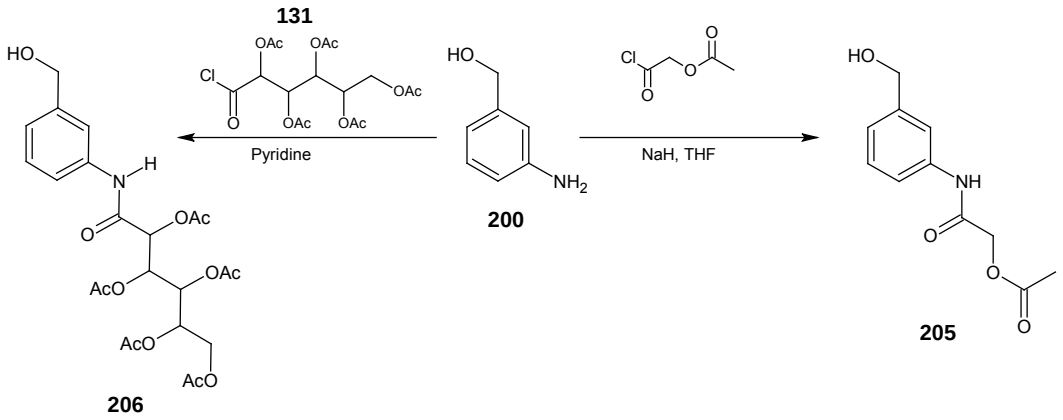

Scheme 51. Routes to amide ester 205 and acetylated derivative **206**

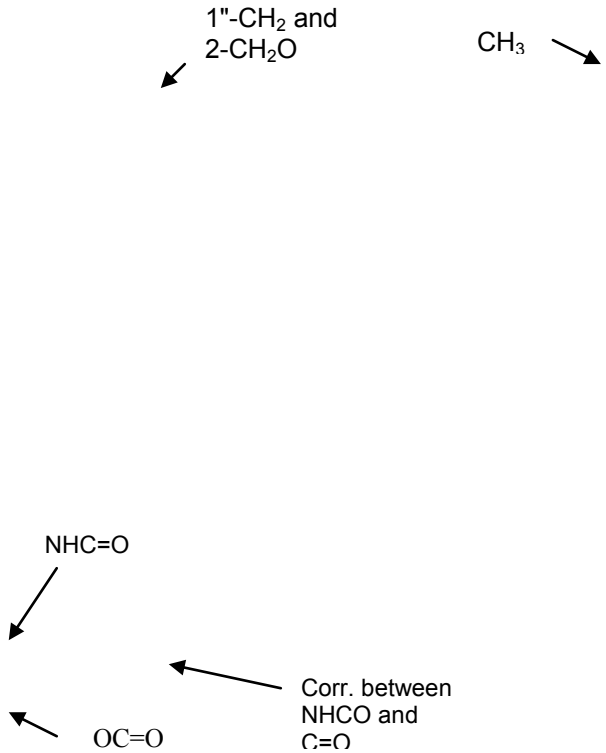

Figure 87. Partial HMBC spectrum of compound **205** in $CDCl_3$.

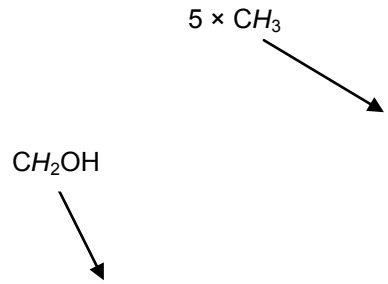

Figure 88. 400 MHz ^{1}H NMR spectrum of compound **206**.

Figure 89. 100 MHz ^{13}C NMR spectrum of compound **206**.

2.4.5. ATP mimics from 3-hydroxy- and 3-aminobenzoic acid

Issues of regioselectivity also arose in the reaction of 3-hydroxy- and 3-aminobenzoic acid with allyl bromide.[169] Treatment of both substrates with 1 e quivalent NaH, followed by allyl bromide yielded the mono-allylated products **208** and **210** respectively, while use of 2 equivalents of NaH yielded the di-allylated products **208A** and **210A**, respectively, (Scheme 52). The position of the methylene proton signals in the ^{1}H NMR spectra of all these allylated compounds as well as comparisons of experimental and predicted ^{13}C NMR data were used to confirm their structures. In the ^{1}H NMR spectra of compounds **208** and **210**, the 1'-methylene protons resonate at 4.81 ppm and 3.74, respectively, (Figure 90), confirming that these methylene groups are in different chemical environments in the mono-allylated compounds.

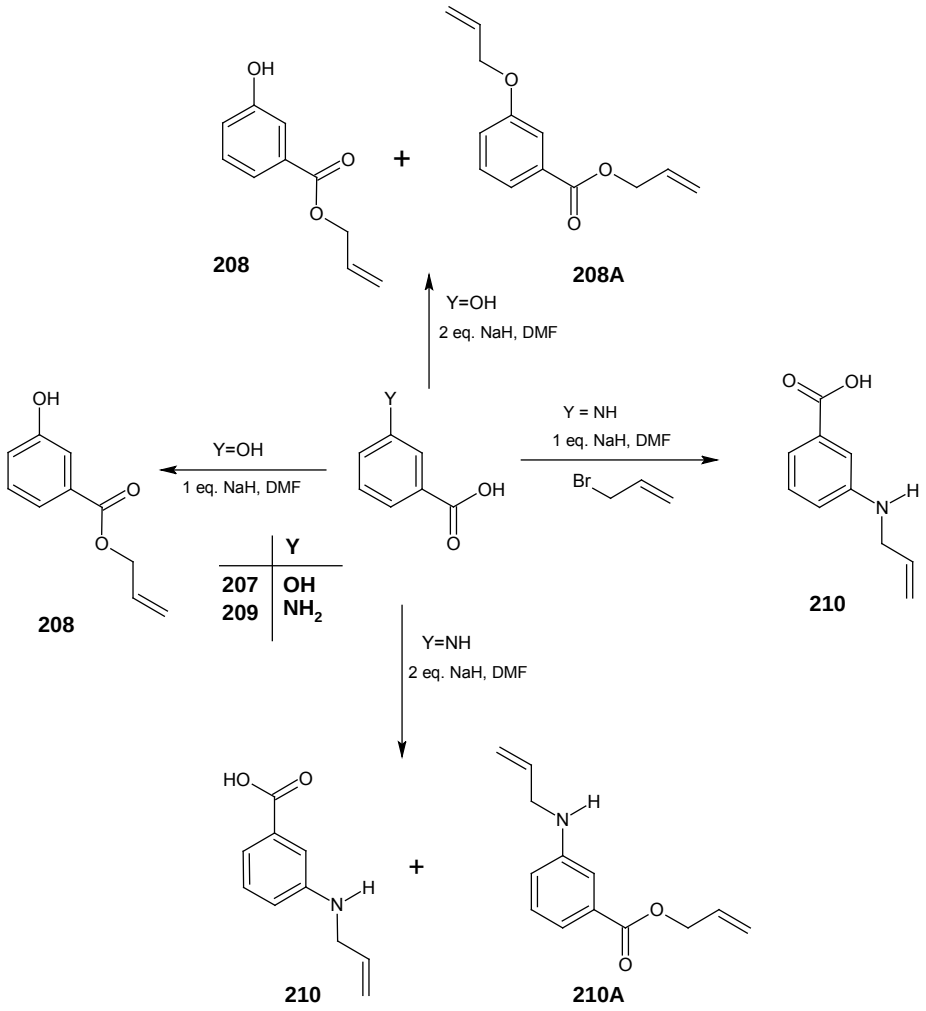

Scheme 52. Synthesis of compounds **208**, **208A**, **210** and **210A**.

These values are very similar to the predictions by the Modgraph NMR predict programme (Section 2.5) which indicate their chemical shifts to be 4.92 ppm and 3.73 ppm, respectively, confirming that the amino group was mono-allylated in compound **210** while the carboxylic acid group was allylated in the mono-allylated product **208**. In the di-allylated compound **210A**, the 2'- (at δ 5.94 ppm) and 2"- (at δ 6.02 ppm) methine protons are clearly observed as separate multiplets confirming that there is no di-substitution on the amine nitrogen (Figure 91). Unfortunately, attempts at dihydroxylating these alkenes were again unsuccessful.

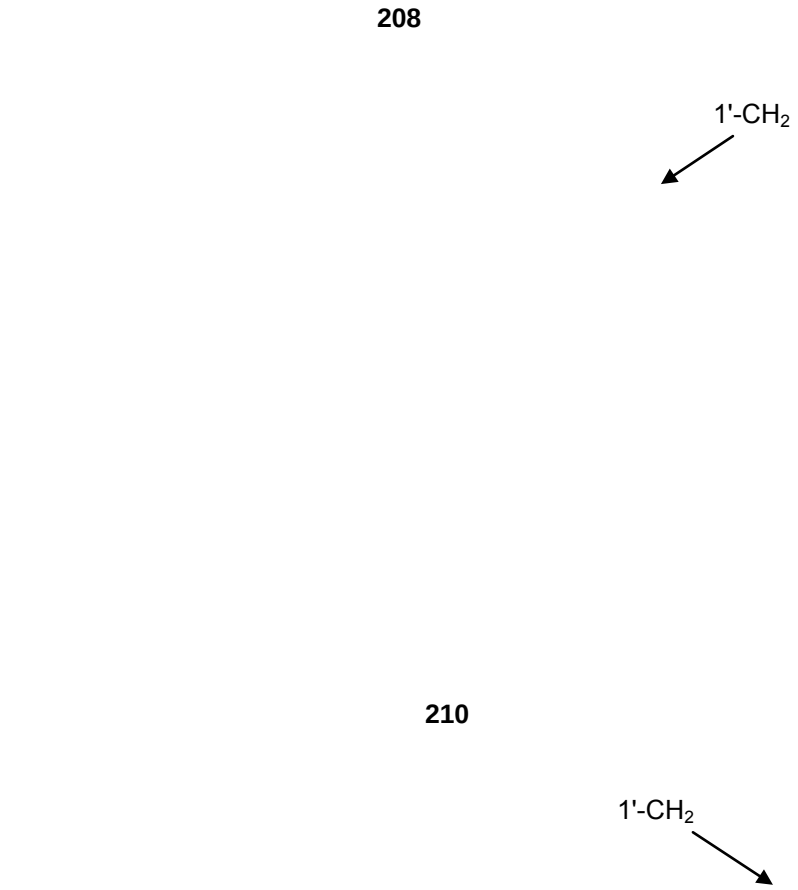

Figure 90. Comparison of 400 MHz ^{1}H NMR spectra of mono-allylated derivatives **208** and **210**.

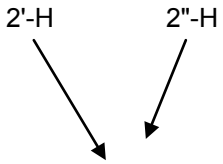

Figure 91. 400 MHz ^{1}H NMR spectra of di-allylated derivative **210A** in $CDCl_3$.

2.5. Application of NMR chemical shift prediction programmes

The Modgraph NMRPredict programme (version 3.2.2) was used to verify chemical shift assignments of selected systems. This programme can be used to predict both ^{1}H and ^{13}C chemical shifts. The Hierarchical Organization of Spherical Environments (HOSE) code and the Neural Network (Nnet) algorithm are the two approaches used for prediction. The HOSE code looks at a carbon atom relative to its spherical environments and uses this information based on the NMR spectral data base of thousands of compounds it contains as references. The draw-back of this approach is that if the query compound is not well represented in the data base, the prediction is not reliable as the programme can only make a prediction to a maximum of two spheres. Another disadvantage of this method is that it uses the contents of the data base and, hence, it is prone to inherent errors or bias. The Nnet is a general and more reliable approach as it is much more error tolerant and more accurate in predicting the chemical shifts of atoms not encountered before.[190] The Modgraph data presented in this section is a combination of both the HOSE and Nnet approaches. For comparative purposes, use was also made of the ChemWindow C-13 prediction module. The relevant ^{13}C data is tabulated on the following pages and, while comment is generally limited to particular assignments, significant discrepancies between experimental and predicted data are highlighted in the various tables.

2.5.1. NMR chemical shift prediction for adenosine analogues

2-(6-Aminopurin-9-yl)-5[7-diethylphosphoryloxy)-2-5-dioxaheptyl]-3,4-dihydroxy-tetrahydrofuran 3,4-acetonide 138

The experimental chemical shifts assigned for compound **138** were compared with shift values provided by both NMR predict programmes, Modgraph and ChemWindow. Generally the Modgraph data is more comparable to the experimental data than the ChemWindow data. The CH_3CH_2OP protons resonate as superimposed triplets at 1.38 ppm in the experimental spectrum while Modgraph predicts them to be at 1.29 ppm. The ^{13}C signals for the polyoxyalkyl centres, C-1", C-3", C-4", C-6" and C-7", are present in the ^{13}C NMR spectrum between 66.6 and 66.7 ppm, while both ChemWindow and Modgraph predict them to be between 66.5 and 71.2 ppm (Table 3). However, the ChemWindow predictions tend to vary significantly from the

experimentally established values, *over-estimating* certain aromatic carbons by as much as 9 ppm and *under-estimating* alkyl carbons by as much as 13 ppm (data highlighted in yellow).

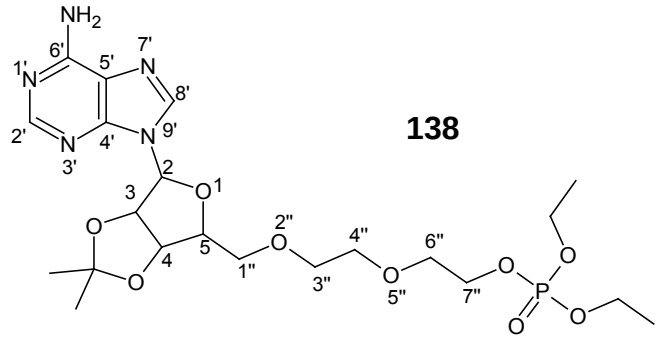

138

Table 3. Experimental and predicted ^{13}C NMR data for compound **138**

^{13}C nuclei	**a**	**b**	**c**
CH_3P	16.02	15.8	14.3
CH_3P	16.09	15.8	14.3
C.$(CH_3)_2$	25.3	25.9	28.6
C.$(CH_3)_2$	27.1	25.9	28.6
CH_2P	64.08	63.8	58.6
CH_2P	64.10	63.8	58.6
1",3",4",6"and 7"	66.6-66.7	66.3-71.4	66.5-71.2
5	81.8	86.2	71.6
3	84.4	85.2	78.1
4	85.4	81.7	72.7
2	91.0	91.1	83.1
C.$(CH_3)_2$	114.7	114.1	101.6
5'	119.9	119.7	113.7
8'	140.2	139.4	147.9
4'	149.0	149.0	157.2
2'	150.8	152.4	151.1
6'	154.4	156.0	156.1

a = Experimental values, b = Modgraph predict, c = ChemWindow predict

2-(6-Aminopurin-9-yl)-5-[(2-chloroacetoxy)methyl]-3,4-dihydroxytetrahydrofuran 3,4-acetonide 141 and 2-[6-(2-chloroacetamido)purin-9-yl]-5-[(2-chloroacetoxy)-methyl]-3,4-dihydroxytetrahydrofuran 3,4-acetonide 141A

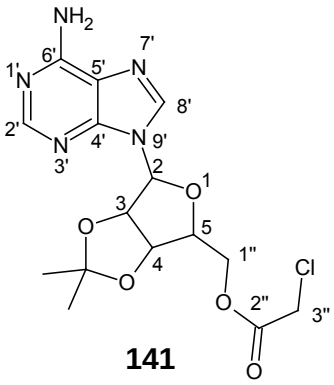

141

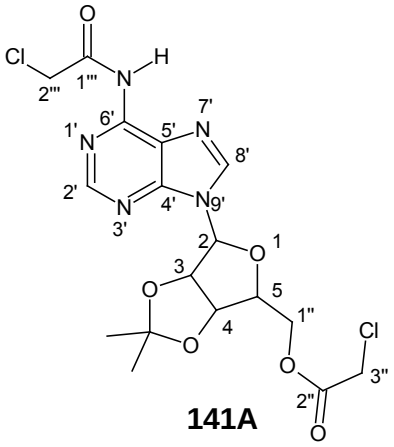

141A

Table 4. Experimental and predicted ^{13}C NMR data for compounds **141** and **141A**

142

^{13}C nuclei	**a**	**b**	**c**
C.CH_3	25.3	25.9	28.6
C.CH_3	27.1	25.9	28.6
CH_2Cl	44.5	40.6	48.3
1"	65.4	64.0	65.1
5	81.5	83.8	70.5
3	84.1	83.2	77.8
4	84.6	80.9	72.6
2	90.9	91.9	82.8
$C.(CH_3)_2$	114.7	114.1	101.6
5'	120.3	119.7	113.7
8'	139.8	139.4	147.9
4'	149.1	149.0	157.2
2'	153.1	152.4	151.1
6'	155.7	156.0	156.1
C=O	166.8	167.5	166.4

142A

^{13}C nuclei	**a**	**b**	**c**
C.CH_3	25.3	25.9	28.6
C.CH_3	27.1	25.9	28.6
3"	40.5	40.6	48.3
2'''	44.6	43.8	48.6
1"	65.3	64.0	65.1
5	81.3	83.8	70.5
3	84.1	83.2	77.8
4	84.6	80.9	72.6
2	91.1	91.1	82.8
$C.(CH_3)_2$	115.0	114.1	101.6
5'	122.5	122.6	119.6
8'	142.8	142.2	147.9
4'	148.5	150.2	157.6
2'	152.4	151.9	149.7
6'	166.0	155.1	147.5
1'''-C=O	166.8	166.9	163.2
1-C=O	166.83	167.5	166.4

a = Experimental values, b = Modgraph predict, c = ChemWindow predict

In the ^{1}H NMR spectrum of compound **141** the 3"-CH_2 protons and 2'-H aromatic proton resonate as singlets at 4.00 ppm and 8.32 ppm, respectively in the experimental spectrum while Modgraph predicts them to be at 4.34 ppm and 8.58 ppm. The signals for the C-8' and carbonyl ^{13}C signals observed at 139.4 ppm and 166.8 ppm are predicted to be at 139.4 and 167.5 ppm by Modgraph and at 147.9 and 166.4 ppm respectively by ChemWindow. The ChemWindow ^{13}C value for C-8' is clearly not

comparable with the Modgraph and experimental data values. The ChemWindow values for the tetrahydrofuran carbons, C-2, C-3, C-4 and C-5, similarly exhibit large discrepancies from the experimental values. In compound **141A**, the di-acylated derivative, the 3"-H and 2'"-H protons resonate at 4.01 ppm and 4.68 ppm respectively and are predicted by Modgraph to be resonate at 4.34 ppm and 3.63 ppm respectively. The C-3" carbon signal at 40.5 ppm is predicted to resonate at 40.6 ppm and 48.3 ppm by Modgraph and ChemWindow respectively while the C-2'" signal at 44.6 ppm is predicted by Modgraph and ChemWindow to resonate at 43.8 ppm and 48.6 ppm. In fact, going down Table 4, the discrepancies between the ChemWindow values, on one hand, and the Modgraph and experimental values, on t he other, continue to be significant; in some cases, the ChemWindow values are *over-estimated* by up to 9 ppm or *under-estimated* by up to 14 ppm.

2 -(6-Aminopurin-9-yl)-5-acetoxyacetyl-3,4-dihydroxytetrahydrofuran 3,4-acetonide 140 and 2-[6-(acetoxyacetylamino)purin-9-yl)-5-acetoxyacetyl-3,4-dihydroxytetra-hydrofuran 3,4-acetonide 140A

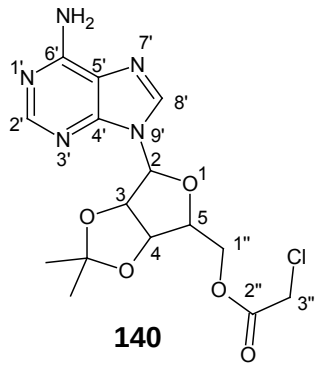

140

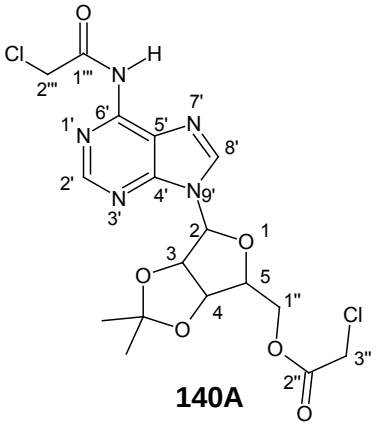

140A

There is a generally good corellation between the experimental assignments and the Modgraph ^{13}C predict values for compounds **140** and **140A** (Table 5). ChemWindow values however show considerable differences from the other two values in some instances as indicated by the highlighted data. Again the discrepancies are far greater for the ChemWindow data which *over-estimates* by as much as 8 ppm and *under-estimates* by as much as 13 ppm.

Table 5. Experimental and predicted ^{13}C NMR data for compounds **140**and **140A**

140

^{13}C nuclei	a	b	c
7"	20.4	20.7	17.0
C.CH_3	25.3	26.6	28.6
C.CH_3	27.1	26.6	28.6
4"	60.5	63.0	69.7
1"	64.6	63.0	65.6
5	81.6	85.2	70.5
3	84.1	84.5	77.8
4	84.7	82.3	72.6
2	90.9	90.6	82.8
C.$(CH_3)_2$	114.7	112.0	101.6
5'	120.4	119.5	113.7
8'	139.8	140.9	147.9
4'	149.2	151.1	157.2
2'	153.2	152.4	151.1
6'	155.5	154.5	156.1
3"	167.4	169.3	171.0
6"	170.3	171.3	171.0

140A

^{13}C nuclei	a	b	c
7"	20.4	20.7	17.0
5"'	20.6	20.7	16.6
C.CH_3	25.3	26.6	28.6
C.CH_3	27.1	26.6	28.6
4"	60.4	63.0	69.7
1"	64.4	63.0	65.6
2"'	64.6	61.6	70.0
5	81.4	85.2	70.5
3	84.1	84.5	77.8
4	84.7	82.3	72.6
2	91.1	90.6	82.8
C.$(CH_3)_2$	114.9	112.0	101.6
5'	122.0	121.8	119.6
8'	142.7	141.8	147.9
4'	148.7	150.0	157.6
2'	150.7	151.0	149.7
6'	152.3	154.7	147.5
1"'	167.3	167.9	168.2
3"	167.3	169.3	171.0
4"'	170.3	171.3	171.0
6"	170.3	171.3	171.0

a = Experimental values, b = Modgraph predict, c = ChemWindow predict

2.5.2 NMR chemical shift prediction for adenine analogues

6-(*N*-Allylamino)purine 150* and *1-allyl-[6-amino(*N*-allylamino)]purine 150A

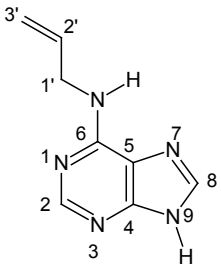

150

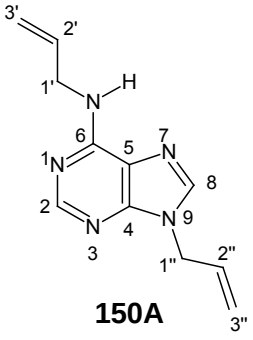

150A

The chemical shift predictions for the 1'-methylene carbons in compound **150** are quite different; Modgraph *under-estimates* by 4 ppm and ChemWindow *over-estimates* by 9 ppm. The predictions for the C-3' carbon compare well with each other

(*ca.* 114 ppm) but both under-estimate the experimental value by 5 ppm. The experimental assignments for the pyrimidine carbons are observed to correlate well with the Modgraph prediction values (Table 6). The predictions for the C-3' and the C-3" methylene carbons in compound **150A** correlate reasonably with experimental values but, generally, the ChemWindow values tend to be considerably less accurate.

Table 6. Experimental and predicted ^{13}C NMR data for compounds **150 and 150A**

150

^{13}C nuclei	a	b	c
1'	46.1	42.0	54.8
3'	119.6	114.8	114.9
5	120.4	126.2	113.7
2'	131.2	136.0	134.3
8	144.2	144.2	147.9
4	149.3	151.9	157.2
6	151.9	152.3	156.1
2	152.5	150.0	151.1

150A

^{13}C nuclei	a	b	c
1'	45.7	42.0	54.8
1"	45.7	45.5	55.6
3'	116.4	114.8	114.9
3"	118.9	117.4	114.9
5	119.6	126.2	113.7
2"	131.9	133.7	134.3
2'	134.3	136.0	134.3
8	139.7	141.1	147.9
4	152.5	151.1	157.2
2	153.0	152.4	151.1
6	154.7	158.1	156.1

a = Experimental values, b = Modgraph predict, c = ChemWindow predict

2.5.3 NMR chemical shift prediction for truncated adenine analogues

While the discussion in Sections 2.5.1 and 2.5.2 has focused on an assessment of the relative accuracy of the two prediction approaches, Sections 2.5.3 – 2.5.5 will illustrate their application in supporting structural assignments.

3-Hydroxyphenyl acrylate 192 and 3-(acryloyloxy)phenyl acrylate 192A

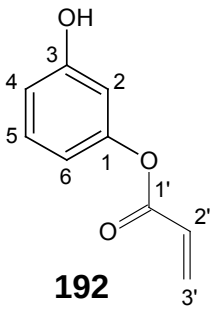

192

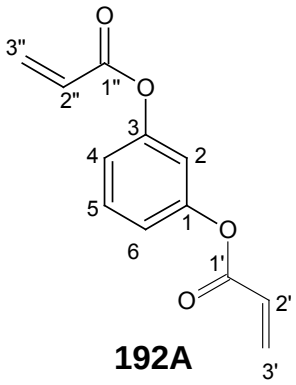

192A

Table 7. Experimental and predicted ^{13}C NMR data for compounds **192** and **192A**

192

^{13}C nuclei	a	b	c
2	109.1	106.2	108.6
6	113.2	112.3	114.0
4	113.5	114.0	112.5
2'	127.8	127.9	130.4
5	130.1	131.1	130.3
3'	133.0	130.9	128.8
1	151.3	154.3	154.5
3	156.6	158.4	157.7
C=O	164.0	164.8	162.0

192A

^{13}C nuclei	a	b	c
2	115.4	113.5	114.3
4	119.0	117.7	118.2
6	119.0	117.7	118.2
2'	127.6	127.9	130.4
2"	127.6	127.9	130.4
5	129.7	131.0	129.3
3'	132.9	130.9	128.8
3"	132.9	130.9	128.8
1	150.9	152.5	153.5
3	150.9	152.5	153.5
1'-C=O	164.1	164.8	162.0
1"C=O	164.1	164.8	162.0

a = Experimental values, b = Modgraph predict, c = ChemWindow predict

There is a generally good correlation between the experimental assignment, the Modgraph predict values and the ChemWindow ^{13}C values for compound **192**, with the C-1 quartenary and C-2' methine carbons experimental assignments varying from prediction values by *ca.* 3 ppm (Table 7). Similar patterns are observed for compound **192A**, with the C-1 and C-3 quartenary carbons being indistinguishable and, hence, having the same chemical shifts and confirming formation of the di-substituted product.

N-*Allyl-3-hydroxyaniline 194*, N-*allyl-3-allyloxyaniline 194A and* N,N-*diallyl-3-hydroxyaniline 194B*

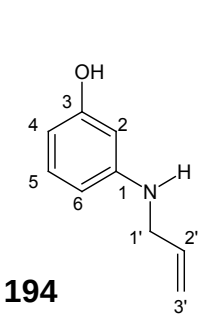

194

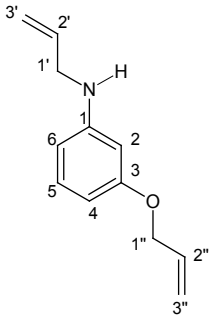

194A

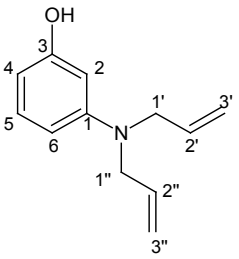

194B

Comparison of the 1'- and 1"- methylene assignments was used to establish the position of allylation in compounds **194**, **194A** and **194B**. In all the compounds the experimental 1'-methylene carbon shifts compare very favourably with the Modgraph values (Tables 8 and 9); ChemWindow, however, over-estimates the chemical shifts by *ca.* 8 ppm. In compound **194A**, the 1"-methylene carbon resonates at the higher chemical shift value of 68.6 ppm (Modgraph 69.0 ppm), consistent with acylation of the phenolic group. The aromatic carbon predictions for these compounds generally show good correlation with the experimental assignments as indicated in the Tables.

Table 8. Experimental and predicted ^{13}C NMR data for compounds **194 and 194A**

195

^{13}C nuclei	a	b	c
1'	46.6	46.2	54.8
2	100.3	102.8	99.5
6	105.0	105.3	104.9
4	106.2	113.0	104.1
3'	116.4	116.4	114.9
5	130.1	130.9	130.7
2'	135.1	134.6	134.3
1	149.4	150.2	144.9
3	156.6	159.0	158.1

195A

^{13}C nuclei	a	b	c
1'	46.5	46.2	54.8
1"	68.6	69.0	75.5
2	99.7	101.7	98.0
4	103.4	104.8	103.9
6	106.3	107.6	102.6
3'	116.1	116.4	114.9
3"	117.3	117.7	115.1
5	129.8	129.7	129.9
2"	133.5	133.2	137.5
2'	135.3	134.6	134.3
3	149.4	150.6	144.1
1	159.8	159.8	159.6

a = Experimental values, b = Modgraph predict, c = ChemWindow predict

Table 9. Experimental and predicted ^{13}C NMR data for compound **194B**

^{13}C nuclei	a	b	c
1'-CH_2	52.7	51.4	59.6
1"-CH_2	52.7	51.4	59.6
2	99.6	151.1	100.3
6	103.5	107.3	105.7
4	105.3	113.0	105.2
3'	116.0	117.8	114.9
3"	116.0	117.8	114.9
5	129.9	131.7	130.8
2'	133.8	133.3	134.3
2"	133.8	133.3	134.3
1	150.2	151.1	145.9
3	156.4	160.2	158.2

a = Experimental values, b = Modgraph predict, c = ChemWindow predict

N-*Allyl-3-(hydroxymethyl)aniline 201*, N-*allyl-3-[(allyloxy)methyl]aniline 201A*, N,N-*di-allyl-3-(hydroxymethyl)aniline 201B and 3-[(allyloxy)methyl]aniline 201C*

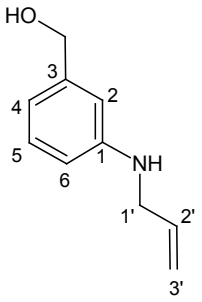

201

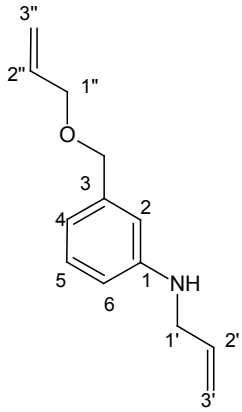

201A

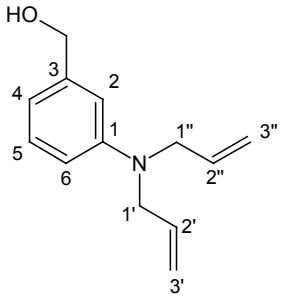

201B

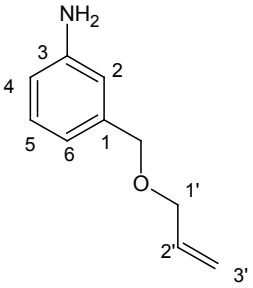

201C

Table 10. Experimental and predicted ^{13}C NMR data for compounds **201** and **201A**

201

^{13}C nuclei	a	b	c
1'-CH_2	46.5	46.2	54.8
CH_2OH	65.6	64.3	68.5
2	111.4	113.1	111.1
6	112.2	117.2	111.2
4	116.0	118.5	115.7
3'	116.2	116.4	114.9
5	129.4	129.6	129.5
2'	135.3	134.6	134.3
1	142.1	146.5	143.7
3	148.3	143.5	141.7

201A

^{13}C nuclei	a	b	c
1'	46.5	46.2	54.8
1"	71.0	71.0	73.0
7-CH_2	72.3	73.7	75.8
2	112.15	114.13	111.4
6	112.20	117.1	111.4
3'	116.2	116.4	114.9
3"	116.91	116.9	114.5
4	116.93	118.7	116.0
5	129.2	129.5	129.2
2"	134.8	135.6	135.6
2'	135.3	134.6	134.3
3	139.4	142.2	138.0

1	148.2	147.1	143.4

a = Experimental values, b = Modgraph predict, c = ChemWindow predict

Table 11. Experimental and predicted ^{13}C NMR data for compounds **202B** and **202C**

201B

^{13}C nuclei	a	b	c
1'-CH_2	52.7	51.4	59.6
1"-CH_2	52.7	51.4	59.6
CH_2	65.9	64.3	68.5
2	110.8	115.1	111.9
6	111.7	119.3	112.0
4	114.9	119.2	116.8
3'	116.0	117.8	114.9
3"	116.0	117.8	114.9
5	129.3	130.6	129.6
2'	133.8	133.3	134.3
2"	133.8	133.3	134.3
3	141.9	144.1	141.8
1	148.9	147.4	144.7

201C

^{13}C nuclei	a	b	c
1'-CH_2	71.0	71.0	73.0
7	72.1	73.7	75.8
2	114.2	114.0	114.2
6	117.0	114.7	114.2
4	117.9	118.7	117.6
5	129.2	129.4	129.2
2'	134.8	135.6	135.6
3	139.5	139.3	138.0
1	146.5	146.5	146.6

a = Experimental values, b = Modgraph predict, c = ChemWindow predict

Comparison of the experimental and predicted 1'- and 1"- methylene ^{13}C chemical shifts was also used to establish the position of allylation in compounds **201**, **201A** **201B** and **201C** (Tables 10 and 11). The Modgraph predicted values, in particular, correlate closely with the assignment of experimental data. Thus in compound **201**, the signals at 46.5 and 65.6 ppm correspond to the *N*-allyl- and hydroxymethylene carbons, respectively. Allylation of the hydroxyl group (compound **201A**) results in a downfield shift of the latter carbon signal to 72.3 ppm. In the *N*,*N*-di-allylated product **201B**, both *N*-allyl carbons resonate at 52.7 ppm – a signal which is absent resonate in the spectrum of the *O*-allylated product **201C**.

2.5.4 NMR chemical shift prediction for allopurinol-derived Baylis-Hillman analogues

1-(6-Bromo-3-methyl-2H-chromen-2-one)-4-(tetrahydropyran-2-yloxy)pyrazolo[3,4-d]- pyrimidine 170A

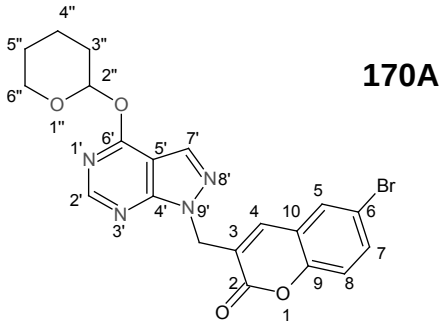

170A

Table 12. Experimental and predicted ^{13}C NMR data for compound **170A**

^{13}C nuclei	a	b	c
5"	22.7	25.6	28.0
4"	24.8	19.7	21.0
3"	29.3	30.6	32.7
NCH_2	45.7	46.9	57.1
6"	68.3	65.1	65.6
2"	82.8	100.2	103.0
3	106.1	127.8	130.4
6	117.4	121.1	119.8
8	118.3	120.0	123.5
5'	120.2	110.8	99.9
10	123.0	120.8	130.0
5	130.7	129.7	129.9
7	135.0	134.3	131.4
2'	135.6	158.1	155.5
7'	143.2	131.6	154.7
4	150.0	134.6	132.9
6'	151.7	166.8	174.5
9	152.4	153.5	149.8
4'	157.3	154.0	170.8
C=O	160.7	162.4	162.0

a = Experimental values, b = Modgraph predict, c = ChemWindow predict.

Comparison of the experimental and Modgraph predicted data for the *N*-methylene carbon was used to confirm the formation of the coumarin **170A**. If the chromene had been formed, the methylene carbon would have been in the lactone ring and resonated at a higher chemical shift (> 65 ppm; Modgraph prediction: 68.7 ppm). There is a good correlation between the experimental assignment and the Modgraph predicted values for most of the pyran carbons except for the C-2" carbon. Some of the purine and coumarin ring predictions, however, show significant differences from the experimental data due, perhaps, to mutual shielding or deshielding of the linked, magnetically anisotropic aromatic systems.

2.5.5. NMR chemcial shift prediction for 3-amino- and 3-hydroxybenzoic acid derivatives **208**, **208A**, **210** and **210A**

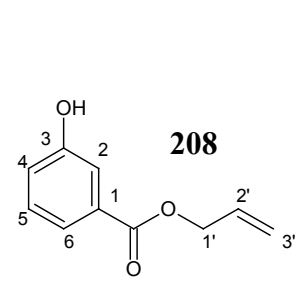

208

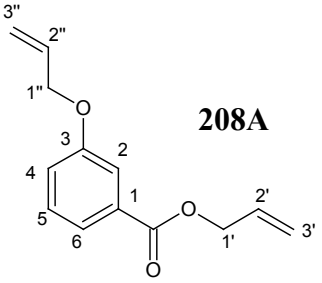

208A

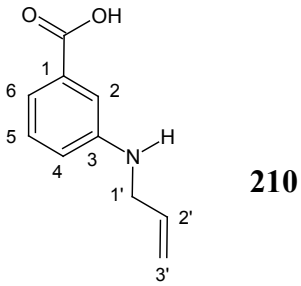

210

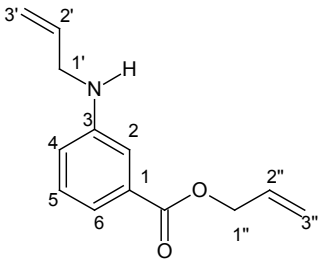

210A

Tables 13 and 14 show the agreement between the ^{13}C NMR experimental assignments and the predictions for the 1'-CH_2 and 1"-CH_2 carbons as well as other carbon atoms in each of the mono- and di-allylated products **208**, **208A**, **210** and **210A**. The data also confirms the structures proposed for the respective compounds. The argument is similar to that for compounds **194**, **194A** and **194B,** a critical point being the resonance of the 1'-CH_2 group at *ca.* 65 ppm and the ester carbonyl carbon at *ca.* 166 ppm in each of the allyl esters **208**, **208A** and **210A**.

Table 13. Experimental and predicted ^{13}C NMR data for compounds **208** and **210**

208

^{13}C nuclei	a	b	c
1'-CH_2	65.8	65.6	69.5
2	116.4	115.5	116.9
3'	118.4	117.4	114.5
4	120.4	122.2	120.0
6	122.0	120.1	122.3
5	129.7	129.5	129.8
2'	131.4	134.1	135.6
1	131.9	131.1	131.9
3	155.9	155.5	157.2
C=O	166.4	168.1	167.0

210

^{13}C nuclei	a	b	c
1'	46.0	44.3	54.8
3'	116.9	114.9	114.9
3	112.9	143.4	149.5
4	115.0	117.8	117.5
6	116.8	119.0	118.5
2	117.3	117.0	113.9
1	119.4	133.2	131.4
6	120.8	119.0	117.5
5	129.8	128.9	129.2
2'	134.2	136.0	134.3
C=O	148.2	167.8	172.0

a = Experimental assignment, b = Modgraph prediction, c = ChemWindow prediction

Table 14. Experimental and predicted ^{13}C NMR data for compounds **208A** and **210A**.

208A

^{13}C nuclei	a	b	c
1"	65.6	70.0	75.5
1'	69.0	65.6	69.5
2	115.1	115.7	115.4
3"	117.9	117.5	115.4
3'	118.2	117.4	114.5
4	120.2	121.6	118.5
6	122.2	120.8	121.3
5	129.4	128.6	129.0
1	131.5	131.4	131.1
2"	132.2	134.5	137.5
2'	132.9	134.1	135.6
3	158.6	158.4	158.7
C=O	166.1	168.1	167.0

210A

^{13}C nuclei	a	b	c
1'	46.4	44.3	54.8
1"	65.4	65.6	69.5
2	113.6	114.8	113.5
3'	116.5	114.8	114.9
4	117.8	120.0	116.6
3"	118.0	117.4	114.5
6	118.7	118.6	118.1
5	129.1	128.9	129.2
1	131.0	132.5	131.3
2"	132.3	134.1	135.6
2'	134.9	136.0	134.3
3	150.0	147.0	143.4
C=O	166.0	168.1	167.6

a = Experimental assignment, b = Modgraph prediction, c = ChemWindow prediction

2.6. Computer Modelling of ATP Mimics

A vital tool in rational drug design is the use of computer modelling to explore enzyme-receptor interactions. A number of successes have been recorded in this rational approach to drug discovery in finding therapeutic agents such ritonavir and its analogues that are administered to AIDS patients[191] and relenza[192] for treating flu. Computer modelling at the molecular mechanics level has been used to explore the GS receptor-binding potential of compounds prepared in this study. The first step was to find the global minima of selected deprotected ATP analogues by subjecting each to a molecular dynamics routine, the assumption being that, *in vivo*, accessible ester moieties would be hydrolysed prior to binding. The most stable conformation, in each case, was subjected to various docking options in the receptor cavity of glutamine synthetase *in silico*, each option involving a different orientation and/or conformational change in the ligand. The crystal structure data for 1F52, the glutamine synthetase of *Salmonella typhimurium* co-crystallized with ADP reported by Eisenberg and co-workers (Figure 92)[193,194,195] was used for this study. The relevant residues with their catalytic roles both in the biosynthetic reaction as well as the allosteric control of the enzyme by adenylylation, as identified by Eisenberg, have been confirmed, *in silico* and are summarized below.

2.6.1. Docking of ATP and ATP mimics into the MTB-GS receptor site

The computer modelling studies of the selected, synthesized ATP mimics were conducted on the ACCELERYS Cerius^2 platform. The OFF METHODS and OFF SET UP modules were used for the conformational search while the LIGANDFIT module was used for receptor-docking. A reconstructed model of the crystal structure of MTB-GS determined by Eisenberg and co-workers was used and attention was focused on the 'active site' which is a region defined by amino acid residues within 5Å of the ATP ligand site on GS. The divalent metal ions (Mg^{2+} or Mn^{2+}) were adequately taken into consideration because of the vital role they play in phosphoryl transfer during nitrogen biosynthesis. Particular attention was given to residues which might interact with ATP, and we used the B-subunit (in light brown colour) of the

1F52 *Salmonella* GS, which contains one ATP binding site (Figure 93). The conformational homology and 'active-site' docking of ATP and selected mimics will be illustrated in the following sub-sections.

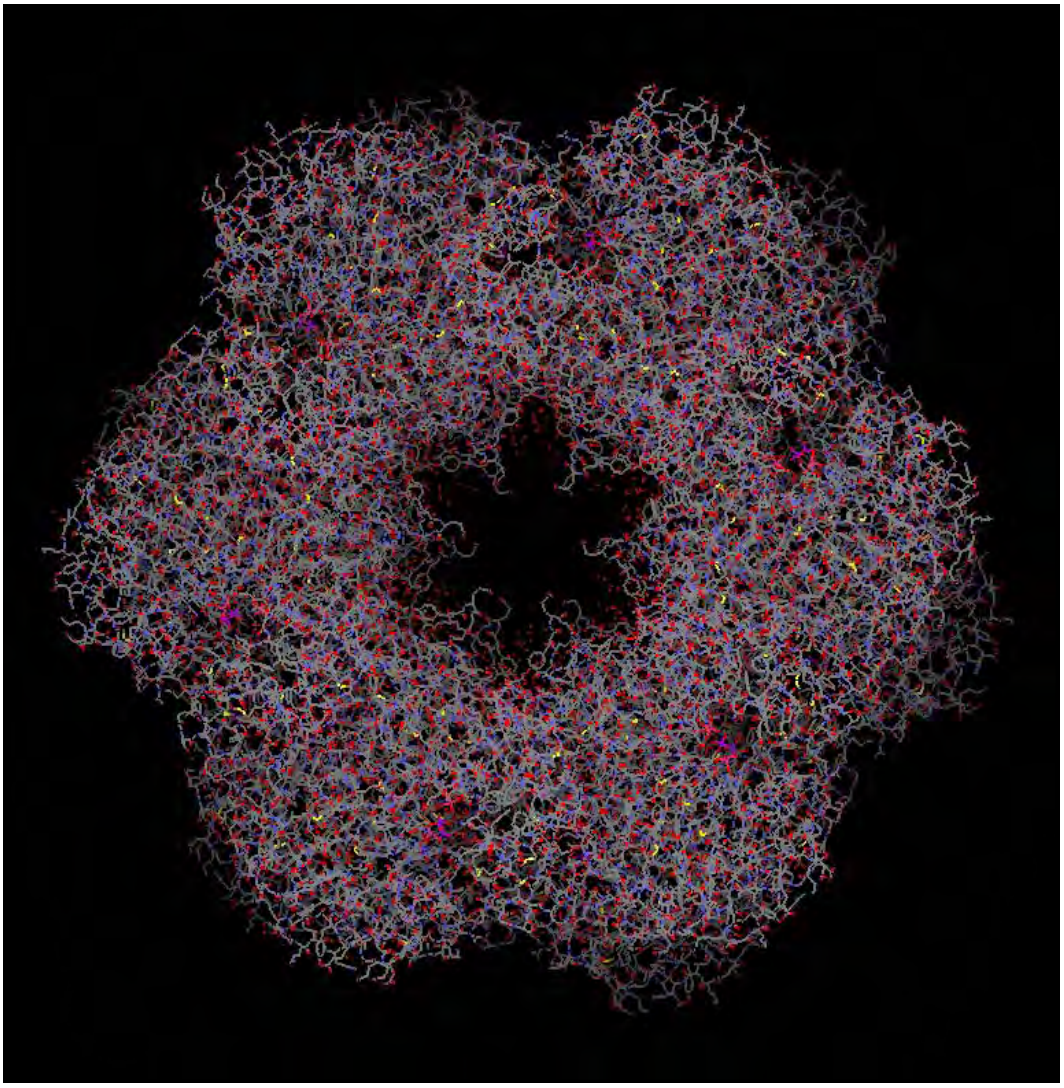

Figure 92. Crystal structure of 1F52, the glutamine synthetase of *Salmonella typhimurium* co-crystallized with ADP. The structure is made up of 25 chains containing 9180 residues. Downloaded from the pdb site at http://www.rcsb.org/pdb/explore.do?structureId=1F52 .

The following interactions were observed between ADP and amino acid residues in the ATP site in the B-subunit (Figure 94).

i. Ser 273 acting as donor in hydrogen-bonding to the amino group on adenine;
ii. Glu 129 interacting with ribose of ADP *via* donor hydrogen-bonding;

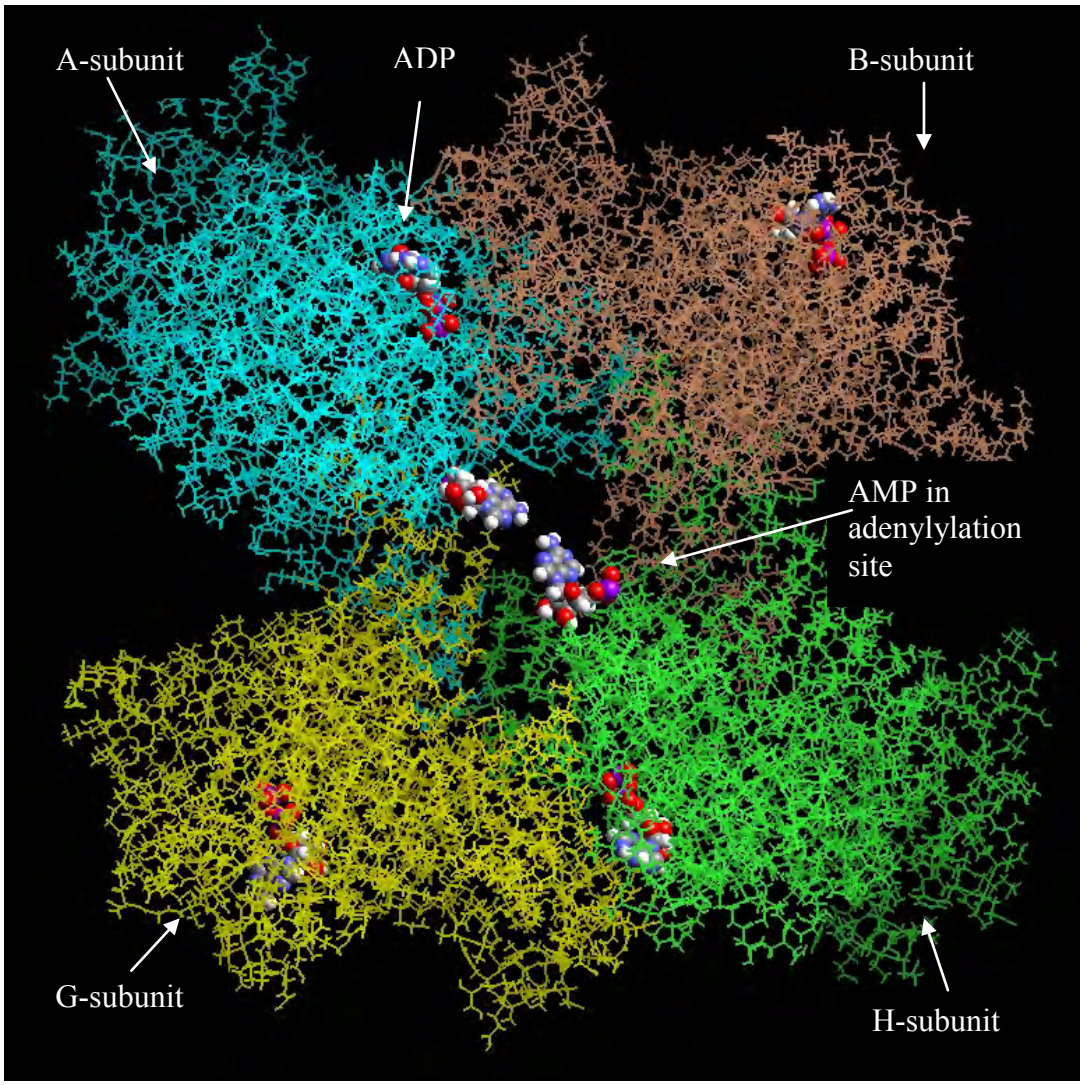

Figure 93. Reconstructed 1F52 *Salmonella typhimurium* GS with A-subunit (in light blue), B-subunit (in light brown), G-subunit (in yellow) and H-subunit (in light-green), showing ADP molecules in the ATP sites and AMP molecules in the adenylylation sites.

iii. Thr 223 interacting with ribose hydroxyl group *via* donor hydrogen-bonding;

iv. Arg 355 acting as an acceptor *via* hydrogen-bonding with an oxygen of the β-phosphate group and the pyrimidine ring of ADP;

v. His 271, Arg 344, His 210 and Glu 220 interacting with the phosphate groups of ADP *via* acceptor hydrogen-bonding.

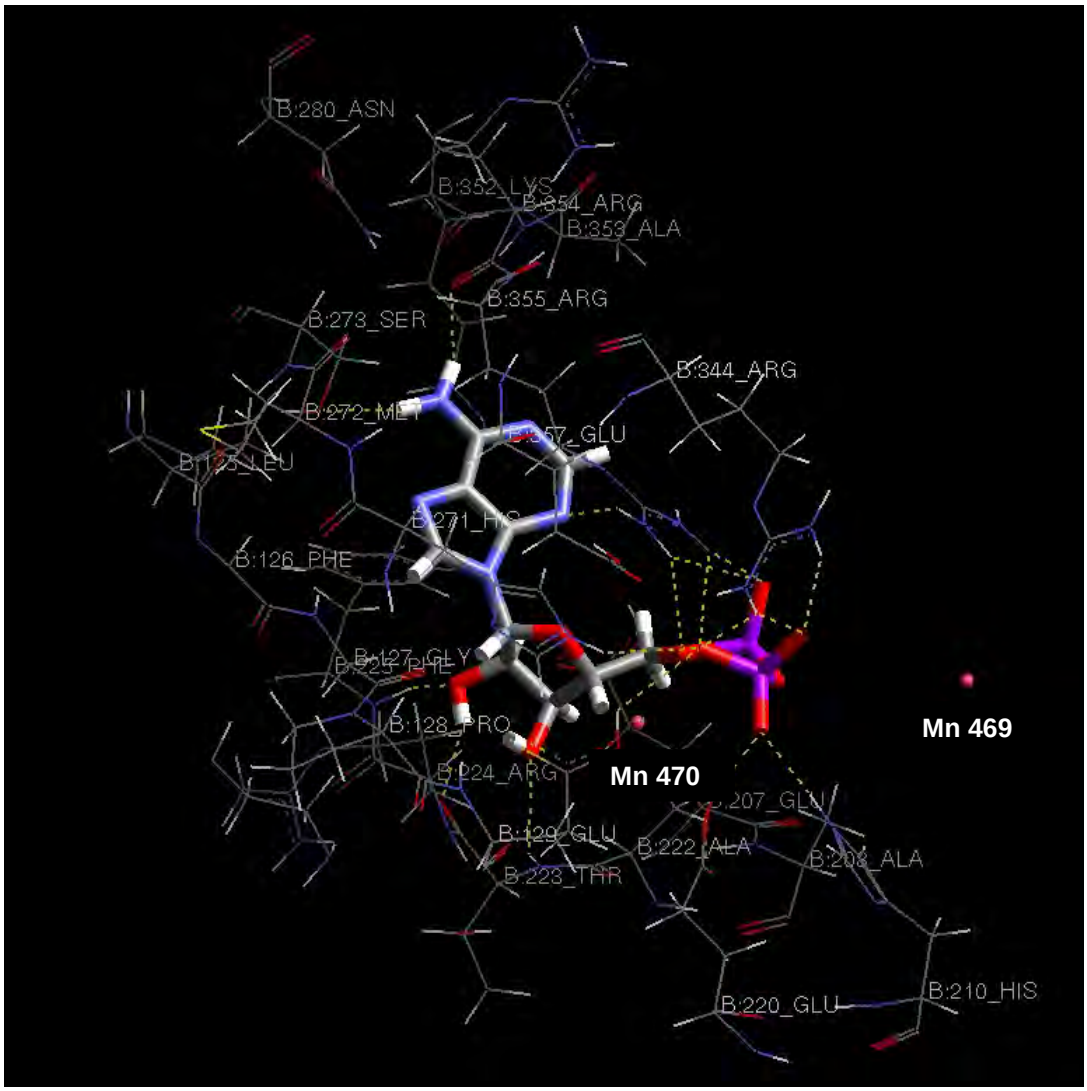

Figure 94. ADP interaction with 'active-site' residues in GS, showing potential hydrogen-bonds in yellow, dashed lines.

2.6.1.1. Modelling of ATP in the GS active site

ATP plays a vital role in biosynthesis and also in the covalent modification of GS by adenylylation, and it is important to explore its interaction with the active site *in silico* since no X-ray structure is available of ATP-bound GS. Hence, the global minimum of ATP was found by conducting a molecular dynamics conformational search at 600K. ATP was then docked into the 'B-sub-unit' active site of GS (Figure 93) and its interaction with active-site residues and its binding potential were analyzed. The non-bonded intermolecular interaction between the ligand and protein is measured in terms of the 'Dock score'. The 'Ligscore' is a measure of the protein-ligand interaction,

while 'vdW' is the Leonard-Jones soft potential. Table 15 shows the scores for the best twenty, bound conformations of ATP in descending order of the 'dock score'. There are few differences between the interactions of ATP with active-site amino acid residues compared with ADP, but it was observed that ATP interacts with Lys 354 *via* acceptor hydrogen-bonding and with Arg 354 *via* donor hydrogen-bonding – interactions not exhibited by ADP. Figure 95 shows the interaction of ATP with active site residues.

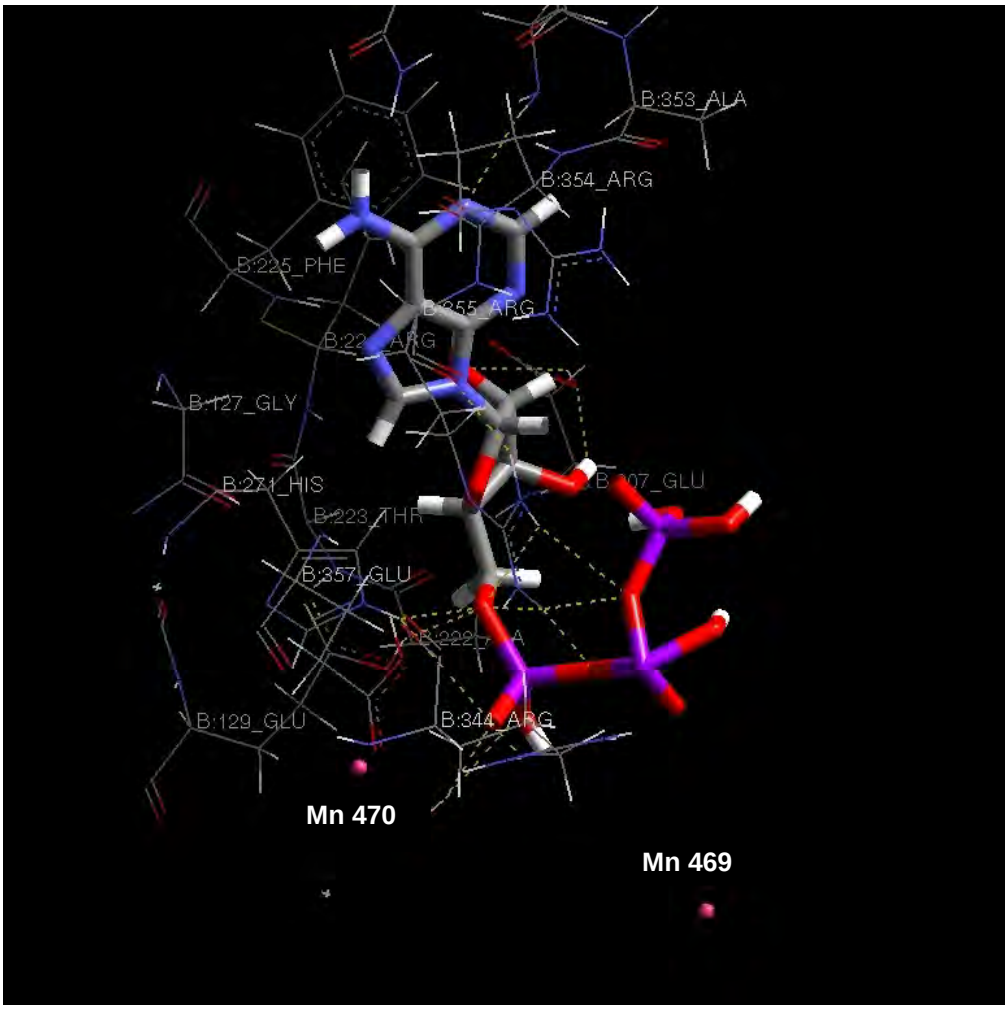

Figure 95. ATP interaction with amino acid residues within 3Å in the 'active-site' of GS, showing potential hydrogen-bonds in yellow, dashed lines.

Table 15. Summary of scores of the docking of ATP into the 'B-subunit' GS active-site.

Conformer	Dock score (kcal/mol)	Ligscore (kcal/mol)	vdW energy (kcal/mol)
1	87.41	-3.06	58.10
2	64.10	-3.43	65.93
3	40.16	-8.15	166.83
4	31.93	-3.51	67.68
5	30.31	-1.10	16.12
6	26.05	-4.46	88.01
7	18.49	-4.50	88.75
8	14.83	-6.10	122.96
9	7.89	-4.93	97.91
10	0.06	-3.61	69.73
11	-0.77	-14.96	312.73
12	-12.56	-3.02	57.20
13	-13.14	-6.27	126.75
14	-25.75	-5.60	112.40
15	-33.01	-0.58	4.88
16	-35.02	-6.87	139.42
17	-36.75	-9.38	193.18
18	-38.32	-7.90	161.60
19	-44.18	-2.09	37.18
20	-47.15	-5.33	106.60

2.6.1.2. Computer modelling of adenosine, adenine and allopurinol derivatives in the GS active site

The homology of selected synthetic ATP mimics and their interaction with active-site residues were explored. A 'target model' alignment of each of the mimics with ATP was conducted using the DRUG DISCOVERY module in Cerius[2]. The global minimum conformation of each of the analogues was aligned with ATP to check their *in vacuo* similarities with ATP. Docking of the energy-minimized mimics into the active-site of the enzyme *in vacuo* was undertaken and docking scores were examined to assess binding with the amino acid residues in the GS 'active-site' (Table 16).

Table 16. Scores for the best binding conformations of ATP and selected adenosine, adenine and allopurinol derivatives.

Compound	Dock score (kcal/mol)	Ligscore (kcal/mol)	vdW (kcal/mol)
ATP	87.41	-3.06	58.10
132	-43.83	-12.29	255.55
138	91.09	-2.56	47.25
140	11.86	0.55	-19.33
149	-52.76	-3.28	62.72
170	44.61	1.64	-42.50

The 'target model' alignment of compound **132** with ATP (in yellow) shown in Figure 96 illustrates good structural homology and the ligand **132** was found to have common interactions with amino acid residues in common with those exhibited by ADP and ATP (Figure 98). In addition, the following interactions were observed.

i. Lys 352 interacts with the 6-amino group *via* donor hydrogen-bonding;
ii. Asn 280 and Arg 354 interacts with the 6-amino group *via* acceptor hydrogen-bonding;
iii. Mn 469 was found to be at a distance of 2.64Å to the terminal acetyl group of ligand **132**.

Figure 97 shows the alignment of the binding conformation of ATP with the binding conformation of ligand **132**. While compound **132** exhibits good homology with ATP

when comparing both global minima (Figure 96) and fair homology when comparing binding conformations (Figure 97), it has a very low 'dock score'.

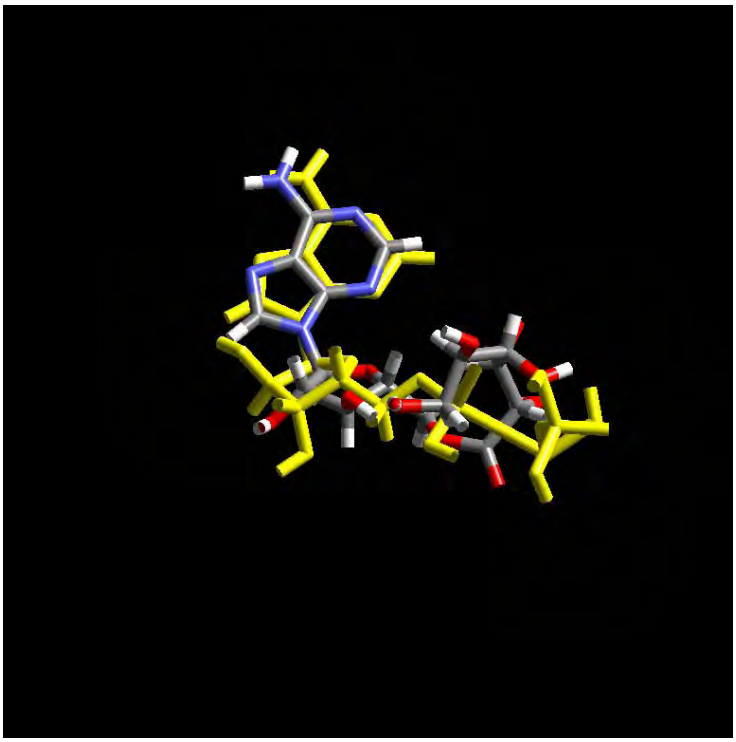

Figure 96. **'**Target model' alignment of ATP (in yellow) with ligand **132**.

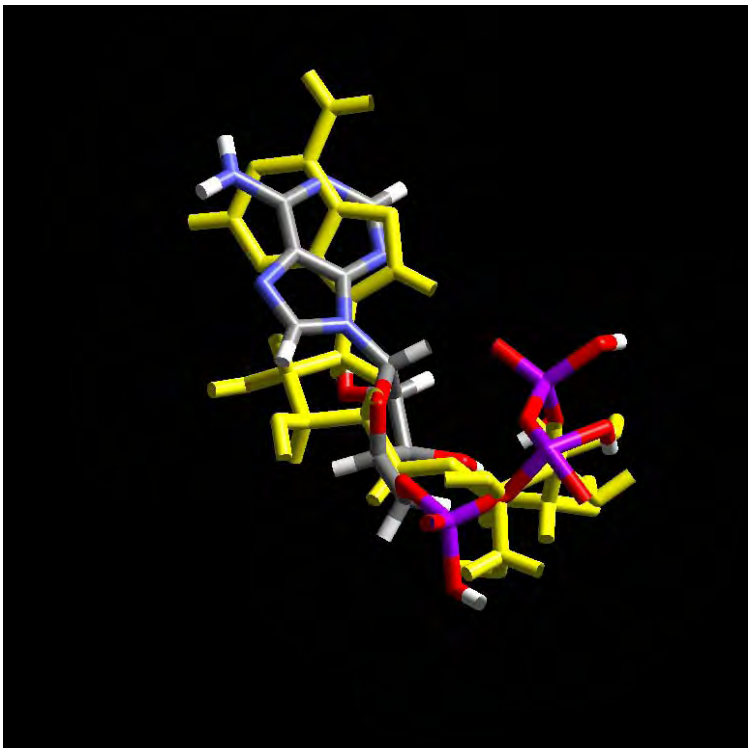

Figure 97. **'**Binding conformation' alignment of ATP with ligand **132** (in yellow).

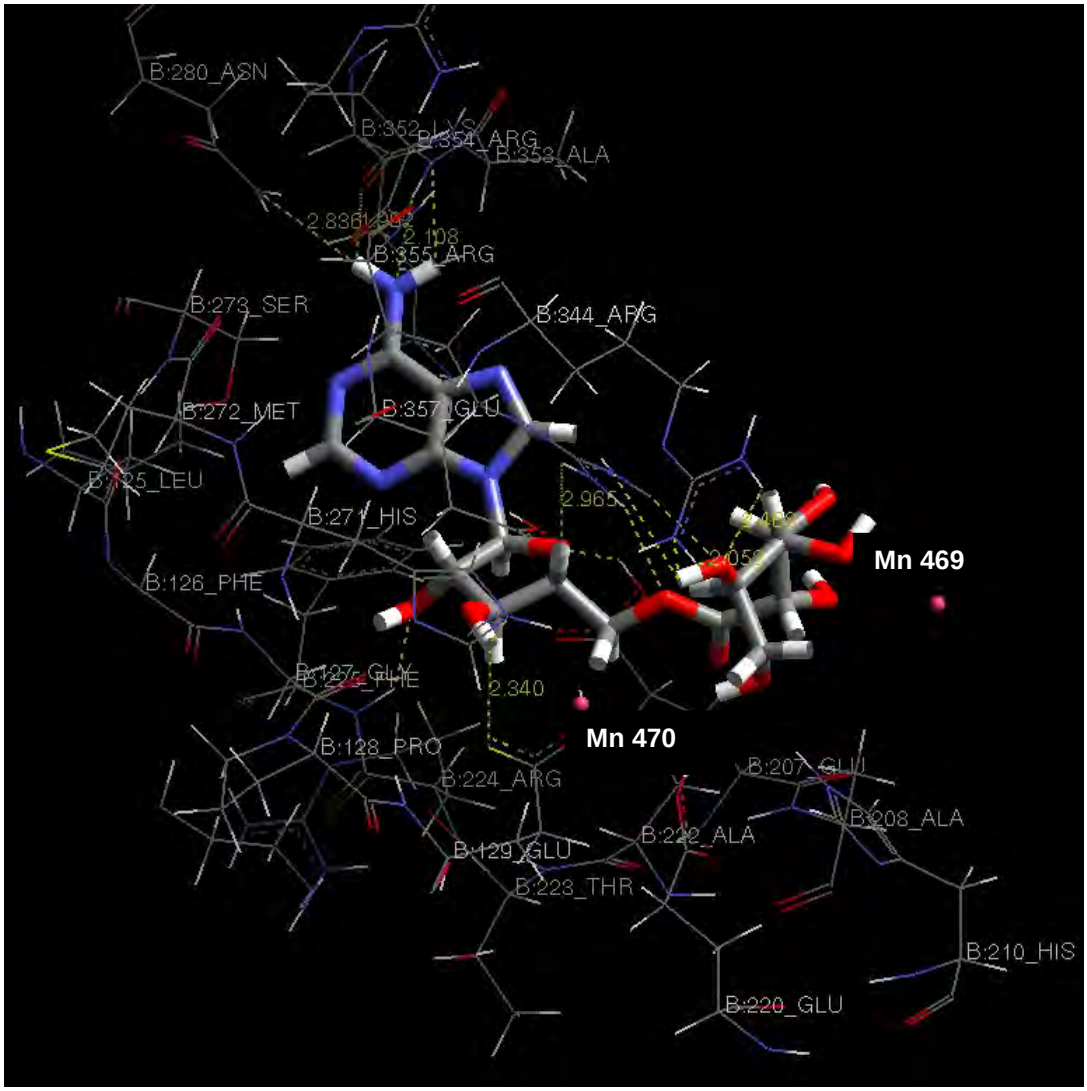

Figure 98. Interaction of ligand **132** with active-site-residues within 3Å in the active-site of GS, showing potential hydrogen-bonds in yellow, dashed lines.

On the other hand, although the global minimum and bound conformations of compound **138** show poor structural homology with ATP (Figures 99 and 100), the ligand appears to bind very well to the active-site of the protein! Its dock score of 91.09 kcal/mole is better than the value for ATP and is an indication of high affinity for the GS active site. Compound **138** appears to interact (Figure 101) with almost all the amino acid residues that ATP interacts with and exhibits the following additional interactions: - (i) acceptor hydrogen-bond interaction *via* one of the amino hydrogens

on adenine with Lys 352; (ii) a donor hydrogen-bond interaction between Gly 127 and the ribose moiety; and (iii) the side-chain that contains the alkyl phosphate group interacts with Ile 345 *via* an acceptor hydrogen-bond. The metal atoms, however, are too far off in this case to have any significant interaction with the ligand.

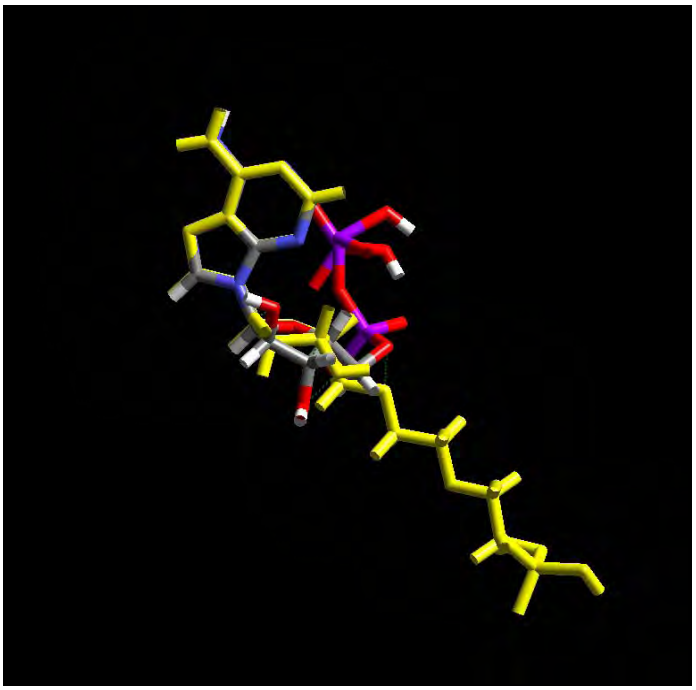

Figure 99. 'Target model' alignment of ATP with ligand **138** (in yellow).

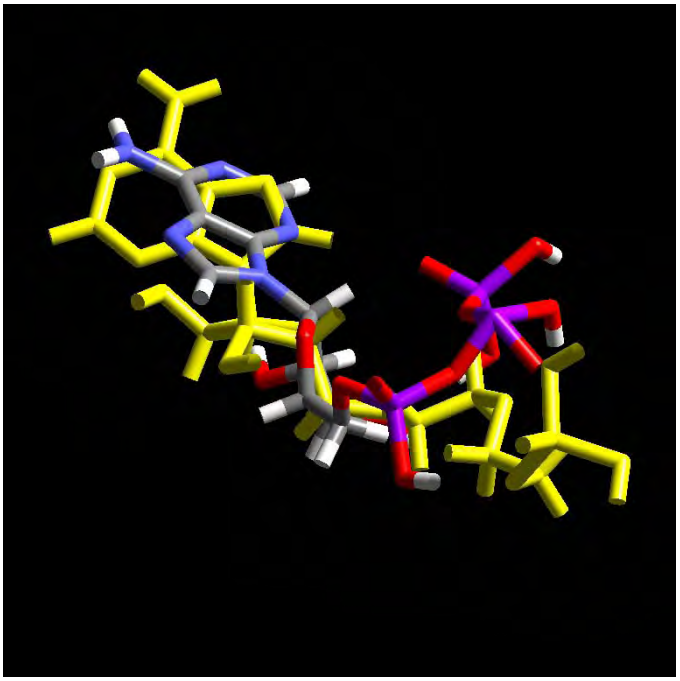

Figure 100. 'Binding conformation' alignment of ATP with ligand **138** (in yellow).

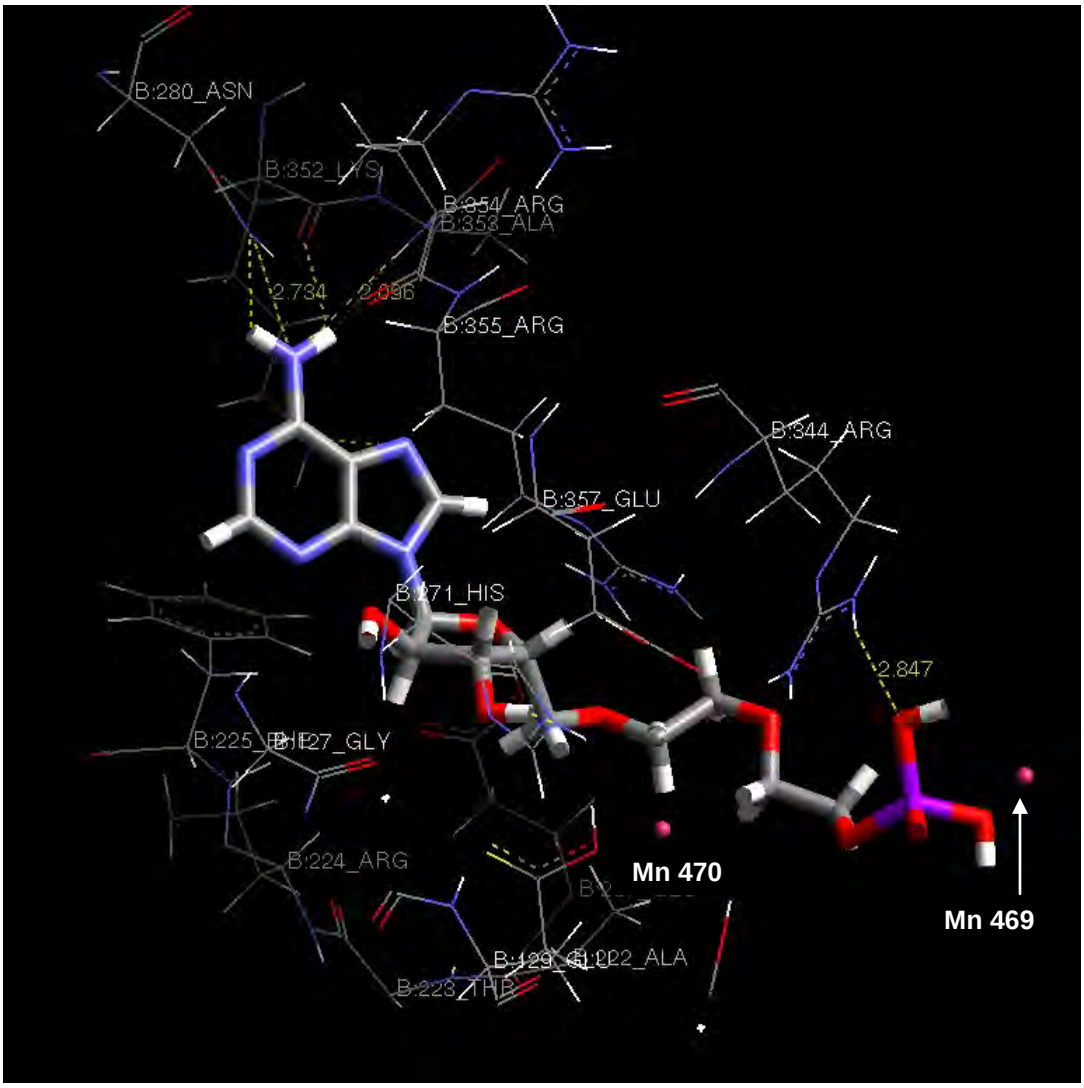

Figure 101. Interaction of ligand **138** with active-site-residues within 3Å in the active-site of GS, showing potential hydrogen-bonds in yellow, dashed lines.

2.6.1.3. Computer modelling of truncated adenine derivatives in the active site of GS

Molecular dynamics to find the global minimum conformation was conducted for each of the truncated mimics listed in Table 17 and their alignment with ATP explored. While the global minimum conformations of the truncated systems exhibit fair to poor structural homology with ATP, several appear to interact with the GS active-site residues *via* both acceptor and donor hydrogen-bonds, indicating their

binding potential. Figures 102 and 103 illustrate the 'target model alignment' and the 'binding conformation' alignment of compound **203** and ATP, while Figure 104 summarises the interaction of the ligand **203** with active-site residues. It is interesting to note the significant conformational differences between the global-minimum (Figure 102) and bound conformations (Figure 103) of the ligand **203**.

Table 17. Comparison of the ligands scores of truncated adenine mimics with ATP

Compound	**Dock score (kcal/mol)**	**Ligscore (kcal/mol)**	**vdW (kcal/mol)**
ATP	87.41	-3.06	58.10
186	-2.48	-0.61	5.49
191	4.90	0.39	-15.91
196	20.83	0.81	-24.83
198	1.93	0.05	-8.65
203	28.87	1.10	-30.95
206	9.07	0.66	-21.60

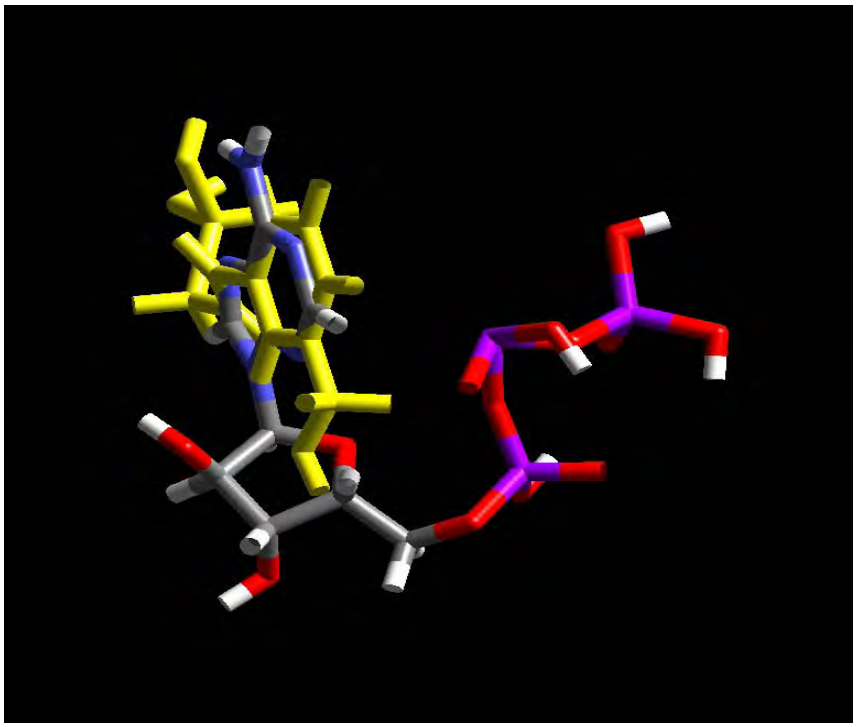

Figure 102. 'Target model' alignment of ATP with ligand **203** (in yellow).

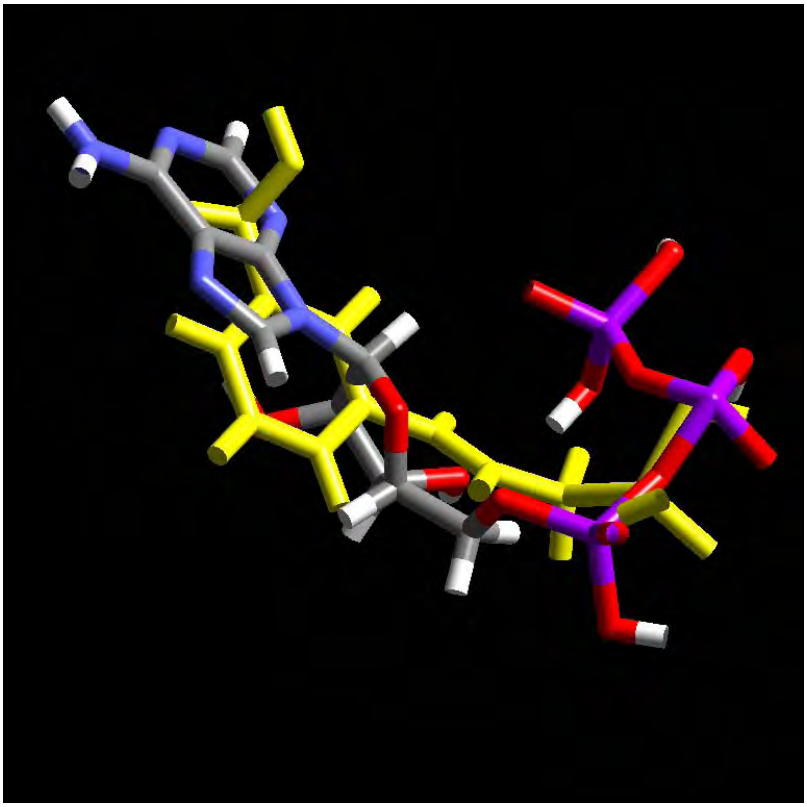

Figure 103. 'Binding conformation' alignment of ATP with ligand **203** (in yellow).

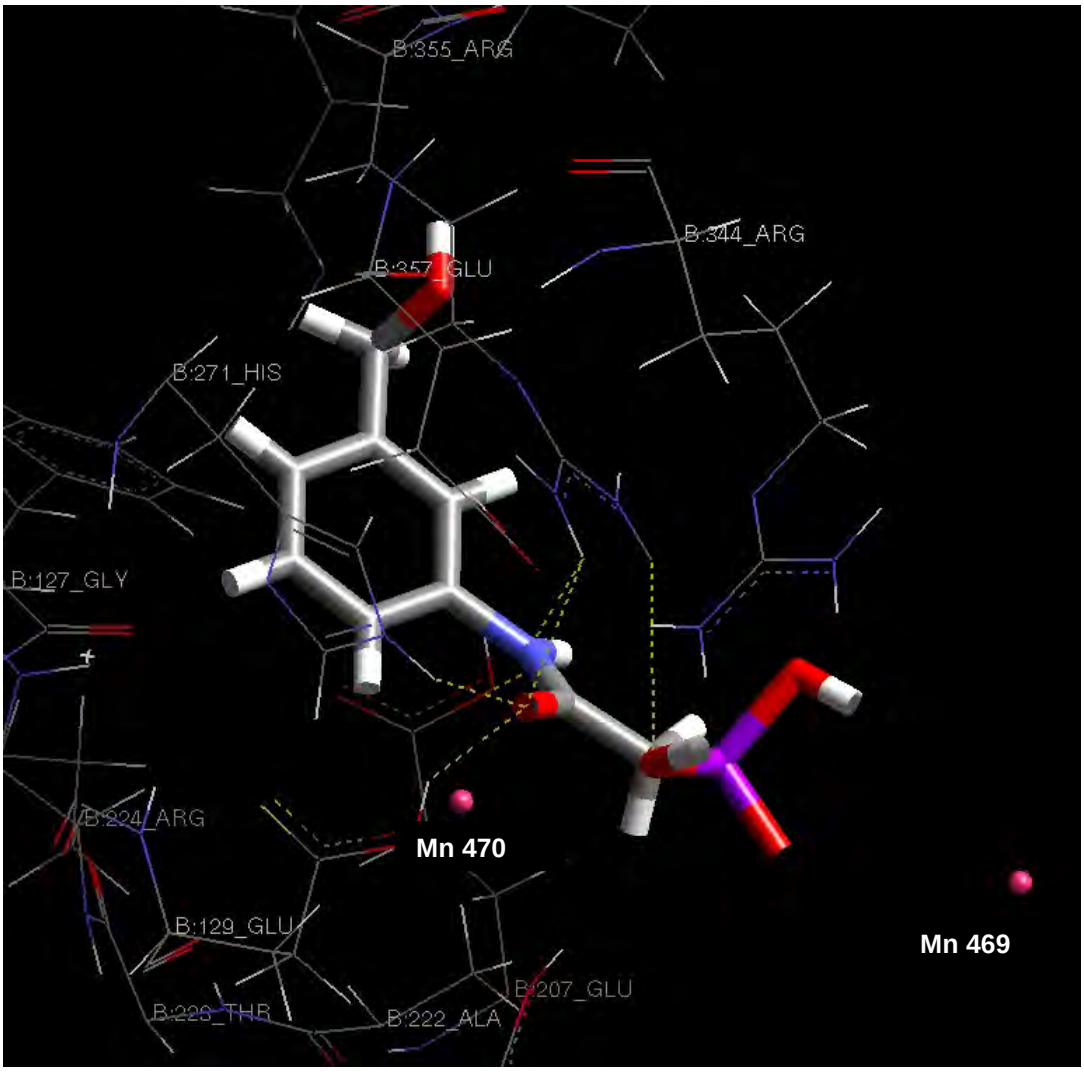

Figure 104. Interaction of ligand **203** with active-site-residues within 3Å in the active-site of GS, showing potential hydrogen-bonds in yellow, dashed lines.

Figures 105 and 106 illustrate the 'target model' alignment and the 'binding conformation' alignment of compound **196** with ATP, while Figure 107 summarises the interaction of the ligand **196** with active-site residues. While the global minimum conformations (Figure 105) exhibit poor structural homology, the alignment of the binding conformations (Figure 106) is clearly much better.

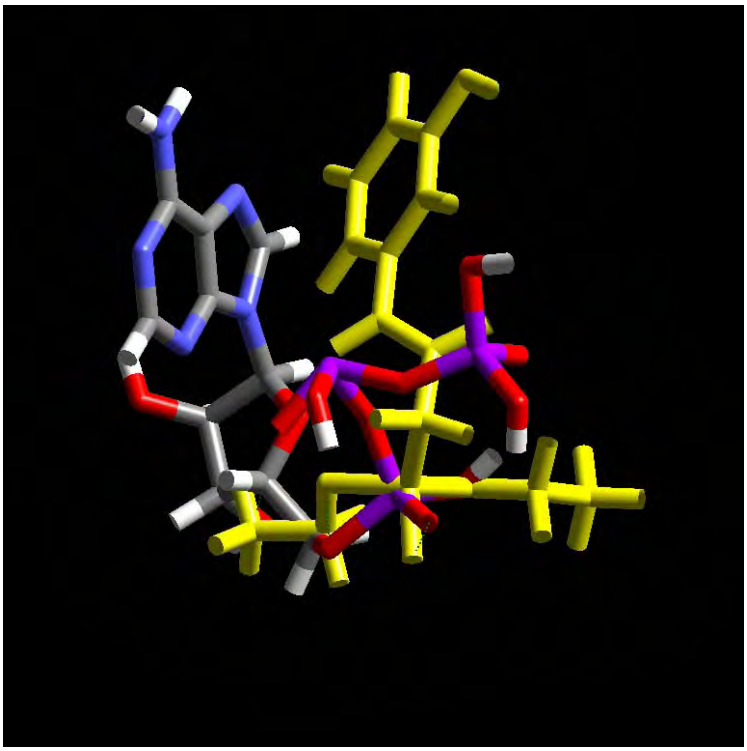

Figure 105. 'Target model' alignment of ATP with ligand **196** (in yellow).

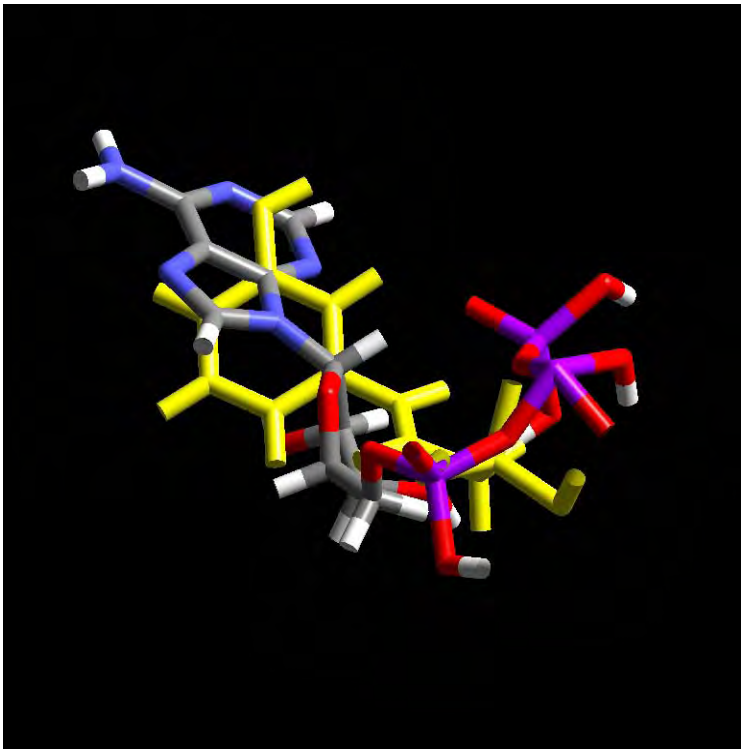

Figure 106. 'Binding conformation' alignment of ATP with ligand **196** (in yellow).

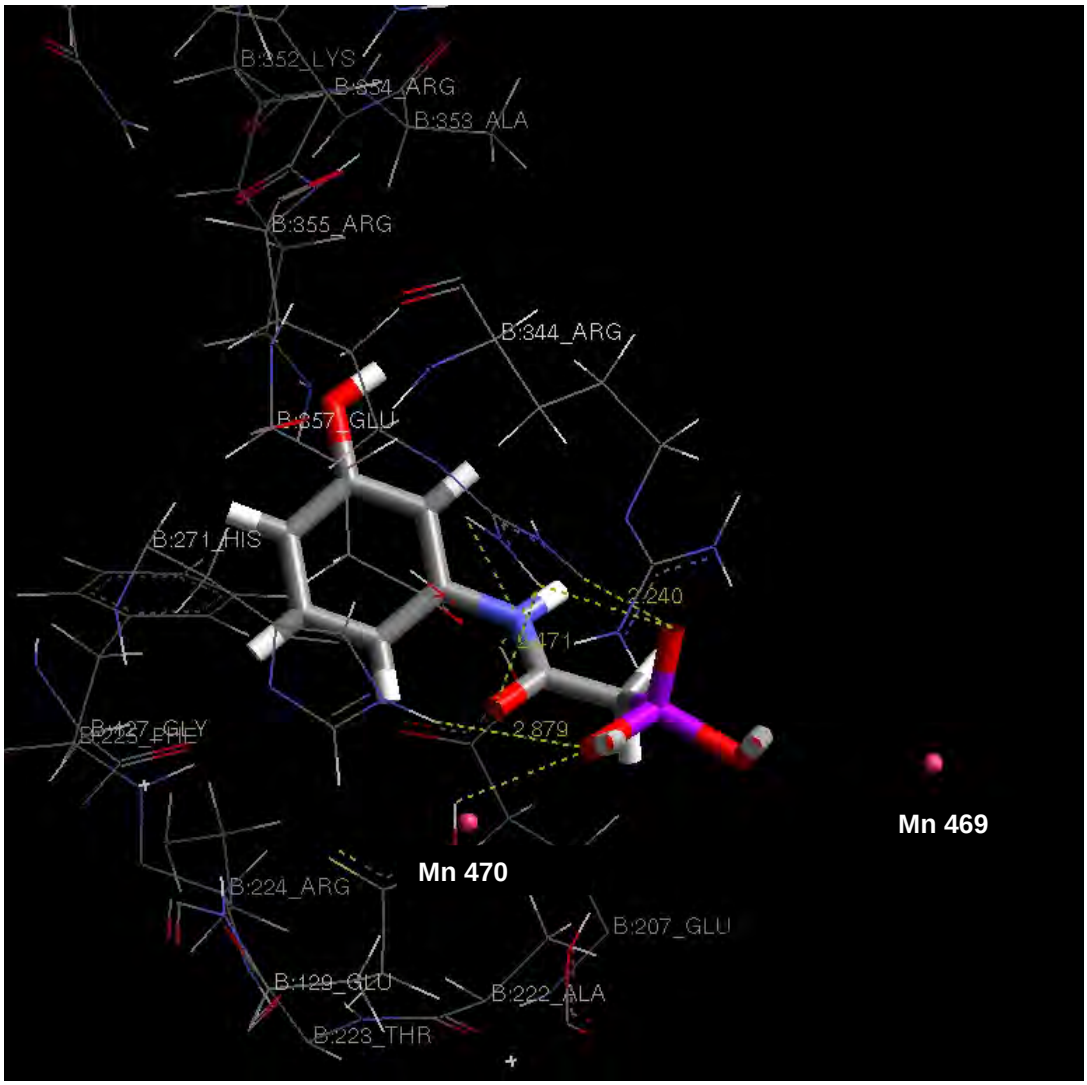

Figure 107. Interaction of ligand **196** with active-site-residues within 3Å in the active-site of GS, showing potential hydrogen-bonds in yellow, dashed lines.

The *in silico* data obtained thus far suggest a measure of complementarity between various synthetic ligands and the GS-ATP active-site and some degree of conformational homology with ATP. Issues of enzyme inhibition and selectivity, aqueous solubility, and free energies of solvation/desolvation and binding have yet to be explored. However, on the basis of modelling data, it seems that a number of the ATP mimics have potential as GS inhibitors and will be investigated further.

2.7. Conclusions

This research has formed part of a col laborative programme aimed at developing glutamine synthetase inhibitors as potential therapeutics for TB – a disease for which drug resistance to current treatment regimens makes it an even greater threat to life.

A mechanism-based approach to drug discovery has been pursued in attempts to discover better drugs. Hence, attention has been focused on synthesizing novel ATP mimics that can act as inhibitors of bacterial glutamine synthetase – an enzyme that is essential for the virulence of *Mycobacterium tuberculosis*, the organism that causes tuberculosis. Consideration has been given to issues of structural homology in designing potential ATP mimics. Initially various purine derivatives were identified as scaffolds for the construction of novel ATP analogues and a range of adenosine, adenine and allopurinol derivatives have been prepared as primary targets *via* alkylation and acylation reactions. Attention was then turned to developing "truncated" ATP analogues and a range of 3-aminobenzonitrile, 3-aminophenol, resorcinol, 3-aminobenzyl alcohol, 3-hydroxybenzoic acid and 3-aminobenzoic acid derivatives have been successfully prepared. A number of alkylating and acylating agents have also been prepared and then reacted, with mixed success, with the purine substrates and the truncated analogues.

Allylation of the hydroxyl, amino or N-9 centres of the various substrates was achieved readily in low to high yield (10-87%). Mono- and di-substituted derivatives were isolated in almost all of these allylation reactions, but attempted dihydroxylation of the resulting terminal alkenes of the mono-allylated derivatives with CTAP, $KMnO_4$ and $NaIO_4$ in the presence of $RuCl_3$ were frustratingly unsuccessful; in one case, attempted epoxidation with *meta*-chloroperbenzoic was also unsuccessful.

Alkylations of the N-9 nitrogen of protected allopurinol with specially prepared Baylis-Hillman products, *tert*-butyl 3-(5-bromo-2-hydroxyphenyl)-3-hydroxy-2-methylenepropanoate, *tert*-butyl 3-hydroxy-3-(2-hydroxyphenyl)-2-methylenepropanoate and 6-bromo-3-(chloromethyl)chromen-2-one were successful and provided access to interesting products.

Acylations were generally successful with substrates having free hydroxyl and/or amino groups but not at the N-9 nitrogen of adenine or protected allopurinol. Mono- and di-acylations were recorded in almost all cases except with 2,3,4,5,6-pentaacetylgluconoyl chloride probably because of steric hindrance in the mono-acylated product. Mono-acylation of resorcinol however, proved difficult as the second hydroxyl group becomes more susceptible to acylation as a result of increased acidity. While tin tetrachloride-catalyzed glycosylation of adenine with acetylated glucose in an inert atmosphere of argon was successfully achieved, the corresponding reaction with 3-aminobenzonitrile as substrate was, surprisingly, unsuccessful. Phosphorylation of a number of hydroxy and chloro derivatives was effected using diethyl chlorophosphate and triethyl phosphite, respectively.

One- and two-dimensional NMR spectroscopic methods were used extensively to confirm the chemical structures of synthesized compounds. Experimental chemical shift data were compared with predicted values using NMR prediction progammes and this approach proved useful in assigning structures in cases of competing reaction centres as well with isomeric di-substituted products.

Molecular modelling with the ACCELERYS Cerius^2 platform was used to conduct *in silico* receptor-ligand docking in the 'active site' of bacterial glutamine synthetase in order to identify potential glutamine synthetase inhibitors. The modelling results certainly indicate the binding potential of certain ligands, *in silico* at least.

The results of this study have provided a basis for future research and for addressing challenges such as: -

i. facilitating N-9 allylation and acylation in purine systems;
ii. effective perhydroxylation of various α,β-unsaturated carbonyl derivatives; and
iii. achieving better regio-control in reactions of bifunctional substrates.

3. EXPERIMENTAL

Reagents were supplied by manufacturers. Solvents such as DMF, THF, actonitrile, pyridine, etc were redistilled by literature methods before use. Dry reactions were carried out in an inert atmosphere either under argon or nitrogen. Plastic TLC plates as supplied by Merck – (precoated with silica gel 60 F_{254}) were used for thin layer chromatography and visualization effected under UV light. Silica gel 60 (particle size 0.040-0.063 nm) was employed as stationary phase for flash column chromatography while silica gel 60 PF_{254} was employed as stationary phase for radial chromatography. For normal phase HPLC a Whatman Partisil[10] semi-preparative column was used, while a Phenomenex C-18 LUNA semi-preparative column was used for reverse phase HPLC.

^{1}H, ^{13}C and ^{31}P NMR experiments were conducted on Bruker AVANCE 400 MHz and 600 MHz spectrometers. Chemical shifts were reported relative to the solvent peaks i.e. δ_H : 7.25 ppm for $CDCl_3$, 4.81 for D_2O, 3.30 for CD_3OD, 2.50 ppm for DMSO-d_6, and 20.5 ppm for $(CD_3)_2C=O$; δ_C : 77.0 ppm for $CDCl_3$, 49.0 ppm for CD_3OD, 39.4 ppm for DMSO-d_6 and 30.8 ppm for $(CD_3)_2C=O$.

Low resolution mass spectra recorded on a Finnigan-MAT GCQ mass spectrometer while high resolution mass spectrometric data was obtained by Martin Brits using APCI (Atmospheric Pressure Chemical Ionization) and Tommie van de Walt (University of Witwatersrand Mass Spectrometry Unit).

Mid-IR spectra recorded on Perkin-Elmer spectrum 2000FT-IR spectrometer as thin films and solid deposits between CsI discs.

Melting points were determined on a Reichert hot-stage apparatus and Gallenkamp melting point apparatus and are not corrected.

Adenosine 3',4'-acetonide 127

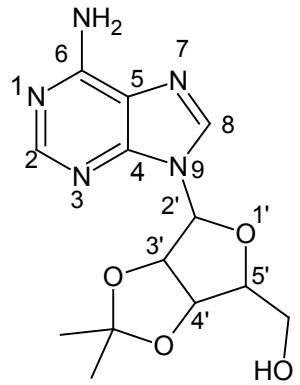

A solution of adenosine **62** (51 mg, 0.19 mmol) and *p*-toluenesulphonic acid (150 mg, 0.79 mmol) in acetone (20 mL) was stirred at room temperature overnight. The reaction was quenched with aqueous Na_2CO_3 (10%, 7 mL). The solvent was removed *in vacuo* and the aqueous residue extracted with CH_2Cl_2 (3 × 10 mL). The combined organic extracts were dried (anhydr. $MgSO_4$) and evaporated *in vacuo* to afford adenosine 3',4'-acetonide **127** as a white powder, (55 mg, 93%), m.p. 215-216°C, (Found: $[\mathbf{M+1}]^+$, 308.14706. $C_{13}H_{17}N_5O_4$ requires: $\mathbf{M}^+$, 307.30518); ν_{max} (solid deposit/cm^{-1}) 3256 (OH), 3095 (NH_2); δ_H/ppm (400MHz; $CDCl_3$) 1.36 and 1.64 (6H, 2 × s, 2 × C*H*$_3$), 3.78 (1H, dd, *J* = 12.8 and 1.9 Hz, C*H*$_a$OH), 3.96 (1H, dd, *J* = 12.8 and 1.4 Hz, C*H*$_b$OH), 4.53 (1H, d, *J* = 1.1 Hz, 4'-H), 5.10 (1H, dd, *J* = 5.9 and 0.9 Hz, 5'-H), 5.19 (1H, t, *J* = 5.4 Hz, 3'-H), 5.85 (1H, d, *J* = 4.9 Hz, 2'-H), 5.94 (2H, s, NH_2), 7.84 (1H, s, 8-H) and 8.30 (1H, s, 2-H); δ_C/ppm (100MHz; $CDCl_3$) 25.2 and 27.6 (2 × *C*H$_3$), 63.4 (*C*H$_2$), 81.7 (C-5'), 83.0 (C-3'), 86.2 (C-4'), 94.3 (C-2'), 114.0 [*C*.(CH$_3$)$_2$], 121.0 (C-5), 140.4 (C-8), 148.4 (C-4), 152.2 (C-2) and 155.7 (C-6).

2,3,4,6-Tetraacetylgluconic acid 129

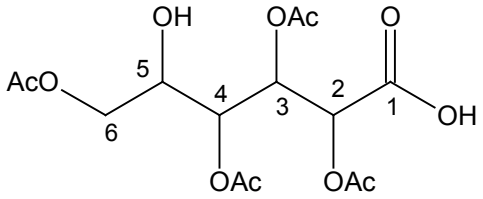

Crushed zinc chloride (8.2 g, 0.060 mol) was dissolved in acetic anhydride (100 mL). The temperature of this solution was reduced to 0ºC, and D-glucono-D-lactone (20 g, 0.11 mol) was added slowly with stirring. The reaction mixture was stirred at 0 ºC for 1 h, and then at room temperature for 24 h, before adding water (400 mL) and stirring for a further 1 h. The product which crystallized out on standing at 0 ºC for 24 h was 2,3,4,6-tetraacetyl-gluconic acid **129** as white crystals (8.2 g, 20%), m.p. 84-88ºC (lit.[165] 113-117°C); ν_{max} (solid deposit/cm^{-1}) 3409 (OH) and 1735 (C=O); δ_H/ppm [600 MHz; $(CD_3)_2C=O$] 2.00 (3H, s, 6-CH_3), 2.03 (3H, 2 × s, 3-CH_3 and 4-CH_3), 2.10 (3H, s, 2-CH_3), 3.98 (1H, dd, *J* = 12.0 and 4.8 Hz, 5-H), 4.08 (2H, d, *J* = 4.9 Hz, 6-H), 4.72 (1H, d, *J* = 0.5 Hz, 5-OH), 5.28 (1H, dd, *J* = 7.6 and 5.0 Hz, 4-H), 5.33 (1H, d, *J* = 3.6 Hz, 2-H) and 5.78 (1H, dd, *J* = 4.9 and 3.7 Hz, 3-H); δ_C/ppm [150 MHz; $(CD_3)_2C=O$] 21.4 (6-OCO.*C*H_3), 21.5 and 21.7 (3-OCO.*C*H_3 and 4-OCO.*C*H_3), 21.8 (2-*C*H_3), 66.7 (C-6), 69.7 (C-5), 71.4 (C-2), 72.8 (C-3), 73.0 (C-4), 169.5 (C=O), 171.0 (2-C=O), 171.17 (3-C=O), 171.20 (4-C=O) and 171.9 (6-C=O).

2,3,4,5,6-Pentaacetylgluconic acid 130

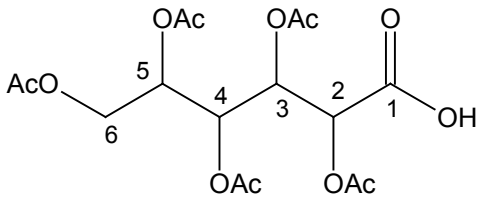

2,3,4,6-Tetraacetyl-gluconic acid (3.0 g, 9.6 m mol) was slowly added to a chilled solution (0ºC) of zinc chloride (1.3 g, 9.5 m mol) in acetic anhydride (13 mL, 0.14 mol) in a 50 mL three necked round bottomed flask equipped with a condenser and a $CaCl_2$ guard tube. The reaction mixture was kept at 0ºC for 1 h a nd then stirred at room temperature for 24 h. T he reaction was quenched with water (70 mL). The aqueous reaction mixture was extracted with $CHCl_3$ (4 × 25 m L). Toluene (75 mL) was added to the combined extract and the volume reduced to 75 mL *in vacuo*. More toluene (75 mL) was added and the volume reduced to 12 mL. Pure 2,3,4,5,6-Pentaacetylgluconic acid **130** crystallized out at 0ºC as white crystals (3.0 g, 77%), m.p. 108-112 ºC (lit.[165] 110-111°C); ν_{max} (solid deposit/cm^{-1}) 3445 (OH) and 1747 (C=O); δ_H/ppm (400MHz; $CDCl_3$) 2.05 (12H, m, 4 × OAc), 2.18 (3H, s, 6-OAc), 4.11 (1H, dd, *J* = 12.2 and 5.5 Hz, 6–H_a), 4.29 (1H, dd, *J* = 12.3 and 4.0 Hz, 6–H_b), 5.06

(1H, dd, J = 10.3 and 5.6 Hz, 5–H), 5.29 (1H, d, J = 3.8 Hz, 2–H), 5.49 (1H, m, 4–H), 5.61 (1H, m, 3–H), and 6.58 (1H, b, OH); δ_C/ppm (100MHz; $CDCl_3$) 20.3, 20.4, 20.6, 20.65 and 20.7 (5 × OAc), 61.4 (C–6), 68.49 (C–3), 68.51 (C–5), 69.3 (C–4), 70.1 (C–2), 169.76 (C–1), 169.83 (C–5'), 169.91 (C–4'), 169.94 (C–3'), 170.4 (C–2') and 170.7 (C–6'); *m/z* = 406 ($\mathbf{M}^+$, 0.52%) and 43 (100%).

2,3,4,5,6-pentaacetylgluconoyl chloride 131

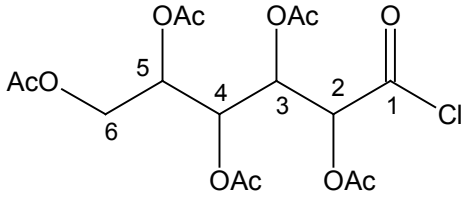

To a solution of 2,3,4,5,6-pentaacetylgluconic acid **130** (1.0 g, 2.5 mmol) in a dry 50 mL round bottomed flask under nitrogen was added oxalyl chloride (0.55 mL, 6.3 mmol) through a septum. There was immediate effervescence and the product precipitated out within 30 minutes. Excess oxalyl chloride was evaporated *in vacuo* to afford 2,3,4,5,6-pentaacetylgluconoyl chloride **131** as a white precipitate (0.52 g, 50%), m.p. 42-44ºC (lit. 68-71°C); ν_{max} (solid deposit/cm^{-1}) 1748 (C=O); δ_H/ppm (400MHz; $CDCl_3$) 2.02-2.10 (12H, overlapping singlets, 4 × CH_3), 2.19 (3H, s, 6-OAc), 4.12 (1H, dd, J = 12.2 and 5.5 Hz, 6-H_a), 4.30 (1H, dd, J = 12.3 and 4.1 Hz, 6-H_b), 5.06 (1H, dt, J = 5.6 and 4.2 Hz, 5-H), 5.31 (1H, d, J = 3.9 Hz, 2-H), 5.50 (1H, dd, J = 6.4 and 5.0 Hz, 4-H) and 5.62 (1H, dd, J = 4.9 and 3.9 Hz, 3-H); δ_C/ppm (100MHz; $CDCl_3$) 20.3, 20.4, 20.6, 20.66 and 20.7 (5 × CH_3), 61.5 (C-6), 68.5 (C-3), 68.55 (C-5), 69.3 (C-4), 70.0 (C-2), 169.7 (C-1), 169.76 (5-O.C=O), 169.8 (4-O.C=O), 169.86 (3-O.C=O), 170.1 (2-O.C=O) and 170.6 (6-O.C=O); *m/z* = 424 ($\mathbf{M}^+$, 0.08%) and 361 (100%).

2-(6-Aminopurin-9-yl)-3,4-dihydroxy-5-[(2,3,4,5,6-pentaacetoxy-hexanoyloxy)-methyl]tetrahydrofuran-3,4-acetonide 132

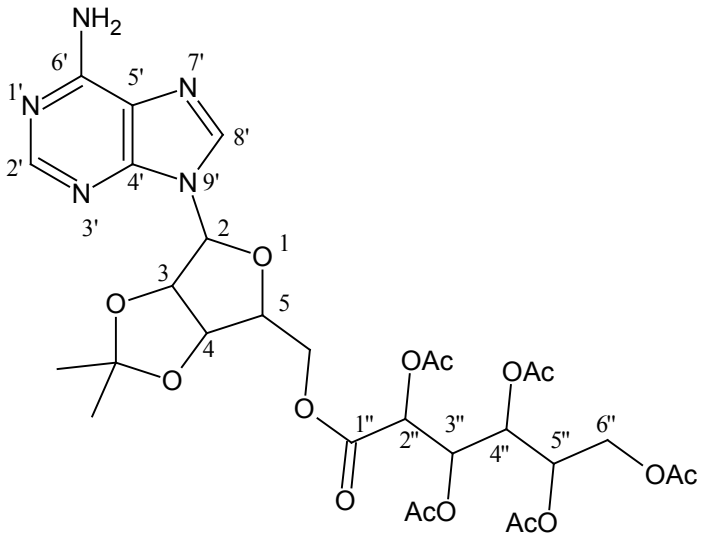

A solution of adenosine 3',4'-acetonide (0.14 g, 0.47 m mol) and 2,3,4,5,6-pentaacetyhlgluconoyl chloride (0.20 g, 0.47 mmol) in pyridine (4 mL) was stirred for 36 h. The solvent was evaporated *in vacuo* and the residue dissolved in $CHCl_3$ (30 mL). The solution was washed with 5% aq. $NaHCO_3$ (2 × 30 mL), water (2 × 30 mL) and brine (2 × 30 mL). The organic layer was then dried (anhydr. $MgSO_4$) and the solvent was evaporated *in vacuo* and the yellow residue was chromatographed [radial chromatography; elution with EtOAc] to afford *2-(6-aminopurin-9-yl)-3,4-dihydroxy-5-[(2,3,4,5,6-pentaacetoxyhexanoyloxy)methyl]tetrahydrofuran-3,4*-acetonide **132** as a yellow oil (46 mg, 14%), ν_{max} (thin film/cm^{-1}) 3345 (NH_2), 1749 (C=O) and 1598 (aromatic C=N) and 1216 (C–N); δ_H/ppm (400MHz; $CDCl_3$) 1.38 and 1.60 (6H, 2 × s, 2 × CH_3, 2.03 (12H, series of singlets, 4 × CH_3), 2.15 (3H, s, 6-CH_3), 4.10 (1H, dd, J = 12.3 and 5.6 Hz, 6"-H_a), 4.28 (2H, m, 6-H_b and CH_{2a}), 4.38 (1H, dd, J = 11.6 and 6.1 Hz, CH_{2a}), 4.45 (1H, m, 4-H), 5.05 (2H, m, 5"-H and 5-H), 5.18 (1H, d, J = 3.6 Hz, 2"-H), 5.45 (2H, m, 3-H and 4"-H), 5.54 (1H, dd, J = 4.8 and 3.7 Hz, 3"-H), 5.93 (2H, s, NH_2), 6.10 (1H, d, J = 2.1 Hz, 2-H), 7.94 (1H, s, 8'-H) and 8.34 (1H, s, 2'-H); δ_C/ppm (100MHz; $CDCl_3$) 20.3, 20.34, 20.56, 20.6 and 20.7 (5 × CH_3), 27.1 and 29.7 (2 × CH_3), 61.5 (C-6"), 65.1 (CH_2), 68.4 (C-3"), 68.6 (C-5"), 69.3 (C-4") , 70.8 (C-2") , 81.6 (C-5), 84.2 (C-3), 84.8 (C-4), 90.8 (C-2), 114.6 [$C.(CH_3)_2$], 120.2 (C-5'), 140.0 (C-8'), 149.2 (C-4'), 152.7 (C-2'), 155.3 (C-6'), 166.4 (C=O), 169.5 (5-O.C=O),

169.6 (4-O.C=O), 169.67 (3-O.C=O), 169.9 (2-O.C=O) and 170.5 (6-O.C=O); *m/z* = 696 ([**M+1**]$^+$, 16%) and (694, 100%).

2-(6-Aminopurin-9-yl)-3,4-dihydroxy-5-[(allyloxy)methyl]tetrahydrofuran-3,4-acetonide 133

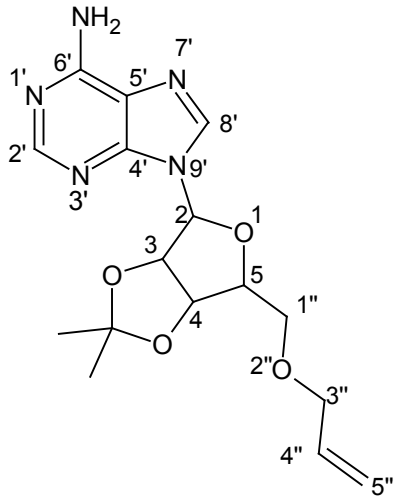

To a stirred solution of adenosine 3',4'-acetonide **127** (0.50 g, . 1.6 mmol) in THF (5 mL) under nitrogen was added NaH (60% dispersion in mineral oil; 42 mg, 1.8 mmol) in small portions to permit controlled evolution of hydrogen. Allyl bromide (0.20 mL, 1.8 m mol) was added through a septum and the resulting solution was refluxed for *ca.* 6h. The reaction was quenched by the addition of water (10 mL). The solvent was evaporated *in vacuo* and the aqueous residue was extracted with CH_2Cl_2 (2 × 20 mL). The organic extract was washed sequentially with water (2 × 40 mL) and brine (2 × 40 m L). The aqueous washings were extracted with CH_2Cl_2 and the organic layers combined and dried (anhydr. $MgSO_4$). Evaporation of the solvent *in vacuo* to afforded a yellow residue, chromatography of which [radial chromatography; elution with 100% EtOAc] afforded *2-(6-aminopurin-9-yl)-3,4-dihydroxy-5-[(allyloxy)methyl]-tetrahydrofuran 3,4-acetonide* **133** as a yellow oil (51 mg, 9%). (Found **[M+1]**$^+$, 348.16276, $C_{16}H_{21}N_5O_4$ requires 347.36904) ν_{max} (thin film/cm^{-1}) 3388 (NH_2); δ_H/ppm (400MHz; $CDCl_3$) 1.38 and 1.62 (6H, 2 × s, 2 × C*H*$_3$), 3.59 (1H, dd, *J* = 10.5 and 4.4 Hz, 1"-CH_a), 3.66 (1H, dd, *J* = 10.5 and 3.5 Hz, 1"-CH_b), 3.94 (1H, dd, *J* = 4.6 and 1.2 Hz, 3"-H), 4.50 (1H, dd, *J* = 6.6 and 3.7 Hz, 4'-H), 4.98 (1H, dd, *J* = 6.1 and 2.5 Hz, 5"-H_a), 5.17 (2H, m, 5'-H and 8'-H,), 5.29 (1H, dd, *J* = 6.1 and 2.4 Hz, 5'-H_b), 5.78 (1H, tdd, *J* = 16.2, 10.4 and 5.8 Hz, 4"-H), 5.98 (2H, s,

NH_2), 6.19 (1H, d, *J* = 2.4 Hz, 2-H), 8.06 (1H, s, 8'-H) and 8.35 (1H, s, 2'-H); δ_C/ppm (100MHz; $CDCl_3$) 25.4 and 27.4 (2 × *C*H_3), 70.2 (C-1"), 72.4 (C-3"), 81.8 (C-5), 85.0 (C-3), 86.0 (C-4), 91.4 (C-2), 114.2 [*C*.$(CH_3)_2$], 117.8 (C-5"), 119.9 (C-5') 133.8 (C-4"), 139.6 (C-8'), 149.5 (C-4'), 152.4 (C-2') and 155.1 (C-6').

2-(6-Aminopurin-9-yl)-3,4-dihydroxy-5-(7-hydroxy-2,5-dioxaheptyl)tetrahydrofuran 3,4-acetonide 137

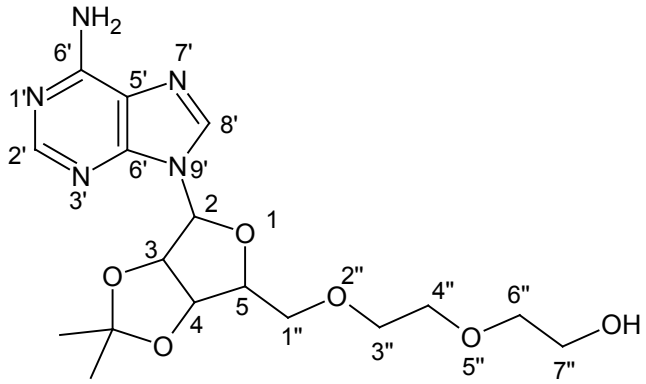

To a stirred solution of adenosine 3',4'-acetonide **127** (0.50 g, 1.6 mmol) in THF (33 mL) under nitrogen was added NaH (60% dispersion in mineral oil; 0.043 g, 1.8 mmol) in small portions to permit controlled evolution of hydrogen. 2-(2-chloroethoxy)ethanol (0.20 mL, 1.8 m mol) was added through a septum and the resulting solution was refluxed for *ca.* 6h. The reaction was quenched by the addition of water (40 mL). The solvent was evaporated *in vacuo* and the aqueous residue was extracted with CH_2Cl_2 (2 × 40 mL). The organic extract was washed sequentially with water (2 × 80 mL) and brine (2 × 80 mL). The aqueous washings were extracted with CH_2Cl_2 and the organic layers combined and dried (anhydr. $MgSO_4$). Evaporation of the solvent *in vacuo* afforded *2-(6-aminopurin-9-yl) 3,4-dihydroxy-5-(7-hydroxy-2,5-dioxaheptyl)tetrahydrofuran - 3,4- acetonide* **137** as a white powder (0.46 g, 72%), m.p. 174-176°C. ν_{max} (solid deposit/cm^{-1}) 3219 (NH_2) and 3112 (OH); δ_H/ppm (400MHz; $CDCl_3$) 1.38 and 1.60 (6H, 2 × s, 2 × CH_3), 2.03-2.64 (1H, br s, OH), 3.63 (4H, dd, *J* = 10.4 and 5.3 Hz, 6"-H and 4"-H), 3.76 (5H, m, 1"–H_a, 7"-H and 3"-H), 3.96 (1H, dd, *J* = 12.8 and 1.4 Hz, 1"-H_b), 4.53 (1H, d, *J* = 1.1 Hz, 4-H), 5.10 (1H, dd, *J* = 5.9 and 0.9 Hz, 5-H), 5.19 (1H, t, *J* = 5.4 Hz, 3-H), 5.85 (1H, d, *J* = 4.9 Hz, 2-H), 5.94 (2H, s, NH_2), 7.84 (1H, s, 8'-H) and 8.30 (1H, s, 2'-H); δ_C/ppm (100MHz; $CDCl_3$) 25.2 and 27.6 (2 × *C*H_3), 42.9 (C-6"), 61.6 (C-7"), 63.4 (C-1"),

71.1 (C-3"), 72.4 (C-4"), 81.7 (C-8'), 83.0 (C-3), 86.1 (C-4), 94.3 (C-2), 114.0 [*C*.$(CH_3)_2$], 121.0 (C-5'), 140.3 (C-8'), 148.4 (C-4'), 152.3 (C-2') and 155.8 (C-6'); *m/z* = 395 ($\mathbf{M}^+$, 0.39%) and 218 (100%).

2-(6-Aminopurin-9-yl)-5[7-diethylphosphoryoxy)-2-5-dioxaheptyl]-3,4-dihydroxytetrahydrofuran 3,4-acetonide 138

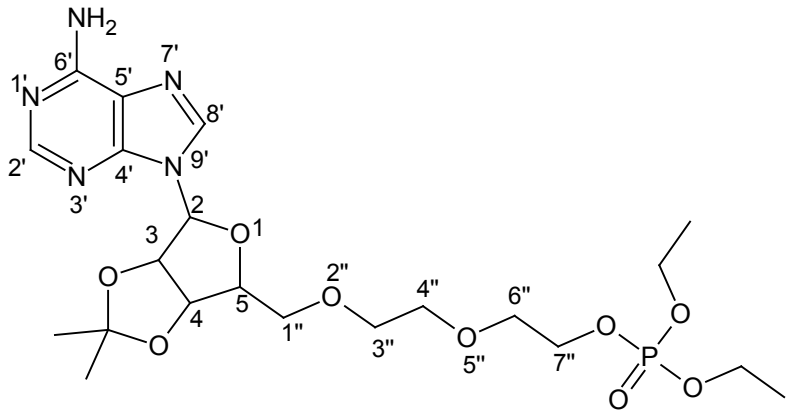

A solution of 2-(6-aminopurin-9-yl)-3,4-dihydroxy-5-(7-hydroxy-2,5-dioxaheptyl)-tetrahydrofuran 3,4-acetonide **137** (260 mg, 0.67 mmol) in THF (10 mL) at room temperature was cooled (-1 ºC). Buthyllithium (300 µL, 0.74 mmol) was added and after stirring for 2 h diethyl chlorophosphate (110 µL, 0.72 mmol) was added and the resulting mixture stirred at room temperature for 24 h. The reaction was quenched by the addition of satd. aq. NH_4Cl solution (10 mL). The THF was evaporated *in vacuo* and the aqueous residue extracted with CH_2Cl_2 (2 × 15 mL). The organic extract was washed with aq. NH_4Cl (2 × 60 mL), water (2 × 60 mL) and brine (2 × 60 mL). The aqueous fractions were extracted with CH_2Cl_2 and the organic layers combined and dried (anhydr. $MgSO_4$). The brown oil obtained after evaporation of the solvent *in vacuo* was washed with hexane (3 × 15 mL) to afford *2-(6-aminopurin-9-yl)-5[7-diethylphosphoryoxy)-2-5-dioxaheptyl]-3,4-dihydroxyltetrahydrofuran 3,4-acetonide* **138** as a yellow oil, (130 mg, 37%). ν_{max} (solid deposit/cm^{-1}) 3337 (NH_2) and 1028 (P=O); δ_H/ppm (400MHz; $CDCl_3$) 1.28 (6H, td, J_{P-H} = 16.5 and 7.1 Hz, 2 × CH_3), 1.38 and 1.61 (6H, 2 × s, 2 × CH_3), 4.06 (5H, m, 2 × CH_2 and 1"-H_a), 4.21 (9H, series of multiplets, 1"-H_b, 7"-H, 6"-H, 4"-H and 3"-H), 4.48 (1H, m, 4-H), 5.06 (1H, dd, *J* = 6.2 and 2.9 Hz, 5-H), 5.35 (1H, dd, *J* = 6.2 and 2.3 Hz, 3-H), 6.14 (1H, d, *J* = 4.9 Hz, 2-H), 6.76 (2H, s, NH_2), 8.05 (1H, s, 2'-H) and 8.32 (1H, s, 8'-H); δ_C/ppm

(100MHz; $CDCl_3$) 16.05 (d, J_{P-C} = 6.5 Hz, 2 × CH_3), 25.3 and 27.1 (2 × CH_3), 64.1 (dd, J_{P-C} = 5.8 and 2.1 Hz, 2 × CH_2), 66.6 and 66.7 (5C, series of singlets, C-1", C-3",C-4",C-6" and C-7"), 81.3 (C-5'), 84.4 (C-3'), 85.4 (C-4), 91.0 (C-2), 114.7 [*C*.$(CH_3)_2$], 119.9 (C-5'), 140.2 (C-8'), 149.0 (C-4'), 150.8 (C-2') and 154.4 (C-6'); δ_P/ppm (162 MHz; $CDCl_3$) 0.8 (P=O); *m/z* 532.31 (**M**$^+$+**1**,3%) and 444.25 (100%).

2-(6-Aminopurin-9-yl)-3,4- dihydroxy-5-(10-hydroxy-2,5,8 - trioxadecyl)tetra-hydrofuran 3,4-acetonide 139 and 2-[6-(8-hydroxy-3,6,-dioxaoctylamino)-purin-9-yl]-3,4-dihydroxy-5-(10-hydroxy-2,5,8- trioxadecyl)tetrahydrofuran 3,4-acetonide 139A

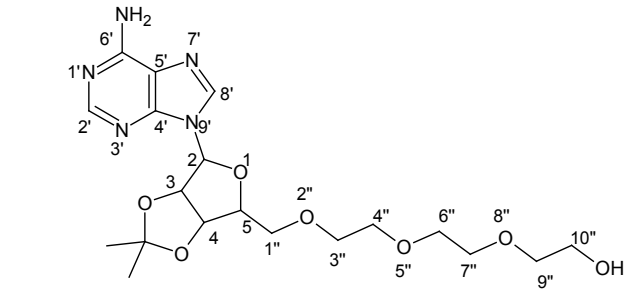

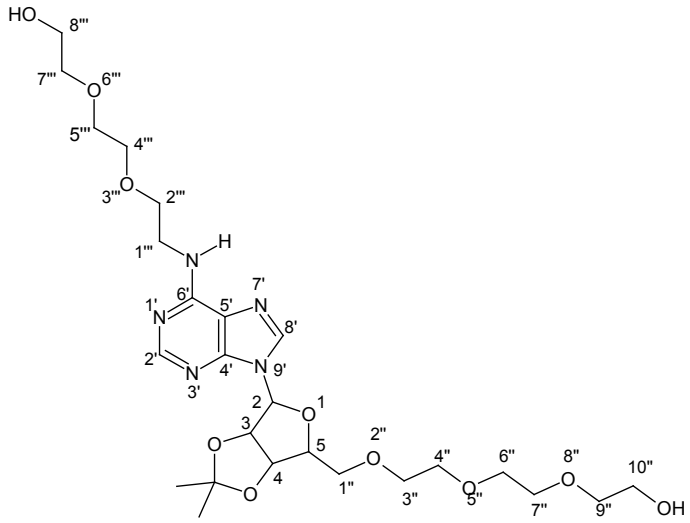

To a stirred solution of adenosine 3',4'-acetonide **127** (0.50 g, 1.6 mmol) in THF (33 mL) under nitrogen was added NaH (60% dispersion in mineral oil; 43 mg, 1.8 mmol) in small portions to permit controlled evolution of hydrogen. 2-[2-(2-chloroethoxy)ethoxy]ethanol (0.30 mL, 1.8 mmol) was then added through a septum and the resulting solution refluxed for *ca.* 5h. The reaction was quenched by the addition of water (40 mL). The solvent was taken off *in vacuo* and the aqueous

residue extracted with CH_2Cl_2 (2 × 40 mL). The organic extract was washed sequentially with satd. $NaHCO_3$ (2 × 80 mL), water (2 × 80 mL) and brine (2 × 80 mL). The aqueous washings were extracted with CH_2Cl_2 and the organic layers combined and dried (anhydr. $MgSO_4$). Evaporation of the solvent *in vacuo* afforded a yellow residue that was chromatographed [column chromatography; elution with EtOH:$CHCl_3$:hexane = 1:2:2] to afford two products:

(i) *2-(6-Aminopurin-9-yl)-3,4-dihydroxy-5-(10-hydroxy-2,5,8-trioxadecy)tetrahydro-furan 3,4-acetonide* **139** as yellow oil (23 mg, 3%). ν_{max} (thin film/cm^{-1}) 3414 (NH_2 and OH); δ_H/ppm (600MHz; $CDCl_3$) 1.37 and 1.64 (6H, 2 × s, 2 × CH_3), 3.58-3.82 (13H, series of multiplets, 1"-CH_a, 3"-H, 4"-H, 6"-H, 7"-H, 9"-H and 10"-H), 3.96 (1H, d, *J* = 13.0 Hz, 1"-CH_b), 4.53 (1H, s, 4-H), 5.10 (1H, d, *J* = 5.9 Hz, 5-H), 5.19 (1H, t, *J* = 5.4 Hz, 3-H), 5.74 (2H, d, *J* = 0.9 Hz, NH_2), 5.84 (1H, d, *J* = 4.9 Hz, 2-H), 7.83 (1H, s, 8'-H) and 8.31 (1H, s, 2'-H); δ_C/ppm (150MHz; $CDCl_3$) 25.2 and 27.7 (2 × *C*H_3), 63.4 (1"-CH_2), 61.5-72.8 (C-3", C-4", C-5", C-6", C-7", C-9" and C-10"), 81.7 (C-5), 82.9 (C-3), 86.1 (C-4), 94.4 (C-2), 114.0 [*C*.$(CH_3)_2$], 121.1 (C-5'), 140.3 (C-8'), 148.4 (C-4'), 152.7 (C-2') and 155.9 (C-6').

ii. *2-[6-(8-hydroxy-3,6-dioxaoctylamino)-purin-9-yl]-3,4-dihydroxy-5-(10-hydroxy -2,5,8 -trioxadecy tetrahydrofuran 3,4-acetonide* **139A** as a pale yellow oil (43 mg, 5%). ν_{max} (thin film/cm^{-1}) 3393 (NH and OH); δ_H/ppm (400MHz; $CDCl_3$) 1.38 and 1.64 (6H, 2 × s, 2 × CH_3), 3.51-3.81 (26H, series of multiplets, 1"-CH_2, 3-H, 4-H, 6-H, 7-H, 9-H, 10-H, 1'"-H, 2'"-H, 4'"-H, 5'"H, 6'"-H, 7'"-H and 8'"-H), 4.52 (1H, d, *J* = 2.1 Hz, 4-H), 4.94 (1H, dd, *J* = 5.8 and 1.6 Hz, 5-H), 5.08 (1H, dd, *J* = 5.8 and 3.3 Hz, 3-H), 6.29 (1H, b, NH), 6.31 (1H, d, *J* = 3.3 Hz, 2-H), 8.34 (1H, s, 2'-H) and 8.50 (1H, s, 8'-H); δ_C/ppm (100MHz; $CDCl_3$) 25.4 and 27.4 (2 × *C*H_3), 61.2-73.1 (1"-CH_2, C-3",C-4", C-6", C-7", C-9", C-10", C-1'", C-2'", C-4'", C-5'", C-7'" and C-8'"), 81.7 (C-5), 84.9 (C-3), 85.4 (C-4), 90.6 (C-2), 114.0 [*C*.$(CH_3)_2$], 118.8 (C-5'), 139.5 (C-8'), 149.8 (C-4'), 153.2 (C-2') and 155.3 (C-6').

2 - (6-Aminopurin-9-yl)-5-acetoxyacetyl-3,4-dihydroxytetrahydrofuran 3,4-acetonide 140 and 2-[6-(acetoxyacetylamino)purin-9-yl)-5-acetoxyacetyl 3,4-dihydroxytetrahydrofuran 3,4-acetonide 140A

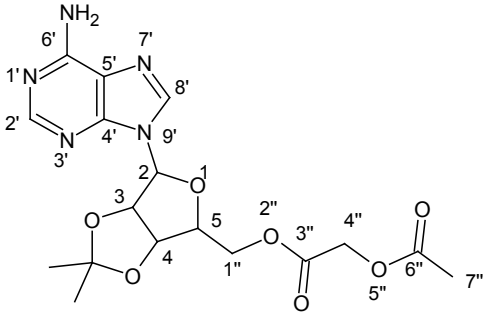

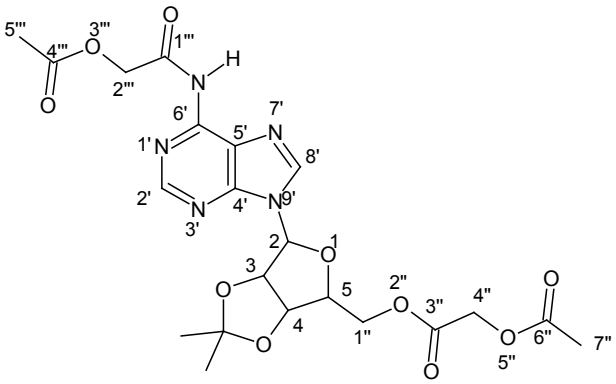

NaH (60% dispersion in mineral oil; 43 mg, 1.8 mmol) was added in small portions to a stirred solution of adenosine 3',4'-acetonide **127** (0.50 g, 1.6 mmol) in THF (33 mL) under nitrogen. Acetoxyacetyl chloride (0.20 mL, 1.8 mmol) was then added through a septum and the resulting solution was refluxed for *ca.* 5 h. The reaction was quenched by the addition of water (50 mL). The solvent was evaporated *in vacuo* and the aqueous residue extracted with CH_2Cl_2 (2 × 50 mL). The combined organic extract was washed sequentially with satd. aq. $NaHCO_3$ (2 × 100 mL), water (2 × 100 mL) and brine (2 × 100 mL). The aqueous washings were extracted with CH_2Cl_2 and the organic layers combined and dried (anhydr. $MgSO_4$). Evaporation of the solvent *in vacuo* afforded a brownish white residue that was chromatographed [radial chromatography; elution with EtOAc] to afford two products:

i. *2-(6-aminopurin-9-yl)-5-acetoxyacetyl-3,4-dihydroxy-tetrahydrofuran 3,4-acetonide* **140**, light yellow oil (230 mg, 35%). ν_{max} (thin film/cm^{-1}) 3326 (NH_2), 1750 ($CH_3C{=}O$) and 1644 (aromatic C=N); δ_H/ppm (400MHz; $CDCl_3$) 1.39 and

1.61 (6H, 2 × s, 2 × C*H*$_3$), 2.13 (3H, s, 7"-H), 4.32 (1H, m, 1"-H$_a$), 4.46 (2H, m, 1"-H$_b$ and 4-H), 4.55 (2H, s, 4"-H), 5.07 (2H, dd, *J* = 6.3 and 3.3 Hz, 5-H), 5.46 (1H, dd, *J* = 6.3 and 2.0 Hz, 3-H), 5.71 (2H, s, NH$_2$), 6.08 (1H, d, *J* = 2.0 Hz, 2-H), 7.88 (1H, s, 8'-H) and 8.34 (1H, s, 2'-H); δ_C/ppm (100MHz; $CDCl_3$) 20.4 (C-7"), 25.3 and 27.1 (2 × *C*H$_3$), 60.5 (C-4"), 64.6 (C-1"), 81.6 (C-5), 84.1 (C-3), 84.7 (C-4), 90.9 (C-2), 114.7 [*C*.(CH$_3$)$_2$], 120.4 (C-5'), 139.8 (C–8'), 149.2 (C–4'), 153.2 (C–2'), 155.5 (C–6'), 167.4 (C-3") and 170.3 (C-6"); *m/z* = 407 (**M**$^+$**-1**, 2.44%) and 408 (100%).

ii. *2-[6-(Acetoxyacetylamino)purin-9-yl)-5-acetoxyacetyl 3,4-dihydroxytetrahydrofuran 3,4-acetonide*, **140A** light yellow oil (330 mg, 40%). ν_{max} (thin film/cm^{-1}) 3422 (NH), 2957 (CH), 1725 (CH$_3$*C*=*O*) 1610 (aromatic C=N) and 1589 (NHC=O); δ_H/ppm (400MHz; $CDCl_3$) 1.39 and 1.62 (6H, 2 × s, 2 × C*H*$_3$), 2.11 (3H, s, 7'"-H), 2.22 (3H, s, 5'"–H), 4.34 (1H, dd, *J* = 11.7 and 6.1 Hz, 1"–Ha), 4.48 (4H, m, 4–H, 1"–Hb and 4"-H), 5.04 (1H, dd, *J* = 6.3 and 3.4 Hz, 5–H), 5.30 (2H, d, *J* = 3.0 Hz, 2'"–H), 5.43 (1H, dd, *J* = 6.3 and 2.11 Hz, 3–H), 6.15 (1H, d, *J* = 2.1 Hz, 2–H), 8.20 (1H, s, 2'–H), 8.66 (1H, s, 8'–H) and 9.40 (1H, s, NH); δ_C/ppm (100MHz; $CDCl_3$) 20.4 (C-7"), 20.6 (C–5'"), 25.3 and 27.1 (2 × *C*H$_3$), 60.4 (C-4"), 64.4 (C–1"), 64.6 (C–2'"), 81.4 (C–5), 84.1 (C–3), 84.7 (C–4), 91.1 (C–2), 114.9 [(.(CH$_3$)$_2$], 122.0 (C–5'), 142.7 (C–8'), 148.7 (C–4'), 150.7 (C–2'), 152.3 (C–6'), 167.3 (C–1'" and C-3"), 170.3 (C–4'") and 170.3 (C-6"); *m/z* = 507 (**M**$^+$, 17.32%) and 157 (100%).

2-(6-Aminopurin-9-yl)-5-[(2-chloroacetoxy)methyl]-3,4-dihydroxytetrahydrofuran 3,4-acetonide 141 and 2-[6-(2-chloroacetamido)purin-9-yl]-5-[(2-chloroacetoxy)-methyl] 3,4-dihydroxytetrahydrofuran 3,4-acetonide 141A

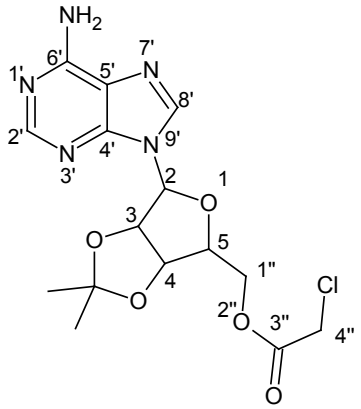

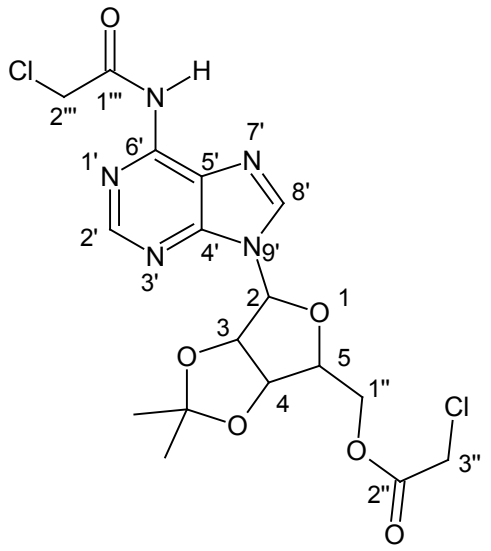

A mixture of adenosine 3',4'-acetonide **127** (0.50 g, 1.6 m mol) in chloroacetyl chloride (1.4 mL, 1.8 mmol) was stirred under argon. The crude ester crystallized out within 0.5 h. T he excess acid chloride was evaporated *in vacuo* and the residue was dissolved in $CHCl_3$ (2 × 50 mL). This solution was washed sequentially with satd. aq. $NaHCO_3$ (2 × 100 mL) and brine (2 × 100 mL). The aqueous washings were extracted with $CHCl_3$ and the organic layers combined and dried (anhydr. $MgSO_4$). Evaporation of the solvent *in vacuo* afforded the pure *2-(6-aminopurin-9-yl)-5-[(2-chloroacetoxy)methyl]-3,4-dihydroxytetrahydrofuran 3,4-acetonide* **141** as light yellow crystals, (0.59 g, 94%), m.p. 150 -151°C. ν_{max} (solid deposit/cm^{-1}) 3398 (NH_2), 1738 (C=O); δ_H/ppm (400MHz; $CDCl_3$) 1.38 and 1.59 (6H, 2 × s, 2 × CH_3), 4.00 (2H, s, 4"-H), 4.34 (1H, dd, *J* = 13.0 and 7.6 Hz, 1"-CH_a), 4.48 (2H, m, 1"-CH_b and 4-H), 5.08 (1H, dd, *J* = 6.3 and 3.2 Hz, 5-H), 5.46 (1H, dd, *J* = 6.3 and 1.9 Hz, 3-H), 6.09 (1H, d, *J* = 1.9 Hz, 2-H), 6.14 (2H, s, NH_2), 7.88 (1H, s, 8'-H) and 8.32 (1H, s, 2'-H); δ_C/ppm (100MHz; $CDCl_3$) 25.3 and 27.1 (2 × *C*H_3), 40.5 (C-4"), 65.4 (C-1"), 81.5 (C-5), 84.1 (C-3), 84.6 (C-4), 90.9 (C-2), 114.7 [*C*.$(CH_3)_2$], 120.3 (C-5'), 139.8 (C-8'), 149.1 (C-4'), 153.1 (C-2'), 155.7 (C-6') and 166.8 (C=O); *m/z* = 384.22 (**M**$^+$**+1**, 9%) and 346 (100%).

In a separate reaction the acetonide **127** was treated with the same reagent following the procedure above. Work up afforded (i) **141** and (ii) *2-[6-(2-chloroacetamido)-purin-1-yl]-5-[(2-chloroacetoxy)methyl]-3,4-dihydroxytetrahydrofuran 3,4-acetonide* **141A** as a yellow oil.

ii *2[6-(2-chloroacetamido) purin-9-yl]-5-[(2-chloroacetoxy)methyl] 3,4-dihydroxy tetra-hydrofuran 3,4-acetonide* **141A** as light yellow crystals. ν_{max} (solid deposit/cm^{-1}) (NH), (C=O); δ_H/ppm (400MHz; $CDCl_3$) 1.39 and 1.62 (6H, 2 × s, 2 × C*H*$_3$), 4.01 (2H, s, 4"-CH_2), 4.45 (4H, m, 1"-CH_2, 4-H and NH), 4.68 (1H, s, 2'"-CH_2), 5.06 (1H, dd, *J* = 6.2 and 3.4 Hz, 5-H), 5.45 (1H, dd, *J* = 6.2 and 1.9 Hz, 3-H), 6.18 (1H, d, *J* = 1.9 Hz, 2-H), 8.25 (1H, s, 2'-H) and 8.72 (1H, s, 8'-H); δ_C/ppm (100MHz; $CDCl_3$) 25.3 and 27.1 (2 × *C*H$_3$), 40.5 (C-4"), 44.6 (C-2'"), 65.3 (C-1"), 81.3 (C-5), 84.1 (C-3), 84.6 (C-4), 91.1 (C-2), 115.0 [*C*.$(CH_3)_2$], 122.5 (C-5'), 142.8 (C-8'), 148.5 (C-4'), 152.4 (C-2'), 166.0 (C-6'), 166.8 (NH-*C*=O) and 166.83 (O-*C*=O).

5-[(Acryloyloxy)methyl]-2-(6-aminopurin-9-yl)-3,4-dihydroxytetrahydrofuran 3,4-acetonide 143

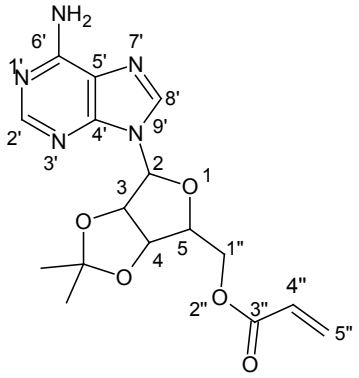

To a stirred solution of adenosine 3',4'-acetonide **127** (1.0 g, 3.3 mmol) in THF (30 mL) under nitrogen was added NaH (60% dispersion in mineral oil; 0.15 g, 3.3 mmol) in small portions to permit controlled evolution of hydrogen. Acryloyl chloride (0.27 mL, 3.3 mmol) was then added with a septum and the resulting solution was refluxed for *ca.* 5h. The reaction was quenched by the addition of water (50 mL). The solvent was evaporated *in vacuo* and the aqueous residue extracted with CH_2Cl_2 (2 × 50 mL). The organic extract was washed sequentially with satd. aq. $NaHCO_3$ (2 × 100 mL) and brine (2 × 100 mL). The aqueous washings were extracted with CH_2Cl_2 and the organic layers combined and dried (anhydr. $MgSO_4$). Evaporation of the solvent *in vacuo* afforded a pale yellow residue. Column chromatography on silica [elution with EtOH-EtOAc (1:20)] afforded *5-[(acryloyloxy)methyl]-2-(6-aminopurin-9-yl)-3,4-dihydroxytetrahydrofuran3,4-acetonide* **143** as a light brown solid (49 mg, 4.1%), m.p. 188-192°C. (Found: $\mathbf{M}^+$, 361.137825. $C_{16}H_{19}N_5O_5$ requires: $\mathbf{M}^+$, 361.138619);

ν_{max} (thin film/cm^{-1}) 3413 (NH_2) and 1714 (C=O); δ_H/ppm (400MHz; $CDCl_3$) 1.39 and 1.61 (6H, 2 × s, 2 × C*H*$_3$), 4.30 (1H, dd, *J* = 11.8 and 6.0 Hz, 1"-H_a), 4.44 (1H, dd, *J* = 11.9 and 4.5 Hz, 1"-H_b), 4.50 (1H, d, *J* = 1.1 Hz, 4-H), 5.08 (1H, dd, *J* = 6.3 and 3.4 Hz, 5-H), 5.48 (1H, dd, *J* = 6.3 and 2.0 Hz, 3-H), 5.80 (1H, dd, *J* = 10.5 and 0.8 Hz, 5"-H_E), 5.87 (2H, s, NH_2), 6.02 (1H, dd, *J* = 17.3 and 10.4 Hz, 4"-H), 6.10 (1H, d, *J* = 1.9 Hz, 2-H), 6.36 (1H, dd, *J* = 17.3 and 0.9 Hz, 5"-H_Z), 7.87 (1H, s, 8'-H) and 8.33 (1H, s, 2'-H); δ_C/ppm (100MHz; $CDCl_3$) 25.4 and 27.1 (2 × *C*H_3), 64.0 (C-1"), 81.7 (C-5), 84.2 (C-3), 85.0 (C-4), 91.0 (C-2), 114.6 [*C*.$(CH_3)_2$], 120.3 (C-5'), 127.6 (C-4"), 131.6 (C-5"), 139.7 (C-8'), 149.2 (C-4'), 153.2 (C-2'), 155.6 (C-6') and 165.5 (C=O).

4-Bromomethyl-2,2-dimethyl-[1,3]dioxolane 145

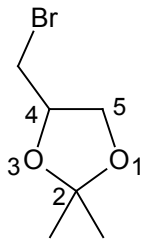

A solution of 3-bromo-1,2-proanediol (0.50 mL, 5.7 mmol) and *p*-toluenesulphonic acid (4.1 g, 24 mmol) in acetone (600 mL) was stirred at room temperature overnight. The reaction was quenched with aqueous Na_2CO_3 (10%, 210 mL). The solvent was removed *in vacuo* and the aqueous residue extracted with CH_2Cl_2 (3 × 250 mL). The combined organic extracts were dried (anhydr. $MgSO_4$) and evaporated *in vacuo* to afford 4-bromomethyl-2,2-dimethyl-[1,3]dioxolane **145** as a yellow oil (730 mg, 66%). δ_H/ppm (400MHz; $CDCl_3$) 1.34 and 1.43 (6H, 2 × s, 2 × CH_3), 3.30 (1H, dd, *J* = 9.9 and 8.3 Hz, CH_a), 3.42 (1H, dd, *J* = 10.0 and 4.7 Hz, CH_b), 3.86 (1H, dd, *J* = 8.7 and 5.2 Hz, 5-H_a), 4.12 (1H, dd, *J* = 8.7 and 6.1 Hz, 5-H_b) and 4.33 (1H, ddd, *J* = 11.0, 8.2 and 5.4 Hz, 4-H); δ_C/ppm (100MHz; $CDCl_3$) 25.4 and 27.0 (2 × *C*H_3), 32.7 (*C*H_2), 63.3 (C-5), 75.3 (C-4) and 110.3 (C-2).

(3,4,5,6-Tetraacetoxy 2-acetoxymethyl)pyran 148

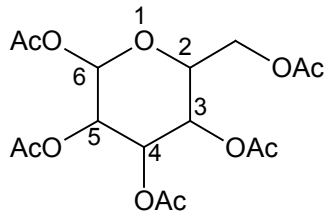

A mixture of zinc chloride (0.5 g, 3.7 mmol) in acetic anhydride (13 mL, 13.0 mmol) was heated for *ca.* 10 minutes. D-glucose (2.5 g, 1.4 mmol) was then added slowly a little at a time to control the evolution of hydrogen. The mixture was then heated without reflux for *ca.* 1 h. Ice-water (125 mL) was added with gentle stirring to quench the reaction in a period of *ca.* 30 minutes. Further stirring was done for 30 minutes by which time the crude product had started crystallizing out of solution. The crude product mixture was allowed to stand at 0ºC for 24 h and the white solid filtered off and recrystallised from methanol to afford pure pentaacetylated α–D-glucopyranose **148** as a white crystalline solid (4.7 g, 87%), m.p. 84-86°C (lit.[181] 110-111°C). ν_{max} (solid deposit/cm^{-1}) 1750 (C=O); δ_H/ppm (400MHz; $CDCl_3$) 2.01 (9H, series of singlets, 3 × CH_3), 2.08 (3H, s, 2-CH_3), 2.16 (3H, s, 6-CH_3), 4.09 (2H, m, CH_a and 2-H,), 4.25 (1H, dd, *J* = 12.5 and 4.1 Hz, CH_b), 5.11 (2H, m, 3-H and 5-H), 5.45 (1H, t, *J* = 9.9 Hz, 4-H) and 6.31 (1H, d, *J* = 3.7 Hz, 6-H); δ_C/ppm (100MHz; $CDCl_3$) 20.4, 20.5, 20.6, 20.7 and 20.9 (series of singlets, 5 × CH_3), 61.5 (CH_2), 67.9 (C-3), 69.2 (C-5), 69.8 (C-2 and C-4), 89.1 (C-6), 168.7 (6-*C* =O), 169.4, 169.6 and 170.2 (3 × *C* =O), and 170.6 (2-*C*=O); *m/z* = 390 (**M**$^+$, 0.03%) and 98 (100%).

3,4,5-Triacetoxy-6-acetoxymethyl-2-(6-aminopurin-9-yl)pyran 149

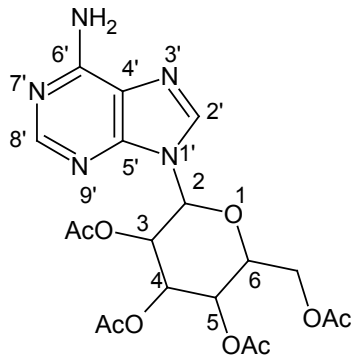

Adenine **61** (0.5 g, 3.7 mmol) and acetylated glucose **148** (1.4 g, 3.5 m mol) were placed in a 100 mL dried 3-neck flask equipped with a reflux condenser. Acetonitrile (20 mL) was added through a septum and the reaction mixture stirred. Tin tetrachloride (1.0 mL, 9.3 mmol) was then added and the reaction mixture refluxed under argon for *ca.* 6 h. The reaction was quenched with satd. $NaHCO_3$ (50 mL). The solvent was evaporated *in vacuo* and the aqueous residue extracted with EtOAc (2 × 25 mL). The organic extract was washed sequentially with satd. aq. $NaHCO_3$ (2 × 50 mL) and brine (2 × 50 mL). The aqueous washings were extracted with EtOAc and the organic layers combined and dried (anhydr. $MgSO_4$). Evaporation of the solvent *in vacuo* afforded a pale yellow residue. Column chromatography on silica [elution with EtOH-$CHCl_3$ (1:19)] afforded 2-[(6-aminopurin-9-yl)-6-acetoxymethyl-3,4,5-triacetoxy)] pyran **149** as yellow crystals (510 mg, 30%), m.p. 63-65°C. (Found: $\mathbf{M}^+$, 465.14892. $C_{19}H_{23}N_5O_9$ requires: $\mathbf{M}^+$, 465.41498); ν_{max} (solid deposit/cm^{-1}) 3339 (NH_2) and 1744 (C=O); δ_H/ppm (400MHz; $CDCl_3$) 2.00 – 2.08 (12H, series of singlets, 4 × CH_3), 4.02 (1H, ddd, *J* = 10.1, 4.8 and 2.1 Hz, 6-H), 4.14 (1H, dd, *J* = 12.6 and 2.1 Hz, C*H*$_a$), 4.29 (1H, dd, *J* = 12.6 and 4.9 Hz, C*H*$_b$) 5.27 (1H, t, *J* = 9.8 Hz, 5-H), 5.44 (1H, t, *J* = 9.5 Hz, 4-H), 5.58 (1H, t, *J* = 9.5 Hz, 3-H), 5.76 (1H, s, NH_2), 5.88 (1H, d, *J* = 9.5 Hz, 2-H), 8.00 (1H, s, 8'-H) and 8.36 (1H, s, 2'-H); δ_C/ppm (100MHz; $CDCl_3$) 20.1, 20.5, 20.6 and 20.7 (series of singlets, 5 × CH_3), 61.6 (*C*H_2), 67.9 (C-5), 70.4 (C-3), 72.9 (C-4), 75.1 (C-6), 80.3 (C-2), 119.2 (C-5'), 138.3 (C-8'), 150.7 (C-4'), 153.4 (C-2'), 155.4 (C-6'), 169.0 (3-*C*=O), 169.4(5-*C*=O), 169.8(4-*C*=O) and 170.5 (6-*C*=O).

6-(*N*-Allylamino)purine 150 and 9-Allyl-[6-amino(*N*-allylamino)] purine 150A

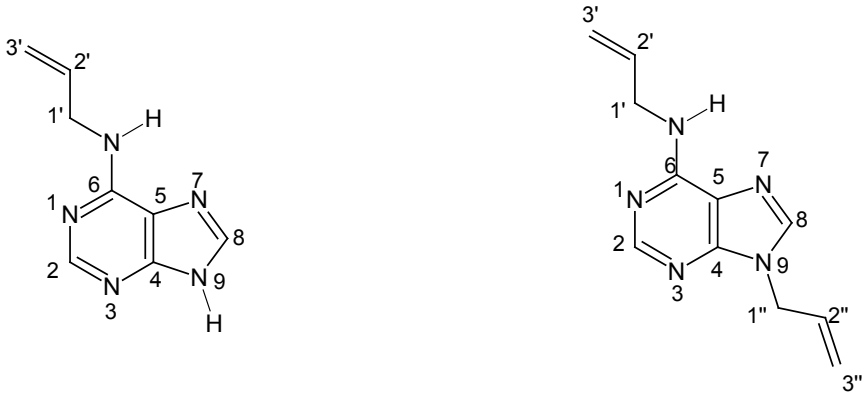

NaH (60% dispersion in mineral oil; 100 mg, 4.0 mmol) was added in small portions permit controlled evolution of hydrogen, to a stirred solution of adenine **61** (300 mg, 2.2 mmol) in dry DMF (20 mL) under nitrogen at 0ºC. Allyl bromide (230 µL, 2.7 mmol) was then added with through a septum and the resulting solution refluxed for *ca.* 6 h. The reaction was quenched by the addition of water (25 mL). The solvent was evaporated *in vacuo* and the aqueous residue extracted with $CHCl_3$ (2 × 25 mL). The combined organic extracts were washed sequentially with satd. $NaHCO_3$ (2 × 50 mL), water (2 × 50 mL) and brine (2 × 50 mL). The aqueous washings were extracted with $CHCl_3$ and the organic layers combined and dried (anhydr. $MgSO_4$). The solvent was evaporated *in vacuo* and the residue chromatographed on s ilica [column chromatography; elution with EtOH-EtOAc (1:20)] to afford two fractions.

(i) *6-(N-allylamino)purine* **150** as a yellow solid (45 mg, 12%), m.p. 165-167°C. (Found: $\mathbf{M}^+$, 175.085842. $C_8H_9N_5$ requires: $\mathbf{M}^+$, 175.085795); ν_{max} (solid deposit/cm^{-1}) 3382 (NH); δ_H/ppm (400MHz; $CDCl_3$) 4.91 (2H, d, *J* = 5.8 Hz, 1'-H), 5.25 (1H, d, *J* = 17.1 Hz, 3'-Ha, CH=C*H*$_Z$), 5.35 (1H, d, *J* = 10.2 Hz, 3'-Hb CH=C*H*$_E$), 6.07 (1H, tdd, *J* = 16.1, 10.4 and 5.8 Hz, 2'-H), 8.43 (1H, s, 8-H), 8.70 (1H, s, 2-H), 10.01 (1H, d, *J* = 10.0 Hz, 6-NH) and 11.12 (1 H , d, *J* = 9.4 Hz, 1-NH); δ_C/ppm (100MHz; $CDCl_3$) 46.1 (C-1'), 119.6 (C-3'), 120.4 (C-5), 131.2 (C-2'), 144.2 (C-8), 149.3 (C-4), 151.9 (C-6) and 152.5 (C-2).

(ii) *9-allyl-[6-amino(N-allylamino)] purine* **150A** as a yellow solid (8.0 mg, 2.0%), m.p. 103-105°C. (Found: $\mathbf{M}^+$, 215.118412. $C_{11}H_{13}N_5$ requires: $\mathbf{M}^+$, 215.117096); ν_{max} (thin film/cm^{-1}) 3383 (NH); δ_H/ppm (400MHz; $CDCl_3$) 4.80 (4H, d, *J* = 5.27 Hz, 1'-CH_2 and 1"-CH_2), 5.19 (2H, m, 3"-H), 5.30 (1H, m, 3'-H), 6.02 (2H, m, 2'-H and 2"-H), 7.77 (1H, s, 2-H) and 8.40 (1H, s, 8-H); δ_C/ppm (100MHz; $CDCl_3$) 45.7 (C-1' and C-1"), 116.4 (C-3'), 118.9 (C-3"), 119.6 (C-5), 131.9 (C-2"), 134.3 (C-2'), 139.7 (C-2), 152.5 (C-4), 153.2 (C-2) and 154.7 (C-6).

4-(Tetrahydropyran-2-yloxy)-1*H*-pyrazolo[3,4]pyrimidine 157

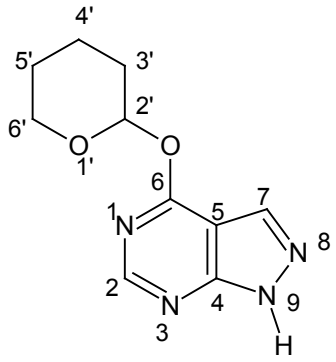

A stirred mixture of allopurinol (1.0 g, 7.4 mmol) in 50 mL reagent grade DMF (50 mL) was heated to *ca.* 75 ºC to dissolve the substrate. To the resulting solution was added dihydropyran (20 mL) followed by the addition of para-toluene sulphonic acid [16 mg in benzene (4 mL) i.e. 0.4% p-TSA in dry benzene]. The reaction mixture was stirred for 24 h. at room temperature. The reaction was quenched with a 4% pyridine in benzene solution (0.5 mL) at end of which the solvent was evaporated *in vacuo* at 40ºC and the crude product dissolved in petroleum ether (100 mL) and allowed to crystallize overnight at 0ºC. Recrystallisation from EtOAc-acetone afforded 4-(tetrahydropyran-2-yloxy)-1*H*-pyrazolo[3,4]pyrimidine **157** as white crystals, (0.40 g, 25%); m.p. 190-193°C (lit.[184] 200-201°C). ν_{max} (solid deposit/cm^{-1}) 3403 (NH); δ_H/ppm (400MHz; $CDCl_3$) 1.62 (1H, dd, *J* = 7.0 and 4.6 Hz, 4'-CH_a), 1.77 (2H, m, 4'-CH_b and 5'-CH_a), 1.94 (1H, dd, *J* = 12.8 and 2.7 Hz, 3'-CH_a), 2.13 (1H, m, 5'-CH_b), 2.55 (1H, m, 3'-CH_b), 3.76 (1H, dt, *J* = 11.4, 11.3 and 2.5 Hz, 6'-CH_a), 4.12 (1H, dd, *J* = 7.6 and 6.0 Hz, 6'-CH_b), 5.89 (1H, dd, *J* = 10.2 and 2.5 Hz, 2'-H), 8.03 (1H, s, 7-H), 8.15 (1H, s, 2-H) and 12.22 (1H, s, NH); δ_C/ppm (100MHz; $CDCl_3$) 22.7 (C-5'),

24.8 (C-4'), 29.4 (C-3'), 68.3 (C-6'), 83.0 (C-2'), 106.5 (C-4), 135.4 (C-7), 146.4 (C-2), 152.4 (C-6) and 159.9 (C-5).

1-Allyl-4-(tetrahydropyran-2-yloxy)-1*H*-pyrazolo[3,4]pyrimidine 158

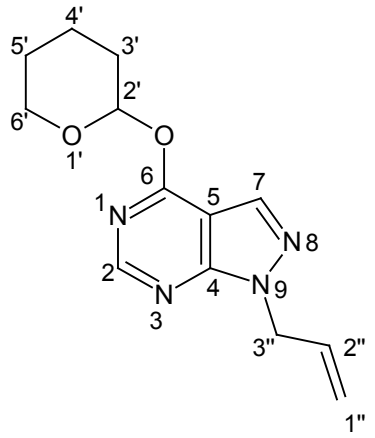

To a stirred solution of protected allopurinol **157** (200 mg, 0.91 mmol) in dry THF (50 mL) under nitrogen was added NaH (60% dispersion in mineral oil; 40 mg, 0.91 mmol) in small portions to permit controlled evolution of hydrogen. Allyl bromide (80 μL, 0.91 mmol) was then added through a septum and the resulting solution was refluxed for *ca.* 6h. The reaction was quenched by the addition of water (50 mL). The solvent was evaporated *in vacuo* and the aqueous residue extracted with CH_2Cl_2 (2 × 50 mL). The combined organic extracts were washed sequentially with water (2 × 100 mL) and brine (2 × 100 mL). The aqueous washings were extracted with CH_2Cl_2 and the organic layers combined and dried (anhydr. $MgSO_4$). Evaporation of the solvent *in vacuo* afforded *1-allyl-4-(tetrahydropyran-2-yloxy)-1H-pyrazolo[3,4-d]pyrimidine* **158** as a pale yellow solid (210 mg, 87%), m.p. 60-62°C. (Found: $\mathbf{M}^+$, 260.12774. $C_{13}H_{16}N_4O_2$ requires: $\mathbf{M}^+$, 260.29174); δ_H/ppm (400MHz; $CDCl_3$) 1.61 (1H, m, 4'-CH_a), 1.75 (2H, m, 4'-CH_b and 5'-CH_a), 1.93 (1H, m, 3'-CH_a), 2.13 (1H, m, 5'-CH_b), 2.54 (1H, m, 3'-CH_b), 3.75 (1H, dt, *J* = 11.4 and 2.5 Hz, 6'-CH_a), 4.10 (1H, m, 6'-CH_b), 4.61 (2H, m, 3"-CH_2), 5.21 (1H, d, *J* = 17.1 Hz, CH_2-CH=C*H*$_Z$), 5.28 (1H, dd, *J* = 10.3 and 0.8 Hz, CH_2-CH=C*H*$_E$), 5.83 (1H, dd, *J* = 10.3 and 2.6 Hz, 2'-H), 5.94 (1H, tdd, *J* = 16.1, 10.4 and 5.7 Hz, 2"-H), 7.94 (1H, s, 7-H) and 8.12 (1H, s, 2-H). δ_C/ppm (100MHz; $CDCl_3$) 22.7 (C-5'), 24.9 (C-4'), 29.3 (C-3'), 47.8 (C-3"), 68.2 (C-6'), 82.9 (C-2'), 106.3 (C-8), 118.9 (C-1"), 132.1 (C-2"), 135.8 (C-7), 149.0 (C-2), 151.7 (C-6) and 156.8 (C-5).

Tert-Butyl 3-(5-bromo-2-hydroxyphenyl)-3-hydroxy-2-methylene propanoate 165a

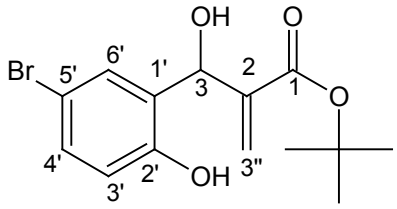

To a solution of *tert*-butyl acrylate **164** (3.2 mL, 22 mmol) in $CHCl_3$ (3 mL) was added 1,4-Diazabicyclo[2.2.2]octane (**DABCO)** (1.3 g, 12 mmol). The solution was stirred for *ca.* 5 mins. 5-bromo-2-hydroxybenzaldehyde **163** (3.0 g, 15 mmol) was then added and the reaction mixture stirred for *ca.* 4 days. The resultant viscous yellow material was eluted through silica with acetone. The solvent was taken evaporated *in vacuo* and the residue recrystallised from $CHCl_3$ to obtain 2-[(5-Bromo-2-hydroxyphenyl) hydroxymethyl] acrylic acid *tert*-butyl ester **165a** as a white powder (4.3 g, 88%), m.p. 185-187ºC (lit.[185] 186-188°C); ν_{max} (solid deposit/cm^{-1}) 3294 OH, 1684 C=O, δ_H/ppm (400MHz; DMSO-d_6) 1.32 (9H, s, Bu^t), 5.59-5.36 (1H, br s, CH-O*H*), 5.65 (1H, dd, *J* = 5.2 and 3.6 Hz, 3-H_a), 5.66 (1H, s, CH), 6.05 (1H, s, 3-H_b), 6.75 (1H, d, *J* = 8.33 Hz, 4'-H), 7.21 (2H, m, 3'-H and 6'-H) and 9.81–9.53 (1H, b, 2' -OH); δ_C (100MHz; DMSO-d_6) 27.4 C(CH_3)$_3$, 64.5 (C-HOH), 80.0 *C*(CH_3)$_3$, 109.5 (C-2'), 117.0 (C-4'), 122.8 (C-3), 129.7 (C-6'), 130.3 (C-5'), 131.8 (C-3'), 144.8 (C-2), 153.7 (C-1') and 164.8 (C=O).

Tert-Butyl 3-hydroxy-3-(2-hydroxyphenyl)-2-methylene propanoate 165b and _tert_-butyl 2-_H_-chromene-2-carboxylate 166b

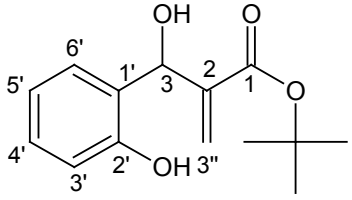

165b

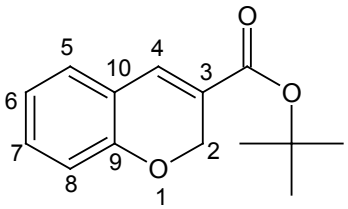

166b

A solution of *tert*-butyl acrylate **164** (5.5 mL, 38 m mol) and 1,4-Diazabicyclo-[2.2.2]octane **(DABCO)** (2.2 g, 20 mmol) in $CHCl_3$ (3 mL) was stirred for *ca.* 5 mins. Salicylaldehyde **163b** (2.6 mL, 25 m mol) was then added and the reaction mixture stirred for *ca.* 3 weeks. The solvent was evaporated *in vacuo* and the reddish residue chromatographed [gravity chromatography; elution with hexane:EtOAc = 7:1] to afford two products.

i. *Tert*-butyl 3-hydroxy-3-(2-hydroxyphenyl)-2-methylene propanoate **165b** as a white powder (0.25 g, 4.1%), m.p. 107-111°C (lit. 108-110ºC); (Found: $[\mathbf{M-1}]^+$, 231.101945. $C_{14}H_{16}O_3$ requires: $\mathbf{M}^+$, 232.109945); ν_{max} (solid deposit/cm^{-1}) 3414 (OH) and 1687 (C=O); δ_H/ppm (400MHz; $CDCl_3$), 1.50 (9H, s, Bu^t), 4.36 (1H, d, *J* = 3.9 Hz, 3-OH), 5.49 (1H, s, 3"-H_a), 5.69 (1H, d, *J* = 3.3 Hz, 3-H), 6.23 (1H, s, 3"-H_b), 6.83 (1H, t, *J* = 7.4 Hz, 5'-H), 6.90 (1H, d, *J* = 8.0 Hz, 3'-H), 6.96 (1H, dd, *J* = 7.6 and 1.5 Hz, 6'-H), 7.20 (1H, m, 4'-H) and 8.14 (1H, s, 2'-OH); δ_C (100MHz; $CDCl_3$) 28.0 C(CH_3)$_3$, 73.6 (C-3), 82.6 *C*(CH_3)$_3$, 117.5 (C-3'), 119.8 (C-5'), 124.1 (C-1'), 126.9 (C-3'), 127.8 (C-6'), 129.5 (C-4'), 140.8 (C-2), 155.9 (C-2') and 166.7 (C=O).

ii. ***Tert*-Butyl 2-*H*-chromene-3-carboxylate 166b**

Tert-Butyl 2-H-chromene-3-carboxylate **166b** (21 mg, 0.37%) as a yellow oil, ν_{max} (thin film/cm^{-1}) 1699 (C=O); δ_H/ppm (400MHz; $CDCl_3$), 1.52 (9H, s, Bu^t), 4.94 (2H, s, 2-H), 6.82 (1H, d, *J* = 8.1 Hz, 5-H), 6.90 (1H, t, *J* = 7.4 Hz, 6-H), 7.11 (1H, d, *J* = 7.4 Hz, 8-H), 7.20 (1H, m, 7-H), and 7.32 (1H, s, 4-H); δ_C (100MHz; $CDCl_3$) 28.1 (3 × C(CH_3)$_3$, 64.6 (C-2), 81.2 *C*(CH_3)$_3$, 116.0 (C-5), 121.1 (C-10), 121.6 (C-6), 124.2 (C-3), 128.7 (C-8), 131.5 (C-7), 132.5 (C-4), 155.0 (C-9) and 163.8 (C=O).

***Tert*-butyl 6-bromo-2*H*-chromene-3-carboxylate 166A**

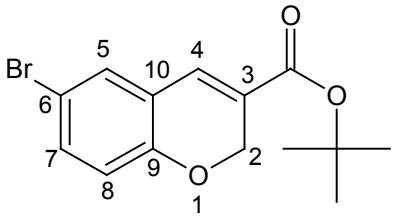

NaH (60% dispersion in mineral oil; 0.03 g, 0.61 mmol) added in small portions, to permit controlled evolution of hydrogen, to a stirred solution of 3-aminobenzonitrile

173 (72 mg, 0.61 mmol) in dry THF (10 mL) under nitrogen at 0°C. The resulting solution was refluxed for 1 h and then allowed to cool. *Tert*-butyl 3-(5-bromo-2-hydroxyphenyl)-3-hydroxy-2-methylene propanoate **165A** (200 mg, 0.61 mmol) was added and the mixture refluxed for *ca.* 6 h. The reaction was quenched by the addition of water (15 mL). The solvent was evaporated *in vacuo* and the aqueous residue was extracted with EtOAc (2 × 30 mL). The combined organic extracts were washed sequentially with water (2 × 60 mL) and brine (2 × 60 mL). The aqueous washings were extracted with EtOAc and the organic layers combined and dried (anhydr. $MgSO_4$). Flash chromatography [on silica gel; elution with hexane-EtOAc (8:2)] afforded *tert-butyl 6-bromo-2H-chromene-3-carboxylate* **166a**, as a yellow oil, (47 mg, 25%). (Found: $\mathbf{M}^+$, 310.020638. $C_{14}H_{15}{}^{79}BrO_3$ requires: $\mathbf{M}^+$, 310.185966); ν_{max} (solid deposit/cm^{-1}) 1703 (C=O); δ_H/ppm (400MHz; $CDCl_3$), 1.52 (9H, s, Bu^t), 4.94 (2H, d, *J* = 1.3 Hz, 2-H), 6.71 (1H, d, *J* = 8.6 Hz, 7-H), 7.23 (2H, m, 5-H and 8-H) and 7.27 (1H, dd, *J* = 8.6 and 2.4 Hz, 4-H); δ_C (100MHz; $CDCl_3$) 28.1 C(CH_3)$_3$, 64.8 (C-2), 81.6 $C(CH_3)_3$, 113.5 (C-6), 117.8 (C-7), 122.9 (C-10), 125.5 (C-3), 130.9 (C-5), 131.1 (C-8), 134.0 (C-4), 154.0 (C-9) and 163.4 (*C*=O).

6-Bromo-3-(chloromethyl)chromen-2-one 167, 6-Bromo-3-(acetoxymethyl)coumarin 168 and 6-Bromo-3-(hydroxymethyl)coumarin 169

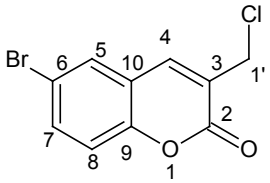

167

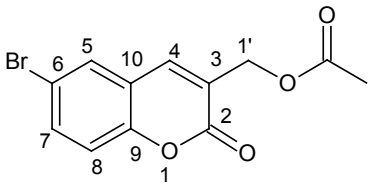

168

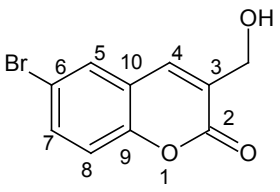

169

A mixture of *tert*-butyl 3-(5-bromo-2-hydroxyphenyl)-3-hydroxy-2-methylene propanoate (2.0 g, 6.1 mmol), conc. HCl (10 mL, 32%) and glacial acetic acid (10 mL) was boiled under reflux for 2.5 h. The reaction mixture was allowed to cool to

room temperature. Ice water (40 mL) was then added and the reaction mixture stirred for 30 mins. The product mixture was allowed to stand at 0ºC for 24 h and the pink solid was filtered off and chromatographed [flash chromatography; elution with hex:EtOAc=7:3] to afford 3 products.

i. 6-Bromo-3-(chloromethyl)chromen-2-one **167** as a white powder (0.52 g, 31%), m.p. 102-104°C. (Found: $\mathbf{M}^+$, 178.064011. $C_{10}H_{10}O_3$ requires: $\mathbf{M}^+$, 178.062994); ν_{max} (solid deposit/cm^{-1}) 1724 C=O, δ_H/ppm (400MHz; $CDCl_3$), 4.53 (2H, s, CH_2), 7.23 (1H, d, *J* = 8.8 Hz, 7-H), 7.62 (1H, dd, *J* = 8.8 and 2.3 Hz, 8-H), 7.65 (1H, d, *J* = 2.3 Hz, 5-H) and 7.80 (1H, s, 4-H); δ_C (100MHz; $CDCl_3$) 40.8 (CH_2), 117.3 (C-6), 118.4 (C-7), 120.3 (C-10), 126.3 (C-3), 130.3 (C-5), 134.7 (C-8), 139.5 (C-4), 152.3 (C-9) and 159.4 (C=O).

ii. *6-Bromo-3-(acetoxymethyl)coumarin* **168** as a white powder (33 mg, 1.8%), m.p. 119-121ºC. (Found: $\mathbf{M}^+$, 297.966202. $C_{12}H_9BrO_4$ requires: $\mathbf{M}^+$, 298.114208); ν_{max} (solid deposit/cm^{-1}) 1720 (C=O), δ_H/ppm (400MHz; $CDCl_3$) 2.16 (3H, s, CH_3), 5.06 (1H, d, *J* = 1.1 Hz, CH_2), 7.22 (1H, d, *J* = 8.7 Hz, 7-H), 7.61 (1H, dd, 8.7 and 2.3 Hz, 8-H) and 7.64 (2H, m, 5-H and 4-H); δ_C (100MHz; $CDCl_3$) 20.8 (CH_3), 60.9 (CH_2), 117.2 (C-6), 118.4 (C-7), 120.3 (C-10), 125.0 (C-3), 130.2 (C-5), 134.5 (C-8), 138.9 (C-4), 152.3 (C-9), 159.4 (2-C=O) and (CH_3C=O).

iii. *6-Bromo-3-(hydroxymethyl)coumarin* **169** as a white powder (0.11 g, 7.3%), m.p. 147-149°C. (Found: $\mathbf{M}^+$, 253.959816. $C_{10}H_7{}^{79}BrO_3$ requires: $\mathbf{M}^+$, 254.079497); ν_{max} (solid deposit/cm^{-1}) 3409 (OH) and 1632 (C=O); δ_H/ppm (400MHz; DMSO-d_6) 4.36 (1H, d, *J* = 5.4 Hz, CH_2), 5.52 (1H, dt, *J* = 5.3 and 1.3 Hz, OH), 7.37 (1H, d, *J* = 8.8 Hz, 7-H), 7.71 (1H, dd, 8.8 and 2.3 Hz, 8-H), 7.94 (1H, d, *J* = 1.1 Hz, 4-H) and 8.05 (1H, d, *J* = 2.2 Hz, 5-H); δ_C (100MHz; DMSO-d_6) 58.1 (CH_2), 116.1 (C-6), 118.2 (C-7), 121.0 (C-10), 130.1 (C-5), 130.5 (C-3), 133.3 (C-8), 135.6 (C-4), 151.3 (C-9) and 159.1 (C=O).

1-(6-Bromo-3-methyl-2*H*-chromen-2-one)-6-(tetrahydropyran-2-yloxy)pyrazolo[3,4-d] pyrimidine 170A

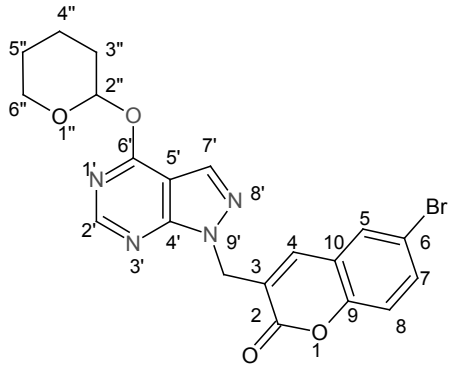

Method 1

To a stirred solution of protected allopurinol **157** (120 mg, 0.55 mmol) in dry THF (10 mL) under nitrogen was added NaH (60% dispersion in mineral oil; 24 mg, 0.99 mmol) in small portions to permit controlled evolution of hydrogen. The resulting solution was refluxed for 1 h and then cooled to room temperature before adding of 6-bromo-3-(chloromethyl)chromen-2-one **167** (150 mg, 0.55 mmol). The reaction mixture was refluxed for *ca.* 6 h at the end of which water (30 mL) was added to quench the reaction. The organic solvent was evaporated *in vacuo* and the aqueous residue extracted with CH_2Cl_2 (2 × 30 mL). The combined organic extracts were washed sequentially with water (2 × 60 mL) and brine (2 ×60 mL). The aqueous washings were extracted with CH_2Cl_2 and the organic layers combined and dried (anhydr. $MgSO_4$). Evaporation of the solvent *in vacuo* afforded pale yellow solid that was chromatographed [flash chromatography; elution with hexane-EtOAc (1:1)] to afford 1-*(6-Bromo-3-methyl-2H-chromen-2-one)-4-(tetrahydropyran-2-yloxy)pyrazolo[3,4] pyrimidine* **170A** as a white powder (77 mg, 31%), m.p. 210-212°C. (Found: $\mathbf{M}^+$, 458.041200. $C_{20}H_{17}{}^{81}BrN_4O_4$ requires: $\mathbf{M}^+$, 458.290594); ν_{max} (solid deposit/cm^{-1}) 1720 (C=O); δ_H/ppm (400MHz; $CDCl_3$) 1.60 (1H, m, 4"-H_a), 1.73 (2H, m, 4"-H_b and 5"-H_a), 1.90 (1H, m, 3"-H_a), 2.11 (1H, m, 5"-H_b), 2.50 (1H, m, 3"-H_b), 3.75 (1H, m, 6"-H_a), 4.10 (1H, m, 6"-H_b), 5.02 (1H, s, CH_2), 5.83 (1H, dd, J = 10.4 and 2.5 Hz, 2"-H), 7.19 (1H, d, J = 8.8 Hz, 8-H), 7.60 (1H, dd, J = 8.8 and 2.3 Hz, 7-H), 7.66 (1H, d, J = 2.3 Hz, 5-H), 8.00 (1H, s, 3'-H), 8.08 (1H, s, 2'-H) and 8.42 (1H, s, 4-H). δ_C/ppm (100MHz; $CDCl_3$) 22.7 (C-5"), 24.8 (C-4"), 29.3 (C-3"), 45.7 (CH_2), 68.3 (C-

6"), 82.8 (C-2"), 106.1 (C-3), 117.4 (C-6), 118.3 (C-8), 120.2 (C-5'), 123.0 (C-10), 130.7 (C-5), 135.0 (C-7), 135.6 (C-2'), 143.2 (C-7'), 150.0 (C-4), 151.7 (C-6'), 152.4 (C-9), 157.3 (C-4') and 160.7 (C=O).

Method 2

In another reaction **157** was reacted with **165A** using the same procedure to afford **170A** in 14% yield.

1-(3-methyl-2*H*-chromen-2-one)-6-(tetrahydropyran-2-yloxy)pyrazolo[3,4-d] pyrimidine 170B

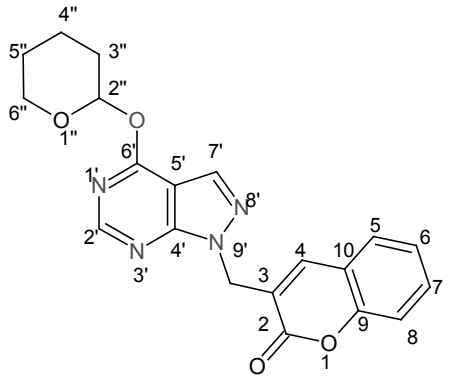

To a stirred solution of protected allopurinol **157** (110 mg, 0.49 mmol) in dry THF (10 mL) under nitrogen was added NaH (60% dispersion in mineral oil; 21 mg, 0.88 mmol) in small portions to permit controlled evolution of hydrogen. The resulting solution was refluxed for 1 h and then cooled to room temperature before adding of ***t****ert*-butyl 3-hydroxy-3-(2-hydroxyphenyl)-2-methylene propanoate **165B** (120 mg, 0.49 mmol). The reaction mixture was refluxed for *ca.* 6h. Water (30 mL) was added to quench the reaction. The organic solvent was evaporated *in vacuo* and the aqueous residue extracted with CH_2Cl_2 (2 × 30 mL). The combined organic extracts were washed sequentially with water (2 × 60 mL) and brine (2 × 60 mL). The aqueous washings were extracted with CH_2Cl_2 and the organic layers combined and dried (anhydr. $MgSO_4$). Evaporation of the solvent *in vacuo* afforded pale yellow solid that was chromatographed [flash chromatography; elution with hexane-EtOAc (3:7)] to afford *1-(2H-chromen-3-carbonyl)-4-(tetrahydropyran-2-yloxy)pyrazolo[3,4] pyrimidine* **170B** as a white powder (45 mg, 24%), m.p. 210-212°C. (Found: $\mathbf{M}^+$,

378.132008. $C_{20}H_{18}N_4O_4$ requires: $\mathbf{M}^+$, 378.382244); ν_{max} (solid deposit/cm^{-1}) 1698 (C=O); δ_H/ppm (600MHz; $CDCl_3$) 1.59 (1H, m, 4"-H_a), 1.74 (2H, m, 4"-H_b and 5"-H_a), 1.90 (1H, m, 3"-H_a), 2.11 (1H, m, 5"-H_b), 2.51 (1H, m, 3"-H_b), 3.74 (1H, m, 6"-H_a), 4.10 (1H, m, 6"-H_b), 5.03 (2H, s, CH_2), 5.84 (1H, dd, *J* = 10.4 and 2.4 Hz, 2"-H), 7.29 (2H, m, 6-H and 8-H), 7.52 (2H, m, 5-H and 7-H), 8.07-8.09 (2H, 2 × s , 2'-H and 7'-H) and 8.46 (1H, s, 4-H). δ_C/ppm (150MHz; $CDCl_3$) 22.7 (C-5"), 24.8 (C-4"), 29.4 (C-3"), 45.7 (*C*H_2), 68.3 (C-6"), 82.8 (C-2"), 106.2 (C-3), 116.6 (C-6), 118.7 (C-7), 121.9 (C-10), 124.8 (C-8), 128.5 (C-5'), 132.3 (C-5), 135.6 (C-4), 144.5 (C-7'), 150.2 (C-2'), 151.8 (C-4'), 153.7 (C-9), 157.4 (C-6') and 161.4 (C=O).

_N_-Allyl-3-cyanoaniline 177 and _N,N_-Diallyallyl-3-cyanoaniline 177A

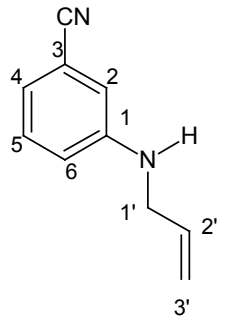

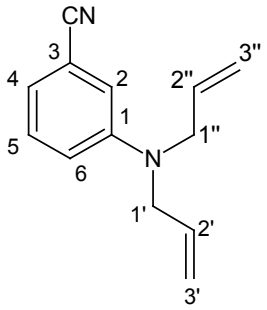

To a stirred solution of 3-aminobenzonitrile **173** (0.50 g ,4.2 mmol) in dry THF (42 mL) under nitrogen was added NaH (60% dispersion in mineral oil; 0.10 g, 4.2 mmol) in small portions to permit controlled evolution of hydrogen. Allyl bromide (0.37 mL, 4. 2 mmol) was then added through a septum and the resulting solution was refluxed for *ca.* 48 h. The reaction was quenched by the addition of water (45 mL). The solvent was evaporated *in vacuo* and the aqueous residue extracted with EtOAc (2 × 90 mL). The combined organic extracts were washed sequentially with water (2 × 180 mL) and brine (2 × 180 mL). The aqueous washings were extracted with EtOAc and the organic layers combined and dried (anhydr. $MgSO_4$). Radial chromatography [on silica gel; elution with hexane-EtOAc (4:1)] afforded N-*Allyl-3-cyanoaniline* **177** as a yellow oil (300 mg, 45%). (Found: $\mathbf{M}^+$, 158.085475. $C_{10}H_{10}N_2$ requires: $\mathbf{M}^+$, 158.200253); ν_{max} (thin film/cm^{-1}) 3391 (NH) 2228 (CN); δ_H/ppm (400MHz; $CDCl_3$) 3.76 (2H, m, 1'-CH_2), 4.13 (1H, s, NH), 5.18 (1H, ddd, *J* = 10.3, 2.8 and 1.4 Hz, CH=CH_E), 5.26 (1H, ddd, *J* = 17.2, 3.1 and 1.6 Hz, CH=CH_Z), 5.89 (1H, tdd, *J* =

17.1, 10.4 and 5.2 Hz, 2'-H), 6.78 (2H, m, 4-H and 6-H), 6.92 (1H, m, 2-H) and 7.19 (1H, m, 5-H); δ_C/ppm (100MHz; $CDCl_3$) 45.9 (C-1'), 112.7 (CN), 114.9 (C-6), 116.6 (C-3'), 117.3 (C-4), 119.4 (C-3), 120.6 (C-2), 129.7 (C-5), 134.1 (C-2') and 148.2 (C-1).

In a separate reaction 3-aminobenzonitrile **173** (1.0 g, 8.5 m mol) in THF (20 mL) under nitrogen was NaH (60% dispersion in mineral oil; 370 mg, 15 mmol) and allyl bromide (0.74 mL, 8.5 mmol). Radial chromatography [on silica gel; elution with hexane-EtOAc (4:1)] afforded (i) *N-Allyl-(3-cyano)aniline* **177** as a yellow oil (410 mg, 32%) and

(ii) N,N-*Diallyallyl-3-cyanoaniline* **177A** as yellow oil. (130 mg, 7.6%). (Found: **[M-1]**$^+$, 197.107123. $C_{13}H_{14}N_2$ requires: **M**$^+$, 198.115699); ν_{max} (thin film/cm^{-1}) 2228 (CN); δ_H/ppm (400MHz; $CDCl_3$) 3.92 (4H, m, 1'-CH_2 and 1"-CH_2), 5.16 (4H, m, 3'-CH_2 and 3"-CH_2), 5.81 (2H, m, 2'-H and 2"-H), 6.85 (2H, m, 4-H and 6-H), 6.91 (1H, d, *J* = 7.36 Hz, 2-H) and 7.22 (1H, m, 5-H); δ_C/ppm (100MHz; $CDCl_3$) 52.7 (C-1' and C-1"), 112.7 (CN), 114.9 (C-4 or C-6), 116.2 (C-4 or C-6), 116.4 (C-3' and C-3"), 119.4 (C-2), 119.7 (C-3), 129.6 (C-5), 132.6 (C-2' and C-2"), and 148.6 (C-1).

2-Chloro-*N*-(3-cyanophenyl)acetamide 181

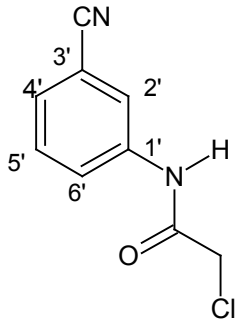

A mixture of 3-aminobenzonitrile (0.50g, 4.2 m mol) **173** and chloroacetyl chloride (3.3 mL, 42 mmol) was stirred under argon at room temperature for *ca.* 4 days. Excess chloroacetyl chloride was evaporated *in vacuo* and the residue dissolved in EtOAc (50 mL). The solution was washed sequentially with satd. aq. $NaHCO_3$ (2 × 50 mL) and brine (2 × 50 mL). The aqueous washings were extracted with EtOAc and the organic layers were combined and dried (anhydr. $MgSO_4$). The solvent was evaporated *in vacuo* to afford 2-chloro-*N*-(3-cyanophenyl)acetamide **181** as light brown flakes (0.79

g, 95%), m.p. 141–144 ºC (lit.[1] 144–146 ºC) (Found: $\mathbf{M}^+$, 194.02431. Calc. for $C_9H_7ClN_2O$ $\mathbf{M}^+$, 194.02469); ν_{max} (solid deposit/cm^{-1}) 3451 (NH), 2232 (C≡N) and 1676 (NHC=O); δ_H/ppm (400MHz; $CDCl_3$) 4.20 (2H, s, CH_2), 7.45 (1H, d, J = 1.0 Hz, 4'-H), 7.46 (1H, m, 6'-H), 7.73 (1H, m, 5'-H), 7.98 (1H, s, 2'-H) and 8.35 (1H, s, NH); δ_C (100MHz; $CDCl_3$) 42.7 (CH_2), 113.3 (C-3'), 118.1 (C-1'), 123.1 (C-2'), 124.1 (C-5'), 128.6 (C-6'), 130.0 (C-4'), 137.5 (C≡N) and 164.1(C=O).

Diethyl [(3-cyanophenyl)carbamoyl]methyl phosphonate 182

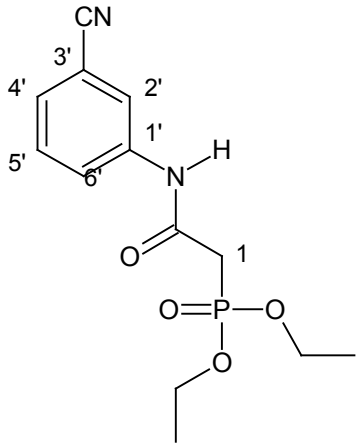

2-Chloro-*N*-(3-cyanophenyl)acetamide **181** (1.0 g, 5.1 mmol) was placed in an oven-dried round bottomed flask equipped with a reflux condenser. Triethyl phosphite (4.4 mL, 26 mmol) was added under nitrogen through a septum. The resulting mixture was refluxed until the substrate **181** was shown by TLC to have been completely consumed (*ca.* 5.5h). The cooled mixture was then stirred with hexane (20 mL) for *ca.* 10 minutes followed by decantation of the hexane layer to remove the excess phosphite. This procedure was repeated twice. The crude solid was transferred to a Buchner funnel and washed with more hexane to afford *diethyl [(3-cyanophenyl)carbamoyl]methyl phosphonat*e **182** as a cream powder (1.3 g, 84%), m.p. 119-125ºC (Found: $\mathbf{M}^+$, 296.09163. $C_{13}H_{17}N_2O_4P$ requires: $\mathbf{M}^+$, 296.09260); ν_{max} (solid deposit/cm^{-1}) 3423 (NH), 2231 (C≡N), 1685 (C=O), 1220 (P=O) and 1024 (P−O−C_2H_5); δ_H/ppm (400MHz; $CDCl_3$) 1.39 (6H, t, J = 7.1 Hz, 2 × CH_3), 3.09 (2H, d, $J_{P–H}$ = 21.6 Hz, CH_2P), 4.22 (4H, p, J = 7.1 Hz, 2 × CH_3CH_2), 7.21 (2H, m,

[1] http://www.acros.com/DesktopModules/Acros_Search_Results/Acros_Search_Results.aspx?search_type=CatalogSearch&SearchString=BTB02751

4'-H and 5'-H), 7.52 (1H, td, J = 6.9 and 2.3 Hz, 6'-H), 7.87 (1H, s, 2'-H) and 9.92 (1H, s, NH); δ_C (100MHz; $CDCl_3$) 16.3 (d, J_{P-C} =24.8 Hz, 2 × CH_3), 36.3 (d, J_{P-C} = 129.6 Hz, CH_2P), 63.3 (d, J_{P-C} = 26.8 Hz, 2 × CH_2CH_3), 112.6 (C-1'), 118.4 (C-3'), 122.4 (C-2'), 123.2 (C-6'), 127.3 (C-5'), 129.5 (C-4'), 138.9 (C≡N) and 162.6 (C=O, d, J_{P-C} = 4.5,); δ_P/ppm (162 MHz; $CDCl_3$) 18.3 (P=O).

2-Acetoxy-*N*-(3-cyanophenyl)acetamide 184

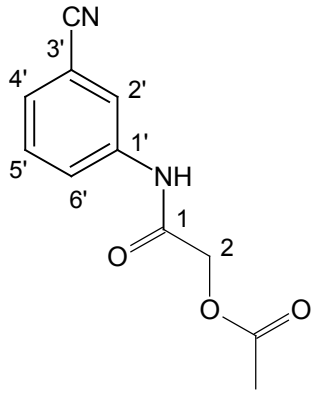

NaH (60% dispersion in mineral oil; 0.17 g, 8.1 mmol) in small portions to permit controlled evolution of hydrogen, to a stirred solution of 3-aminobenzonitrile **176** (0.50 g, 4.2 mmol) in dry THF (43 mL) under nitrogen at 0ºC. Acetoxyacetyl chloride (0.50 mL, 4.2 m mol) was then added through a septum and the resulting solution refluxed and monitored for ca. 5 h during which time the reaction was monitored for the disappearance of the substrate **173**. The reaction was quenched by the addition of water (40 mL). The solvent was evaporated *in vacuo* and the aqueous residue extracted with CH_2Cl_2 (2 × 40 mL). The combined organic extracts were washed sequentially with 10% aq. $NaHCO_3$ (2 × 80 mL), water (2 × 80 mL) and brine (2 × 80 mL). The aqueous washings were extracted with CH_2Cl_2 and the organic layers combined and dried (anhydr. $MgSO_4$). Evaporation of the solvent *in vacuo* afforded *2-acetoxy-N-(3-cyanophenyl)acetamide* **184** as light yellow crystals (0.78 g, 85%), m.p. 96-100°C. (Found $\mathbf{M}^+$, 218.06803, $C_{11}H_{10}N_2O_3$ requires $\mathbf{M}^+$, 218.20920), ν_{max} (solid deposit/cm^{-1}) 3344 (NHC=O), 2230 (CN) and 1735 (CH_3C=O); δ_H/ppm (400MHz;$CDCl_3$) 2.20 (3H, s, CH_3), 4.68 (2H, s, C-2), 7.40 (2H, m, 5'-H and 6'-H), 7.74 (1H, td, J = 7.6 and 2.0 Hz, 4'-H) and 7.94 (1H, s, 2'-H); δ_C/ppm (100MHz; $CDCl_3$) 20.6 (CH_3), 63.0 (C-2), 112.7 (C-3'), 118.3 (C-1'), 123.2 (C-2'), 124.3 (C-4'), 128.1 (C-5'), 129.9 (C-6'), 137.7 (C≡N), 165.6 (NHC=O) and 169.6 (CH_3C=O); m/z = 217.10 ($\mathbf{M}^+$**-1**, 4%) and 294.12 (100%).

2,3,4,5,6-Pentaacetyl-*N*-(3-cyanophenyl)gluconamide 186

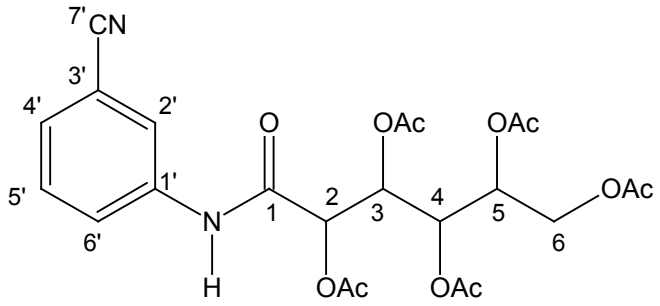

To a solution of 3-aminobenzonitrile (0.10 g, 0.85 mmol) in pyridine (2 mL) was added NaH (60% dispersion in mineral oil; 0.035 g, 0.85 mmol) in small portions to permit controlled evolution of hydrogen. 2,3,4,5,6-pentaacetylgluconoyl chloride **131** (0.36 g, 0.85 mmol) was then added and the reaction mixture stirred at room temperature for 2.5 days. The solvent was evaporated *in vacuo* and the residue dissolved in EtOAc (30 mL). The solution was washed with water (2 × 30 mL) and brine (2 × 30 mL), dried (anhydr. $MgSO_4$) and evaporated *in vacuo* to afford a yellow residue, chromatography [radial chromatography; elution with hexane-EtOAc (1:1)] of which afforded *2,3,4,5,6-pentaacetyl-N-(3-cyanophenyl)-gluconamide* **186** as yellow crystals (180 mg, 41%), m.p. 103-105ºC. (Found: $\mathbf{M}^+$, 506.15293. $C_{23}H_{26}N_2O_{11}$ requires: $\mathbf{M}^+$, 506.46033); ν_{max} (solid deposit/cm^{-1}) 3431 (NH), 2231 (CN), 1747 (CH_3C=O) and 1600 (NHC=O); δ_H/ppm (400MHz; $CDCl_3$) 2.05-2.11 (12H, series of singlets, 4 × OAc), 2.23 (3H, s, CH_3, 6-OAc), 4.12 (1H, dd, *J* = 12.5 and 5.3 Hz, 6-H_a), 4.36 (1H, dd, *J* = 12.5 and 3.2 Hz, 6-H_b), 5.05 (1H, ddd, *J* = 6.6, 5.3 and 3.2 Hz, 5-H), 5.28 (1H, d, *J* = 5.9 Hz, 2-H), 5.47 (1H, dd, *J* = 6.7 and 4.6 Hz, 4-H), 5.72 (1H, dd, *J* = 5.81 and 4.58 Hz, 3-H), 7.41 (2H, m, 4'-H and 6'-H), 7.72 (1H, m, 5'-H), 7.89 (1H, s, 2'-H) and 8.23 (1H, s, NH); δ_C/ppm (100MHz; $CDCl_3$) 20.4, 20.6, 20.67, 20.70 and 20.73 (5 × CH_3), 61.8 (C-6), 68.6 (C-3), 68.9 (C-5), 69.1 (C-4), 71.6 (C-2), 113.1 (C-3'), 118.2 (C-1'), 123.1 (C-2'), 124.2 (C-5'), 128.4 (C-6') 130.0 (C-4') 137.7 (C-7'), 164.6 (NH-C=O), 169.4 (2-C=O), 169.9 (3-C=O), 170.0 (5-C=O), 170.3 (4-C=O) and 170.9 (6-C=O); *m/z* = 507.07 ($\mathbf{M}^+$+**1**, 100%).

3-(Allyloxy)phenol 188

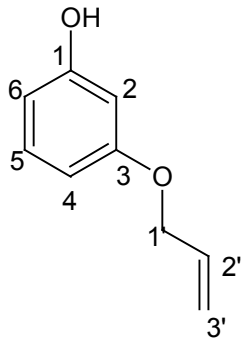

NaH (60% dispersion in mineral oil; 0.36 g, 9.1 mmol) was added in small portions to permit controlled evolution of hydrogen, to a stirred solution of 3-aminophenol (1.0 g, 9.1 mmol) in dry THF (20 mL) under nitrogen at 0ºC. Allyl bromide (0.8 mL, 9.1 mmol) was then added with through a septum and the resulting solution refluxed for *ca.* 6 h. The reaction was quenched by the addition of water (50 mL). The solvent was evaporated *in vacuo* and the aqueous residue extracted with EtOAc (2 × 50 mL). The combined organic extracts were washed sequentially with water (2 × 100 mL) and brine (2 × 100 m L). The aqueous washings were extracted with EtOAc and the organic layers combined and dried (anhydr. $MgSO_4$). The solvent was evaporated *in vacuo* and the residue chromatographed [radial chromatography; elution with hexane-EtOAc (7:3)] to afford 3-(allyloxy)phenol **188** as a reddish brown oil (0.38 g, 28%). (Found: $\mathbf{M}^+$, 150.067020. $C_9H_{10}O_2$ requires: $\mathbf{M}^+$, 150.068080); ν_{max} (thin film/cm^{-1}) (OH); δ_H/ppm (400MHz; $CDCl_3$) 4.50 (2H, dt, J = 5.2 and 1.5 Hz, 1'-CH_2), 5.28 (1H, qd, J = 10.5 and 1.4 Hz, CH=CH_E), 5.40 (2H, m, HC=CH_Z and OH), 6.04 (1H, m, 2'-H), 6.43 (2H, m, 2-H and 6-H), 6.52 (1H, ddd, J = 8.3, 2.2 and 1.1 Hz, 4-H) and 7.12 (1H, t, J = 8.5, 5-H); δ_C/ppm (100MHz; $CDCl_3$) 68.9 (C-1'), 102.4 (C-2), 107.3 (C-4), 108.0 (C-6), 117.8 (C-3'), 130.2 (C-5), 133.1 (C-2'), 156.6 (C-1) and 159.8 (C-3).

1,3-Bis(chloroacetoxy)phenol 189A

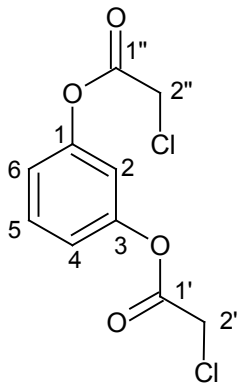

NaH (60% dispersion in mineral oil; 0.22 g, 9.1 mmol) was added in small portions to permit controlled evolution of hydrogen, to a stirred solution of resorcinol **187** (1.0 g, 9.1 mmol) in dry THF (20 mL) under nitrogen at 0 ºC. Chloroacetyl chloride (0.71 mL, 9.1 mmol) was then added through a septum and the resulting solution refluxed for *ca.* 6 h. The reaction was quenched by the addition of water (20 mL). The solvent was evaporated *in vacuo* and the aqueous residue extracted with EtOAc (2 × 40 mL). The combined organic extracts were washed sequentially with water (2 × 80 mL) and brine (2 × 80 mL). The aqueous washings were extracted with EtOAc and the organic layers combined and dried (anhydr. $MgSO_4$). The solvent was evaporated *in vacuo* and the residue chromatographed [radial chromatography; elution with hexane-EtOAc (6:4)] to afford *1,3-(bischloroacetoxy)phenol* **189A** as a yellow oil. (570 mg, 24%), (Found: $\mathbf{M}^+$, 261.978798 $C_{10}H_8{}^{35}Cl_2O_4$ requires: $\mathbf{M}^+$, 262.106210) ; ν_{max} (thin film/cm^{-1}) 1776 (*C*=O); δ_H/ppm (400MHz; $CDCl_3$) 4.27 (4H, s, 2'-H and 2"-H), 7.03 (1H, t, *J* = 2.2 Hz, 2-H), 7.06 (1H, d, *J* = 2.3 Hz, 4-H or 6-H), 7.08 (1H, d, *J* = 2.15 Hz, 4-H or 6-H) and 7.41 (1H, t, *J* = 8.2 Hz, 5-H); δ_C/ppm (100MHz; $CDCl_3$) 40.7 (C-2' and C-2"), 114.7 (C-2), 119.1 (C-4 and C-6), 130.1 (C-5), 150.7 (C-3 and C-1) and 165.3 (C-1' and C-1").

Resorcinol bis [(acetyloxy)acetate] 190A

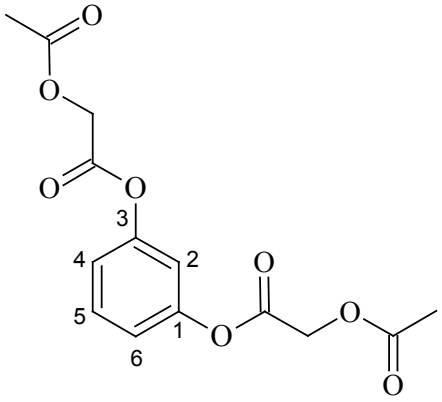

NaH (60% dispersion in mineral oil; 48 mg, 2.0 mmol) was added in small portions to permit controlled evolution of hydrogen, to a stirred solution of resorcinol **187** (220 mg, 2.0 m mol) in dry THF (15 mL) under nitrogen at 0ºC. Acetoxyacetyl chloride (0.22 mL, 2.0 m mol) was then added through a septum and the resulting solution refluxed for ca. 5 h dur ing which time the reaction was monitored for the disappearance of the substrate resorcinol **187**. The reaction was quenched by the addition of water (20 mL). The solvent was evaporated *in vacuo* and the aqueous residue extracted with EtOAc (2 × 20 mL). The combined organic extracts were washed sequentially with water (2 × 40 m L) and brine (2 × 40 m L). The aqueous washings were extracted with EtOAc and the organic layers combined and dried (anhydr. $MgSO_4$). Evaporation of the solvent *in vacuo* and chromatography of the residue [column chromatography with EtOH:$CHCl_3$:hexane = 0.5:1.5:2.5] afforded *resorcinol bis[(acetyloxy)acetate]* **190A** as a yellow oil (25 mg, 40%). (Found $\mathbf{M}^+$, 310.067879, $C_{14}H_{14}O_8$ requires 310.068868); ν_{max} (solid deposit) 1746 δ_H/ppm (400MHz; $CDCl_3$) 2.18 (6H, 2 × s, 2× CH_3), 4.81 (4H, 2 × s, 2 × CH_2), 6.96 (1H, t, *J* = 2.2 Hz, 2-H), 7.03 (2H, dd, *J* = 8.2 and 2.2 Hz, 4-H and 6-H) and 7.38 (1H, t, *J* = 8.2 Hz, 5-H); δ_C/ppm (100MHz; $CDCl_3$) 20.4 (2 × CH_3), 60.7 (2 × CH_2), 115.0 (C-2), 119.2 (C-4 and C-6), 129.9 (C-5), 150.4 (C-1 and C-3), 167.8 (2 × CH_2*C*=O) and 170.3 (2 × CH_3*C*=O).

2,3,4,5,6-Pentaacetyl-*O*-(3-hydroxyphenyl)gluconate 191

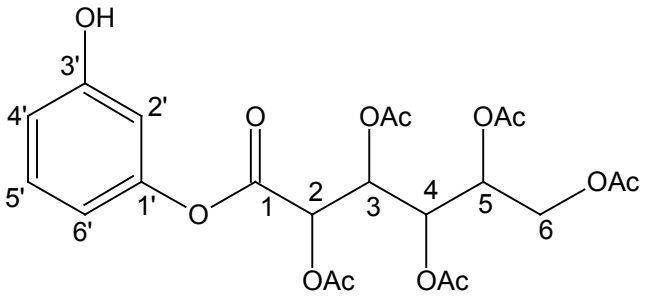

To a solution of resorcinol (200 mg, 0.91 mmol) in pyridine (2 mL) was added NaH (60% di spersion in mineral oil; 41 mg, 1.7 mmol) in small portions to permit controlled evolution of hydrogen. 2,3,4,5,6-pentaacetylgluconoyl chloride **131** (400 mg, 0.94 mmol) was then added and the reaction mixture stirred at room temperature for *ca.* 2.5 days. The solvent was taken off *in vacuo* and the residue dissolved in EtOAc (2 × 25 mL). This solution was washed with water (2 × 50 mL) and brine (2 × 50 mL). The organic layer was then dried (anhydr. $MgSO_4$) and the solvent evaporated *in vacuo* to afford a reddish brown oil, flash chromatography [on silica gel; elution with EtOH:$CHCl_3$:hexane (0.5:1.5:2.5)] of which afforded *2,3,4,5,6-pentaacetyl-O-(3-hydroxyphenyl)-gluconate* **191** as a yellow oil, (64 mg, 14%). (Found: $\mathbf{M}^+$, 498.137550, $C_{22}H_{26}O_{13}$ requires: $\mathbf{M}^+$, 498.434913); ν_{max} (thin film/cm^{-1}) 3419 (OH) and 1747 (C=O); δ_H/ppm (400MHz; $CDCl_3$) 2.08 (12H, series of singlets, 4 × OAc), 2.22 (3H, s, CH_3, 6-OAc), 4.16 (1H, dd, *J* = 12.2 and 5.3 Hz, 6-H_a), 4.32 (1H, dd, *J* = 12.3 and 4.0 Hz, 6-H_b), 5.14 (1H, m, 5-H), (1H, d, *J* = 3.53 Hz, 2-H), 5.58 (1H, dd, *J* = 6.7 and 4.6 Hz, 4-H), 5.74 (1H, t, *J* = 4.10 Hz, 3-H), 6.59 (1H, t, *J* = 2.0 Hz, 2'-H), 6.65 (1H, dd, *J* = 8.0 and 1.8 Hz, 4'-H), 6.71 (1H, dd, *J* = 8.2 and 1.8 Hz, 6'-H) and 7.20 (1H, t, *J* = 8.2 Hz, 5'-H); δ_C/ppm (100MHz; $CDCl_3$) 20.4, 20.45, 20.6, 20.68 and 20.8 (5 × OAc), 61.6 (C-6), 68.3 (C-5), 68.4 (C-3), 69.2 (C-4), 70.8 (C-2), 108.8 (C-2'), 113.2 (C-4'), 113.7 (C-4'), 130.2 (C-5'), 150.8 (C-1'), 156.7 (C-3'), 165.4 (1'-*C*=O), 169.7 (5-*C*=O), 169.8 (3-*C*=O), 169.9 (4-*C*=O), 170.1 (2-*C*=O) and 170.6 (6-*C*=O).

Resorcinol monoacrylate 192 and resorcinol diacrylate 192A

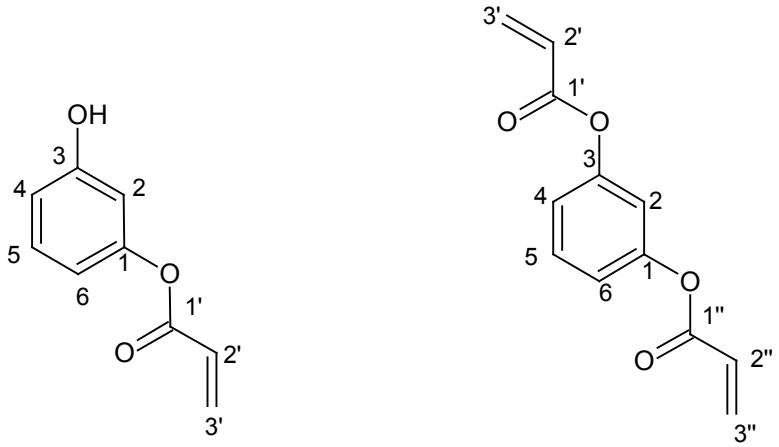

NaH (60% dispersion in mineral oil; 400 mg, 9.1 mmol) was added in small portions permit controlled evolution of hydrogen, to a stirred solution of resorcinol **187** (1.0 g, 9.1 mmol) in dry THF (20 mL) under nitrogen at 0ºC. Acryloyl chloride (0.74 mL, 9.1 mmol) was then added with through a septum and the resulting solution refluxed for *ca.* 6 h. The reaction was quenched by the addition of water (25 mL). The solvent was evaporated *in vacuo* and the aqueous residue extracted with EtOAc (2 × 25 mL). The combined organic extracts were washed sequentially with water (2 × 50 mL) and brine (2 × 50 mL). The aqueous washings were extracted with EtOAc and the organic layers combined and dried (anhydr. $MgSO_4$). The solvent was evaporated *in vacuo* and the residue chromatographed [preparative TLC; elution with hexane-EtOAc (1:1)] to afford two fractions.

(i) *Resorcinol monoacrylate* **192** as a yellow oil (120 mg, 8%). (Found: $\mathbf{M}^+$, 164.046723. $C_9H_8O_3$ requires: $\mathbf{M}^+$, 164.047344); ν_{max} (thin film/cm^{-1}) 3393 (OH) 1721 (C=O); δ_H/ppm (400MHz; $CDCl_3$) 5.68 (1H, s, OH), 6.02 (1H, d, *J* = 10.5 Hz, CH=CH_E), 6.31 (1H, dd, *J* = 17.3 and 10.5 Hz, 2'-H), 6.60 (1H, m, 2-H and CH=CH_Z), 6.66 (1H, d, *J* = 2.2 Hz, 4-H), 6.68 (1 H, d, *J* = 2.1 Hz, 6-H) and 7.21 (1H, t, *J* = 8.2 Hz, 5-H); δ_C/ppm (100MHz; $CDCl_3$) 109.1 (C-2), 113.2 (C-6), 113.5 (C-4), 127.8 (C-2'), 130.1 (C-5), 133.0 (C-3'), 151.3 (C-1), 156.6 (C-3) and 164.8 (C=O).

(ii) *Resorcinol diacrylate* **192A** as a yellow oil (260 mg, 13%). (Found: $\mathbf{M}^+$, 218.058102. $C_{12}H_{10}O_4$ requires: $\mathbf{M}^+$, 218.057909.); ν_{max} (thin film/cm^{-1}) 1743 (C=O);

δ_H/ppm (400MHz; $CDCl_3$) 6.01 (1H, 2 × dd, *J* = 10.4 and 0.8 Hz, 2 × CH=C*H*$_E$), 6.30 (1H, dd, *J* = 17.3 and 10.4 Hz, 2'-H and 2"-H), 6.60 (2H, 2 × dd, *J* = 17.3 and 0.8 Hz, 2 × CH=C*H*$_Z$), 7.01 (1H, m, 2-H), 7.03 (1H, d, *J* = 2.1 Hz, 4-H), 7.05 (1H, d, *J* = 2.1 Hz, 6-H) and 7.39 (1H, t, *J* = 8.1 Hz, 5-H); δ_C/ppm (100MHz; $CDCl_3$) 115.4 (C-2), 119.0 (C-4 and C-6), 127.6 (C-2' and C-2"), 129.7 (C-5), 132.9 (C-3' and C-3"), 150.9 (C-1 and C-3) and 164.1 (2 × C=O).

_N_-Allyl-(3-hydroxy)aniline 194, _N_-Allyl-3-(allyloxy)aniline 194A and _N,N_-diallyl-3-hydroxyaniline 194B

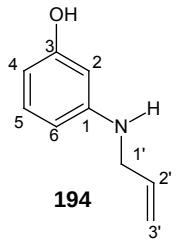

194

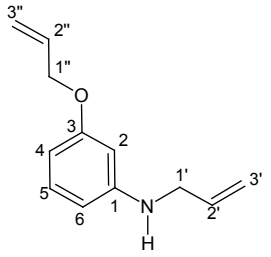

194A

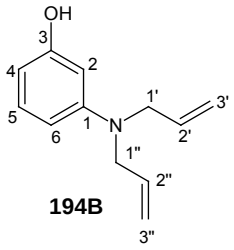

194B

To a stirred solution of 3-aminophenol **193** (3.0 g, 28 mmol) in dry THF (30 mL) under nitrogen was added NaH (60% dispersion in mineral oil; 1.1 g, 28 mmol) in small portions to permit controlled evolution of hydrogen. Allyl bromide (2.4 mL, 28 mmol) was then added through a septum and the resulting solution was refluxed for *ca.* 4.5 h. The reaction was quenched by the addition of water (50 mL). The solvent was evaporated *in vacuo* and the aqueous residue extracted with EtOAc (2 × 50 mL). The combined organic extracts were washed sequentially with water (2 × 100 mL) and brine (2 × 100 mL). The aqueous washings were extracted with EtOAc and the organic layers combined and dried (anhydr. $MgSO_4$). Flash chromatography [on silica gel; elution with hexane-EtOAc (8:2)] afforded 3 fractions.

(i) *N*-Allyl-(3-hydroxy)aniline **194** a dark brown oil (680 mg, 17%). (Found $\mathbf{M}^+$, 149.083104. $C_9H_{11}NO$ requires 149.084064); ν_{max} (thin film/cm^{-1}) 3388 (NH); δ_H/ppm (400MHz; $CDCl_3$) 3.70 (2H, dt, *J* = 5.4 and 1.6 Hz, 1'-C*H*$_2$), 5.16 (1H, qd, *J* = 10.3 and 1.40 Hz, CH=C*H*$_E$), 5.26 (1H, qd, *J* = 17.2 and 1.6 Hz, CH=C*H*$_Z$), 5.92 (1H, m, 2'-H), 6.10 (1H, t, *J* = 2.3 Hz, 2-H), 6.20 (1H, dd, *J* = 8.0 and 2.3 Hz, 6-H), 6.23 (1H, dd, *J* = 8.1 and 2.1 Hz, 4-H) and 7.02 (1H, t, *J* = 8.0 Hz, 5-H); δ_C/ppm

(100MHz; $CDCl_3$) 46.6 (C-1'), 100.3 (C-2), 105.0 (C-6), 106.2 (C-4), 116.4 (C-3'), 130.1 (C-5), 135.1 (C-2'), 149.4 (C-1) and 156.6 (C-3).

(ii) *N-Allyl-3-(allyloxy)aniline* **194A** a dark brown oil (270 mg, 5.2%). (Found $\mathbf{M}^+$, 189.115840. $C_{12}H_{15}NO$ requires 189.115364); ν_{max} (thin film/cm^{-1}) 3406 (NH_2); δ_H/ppm (400MHz; $CDCl_3$) 3.77 (2H, dt, *J* = 5.4 and 1.6 Hz, 1'-C*H*$_2$), 4.51 (2H, td, *J* = 5.3 and 1.5 Hz, 1"-C*H*$_2$), 5.18 (1H, m, 3'-Ha), 5.30 (2H, m, 3'-Hb and 3"-Ha), 5.42 (1H, m, 3"-Hb), 5.97 (1H, m, 2'-H), 6.07 (1H, m, 2"-H), 6.23 (1H, t, *J* = 2.3 Hz, 2-H), 6.26 (1 H, dd, *J* = 8.0 and 2.2 Hz, 6-H), 6.31 (1H, dd, *J* = 8.1 and 2.3 Hz, 4-H) and 7.08 (1H, t, *J* = 8.1 Hz, 5-H); δ_C/ppm (100MHz; $CDCl_3$) 46.5 (C-1'), 68.6 (C-1"), 99.7 (C-2), 103.4 (C-4), 106.3 (C-6), 116.1 (C-3'), 117.3 (C-3"), 129.8 (C-5), 133.5 (C-2"), 135.3 (C-2'), 149.4 (C-1) and 159.8 (C-3).

(iii) *N,N-Diallyl-3-(hydroxy)aniline* **194B** as a dark brown oil (830 mg, 16%). (Found $\mathbf{M}^+$, 189.114166. $C_{12}H_{15}NO$ requires 189.115364); ν_{max} (thin film/cm^{-1}) 3363 (NH); δ_H/ppm (400MHz; $CDCl_3$) 3.89 (4H, m, 1'-C*H*$_2$ and 1"-C*H*$_2$), 5.18 (4H, m, 3'-C*H*$_2$ and 3"-C*H*$_2$), 5.85 (2H, m, 2'-H and 2"-H), 6.19 (1H, m, 6-H), 6.22 (1H, s, 2-H), 6.32 (1H, m, 4-H), and 7.06 (1H, t, *J* = 8.1 Hz, 5-H); δ_C/ppm (100MHz; $CDCl_3$) 52.7 (C-1' and C-1"), 99.6 (C-2), 103.5 (C-6), 105.3 (C-4), 116.0 (C-3' and C-3"), 129.9 (C-5), 133.8 (C-2' and C-2"), 150.2 (C-1) and 156.4 (C-3).

2-Chloro-*N*-(3-hydroxyphenyl)acetamide 195

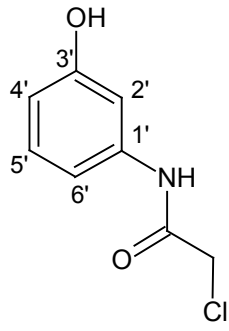

To a stirred solution of 3-aminophenol (3.0 g, 28 mmol) in THF (30 mL) under nitrogen was added NaH (60% dispersion in mineral oil; 1.2 g, 50 mmol) in small portions to permit controlled evolution of hydrogen. Chloroacetyl chloride (2.2 mL,

28 mmol) was then added through a septum and the resulting solution was stirred for *ca.* 6 h. The solvent was evaporated *in vacuo* and the residue dissolved in EtOAc (2 x 50 mL). The organic extract was washed sequentially with satd. aq. $NaHCO_3$ (2 × 100 mL), water (2 x 100 m L) and brine (2 × 100 mL). The aqueous washings were extracted with EtOAc and the combined organic solutions were (anhydr. $MgSO_4$). Evaporation of the solvent *in vacuo* afforded 2-chloro-*N*-(3-hydroxyphenyl)acetamide **195** as a grey solid (3.9 g, 76%) m.p. 119-120°C. ν_{max} (solid deposit/cm^{-1}) 3360 (OH) and 1642 (CO); δ_H/ppm (400MHz; DMSO-d_6) 4.22 (2H, s, CH_2), 6.48 (1H, dd, *J* = 8.0 and 2.0 Hz, 6'-H), 6.94 (1H, d, *J* = 8.5 Hz, 4'-H), 7.09 (1H, t, *J* = 8.1 Hz, 5'-H), 7.17 (1H, t, *J* = 2.0 Hz, 2'-H), 9.48 (1H, s, OH) and 10.18 (1H, s, NH); δ_C/ppm (100MHz; DMSO-d_6) 43.6 (*C*H_2), 106.3 (C-2'), 110.0 (C-6'), 110.9 (C-4'), 129.5 (C-5'), 139.5 (C-1'), 157.6 (C-3') and 164.4 (C=O).

[(3-Hydroxyphenyl)carbamoyl)methyl]phosphonate 196

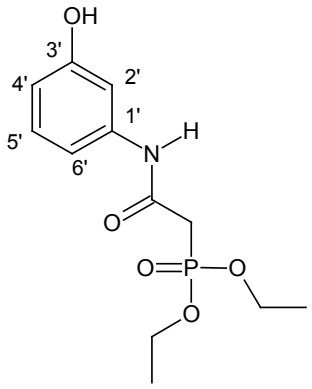

To 2-Chloro-*N*-(3-hydroxyphenyl)-acetamide **195** (500 mg, 30 m mol) in an oven-dried round bottomed flask equipped with a reflux condenser was added triethyl phosphite (2.6 mL, 15 mmol) under nitrogen through a septum. The resulting mixture was refluxed for *ca.* 9 h during which time the reaction was monitored by TLC. The cooled mixture was then stirred with hexane (20 mL) for *ca.* 10 minutes followed by decantation of the hexane layer to remove the excess phosphite; this was repeated twice. Evaporation of the solvent *in vacuo* afforded *[(3-hydroxyphenyl)-carbamoyl)methyl]phosphonate* **196** as white crystals (370 mg, 48%), m.p. 115-117°C. (Found: $\mathbf{M}^+$, 287.093363. $C_{12}H_{18}NO_5P$ requires: $\mathbf{M}^+$, 287.092261); ν_{max} (solid deposit/cm^{-1}) 3263 (OH), 1667 (C=O), 1230 (P=O) and 1024 (O[illegible]P $_2H_5$);

δ_H/ppm (400MHz; $CDCl_3$) 1.32 (6H, t, J = 6.8 Hz, 2 × CH_3), 3.05 (2H, d, $J_{P–H}$ = 21.1 Hz, 1-CH_2), 4.17 (4H, p, $J_{P–H}$ = 7.1 Hz, 2 × CH_3CH_2), 6.60 (1H, d, J = 8.0 Hz, 4'-H), 6.80 (1H, d, J = 7.9 Hz, 6'-H), 7.09 (1H, t, J = 8.0 Hz, 5'-H), 7.46 (1H, s, 2'-H), 7.99 (1H, s, OH) and 8.96 (1H, s, NH); δ_C (100MHz; $CDCl_3$) 16.3 (2C, d, $J_{P–C}$ = 6.0 Hz, 2 × CH_3), 36.4 (1C, d, $J_{P–C}$ = 130.4 Hz, 1-CH_2), 63.3 (2C, d, $J_{P–C}$ = 6.6 Hz, 2 × CH_2), 107.3 (C-2'), 111.1 (C-6'), 112.1 (C-4'), 129.8 (C-5'), 138.5 (C-1'), 157.3 (C-3') and 162.7 (1C, d, $J_{P–C}$ = 4.1 Hz, C=O); δ_P/ppm (162 MHz; $CDCl_3$) 24.2 (P=O).

2-Acetoxy-*N*-(3-hydroxyphenyl)acetamide 197

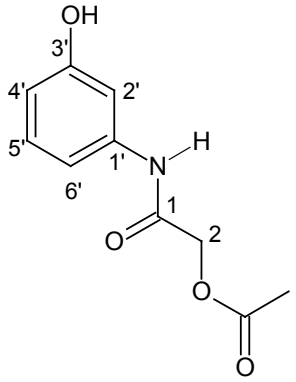

NaH (60% dispersion in mineral oil; 60 mg, 2.5 mmol) was added in small portions to a stirred solution of 3-aminophenol (150 mg, 1.4 mmol) in dry THF (10 mL) under nitrogen at 0ºC, to permit controlled evolution of hydrogen. Acetoxyacetyl chloride (160 µL, 2.5 m mol) was then added through a septum and the resulting solution refluxed for *ca.* 5.0 h. The reaction was quenched by the addition of water (20 mL). The solvent was evaporated *in vacuo* and the aqueous residue was extracted with EtOAc (2 × 40 mL). The combined organic extracts were washed sequentially with water (2 × 80 mL) and brine (2 × 80 mL). The aqueous washings were extracted with EtOAc and the organic layers combined and dried (anhydr. $MgSO_4$). Evaporation of the solvent *in vacuo* and chromatography of the residue [column chromatography with EtOH:$CHCl_3$:hex= (0.5:1.5:2.5)] afforded *2-acetoxy-N-(3-hydroxyphenyl)acetamide* **197** as a grey powder (70 mg, 24%), m.p. 154-156°C. (Found **M$^+$,** 209.068446, $C_{10}H_{11}NO_4$ requires 209.068808), ν_{max} (solid deposit/cm^{-1}) 3424 (OH), 1734 (CH_3C=O), 1678 (NHC=O); δ_H/ppm (400MHz; DMSO-d_6) 2.11 (3H, s, CH_3), 4.61 (2H, s, CH_2), 6.46 (1H, dd, J = 7.9 and 2.2 Hz, 6'-H), 6.93 (1H, d, J = 8.3 Hz, 4'-H),

7.07 (1H, t, *J* = 8.06 Hz, 5'-H), 7.13 (1H, t, *J* = 2.0 Hz, 2'-H), 9.39 (1H, br s, OH) and 9.92 (1H, s, NH); δ_C/ppm (100MHz; DMSO-d_6) 20.4 (*C*H_3), 62.5 (C*H*$_2$), 106.3 (C-2'), 109.9 (C-4'), 110.5 (C-6'), 129.3 (C-5'), 139.3 (C-1'), 157.5 (C-3'), 165.2 (C-1) and 169.9 (CH_3*C*=O).

2,3,4,5,6-Pentaacetyl-*N*-(3-hydroxyphenyl)-gluconamide 198

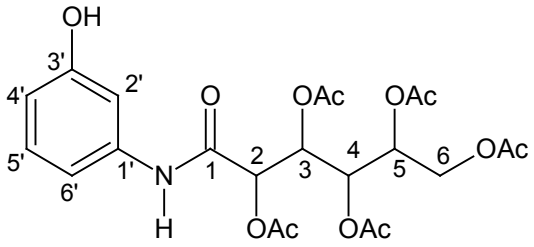

To a solution of 3-aminophenol (0.10 g, 0.92 mmol) in pyridine (2 mL) was added NaH (60% dispersion in mineral oil; 0.041 g, 0.92 mmol) in small portions to permit controlled evolution of hydrogen. 2,3,4,5,6-pentaacetylgluconoyl chloride **131** (0.40 g, 0.92 mmol) was then added and the reaction mixture stirred at room temperature for *ca.* 2.5 days. The solvent was taken off *in vacuo* and the residue dissolved in EtOAc (30 mL). This solution was washed with water (2 × 30 mL) and brine (2 × 30 mL). The organic layer was then dried (anhydr. $MgSO_4$) and the solvent was evaporated *in vacuo* to afford a reddish brown oil, flash chromatography [on silica gel; elution with hexane-EtOAc (4:6)] of which afforded *2,3,4,5,6-pentaacetyl-N-(3-hydroxyphenyl)-gluconamide* **198** as a reddish brown oil, (93 mg, 20%). (Found: $\mathbf{M}^+$, 497.15132. $C_{22}H_{27}NO_{12}$ requires: $\mathbf{M}^+$, 497.45019); ν_{max} (solid deposit/cm^{-1}) 3427 (OH), 1740 (CH_3*C*=O) and 1605 (NH*C*=O); δ_H/ppm (400MHz; $CDCl_3$) 2.06 (12H, series of singlets, 4 × OAc), 2.22 (3H, s, CH_3, 6-OAc), 4.12 (1H, dd, *J* = 12.4 and 5.5 Hz, 6-H_a), 4.34 (1H, dd, *J* = 12.4 and 3.3 Hz, 6-H_b), 5.06 (1H, dt, *J* = 6.0, 5.8 and 3.4 Hz, 5-H), 5.34 (1H, d, *J* = 5.4 Hz, 2-H), 5.47 (1H, dd, *J* = 6.5 and 4.7 Hz, 4-H), 5.70 (1H, t, *J* = 5.00 Hz, 3-H), 6.63 (1H, dd, *J* = 8.1 and 2.0 Hz, 4'-H), 6.81 (1H, dd, *J* = 8.0 and 1.1 Hz, 6'-H), 7.13 (1H, t, *J* = 8.1 Hz, 5'-H), 7.33 (1H, s, 2'-H) and 8.10 (1H, s, NH); δ_C/ppm (100MHz; $CDCl_3$) 20.4, 20.6, 20.66 and 20.72 (5 × OAc), 61.7 (C-6), 68.9 (C-3), 69.0 (C-5), 69.2 (C-4), 71.8 (C-2), 107.4 (C-2'), 111.6 (C-6'), 112.4 (C-4'), 130.0 (C-5'), 137.6 (C-3'), 156.9 (C-1'), 164.6 (NH-*C*=O), 169.6 (5-*C*=O), 169.9 (3-

C=O), 170.0 (2-*C*=O), 170.3 (4-*C*=O) and 170.9 (6-*C*=O); m/z = 496.11 (**M**$^+$**-1**, 28 %) and 412.25 (100%).

_N_-(3-Hydroxyphenyl) acryloyl amine 199 and 3-(acryloylamino)phenyl acrylate 199A

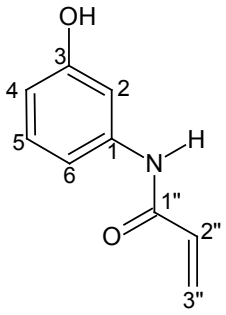

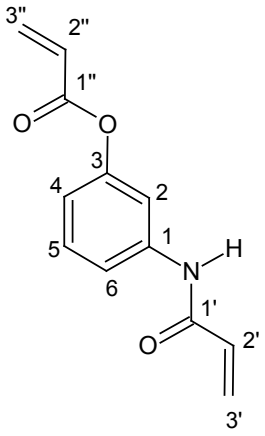

To a stirred solution of 3-aminophenol (0.50 mg, 4.6 m mol) in dry THF (15 mL) under nitrogen was added NaH (60% dispersion in mineral oil; 0.11 g, 4.6 mmol) in small portions to permit controlled evolution of hydrogen. Acryloyl chloride (0.37 mL, 4.6 mmol) was then added through a septum and the resulting solution was refluxed for *ca.* 6 h. The reaction was quenched by the addition of water (20 mL). The solvent was evaporated *in vacuo* and the aqueous residue extracted with EtOAc (2 × 40 mL). The combined organic extracts were washed sequentially with water (2 × 80 mL) and brine (2 × 80 mL). The aqueous washings were extracted with EtOAc and the organic layers combined and dried (anhydr. $MgSO_4$). Preparative thin layer chromatography [on silica gel; elution with hexane-EtOAc (4:6)] afforded two fractions.

(i) *N-(3-hydroxyphenyl)acryloyl amine* **199** as a yellow oil, (5.4 mg, 0.72%). (Found: **M**$^+$, 163.076095. $C_9H_9NO_2$ requires: **M**$^+$, 163.063329); ν_{max} (thin film/cm^{-1}) 3419 (OH) 1667 (C=O); δ_H/ppm (400MHz; $CDCl_3$) 6.01 (1H, d, *J* = 10.5 Hz, 3'-H_a), 6.30 (1H, dd, *J* = 17.3 and 10.5 Hz, 2'-H), 6.60 (1H, d, *J* = 17.3 Hz, 3'-H_b), 6.89 (1H, d, *J* = 7.0 Hz), 7.34 (2H, m, 5-H and 6-H) and 7.50 (1H, s, 2-H); δ_C/ppm (150MHz; $CDCl_3$) 113.5 (C-2), 117.1 (C-6), 17.6 (C-4), 127.8 (C-2'), 129.7 (C-5), 132.9 (C-3'), 138.5 (C-1), 150.9 (C-3) 164.6 and 167.7 (H-N-C=O).

(ii) *3-(Acryloylamino)phenyl acrylate* **199A** as yellow oil, (12 mg, 1.2%). (Found: $\mathbf{M}^+$, 217.072324. $C_{12}H_{11}NO_3$ requires: $\mathbf{M}^+$, 217.073893); ν_{max} (thin film/cm^{-1}) 1731(C=O) and 1663 (NHC=O); δ_H/ppm (400MHz; $CDCl_3$) 5.70 (1H, d, *J* = 10.2 Hz, 3"-H_a), 6.03 (1H, d, *J* = 10.4 Hz, 3'-H_a), 6.16 (1H, dd, *J* = 16.8 and 10.3 Hz, 2"-H), 6.32 (2H, m, 2'-H and 3"-H_b), 6.60 (1H, d, *J* = 17.3 Hz, 3'-H_b), 6.82 (1H, d, *J* = 7.09 Hz, 6-H), 7.24 (2H, m, 4-H and 5-H), 7.58 (1H, s, 2-H) and 7.95 (1H, s, NH); δ_C/ppm (100MHz; $CDCl_3$) 113.5 (C-2), 117.2 (C-4), 117.3 (C-6), 127.7 (C-2'), 127.9 (C-3"), 129.6 (C-5),130.9 (C-1),133.1 (C-3'), 139.1 (C-3), 150.7 (C-1), 163.7 (C=O) and 165.0 (NHC=O).

_N_-Allyl-3-(hydroxymethyl) aniline 201, _N_-allyl-3-[(allyloxy)methyl] aniline 201A, _N,N_-diallyl-3-(hydroxymethyl)aniline 201B and 3-[Allyloxy)methyl]aniline 201C

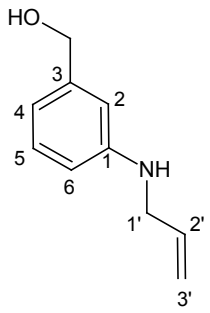

201

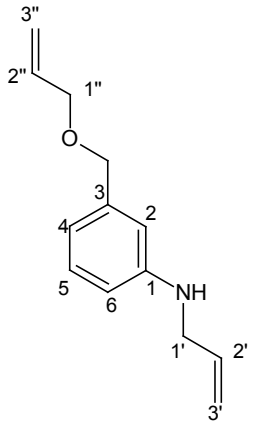

201A

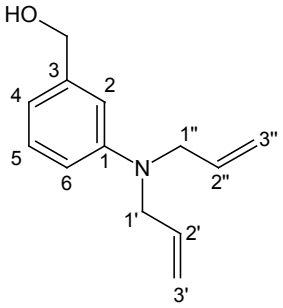

201B

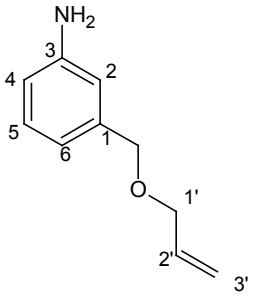

201C

To a stirred solution of 3-aminobenzyl alcohol **200** (1.0 g, 8.1 mmol) in dry THF (41 mL) under nitrogen was added NaH (60% dispersion in mineral oil; 0.30 g, 8.1 mmol) in small portions to permit controlled evolution of hydrogen. Allyl bromide (0.80 mL,

8.1 mmol) was then added through a septum and the resulting solution was refluxed for *ca.* 6h. The reaction was quenched by the addition of water (50 mL). The solvent was evaporated *in vacuo* and the aqueous residue extracted with EtOAc (2 × 50 mL). The combined organic extracts were washed sequentially with water (2 × 100 mL) and brine (2 × 100 mL). The aqueous washings were extracted with EtOAc and the organic layers combined and dried (anhydr. $MgSO_4$). Flash chromatography [on silica gel; elution with hexane-EtOAc (7:3)] afforded four fractions.

i. *N-Allyl-3-(hydroxymethyl) aniline* **201** a reddish brown oil (130 mg, 10%). (Found $\mathbf{M}^+$, 163.098763. $C_{10}H_{13}NO$ requires 163.099714); ν_{max} (thin film/cm^{-1}) 3347 (OH and NH); δ_H/ppm (400MHz; $CDCl_3$) 3.76 (2H, td, *J* = 5.4 and 1.6 Hz, 1'-CH_2), 4.58 (2H, s, 7-CH_2), 5.16 (1H, ddd, *J* = 10.3, 3.0 and 1.5 Hz, CH=CH_E), 5.28 (1H, ddd, *J* = 17.2, 3.3 and 1.6 Hz, CH=CH_Z), 5.95 (1H, m, 2'-H), 6.54 (1H, dd, *J* = 8.0 and 2.2 Hz, 6-H), 6.62 (1H, s, 2-H), 6.68 (1H, d, *J* = 7.47 Hz, 4-H) and 7.15 (1H, t, *J* = 7.8 Hz, 5-H); δ_C/ppm (100MHz; $CDCl_3$) 46.5 (C-1'), 65.6 (C-7), 111.4 (C-2), 112.2 (C-6), 116.0 (C-4), 116.2 (C-3'), 129.4 (C-5), 135.3 (C-2'), 142.1 (C-1) and 148.3 (C-3).

ii. *N-Allyl-3-[(allyloxy)methyl] aniline* **201A** as reddish brown oil (140 mg, 8.5%). (Found: $\mathbf{M}^+$, 203.130341. $C_{13}H_{17}NO$ requires: $\mathbf{M}^+$, 203.131014); ν_{max} (thin film/cm^{-1}) 3393 (NH); δ_H/ppm (400MHz; $CDCl_3$) 3.78 (2H, td, *J* = 5.4 and 1.5 Hz, 1'-CH_2), 4.02 (1H, td, *J* = 5.6 and 1.4 Hz, 3-H), 4.46 (2H, s, CH_2), 5.18 (1H, m, 3'-H), 5.29 (2H, qdd, *J* = 17.2, 9.8 and 1.6 Hz, 3"-H), 5.96 (2H, m, 2"-H and 2'-H), 6.55 (1H, dd, *J* = 8.0 and 2.3 Hz, 6-H), 6.64 (1H, s, 2-H), 6.68 (1H, d, *J* = 7.5 Hz, 4-H), 7.14 (1H, dd, *J* = 9.6 and 5.9 Hz, 5-H). δ_C/ppm (100MHz; $CDCl_3$) 46.5 (C-1'), 71.0 (C-1"), 72.3 (*C*H_2), 112.15 (C-2), 112.20 (C-6), 116.2 (C-3'), 116.91 (C-3"), 116.93 (C-4), 129.2 (C-5), 134.8 (C-2"), 135.3 (C-2'), 139.4 (C-3) and 148.2 (C-1).

iii. *N,N-bis allyl-3-(hydroxymethyl) aniline* **201B** as a reddish brown oil, (82 mg, 6.2%). (Found: $\mathbf{M}^+$, 203.131507. $C_{10}H_{17}NO$ requires: $\mathbf{M}^+$, 203.131014); ν_{max} (thin film/cm^{-1}) 3360 (OH) and (NH); δ_H/ppm (400MHz; $CDCl_3$) 3.93 (4H, m, 1'-H and 1"-H), 4.60 (2H, s, CH_2), 5.17 (4H, m, 3'-H and 3"-H), 5.86 (2H, tdd, *J* = 17.1, 10.1 and 4.9 Hz, 2'-H and 2"-H), 6.63 (1H, dd, *J* = 8.3 and 2.5 Hz, 6-H), 6.67 (1H, d, *J* = 7.4 Hz, 4-H), 6.71 (1H, d, *J* = 1.1 Hz, 2-H) and 7.18 (1H, t, *J* = 7.9 Hz, 5-H); δ_C/ppm (100MHz; $CDCl_3$) 52.7 (C-1' and C-1"), 65.9 (*C*H_2), 110.8 (C-2), 111.7 (C-6), 114.9

(C-4), 116.0 (C-3' and C-3"), 129.3 (C-5), 133.8 (C-2' and C-2"), 141.9 (C-3) and 148.9 (C-1).

iv. *3-[(allyloxy)methyl]aniline* **201C** as a reddish brown oil (140 mg, 11%). (Found: $\mathbf{M}^+$, 163.099525. $C_{10}H_{13}NO$ requires: $\mathbf{M}^+$, 163.099714); ν_{max} (thin film/cm^{-1}) 3356 (NH_2); δ_H/ppm (400MHz; $CDCl_3$) 3.50 (2H, b, NH_2), 4.02 (2H, td, *J* = 5.6 and 1.2 Hz, 1'-C*H*$_2$), 4.44 (2H, s, 7-CH_2), 5.20 (1H, dd, *J* = 10.4 and 1.3 Hz, CH_2−CH=C*H*$_E$), 5.30 (1H, qd, *J* = 17.2 and 1.5 Hz, CH_2-CH=C*H*$_Z$), 5.95 (1H, tdd, *J* = 17.2, 10.5 and 5.6 Hz, 2'-H), 6.60 (1H, dd, *J* = 7.9 and 1.7 Hz, 6-H), 6.69 (1H, s, 2-H), 6.72 (1H, d, *J* = 7.2Hz, 4-H) and 7.11 (1H, dd, *J* = 9.6 and 5.8 Hz, 5-H); δ_C/ppm (100MHz; $CDCl_3$) 71.0 (C-1'), 72.1 (C-7), 114.2 (C-2), 114.3 (C-6), 117.0 (C-3'), 117.9 (C-4), 129.2 (C-5), 134.8 (C-2'), 139.5 (C-3) and 146.5 (C-1).

2-Chloro-*N*-[3-(hydroxymethyl)phenyl]acetamide 202 and 3-(Chloroacetamido)-benzyl chloroacetate 202A

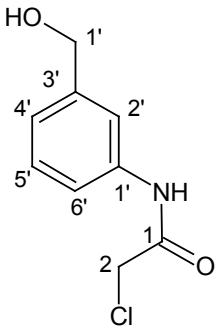

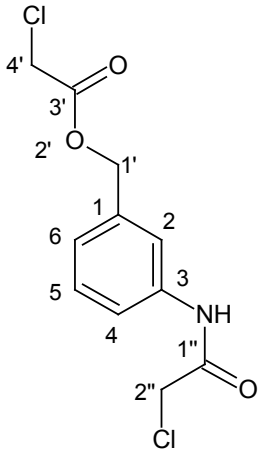

NaH (60% dispersion in mineral oil; 0.20 g, 8.1 mmol) was added in small portions to permit controlled evolution of hydrogen, to a stirred solution of 3-aminobenzyl alcohol **200** (1.0 g, 8.1 mmol) in dry THF (20 mL) under nitrogen at 0°C. Chloroacetyl chloride (0.64 mL, 8.1 mmol) was then added through a septum and the resulting solution refluxed for *ca.* 8h. The reaction was quenched by the addition of water (30 mL). The solvent was evaporated *in vacuo* and the aqueous residue was extracted with EtOAc (2 × 30 mL). The combined organic extracts were washed sequentially with water (2 × 60 mL) and brine (2 × 60 mL). The aqueous washings were extracted with EtOAc and the organic layers combined and dried (anhydr.

$MgSO_4$). The solvent was evaporated *in vacuo* and the residue was chromatographed [Column chromatography; elution with hexane-EtOAc (1:1)] to afford two products:

i. *2-Chloro*-N-*[3-(hydroxymethyl)phenyl]acetamide* **202** as a light brown solid (0.60 g, 37%) m.p. 88-90°C. (Found: $\mathbf{M}^+$, 199.03915. $C_9H_{10}NO_2{}^{35}Cl$ requires: $\mathbf{M}^+$, 199.15044); ν_{max} (solid deposit/cm^{-1}) 3378 (OH), 1681 (C=O) and 1615 (NHCO); δ_H/ppm (400MHz; DMSO-d_6) 4.23 (2H, s, 1"-H), 4.48 (2H, d, J = 5.2 Hz, CH_2Cl), 5.17 (1H, d, *J* = 5.0 Hz, OH), 7.03 (1H, d, *J* = 7.3 Hz, 6'-H), 7.27 (1H, t, *J* = 7.7 Hz, 5'-H), 7.47 (1H, d, *J* = 7.8 Hz, 4'-H), 7.56 (1H, s, 2'-H) and 10.23 (1H, s, NH) ; δ_C/ppm (100MHz; DMSO-d_6) 43.4 (CH_2OH), 62.6 (CH_2Cl), 117.3 (C-2'), 117.6 (C-4'), 121.7 (C-6'), 128.3 (C-5'), 138.2 (C-1'), 143.2 (C-3') and 164.4 (C=O); m/z = 199 ($\mathbf{M}^+$, 10%) and 198 (100%).

ii. *3-(Chloroacetamido)-benzyl chloroacetate* **202A** as a yellow solid (0.41 g, 18%), m.p. 84-86°C. (Found: $\mathbf{M}^+$, 275.01078. $C_{11}H_{11}NO_3{}^{35}Cl_2$ requires: $\mathbf{M}^+$, 275.14811); ν_{max} (solid deposit/cm^{-1}) 3411 (NH), 1747 (O.C=O), 1664 (C=O) and 1617 (NHC=O); δ_H/ppm (400MHz; $CDCl_3$) 4.10 (2H, s, 2-CH_2), 4.18 (2H, s, 2"-CH_2), 5.19 (2H, s, 7'-H), 7.17 (1H, d, *J* = 7.6 Hz, 4'-H), 7.36 (1H, t, *J* = 7.9 Hz, 5'-H), 7.52 (1H, d, *J* = 8.14 Hz, 6'-H), 7.60 (1H, s, 2'-H) and 8.28 (1H, s, NH); δ_C/ppm (100MHz; $CDCl_3$) 40.8 (C-2), 42.8 (C-2"), 67.4 (C-7'), 119.9 (C-6'), 120.2 (C-2'), 125.0 (C-4'), 129.5 (C-5'), 136.1 (C-1'), 137.0 (C-3'), 163.9 (C-1") and 167.1 (C-1); m/z = 274.12 ($\mathbf{M}^+$**-1**, 50%) and 314.02 (100%).

Diethyl {[3-(hydroxymethyl)phenyl]carbamoyl}methyl] phosphonate 203

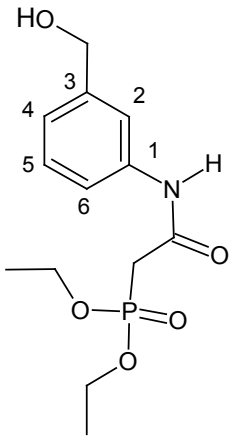

Triethyl phosphite (1.6 mL, 9.3 mmol) was added under nitrogen through a septum to 2-chloro-*N*-(3-hydroxymethylphenyl)acetamide **202** (150 mg, 0.75 mmol) in an oven-dried round bottomed flask equipped with a reflux condenser. The resulting mixture was refluxed for *ca.* 5.5h during which time the reaction was monitored by TLC. The cooled mixture was then stirred with hexane (20 mL) for *ca.* 10 minutes followed by decantation of the hexane layer to remove the excess phosphite; this was repeated twice. The residual brown oil that was chromatographed [column chromatogragpy; elution with EtOAc:EtOH = 20:1] to afford *diethyl {[3-(hydroxymethyl)phenyl]carbamoyl}methyl] phosphonate* **203** as a light yellow oil (77 mg, 34%). (Found: $\mathbf{M}^+$, 301.10706. $C_{13}H_{20}NO_2P$ requires: $\mathbf{M}^+$, 301.27591); ν_{max} (thin film/cm^{-1}) 3400 (OH), 1670 NHC=O (1613), 1232 (P=O) and 1023 (O=PO−C $_2H_5$); δ_H/ppm (400MHz; $CDCl_3$) 1.35 (6H, t, J = 7.1 Hz, 2 × CH_3), 1.78 (1H, br s, OH), 3.04 (2H, d, $J_{P–H}$ = 21.1 Hz, CH_2P), 4.18 (4H, m, 2 × CH_3CH_2), 4.57 (2H, s, 7-H), 6.98 (1H, d, J = 7.5 Hz, 6-H), 7.18 (1H, t, J = 7.8 Hz, 5-H), 7.39 (1H, s, 2-H), 7.43 (1H, d, J = 8.1 Hz, 4-H) and 9.27 (1H, s, NH); δ_C (100MHz; $CDCl_3$) 16.3 (2C, d, $J_{P–C}$ = 6.1 Hz, 2 × CH_3), 36.3 (d, $J_{P–C}$ = 129.9 Hz, CH_2P), 63.1 (d, $J_{P–C}$ = 6.5 Hz, 2 × CH_2CH_3), 64.8 (C-7), 118.1 (C-2), 118.7 (C-4), 122.6 (C-6), 128.9 (C-5), 138.1 (C-1), 141.9 (C-3) and 162.3 (C=O, d, $J_{P–C}$ = 3.9); δ_P/ppm (162 MHz; $CDCl_3$) 23.5 (P=O).

_N_-Acryoyl-3-(hydroxymethyl)aniline 204 and 3-acrylamidobenzyl acrylate 204A

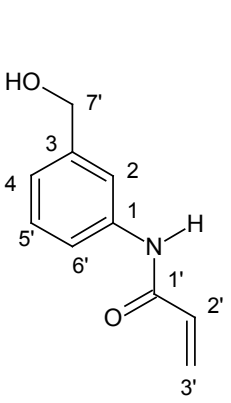

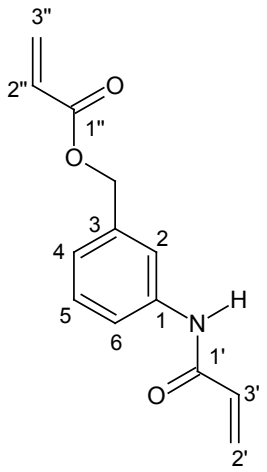

To a stirred solution of 3-aminobenzyl alcohol **200** (0.50 g, 4.1 mmol) in dry THF (20 mL) under nitrogen was added NaH (60% dispersion in mineral oil; 0.098 g, 4.1 mmol) in small portions to permit controlled evolution of hydrogen. Acryloyl chloride (0.33 mL, 4.1 mmol) was then added through a septum and the resulting solution was refluxed for *ca.* 6 h. The reaction was quenched by the addition of water (30 mL). The solvent was evaporated *in vacuo* and the aqueous residue extracted with EtOAc (2 × 30 mL). The combined organic extracts were washed sequentially with water (2 × 60 mL) and brine (2 × 60 mL). The aqueous washings were extracted with EtOAc and the organic layers combined and dried (anhydr. $MgSO_4$). Preparative thin layer chromatography [on silica gel; elution with hexane-EtOAc (4:6)] afforded two fractions.

(i) N-*Acryoyl-3-(hydroxymethyl)aniline* **204** as a yellow oil, (7.2 mg, 1%). Found: $\mathbf{M}^+$, 177.078091. $C_{10}H_{11}NO_2$ requires: $\mathbf{M}^+$, 177.078979); ν_{max} (thin film/cm^{-1}) 3296 (OH) and 1711 (C=O); δ_H/ppm (600MHz; $CDCl_3$) 5.17 (1H, s, 7-CH_2), 5.85 (1H, d, *J* = 10.5 Hz, 3'-H_a), 6.16 (1H, dd, *J* = 17.3 Hz and 10.5 Hz, 2'-H), .45 (1H, d, *J* = 17.3 Hz, 3'-H_b), 7.14 (1H, d, *J* = 7.7 Hz, 4-H), 7.32 (1H, t, *J* = 7.8 Hz, 5-H), 49 (1H, d, *J* = 7.7 Hz, 6-H) and 7.56 (1H, s, 2-H); δ_C/ppm (150MHz; $CDCl_3$) 66.0 (C-7), 119.6 (C-2), 119.9 (C-6), 124.3 (C-4), 128.2 (C-2'), 129.5 (C-5), 131.3 (C-3'), 137.0 (C-1), 137.7 (C-3) and 167.7 (C=O).

(ii) *3-acrylamidobenzyl acrylate* **204A** as a yellow oil, (0.019, 2%). (Found: $\mathbf{M}^+$, 231.088347. $C_{13}H_{13}NO_3$ requires: $\mathbf{M}^+$, 231.089543); ν_{max} (thin film/cm^{-1}) 1713

(C=O) and 1665 NHC=O; δ_H/ppm (400MHz; $CDCl_3$) 5.18 (1H, s, 7-CH_2) , 5.78 (1H, dd, *J* = 10.2 and 1.1 Hz, 3"-H_a), 5.85 (1H, dd, *J* = 10.4 and 1.3 Hz, 3'-H_b), 6.20 (2H, m, 2'-H and 2"-H), 6.42 (1H, dd, *J* = 5.2 and 1.2 Hz, 3"-Hb), 6.46 (1H, dd, *J* = 5.7 and 1.1 Hz, 3'-H_b), 7.14 (1H, d, *J* = 7.5 Hz, 6-H), 7.33 (1H, t, *J* = 7.8 Hz, 5-H), 7.55 (1H, d, *J* = 6.8 Hz, 4-H) and 7.61 (1H, s, 2-H); δ_C/ppm (100MHz; $CDCl_3$) 66.0 (7-*C*H_2), 119.8 (C-4), 124.2 (C-6), 128.2 (C-2' and C-2"), 129.3 (C-5), 131.3 (C-3' and C-3"), 136.9 (C-1 and C-3) and 166.0 (2 × C=O).

2-Acetoxy-*N*-[(3-hydroxymethyl)phenyl]-acetamide 205

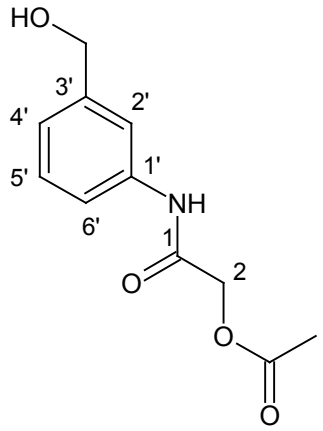

NaH (60% dispersion in mineral oil; 0.33 g, 8.1 mmol) was added in small portions to a stirred solution of 3-aminobenzyl alcohol (1.0 g, 8.1 mmol) in dry THF (20 mL) under nitrogen at 0 ºC , to permit controlled evolution of hydrogen. Acetoxyacetyl chloride (0.90 mL, 8.1 mmol) was then added through a septum and the resulting solution refluxed for *ca.* 5.0 h. The reaction was quenched by the addition of satd. aq. $NaHCO_3$ (50 mL). The solvent was evaporated *in vacuo* and the aqueous residue was extracted with EtOAc (2 × 50 mL). The combined organic extracts were washed sequentially with water (2 × 100 mL) and brine (2 × 100 mL). The aqueous washings were extracted with EtOAc and the organic layers combined and dried (anhydr. $MgSO_4$). Evaporation of the solvent *in vacuo* and chromatography of the residue [radial chromatography with hexane-EtOAc (1:9)] to afforded *2-acetoxy-N-[(3-hydroxymethyl)phenyl]-acetamide* **205** as a light yellow oil (0.26 g, 14%). (Found $\mathbf{M^+}$**,** 223.08369, $C_{11}H_{13}NO_4$ requires 223.22569), ν_{max} (solid deposit/cm^{-1}) 3354 (OH), 1741 (CH_3*C*=O), 1678 (NH*C*=O); δ_H/ppm (400MHz; $CDCl_3$) 2.19 (3H, s, CH_3), 4.62 (2H, s, CH_2OH), 4.63 (2H, s, CH_2), 5.28 (1H, s, OH), 7.09 (1H, d, *J* = 7.6 Hz, 4'-H), 7.27 (1H, t, *J* = 7.8 Hz, 5'-H), 7.43 (1H, d, *J* = 8.40 Hz, 6'-H), 7.47 (1H, s, 2'-H) and

8.04 (1H, s, NH); δ_C/ppm (100MHz; $CDCl_3$) 20.7 (*C*H_3), 63.2 (C-2), 64.7 (C*H*$_2$), 118.7 (C-2'), 119.4 (C-6'), 123.4 (C-4'), 129.2 (C-5'), 136.9 (C-1'), 142.1 (C-3'), 165.3 (C-1) and 169.6 (CH_3*C*=O); m/z = 224.13 (**M**$^+$+**1**, 35%) and 206.21 (100%).

2,3,4,5,6-Pentaacetyl-*N*-[3-(hydroxymethylphenyl)]-gluconamide 206

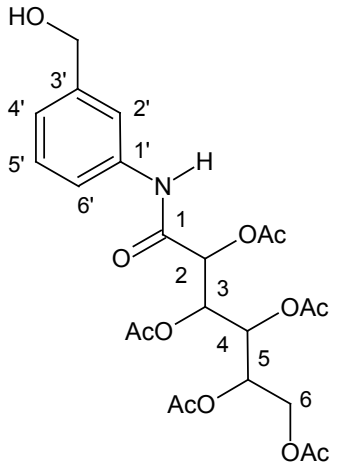

To a solution of 3-aminobenzyl alcohol **200** (100 mg, 0.81 m mol) pyridine (2 mL) was added NaH (60% dispersion in mineral oil; 37 m g, 0.81 m mol) was added in small portions to permit controlled evolution of hydrogen. 2,3,4,5,6-pentaacetoxyhexanoyl chloride **131** (350 mg, 0.81 m mol) was then added and the reaction mixture stirred at room temperature for 2.5 days. The solvent was evaporated *in vacuo* and the residue dissolved in EtOAc (30 mL). This solution was washed with satd. aq. $NaHCO_3$ (2 × 30 mL) and brine (2 × 30 mL). The organic layer was then dried (anhydr. $MgSO_4$) and the solvent was evaporated *in vacuo* to afford a reddish brown oil of which flash chromatography [on silica gel; elution with hexane-EtOAc (4:6)] afforded *2,3,4,5,6-pentaacetyl-N-[3-(hydroxymethylphenyl)]-gluconamide* **206** as a light brown oil, (58 mg, 14%). (Found: **M**$^+$, 511.16685. $C_{23}H_{29}NO_{12}$ requires: **M**$^+$, 511.47681) ν_{max} (solid deposit/cm^{-1}) 3413 (OH), 1747 (CH_3C=O) and 1602 (NHC=O); δ_H/ppm (400MHz; $CDCl_3$) 2.06 (12H, series of singlets, 4 × OAc), 2.23 (3H, s, 6-OAc), 4.11 (1H, dd, *J* = 12.4 and 5.5 Hz, 6-H$_a$), 4.31 (1H, dd, *J* = 12.3 and 3.5 Hz, 1-H$_b$), 4.63 (1H, s, C*H*$_2$), 5.06 (1H, dt, *J* =5.7, 5.6 and 3.8 Hz, 5-H), 5.34 (1H, d, *J* = 5.7 Hz, 2-H), 5.48 (1H, dd, *J* = 6.7 and 4.5 Hz, 4-H), 5.70 (1H, m, 3-H), 7.10 (1H, d, *J* = 7.7 Hz, 6'-H), 7.25 (1H, s, OH), 7.29 (1H, m, 5'-H), 7.40 (1H, d, *J* = 8.2 Hz, 4'-H), 7.47 (1H, s, 2'-H) and 8.07 (1H, s, NH); δ_C/ppm (100MHz; $CDCl_3$) 20.4,

20.6, and 20.7 (5 × OAc), 61.6 (C-6), 64.8 (C-7'), 68.7 (C-3), 68.8 (C-5), 69.1 (C-4), 71.8 (C-2), 118.5 (C-2'), 119.3 (C-4'), 123.4 (C-6'), 129.2 (C-5'), 136.9 (C-1'), 142.1 (C-3'), 164.3 (NH-C=O), 169.4 (3-C=O), 169.8 (2-*C*=O), 169.9 (5-*C*=O), 170.1 (4-*C*=O) and 170.7 (6-C=O).

Allyl (3-hydroxy)benzoate 208 and allyl 3-(allyloxy)benzoate 208A

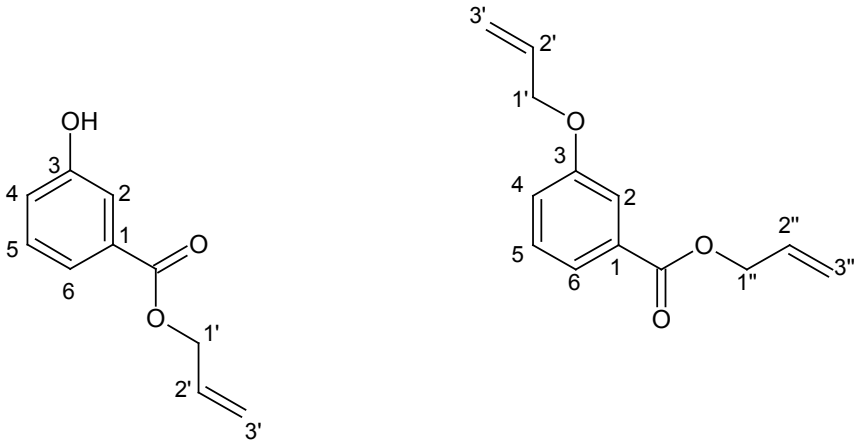

To a stirred solution of 3-hydroxybenzoic acid **207** (0.50 g , 3.6 mmol) in dry DMF (36 mL) under nitrogen was added NaH (60% dispersion in mineral oil; 170 mg, 7.2 mmol) in small portions to permit controlled evolution of hydrogen. Allyl bromide (0.34 mL, 4.0 mmol) was then added through a septum and the resulting solution was refluxed for *ca.* 48 h. The reaction was quenched by the addition of water (40 mL). The solvent was evaporated *in vacuo* and the aqueous residue extracted with EtOAc (2 × 80 mL). The combined organic extracts were washed sequentially with water (2 × 160 mL) and brine (2 × 160 mL). The aqueous washings were extracted with EtOAc and the organic layers combined and dried (anhydr. $MgSO_4$). Radial chromatography [on silica gel; elution with hexane-EtOAc (4:1)] afforded two fractions.

(i) *Allyl 3-hydroxybenzoate* **208** as a yellow oil that crystallized at 0°C. (330 mg, 52%), m.p. 43-45°C. (Found: $\mathbf{M}^+$, 178.064011. $C_{13}H_{14}O_3$ requires: $\mathbf{M}^+$, 178.062994); ν_{max} (thin film/cm^{-1}) 3410 (OH) and 1693 (CO); δ_H/ppm (400MHz; $CDCl_3$) 4.82 (2H, td, *J* = 5.6 and 1.3 Hz, 1'-CH_2), 5.28 (1H, dd, *J* = 10.5 and 1.24 Hz, CH=CH_E) 5.40 (1H, ddd, *J* = 17.2, 2.9 and 1.43 Hz, CH=CH_Z), 5.84 (1H, br s, OH), 6.02 (1H, tdd, *J* = 16.1, 10.6 and 5.6 Hz, 2'-H), 7.07 (1H, ddd, *J* = 8.1, 2.6 and 0.9 Hz, 4-H), 7.31 (1H, t, *J* = 7.9 Hz, 5-H) and 7.61 (2H, m, 2-H and 6-H); δ_C/ppm (100MHz; $CDCl_3$) 65.8

(C-1'), 116.4 (C-2), 118.4 (C-3'), 120.4 (C-4), 122.0 (C-6), 129.7 (C-5), 131.4 (C-2'), 131.9 (C-1), 155.9 (C-3) and 166.4 (C=O).

(ii) *Allyl 3-(allyloxy)benzoate* **208A** as light yellow oil (150 mg, 19%). (Found: $\mathbf{M}^+$, 218.093606. $C_{13}H_{14}NO_3$ requires: $\mathbf{M}^+$, 218.094294); ν_{max} (thin film/cm^{-1}) 1691 (CO); δ_H/ppm (400MHz; $CDCl_3$) 4.58 (2H, d, *J* = 5.3 Hz, 1'-CH_2), 4.81 (2H, d, *J* = 5.6 Hz, 1"-CH_2), 5.35 (4H, m, 3'-Ha and 3"-Ha), 6.04 (2H, m, 2'-H and 2"-H), 7.11 (1H, dd, *J* = 8.2 and 2.0 Hz, 4-H), 7.33 (1H, t, *J* = 8.0 Hz, 5-H), 7.59 (1H, s, 2-H), 7.65 (1H, d, *J* = 7.7 Hz, 6-H); δ_C/ppm (100MHz; $CDCl_3$) 65.6 (C-1"), 69.0 (C-1'), 115.1 (C-2), 117.9 (C-3"), 118.2 (C-3'), 120.2 (C-4), 122.2 (C-6), 129.4 (C-5), 131.5 (C-1), 132.2 (C-2"), 132.9 (C-2'), 158.6 (C-3) and 166.1 (C=O).

In a separate reaction 3-hydroxybenzoic acid **207** (2.0 g, 14 mmol) in DMF (60 mL) under nitrogen was treated with NaH (60% dispersion in mineral oil; 360 mg, 150 mmol) and allyl bromide (1.2 mL, 15 mmol). Radial chromatography [on silica gel; elution with hexane-EtOAc (4:1)] afforded only *allyl 3-hydroxybenzoate* **208** (1.2 g, 45 %).

3-(Allylamino)benzoic acid 210 and Allyl 3-(*N*-allylamino)benzoate 210A

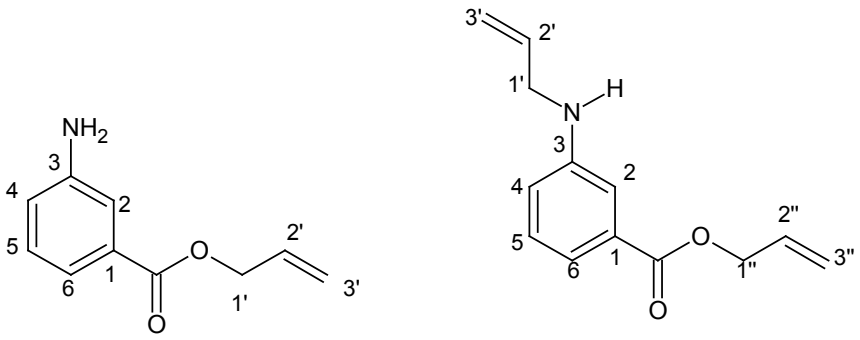

To a stirred solution of 3-aminobenzoic acid **209** (500 mg , 3.7 mmol) in dry DMF (36 mL) under nitrogen was added NaH (60% dispersion in mineral oil; 9.7 mg, 4.1 mmol) in small portions to permit controlled evolution of hydrogen. Allyl bromide (0.32 mL, 3.7 mmol) was then added through a septum and the resulting solution was refluxed for *ca.* 48 h. The reaction was quenched by the addition of water (40 mL). The solvent was evaporated *in vacuo* and the aqueous residue extracted with EtOAc

(2 × 80 mL). The combined organic extracts were washed sequentially with water (2 × 160 mL) and brine (2 × 160 mL). The aqueous washings were extracted with EtOAc and the organic layers combined and dried (anhydr. $MgSO_4$). Radial chromatography [on silica gel; elution with hexane-EtOAc (4:1)] afforded.

(i) *3-(Allylamino)benzoic acid* **210** as a reddish brown oil (160 mg, 25%). (Found: $\mathbf{M}^+$, 177.077749. $C_{10}H_{11}NO_2$ requires: $\mathbf{M}^+$, 177.200260); ν_{max} (thin film/cm^{-1}) 3436 (NH) and 1710 (CO); δ_H/ppm (400MHz; $CDCl_3$ 3.76 (1H, d, *J* = 5.2 Hz, 1'-CH_2), 5.19 (1H, dd, *J* = 10.3 and 1.3 Hz, CH=CH_E) 5.26 (1H, dd, *J* = 17.2 and 1.4 Hz, CH=CH_Z), 5.89 (1H, tdd, *J* = 17.1, 10.4 and 5.2 Hz, 2'-H), 6.78 (2H, m, 2-H and 4-H), 6.93 (1H, d, *J* = 7.4 Hz, 6-H) and 7.20 (1H, m, 5-H); δ_C/ppm (100MHz; $CDCl_3$) 46.0 (C-1'), 112.9 (C-3), 115.0 (C-4), 116.8 (C-3'), 117.3 (C-2), 119.4 (C-1), 120.8 (C-6), 129.8 (C-5), 134.2 (C-2') and 148.2 (C=O).

In a separate reaction 3-aminobenzoic acid **209** (1.0 g, 7.3 mmol) in DMF (20 mL) under nitrogen was treated NaH (60% dispersion in mineral oil; 320mg, 13 mmol) and allyl bromide (0.63 mL, 7.3 mmol). Two fractions were obtained.
(i) **210** (220 mg, 17%) and
(ii) *Allyl 3-(N-allylamino)benzoate* **210A** as a yellow oil (160 mg, 10%). (Found: $\mathbf{M}^+$, 217.109334. $C_{13}H_{15}NO_2$ requires: $\mathbf{M}^+$, 217.264231); ν_{max} (thin film/cm^{-1}) 3391 (OH) and 1711 (CO); δ_H/ppm (400MHz; $CDCl_3$) 3.80 (2H, td, *J* = 5.3 and 1.5 Hz, 1'-CH_2), 3.94 (1H, b s, NH), 4.79 (2H, td, *J* = 5.6 and 1.4 Hz, 1''-CH_2), 5.17 (1H, dd, *J* = 10.3 and 1.4 Hz, 3'-H_a), 5.27 (2H, m,, 3'-H_b and 3''-H_a), 5.40 (1H, m, 3''-H_b), 5.94 (1H, tdd, *J* = 17.1, 10.5 and 5.3 Hz, 2'-H), 6.02 (1H, ddd, *J* = 22.8, 10.8 and 5.6 Hz, 2''-H), 6.79 (1H, dd, *J* = 7.8 and 2.2 Hz, 4-H), 7.22 (1H, t, *J* = 7.9, 5-H), 7.30 (1H, s, 2-H) and 7.40 (1H, d, *J* = 7.7 Hz, 6-H); δ_C/ppm (100MHz; $CDCl_3$) 46.4 (C-1'), 65.4 (C-1''), 113.6 (C-2), 116.5 (C-3'), 117.8 (C-4), 118.0 (C-3''), 118.7 (C-6), 129.1 (C-5), 131.0 (C-1), 132.3 (C-2''), 134.9 (C-2'), 150.0 (C-3) and 166.6 (C=O).

4. REFERENCES

1. P.D.O. Davies, *Clinical Tuberculosis*, 2nd edn., Chapman and Hall, London, 1998, pp. 3-19.
2. N.M.S. Bhat, V.E. Subramaniam, *Am. J. Otolaryng.-Head and Neck Medicine and Surgery*, 2006, **27,** 39-45.
3. D.A. Williams and T.L. Lemke, *Foye's Principles of Medicinal Chemistry*, 5th edn., Lippincott Williams and Wilkins, Philadelphia, 2002, p. 905.
4. M.H. Beers and R. Berkow, *The Merck Manual of Diagnosis and Therapy*, 7th edn., Merck & Co., Inc., New Jersey, 1999, p. 1193.
5. J.Y. Kim, A. Shakow, K. Mate, C. Vanderwarker, R. Gupta and P. Farmer, *Soc. Sci. Med.*, 2005, **61,** 847-859.
6. G. Wan, S. Lu and Y. Tsai, *Am. J. Infect. Control* 2004, **32** (1), 17-22.
7. WHO Fact Sheet No. 104, 2007, accessed on 2nd October 2007 at http://www.-who.int/mediacentre/factsheets/fs104/en/
8. G. Fätkenheuer, H. Taelman, P. Lepage, A. Schwenk and R. Wenzel, *Diag. Microbiol. Infect. Dis.*, 1999, **34,** 139-146.
9. P.D.O. Davies, *Multidrug Resistant Tuberculosis* accessed on http://www.-priory.com/cmol/TBMultid.htm#Return (Accessed 5th October, 2007).
10. S.T. Cole, *Microbiology*, 2002, **148,** 2919-2928.
11. T.M. Doherty, *Vaccine*, 2005, **23,** 2109-2114.
12. C.W. Pratt and K. Cornelly, *Essential Biochemistry*, John Willey and Sons, Inc. New Jersey, 2004, p. 79.
13. M.H. Beers and R. Berkow, *The Merck Manual of Diagnosis and Therapy*, Merck & Co., Inc., New Jersey, 1999, p. 1194
14. J.D. Ernst, G. Trevor-Nunez and N. Banaiee, *J. Clin. Invest.*, 2007, **117,** 1738-1745.
15. The History of Tuberculosis accessed on http://efletch.myweb.uga.edu-/history.htm (Accessed 5th of October, 2007).
16. K. Florey, *Analytical Profiles of Drug Substances*, 1987, **16,** 512.

17. Wikipedia, the Free Encyclopedia accessed on 21st November, 2007 at http://en.wikipedia.org/wiki/Streptomycin.
18. K. Florey, *Analytical Profiles of Drug Substances,* New York, 1987, **10,** p. 2.
19. W. Fox, G.A. Ellard and D.A. Mitchinson, *Int. J. Tuberc. Lung. Dis.*, 1999, **3** (10), 5231-5279.
20. K. Florey, *Analytical Profiles of Drug Substances,* 1977, **6,** p. 186.
21. K. Florey, *Analytical Profiles of Drug Substances,* 1983, **12,** p. 435.
22. K. Florey *Analytical Profiles of Drug substances,* 1989, **18,** p. 584.
23. K. Florey, *Analytical Profiles of Drug Substances,* 1978, **7,** p. 233.
24. K. Florey, *Analytical Profiles of Drug Substances,* 1987, **5,** p. 470.
25. N.W. Schluger and W.N. Rom, *Am. J. Respir. Crit. Care Med.*, 157, 1998, 679-691.
26. A.J. Gehrin,K.M. Dobos, J.T. Belisle, C.V. Harding and W.H. Boom, *J. Immunol.*, 2004, **173,** 2660-2668.
27. C. Manca, L. Tsenova, A. Bergtold, S. Freeman, M. Tovey, J.M. Musser, C.E. Barry, V.H. Freedman and G. Kaplan, *Proc. Natl. Acad. Sci. USA*, 2001, **98** (10), 5752-5757.
28. T. Ludovic, O. Schwartz, J. Hermmann, E. Pivert, M. Jackson, A. Amara, L. Legres, D. Dreher, L.P. Nicod, J.C. Gluckman, P.H. Lagrange, B. Gicquel and O. Neyrolles, *J. Exp. Med.*, 2003, **197** (1), 121-127.
29. M.T. Madigan, J.M. Martinko and J. Parker, *Brock Biology of Microorganisms*, 8th edn., Prentice-Hall, Inc., New Jersey, 1997, p. 939.
30. B. Petrini and S. Hoffner *Int. J. Antimicrob. Ag.*, 1999, **13**, 93-97.
31. M.A. Espinal, *Tuberculosis*, 2003, **83,** 44-51.
32. WHO on *Emergence of XDR-TB* accessed on the 30th nov., 2007 at http://www.who.int/mediacentre/news/notes/2006/np23/en/
33. Extensively Drug Resistant Tuberculosis-United States, CDC document, 1993-2006, *JAMA*, 2007, 297, (**17**), 1871-1873.
34. X. Shen, G. Shen, J. Wu, X. Gui, X. Li, J. Mei, K. DeRemer and Q. Gao, *Anti-microb. Agents Chemother.*, 2007, 2618-2620.

35. D.A. Williams and T.L. Lemke, *Foye's Principles of Medicinal Chemistry*, 5th edn., Lippincott Williams and Wilkins, Philadelphia, 2002, 907.
36. L. Hihghleyman, *Bulletin of the Experimental Treatment for AIDS*, 1998, accessed on 21st Nov. 2007 at http://ww1.aegis.org/pubs/beta/1998/-BE981007.html.
37. D.A. Mitchison, *Am. J. Resp. Crit. Care*, 2005, **171**, 699-706
38. J.S. Blanchard, *Annu. Rev. Biochem*. 1996, **65**, 215-239.
39. Y. Zhang B. Heym and B. Allen, *Nature*, 1992, *358*, 591-593.
40. K. Johnsson and P.G. Schultz, *J. Am. Chem. Soc*., 1994, **116**, 7425-7426.
41. A. Banerjee, E. Dubnau and A. Quemard, *Sci*., 1994, *263*, 227-230.
42. K. Mdluli, D.R. Sherman and M.J. Hickey, *J. Infect. Dis*., 1996, **174**, 1085-1090.
43. L.A. Basso, R. Zheng and J.M. Musser, *J. Infect. Dis*., 1998, **178**, 769-775.
44. E.M. Bavin, B. James and E. Kay, *J. Pharm. Pharmacol*, 1955, 7, 1032-1038.
45. E.M. Bavin, D.J. Drain and M. Seiler, *J. Pharm. Pharmacol*, 1952, 4, 844-855.
46. D.A. Williams and T.L. Lemke, *Foye's Principles of Medicinal Chemistry*, 5th edn., Lippincott Williams and Wilkins, Philadelphia, 2002, 912.
47. P.D.O. Davies, *Clinical Tuberculosis* 2nd edn., Chapman and Hall, London, 1998, p. 235.
48. K. Florey, *Analytical Profiles of Drug Substances*, 1977, **6,** p. 262.
49. D.A. Williams and T.L. Lemke, *Foye's Principle of Medicinal Chemistry*, 5th edn., Lippincott Williams and Wilkins, Philadelphia, 2002, 915.
50. K. Johnsson, D.S. King, P.G. Schultz, *J. Am. Chem. Soc*., 1995, 117, 5009-5010.
51. E. Miyazaki, M. Miyazaki and J.M. Chen, *Antimicrob. Agents Chemother*., 1999, **43**, 85-89.
52. B.Y. Zhao, R. Pine and J. Domagala, *Antimicrob. Agents Chemother*., 1999, **43**, 661-663.
53. X. Yang, et al, *Biochemistry*, 2007, **46**, 9058-9067.
54. J. Hugonnet and J.S. Blanchard, *Biochemistry*, 2007, **46**, 11998-12004.
55. P.B. Jones, *J. Med. Chem*., 2000, **43,** 3304-3314.
56. P.D.O. Davies, *Clinical Tuberculosis*, 2nd edn., Chapman and Hall, London, 1998, pp. 318-338.

57. T.R. Frieden, T.R. Sterling, S.S. Munsiff, C.J. Watt and C. Dye, *The Lancet*, 2003, **362,** 887-899.
58. J.S. Mukherjee, M. L. Rich, A.R. Socci, J.K. Joseph, F.A. Viru, S.S. Shin, J.J. Furin, M.C. Beccerra, D.J. Barry, J.Y. Kim, J. Bayona, P. Farmer, M.C.S. Fawz and K.W. Seung, *The Lancet*, 2004, **363**, 474-481.
59. K. Dereimer, L. Garcia-Garcia, M. Bobadilla-del-Valle, M. Palacios-Martinez, A. Martinez-Gamboa, P.M Small, J. Sifuentes-Orsonio and A. Ponce-de-Leon, *The Lancet*, 2005, **365,** 1239-1245.
60. P.H. Hopewell, M. Pai, D. Maher, M. Uplekar, M.C. Raviglione, *Lancet Infect. Dis.*, 2006, **6,** 710-725.
61. S. Protussananon and K. Peltzer, *J. Health Popul. Nutr*., 2005, **23**, (1), 74-78.
62. J.W. Daily, *Proc. Natl. Acad. Sci. USA*, 1995, **92**, 9-13.
63. A. Sato, *J. Toxicol. Toxin Rev*., 1996, **15**, 171-198.
64. New Science accessed on 30th nov. 2007 on http://www.chemistry.unimelb.edu.au/staff/quiney/www/synchnet/newsciences/rationaldrugs.php
65. S. O'Connor, *J. Aut. Chem*., 1993, **15** (1), pp. 9-12.
66. S. Stern *the case of drug discovery in the 1980s* accessed on 30th Nov., 2007 on http://www.kellogg.northwestern.edu/faculty/sstern/htm/NEWresearchpage/Publications/Stern%20RX%20Organizations.pdf
67. R. Twyman, *Rational drug design*, accessed on 30th Nov., 2007 at http://genome.wellcome.ac.uk/doc_wtd020912.html.
68. D.A. Williams and T.L. Lemke, *Foye's Principle of Medicinal Chemistry*, 5th edn., Lippincott Williams and Wilkins, Philadelphia, 2002, 31.
69. D.A. Williams and T.L. Lemke, *Foye's Principle of Medicinal Chemistry*, 5th edn., Lippincott Williams and Wilkins, Philadelphia, 2002, 37-64.
70. D.A. Williams and T.L. Lemke, *Foye's Principle of Medicinal Chemistry*, 5th edn., Lippincott Williams and Wilkins, Philadelphia, 2002, 100.
71. D.D. Woods, Br. J. Exp. Pathol., 1940, 21, 74-90.
72. D.A. Williams and T.L. Lemke, *Foye's Principle of Medicinal Chemistry*, 5th edn., Lippincott Williams and Wilkins, Philadelphia, 2002, 101.

73. D.A. Williams and T.L. Lemke, *Foye's Principle of Medicinal Chemistry*, 5th edn., Lippincott Williams and Wilkins, Philadelphia, 2002, 68-85.
74. R.M.A. Knegtel, I.D. Kuntz and C.M. Oshiro, *J. Mol. Biol*., 1997, **266**, 424-440.
75. S.T. Cole, *Tubercle Lung Dis*., 1996, **77**, 486-490.
76. G. Jung, *Combinatorial Chemistry*, Wiley-VCH, New York, 1999, p.1.
77. M. Fernandez, *J. Mol. Gr. M.* 2007, **26**, 748-759.
78. *Target based rational drug design* accessed on 27th nov 2007 at http://www.pharmacy.umaryland.edu/courses/PHAR531/lectures_old/compchem_1.html
79. T.S. Balganesh, V. Balasubramanian, S.N. Kumar, *Curr. Sci. India*, 2004, **86** (1), 167-176.
80. R.E. Shoup, *Current Separations*, 1999, **18**, (1), 17-22.
81. D. Zhang et al, *Drug Metabolism and Disposition*, 2005, **33**, (11), 1729-1739.
82. D.A. Williams and T.L. Lemke, *Foye's Principle of Medicinal Chemistry*, 5th edn., Lippincott Williams and Wilkins, Philadelphia, 2002, 960.
83. C. Raynaud, G.Etienne, P. Peyron, M. Lanéelle and M. Daffé, *Microbiology+*, 1998, **144**, 577-587.
84. G. Harth and M.A. Horwitz, *J. Biol. Chem.*, 1997, 272, (36), 22728-22735.
85. G. Harth and M.A. Horwitz, *J. Exp. Med*., 1999, **189**, (9), 1425-1435.
86. G. Harth, D.L. Clemens and M.A. Horwitz, *Proc. Natl. Acad. Sci. USA*, 1994, **91**, 9342-9346.
87. G.R. Hirschfield, M. Mc Neil and P.J. Brennan, *J. Bacteriol*., 1990, **172**, 1005.
88. D. Eisenberg, H.S. Gill, G.M.U., Pfluegl, S.H. Rotstein, *Biochim. Biophys. Acta.*, 2000, **1477**, 122-145.
89. R.H. Garrette and C.M. Grisham, *Biochemistry*, 2nd edn., Sunders College Publishing, New York, p. 860.
90. W.W. Krajewski, T. A. Jones and S.L. Mowbray, *Proc. Natl. Acad. Sci. USA*, 2005, **102**, (30), 10499-10504.
91. H. Gill, G.M.U. Pfluegl and D. Eisenberg, *Acta Cryst. D*. **55**, 1999, 865-868.
92. B.M. Shapiro, E.R. Stadtman, *J. Biol. Chem.*, 1968, 243, 3769-3771.
93. H. Tumani, G.Q. Shen and J.B. Peter, *J. Immunol. Methods*, 1995, **188**, 155-163.

94. R.P. Pillai, F.M. Raushel and J.J. Villafranca, *Arch. Biochem. Biophys.* 1980, **199**, (1), 7-15.

95. S.G. Rhee, P.B. Chochk and E.R. Stadman, *Biochimie*, 1976, **58**, 35-49.

96. M.T. Madigan, J.M. Martinko and J. Parker, *Brock Biology of Microorganisms*, 8th edn., Prentice-Hall, Inc., New Jersey, 1997, pp. 228-229.

97. S. Liaw, C. Pan and D. Eisenberg, *Proc. Natl. Acad. Sci. USA*, 1993, **90**, 4996-5000.

98. R.H. Garrette and C.M. Grisham, *Biochemistry*, 2nd edn., Sunders College Publishing, New York, p. 862.

99. M.T. Tullius, G. Harth and M.A. Horwitz, *Infect. Immun*., 2003, 3927-3936.

100. R.H. Garrette and C.M. Grisham, Biochemistry, 2nd edn., Sunders College Publishing, New York, p. 862.

101. R. Mehta, J.T. Pearson, S. Mahajan, A. Nath, M.J. Hickey, D.R. Sherman and W.M. Atkins, *J. Biol. Chem*., 2004, **279**, (21), 22477-22482.

102. H.R. Kingdon, B.M. Shapiro and E. Stadtman, *Biochemistry-US*, 1967, **58**, 1703-1710.

103. R. J. Almassy, C.A. Janson and R. Hamlin, *Nature*, 1986, **323**, 304-309.

104. P. Jiang, A.A. Pioszak and A.J. Ninfa, *Biochemistry-US*, 2007, **46**, 4117-4132.

105. S. Anishetty, M. Pulimi and G. Pennathur, *Comput. Biol. Chem*., 2005, **29**, 368-378.

106. S.H. Liaw, I. Kuo, D. Eisenberg, *Protein Sci*., 1995, **4**, 2358-2365.

107. M. Alibhali, J. Villafranca, *Biochemistry+*, 1994, **33**, 682-686.

108. S.H. Liaw, G. Jun, D. Eisenberg, *Biochemistry+*., 1994, **33**, 11184-11188.

109. H. Gill, G.M.U. Pfluegl and D. Eisenberg, *Protein Sci*., 1996, **5**, p. 125.

110. H. Liaw, J. Villafranca, *Biochemistry+*, 1993, **32**, 7999-8003.

111. L.M. Abell, J. Schineller, P.J. Keck and J. Villafranca, *Biochemistry+*, 1995, **34**, 16695-16702.

112. S.H. Liaw, C. Pan, D. Eisenberg, *Proc. Natl. Acad. Sci.* USA, 1993, **90**, 4996-5000.

113. R.J. Almassy, C.A. Janson, R. Hamlin, N. Xuong and D. Eisenberg, *Nature*, 1986, **323**, 304-309.

114. J.A. Joules and K. Mills, *Heterocyclic Chemistry*, 4th edn., Blackwell Science, London, 2000, p. 461.

115. L. Stryer, *Molecular design of Life*, W.H. Freeman and Company, New York, 1989, pp. 72 and 86.

116. M.K. Campbell and S.O. Farrell, *Biochemistry*, 4th edn., Thomson Books/Cole, 2003, 14-21.

117. J.A. Joules and G.F. Smith, *Heterocyclic Chemistry*, 2nd edn., Van Nostrand Reinhold Company, London, 1978, pp. 324-327.

118. J. McMurry, *Organic Chemistry*, 2nd edn., Brooks/Cole Publishing Company, Pacific Grove, California, 1984, pp.1045-1047.

119. M.T. Madigan, J.M. Martinko and J. Parker, *Brock Biology of Microorganisms*, 8th edn., Prentice-Hall, Inc., New Jersey, 1997, p. 329.

120. M. Dreyfus, G. Dodin, O. Bensaude and J. Dubois, *J. Am. Chem. Soc*., 1975, **97**, 2369.

121. L. Stryer, *Molecular design of Life*, W.H. Freeman and Company, New York, 1989, p. 92.

122. R.H. Garrette and C.M. Grisham, *Biochemistry*, 2nd edn., Saunders College Publishing, New York, p. 329.

123. C.W. Pratt and K. Cornelly, *Essential Biochemistry*, John Wiley and Sons, New Jersey, 2004, p. 291.

124. J.S. Boyer, M.R. Francis, J. Boerio-Goates, *J. Chem. Thermodyn*., 2003, **35**, 1917-1928.

125. M. Ochiai, R. Marumoto, S. Kobayashi, H. Shimazu and K. Morita, *Tetrahedron*, 1968, **24**, 5731.

126. N.F. Zakirova, A.V. Shipitsyn, E.F. Belanov and M.V. Jasko, *Bioinorg. Med. Chem. Lett.*, 2004, **14**, 3357-3360.

127. R.H. Garrette and C.M. Grisham, *Biochemistry*, 2nd edn., Saunders College Publishing, New York, p. 331.

128. J. Boerio-Goates, M.R. Francis, M.A.V. Ribeiro da Silva, M.D.M.C. Ribeiro da Silva and Y.B. Tewari, *J. Chem. Thermodyn*., 2001, **33**, 929-947.

129. S. Gessi, K. Varani, S. Merighi, E. Ongini and P.A. Borea, *Brit. J. Pharmacol*., 2000, **129**, 2-11.

130. P.J. Scammells, S.P. Baker, L. Bellardinelli, R.A. Olsson, R.A. Russell and D.M.J. Wright, *Tetrahedron*, 1996, **52**, (13), 4735-4744.

131. D.A. Williams and T.L. Lemke, *Foye's Principles of Medicinal Chemistry*, 5th edn., Lippincott Williams and Wilkins, Philadelphia, 2002, p. 372.

132. C.W. Pratt and K. Cornelly, *Essential Biochemistry*, John Wiley and Sons, New Jersey, 2004, 193 and 217.

133. R.H. Garrette and C.M. Grisham, *Biochemistry*, 2nd edn., Saunders College Publishing, New York, 507-508.

134. G. W. Kenner, C.W. Taylor and A.R. Todd, *J. Chem. Soc*., 1949, 1620.

135. L.M. Lerner and G. Mennitt, *Carbohydr. Res*., 1994, **259**, 191-200.

136. L.M. Lerner, *J. Org. Chem*., 1969, **34**, (1), 101-103.

137. I. Krizmanić, A. Višnjevac, M. Luić, Glavaš-Obrovac, M. Žinić and B. Žinić, *Tetrahedron*, 2003, **59**, 4047-4057.

138. S.R. Guppi, M. Zhou and G.A. O'Doherty, *Org. Lett*., 2006, **8** (2), 293-296.

139. R.S. Babu, G.A. O'Doherty, *J. Am. Chem. Soc*., 2003, **125**, 12406-12407.

140. R.S. Babu, M. Zhou and G.A. O'Doherty, *Org. Lett*., 2005, **24**, 169-177.

141. R.H. Garrette and C.M. Grisham, *Biochemistry*, 2nd edn., Saunders College Publishing, New York, p. 139.

142. C.W. Pratt and K. Cornelly, *Essential Biochemistry*, John Wiley and Sons, New Jersey, 2004, p. 293.

143. J. Clayden, N. Greeves, S. Warren and P. Wothers, *Organic Chemistry*, Oxford University Press, New York, 2005, p. 1347.

144. J. Clayden, N. Greeves, S. Warren and P. Wothers, *Organic Chemistry*, Oxford University Press, New York, 2005, p. 1348.

145. J.A. Joules and K. Mills, *Heterocyclic Chemistry*, 4th edn., Blackwell Science, London, 2000, p. 462-463.

146. J.A. Joules and K. Mills, *Heterocyclic Chemistry*, 4th edn., Blackwell Science, London, 2000, p. 463.

147. R.C. Young, M. Jones, K.J. Milliner, K.K. Rana and J.G. Ward, J. *Med. Chem*., 1990, **33**, 2073.

148. E.C. Taylor, O. Vogl and C.C. Cheng, *J. Am. Chem. Soc*., 1959, **81**, 2442.

149. A.H. Alshaar, D.W. Gilmour, D.J. Lythgoe, I. McClenaghan and C.A. Ramsden, J. *Chem. Soc., Chem. Comm.*, 1989, 551.

150. Q. Dang, B.S. Brown, and M.D. Erion, *J. Org. Chem*., 1999, **121**, 5833.

151. J.A. Joules and K. Mills, *Heterocyclic Chemistry*, 4th edn., Blackwell Science, London, 2000, p. 484.

152. E.C. Taylor, Y. Maki and A. McKillop, *J. Org. Chem*., 1969, **34**, 1170.

153. A. Vincze and S. Cohen, *Isr. J. Chem*., 1966, **4**, 23

154. J.A. Montgomery, C. Temple, *J. Am. Chem. Soc*., 1961, 83, 630.

155. L.R. Lewis, F.H. Schneider and R.K. Robins, *J. Org. Chem*., 1961, **26**, 3837.

156. S. Lewin, *J. Chem. Soc*., 1964, 792.

157. R. Brandes and H.J. Roth, *Arch. Pharm. (Weinheim, Ger.)*, 1967, **300**, 1000.

158. M.T. Madigan, J.M. Martinko and J. Parker, *Brock Biology of Microorganisms*, 8th edn., Prentice-Hall, Inc., New Jersey, 1997, pp. 124-126.

159. C.W. Pratt and K. Cornelly, *Essential Biochemistry*, John Wiley and Sons, New Jersey, 2004, p. 7.

160. P. Sykes, *A guidebook to Mechanism in Organic Synthesis*, 2nd edn., Longman Group Ltd, London, 1975, pp 206-208.

161. R.K. Mackie and D.M. Smith *Guidebook to Organic Synthesis*, Longman Inc., New York, 1982, p. 243.

162. Z. Hall, *Synthesis of Novel Glutamine Synthetase Inhibitors*, honours thesis, Rhodes Uni., Grahamstown, South Africa, 2003, 52.

163. A. N. De Belder, *Adv. in Carbohydr. Chem. and Biochem*., 1965, 20, pp. 219-302.

164. C.A. Fyfe, *The chemistry of the hydroxyl group, chap. 2*, John Wiley and Sons, London, 1971, 52-124.

165. C.E. Braune and C.D. Cook, *Org. Synth. Coll*., **5**, 1973, 887-889.

166. R. Adams and L.H. Ulich, *J. Am. chem. soc*., **42**, 1920, 599-611.

167. L.F. Fieser and F. Fieser, Reagents for organic synthesis, John Wiley and Sons, Inc., London, 958.

168. L.F. Fieser, *J. Am. Chem. Soc.*, **75**, 1953, 4400.

169. K.L. Tan, A. Vasudevan, R.G. Bergman, J.A. Ellman and A.J. Souers, *Org. lett.* 2003, **5** (12), S-3.

170. B. Plietker and M. Niggemann, *J. Org. Chem.*, 2005, **70**, 2402-2405.

171. K.B. Wiberg and K.L. Saegebarth, *J. Am. Chem. Soc*., 1957, **79**, 2822-2824.

172. J.E. Coleman, C. Ricciuti and D. Swern, *J. Am. Chem. Soc*., 1956, **78**, 5342-5345.

173. B.S. Furniss, A.J. Hannaford, P.W.G. Smith and A.R. Tatchell, *Vogel's Textbook of Practical Organic Chemistry*, 5th edn., Longman Scientific and Technical, New York, 1989, 547-550.

174. V. Bhushan, R. Rathore and S. Chandrasekaraan, *Communications*, 1984, 431-433.

175. G.N. Vyas and NM. Shah, *organic syntheses*, year, **31**, 90-91.

176. G. R. Pettit, N. Melody and D.L. Herald, *J. Nat. Prod.*, 2004, **67**, 322-327.

177. T. Kanayama, K. Yoshida, H. Miyabe, T. Kimachi and Y. Takemoto, *J. Org. Chem.*, 2003, **68**, 6197-6201.

178. M.J. Robins and P.W. Hatfield, *Can. J. Chem*., 1982, **60**, 547-553.

179. O. Achatz, A. Grandl and K.T. Wanner, *Eur. J. Org. Chem*., 1999, 1967-1978.

180. B.N. Thomas, C.M. Lindermann, R.C. Corcoran, C.L. Cotant, J.E. Kirsch and P.J. Persichini, *J. Am. Chem. Soc*., 2002, **124** (7), 1227-1233.

181. B.S. Furniss, A.J. Hannaford, P.W.G. Smith and A.R. Tatchell, *Vogel's Textbook of Practical Organic Chemistry*, 5th edn., Longman Scientific and Technical, New York, 1989, 644-645.

182. S.M. Jain, A. Kumar, B. Purnima, K.K. Anand, A.K. Saxena and C.K. Atal, *Indian J. Chem*., 1988, (**27B**), PP. 390-393.

183. B.C. Kraybill, L.L. Elkin, J.D. Blethrow, D.O. Morgan and K.M. Shokat, *J. Am. Chem. Soc*., 2002, **124**, 12118-12128.

184. A. Hussain and J. H. Rytting, *J. Pharm. Sci.*, 1974, **63** (5), 798-799.

185. A.M. Musa, *Applications of Baylis-Hillman Reaction in the Synthesis of Coumarin Derivatives*, PhD thesis, Rhodes Uni., 2002, pp. 89-90.

186. B.S. Furniss, A.J. Hannaford, P.W.G. Smith and A.R. Tatchell, *Vogel's Textbook of Practical Organic Chemistry*, 5th edn., Longman Scientific and Technical, New York, 1989, 1132-1136.

187. Z. Rappoport, *The Chemistry of the Cyano Group*, Wiley, New York, 1970, pp. 307 and 340.

188. M. Mayer and B. Meyer, *Communications*, 1999, 38 (12), 1785-1788.

189. D. Uhrin, A.V.K. Prasad, J. Brisson and D.R. Bundle, *Can. J. Chem.*, 2002, **80**, 904-907.

190. HOSE code Prediction accessed on http://www.modgraph.co.uk/product_nmr-_HOSE.htm (Accessed 20th Dec., 2007).

191. R. Kiralj and M.M.C. Ferreira, *J. Mol. Gr. M.*, 2003, **21**, (499-515).

192. *Immunology* accessed on http://www.cgl.ucsf.edu/home/glasfeld/tutorial/sial-/sial.html (accessed 17th august 2007).

193. S. Liaw and D. Eisenberg, *Biochemistry+*, 1994, **33**, 675-681.

194. H.S. Gill and D. Eisenberg, *Biochemistry+*, 2001, **40**, 1903-1912.

195. *Crystal structure of 1F52, the glutamine synthetase of Salmonella typhimurium co-crystallized with ADP*, accessed on http://www.rcsb.org/pdb/explore.do?-structureId=1F52, (accessed 2nd Jan. 2008).